



# **NAVAL POSTGRADUATE SCHOOL**

**MONTEREY, CALIFORNIA**

## **THESIS**

**AUTONOMOUS NON-LINEAR CLASSIFICATION OF LPI  
RADAR SIGNAL MODULATIONS**

by

Taylan O. Gulum

September 2007

Thesis Co-Advisors:

Phillip E. Pace  
Roberto Cristi

**Approved for public release; distribution is unlimited**

THIS PAGE INTENTIONALLY LEFT BLANK

<b>REPORT DOCUMENTATION PAGE</b>			<i>Form Approved OMB No. 0704-0188</i>	
Public reporting burden for this collection of information is estimated to average 1 hour per response, including the time for reviewing instruction, searching existing data sources, gathering and maintaining the data needed, and completing and reviewing the collection of information. Send comments regarding this burden estimate or any other aspect of this collection of information, including suggestions for reducing this burden, to Washington headquarters Services, Directorate for Information Operations and Reports, 1215 Jefferson Davis Highway, Suite 1204, Arlington, VA 22202-4302, and to the Office of Management and Budget, Paperwork Reduction Project (0704-0188) Washington DC 20503.				
<b>1. AGENCY USE ONLY (Leave blank)</b>		<b>2. REPORT DATE</b> September 2007	<b>3. REPORT TYPE AND DATES COVERED</b> Master's Thesis	
<b>4. TITLE AND SUBTITLE</b> Autonomous Non-Linear Classification of LPI Radar Signal Modulations			<b>5. FUNDING NUMBERS</b>	
<b>6. AUTHOR(S)</b> Taylan O. Gulum				
<b>7. PERFORMING ORGANIZATION NAME(S) AND ADDRESS(ES)</b> Center for Joint Services Electronic Warfare Naval Postgraduate School Monterey, CA 93943-5000			<b>8. PERFORMING ORGANIZATION REPORT NUMBER</b>	
<b>9. SPONSORING /MONITORING AGENCY NAME(S) AND ADDRESS(ES)</b> Office of Naval Research, Code 312 Arlington, VA, 22209			<b>10. SPONSORING/MONITORING AGENCY REPORT NUMBER</b>	
<b>11. SUPPLEMENTARY NOTES</b> The views expressed in this thesis are those of the author and do not reflect the official policy or position of the Department of Defense or the U.S. Government.				
<b>12a. DISTRIBUTION / AVAILABILITY STATEMENT</b> Approved for public release; distribution is unlimited.			<b>12b. DISTRIBUTION CODE</b> A	
<b>13. ABSTRACT (maximum 200 words)</b> In this thesis, an autonomous feature extraction algorithm for classification of Low Probability of Intercept (LPI) radar modulations is investigated. A software engineering architecture that allows a full investigation of various preprocessing algorithms and classification techniques is applied to a database of important LPI radar waveform modulations including Frequency Modulation Continuous Waveform (FMCW), Phase Shift Keying (PSK), Frequency Shift Keying (FSK) and combined PSK and FSK. The architecture uses time-frequency detection techniques to identify the parameters of the modulation. These include the Wigner-Ville distribution, the Choi-Williams distribution and quadrature mirror filtering. Autonomous time-frequency image cropping algorithm is followed by a feature extraction algorithm based on principal components analysis. Classification networks include the multilayer perceptron, the radial basis function and the probabilistic neural networks. Lastly, using image processing techniques on images obtained by the Wigner-Ville distribution and the Choi-Williams distribution, two autonomous extraction algorithms are investigated to derive the significant modulation parameters of polyphase coded LPI radar waveform modulations.				
<b>14. SUBJECT TERMS</b> Autonomous Classification, Low Probability of Intercept, LPI, Principal Components Analysis, PCA, Time-Frequency, Multi Layer Perceptron, Radial Basis Function, Parameter Extraction, Radon Transform, 2-D FFT			<b>15. NUMBER OF PAGES</b> 217	
			<b>16. PRICE CODE</b>	
<b>17. SECURITY CLASSIFICATION OF REPORT</b> Unclassified	<b>18. SECURITY CLASSIFICATION OF THIS PAGE</b> Unclassified	<b>19. SECURITY CLASSIFICATION OF ABSTRACT</b> Unclassified	<b>20. LIMITATION OF ABSTRACT</b> UU	

NSN 7540-01-280-5500

Standard Form 298 (Rev. 2-89)  
Prescribed by ANSI Std. Z39-18

THIS PAGE INTENTIONALLY LEFT BLANK

**Approved for public release, distribution is unlimited**

**AUTONOMOUS NON-LINEAR CLASSIFICATION OF  
LPI RADAR SIGNAL MODULATIONS**

Taylan O. Gulum  
Lieutenant Junior Grade, Turkish Navy  
B.S., Turkish Naval Academy, 2001

Submitted in partial fulfillment of the  
requirements for the degree of

**MASTER OF SCIENCE IN ELECTRONIC WARFARE  
SYSTEMS ENGINEERING  
and  
MASTER OF SCIENCE IN ELECTRICAL ENGINEERING**

from the

**NAVAL POSTGRADUATE SCHOOL  
September 2007**

Author: Taylan O. Gulum

Approved by: Phillip E. Pace  
Thesis Co-Advisor

Roberto Cristi  
Thesis Co-Advisor

Dan C. Boger  
Chairman, Department of Information Sciences

Jeffrey B. Knorr  
Chairman, Department of Electrical and Computer Engineering

THIS PAGE INTENTIONALLY LEFT BLANK

## **ABSTRACT**

In this thesis, an autonomous feature extraction algorithm for classification of Low Probability of Intercept (LPI) radar modulations is investigated. A software engineering architecture that allows a full investigation of various preprocessing algorithms and classification techniques is applied to a database of important LPI radar waveform modulations including Frequency Modulation Continuous Waveform (FMCW), Phase Shift Keying (PSK), Frequency Shift Keying (FSK) and combined PSK and FSK. The architecture uses time-frequency detection techniques to identify the parameters of the modulation. These include the Wigner-Ville distribution, the Choi-Williams distribution and quadrature mirror filtering. Autonomous time-frequency image cropping algorithm is followed by a feature extraction algorithm based on principal components analysis. Classification networks include the multilayer perceptron, the radial basis function and the probabilistic neural networks. Lastly, using image processing techniques on images obtained by the Wigner-Ville distribution and the Choi-Williams distribution, two autonomous extraction algorithms are investigated to derive the significant modulation parameters of polyphase coded LPI radar waveform modulations.

THIS PAGE INTENTIONALLY LEFT BLANK



## TABLE OF CONTENTS

<b>I.</b>	<b>INTRODUCTION .....</b>	<b>1</b>
<b>A.</b>	<b>LOW PROBABILITY OF INTERCEPT RADAR.....</b>	<b>1</b>
<b>B.</b>	<b>AUTONOMOUS CLASSIFICATION OF LPI RADAR CW MODULATIONS .....</b>	<b>3</b>
<b>C.</b>	<b>PRINCIPAL CONTRIBUTION.....</b>	<b>6</b>
<b>D.</b>	<b>THESIS OUTLINE .....</b>	<b>8</b>
<b>II.</b>	<b>REVIEW OF LPI RADAR SIGNAL MODULATIONS .....</b>	<b>9</b>
<b>A.</b>	<b>FREQUENCY MODULATION CONTINUOUS WAVE (FMCW).....</b>	<b>9</b>
<b>B.</b>	<b>PHASE SHIFT KEYING TECHNIQUES .....</b>	<b>11</b>
<b>1.</b>	<b>Polyphase Codes .....</b>	<b>12</b>
<b>a.</b>	<i>Frank Code .....</i>	<i>13</i>
<b>b.</b>	<i>P1 Phase Code.....</i>	<i>14</i>
<b>c.</b>	<i>P2 Phase Code.....</i>	<i>15</i>
<b>d.</b>	<i>P3 Phase Code.....</i>	<i>16</i>
<b>e.</b>	<i>P4 Phase Code.....</i>	<i>17</i>
<b>2.</b>	<b>Polytime Codes.....</b>	<b>18</b>
<b>a.</b>	<i>Polytime Code T1(n).....</i>	<i>19</i>
<b>b.</b>	<i>Polytime Code T2(n).....</i>	<i>20</i>
<b>c.</b>	<i>Polytime Code T3(n).....</i>	<i>21</i>
<b>d.</b>	<i>Polytime Code T4(n).....</i>	<i>21</i>
<b>C.</b>	<b>FREQUENCY SHIFT KEYING TECHNIQUES.....</b>	<b>22</b>
<b>1.</b>	<b>Costas Codes .....</b>	<b>23</b>
<b>2.</b>	<b>Hybrid FSK/PSK Technique.....</b>	<b>23</b>
<b>D.</b>	<b>SUMMARY .....</b>	<b>24</b>
<b>III.</b>	<b>DATABASE DESCRIPTION.....</b>	<b>25</b>
<b>A.</b>	<b>SUMMARY .....</b>	<b>30</b>
<b>IV.</b>	<b>DETECTION AND CLASSIFICATION ARCHITECTURE .....</b>	<b>31</b>
<b>A.</b>	<b>DETECTION TECHNIQUES .....</b>	<b>32</b>
<b>1.</b>	<b>Wigner-Ville Distribution.....</b>	<b>32</b>
<b>2.</b>	<b>Choi-Williams Distribution .....</b>	<b>35</b>
<b>3.</b>	<b>Quadrature Mirror Filter Bank Tree .....</b>	<b>36</b>
<b>B.</b>	<b>AUTONOMOUS PREPROCESSING.....</b>	<b>39</b>
<b>1.</b>	<b>T-F Autonomous Cropping and Feature Extraction Algorithm...40</b>	
<b>a.</b>	<i>The 2-D Discrete Fourier Transform and Frequency Domain Filtering.....</i>	<i>43</i>
<b>b.</b>	<i>Determination of the Frequency Band of Interest.....</i>	<i>48</i>
<b>c.</b>	<i>Cropping and Feature Vector Generation.....</i>	<i>54</i>
<b>2.</b>	<b>Principal Components Analysis .....</b>	<b>55</b>
<b>C.</b>	<b>CLASSIFICATION NETWORKS.....</b>	<b>60</b>
<b>1.</b>	<b>MLP Classifiers .....</b>	<b>60</b>

2.	RBF Classifier .....	63
D.	CLASSIFICATION RESULTS .....	66
1.	Optimization of Feature Extraction and Network Parameters ....	67
a.	<i>Optimization for MLPNN</i> .....	67
b.	<i>Optimization for RBFNN</i> .....	72
c.	<i>Optimization for PNN</i> .....	75
2.	Classification Results with MLPNN.....	78
3.	Classification Results with RBFNN.....	82
4.	Classification Results with PNN.....	85
5.	Classification Results using PWVD .....	88
6.	Classification Results Using CWD .....	91
7.	Classification Results using QMFB.....	94
E.	SUMMARY .....	97
V.	PARAMETER EXTRACTION ALGORITHMS .....	99
A.	PARAMETER EXTRACTION OF POLYPHASE CODED LPI RADAR MODULATIONS USING PWVD IMAGES .....	99
B.	PARAMETER EXTRACTION OF POLYPHASE CODED LPI RADAR MODULATIONS USING CWD IMAGES .....	108
C.	PARAMETER EXTRACTION TEST RESULTS.....	117
D.	SUMMARY .....	121
VI.	CONCLUSIONS AND RECOMMENDATIONS .....	123
APPENDIX A.	.....	127
A.	INITIALIZATION OF MLPNN .....	127
B.	INITIALIZATION OF RBFNN .....	131
C.	INITIALIZATION OF PNN.....	137
APPENDIX B.	.....	143
A.	MLPNN CLASSIFICATION CONFUSION MATRICES.....	143
B.	RBFNN CLASSIFICATION CONFUSION MATRICES.....	152
C.	PNN CLASSIFICATION CONFUSION MATRICES .....	161
APPENDIX C.	.....	171
A.	PARAMETER EXTRACTION RESULTS FOR POLYPHASE CODED LPI MODULATIONS USING PWVD IMAGES .....	171
B.	PARAMETER EXTRACTION RESULTS FOR POLYPHASE CODED LPI MODULATIONS USING CWD IMAGES.....	175
C.	COMPARATIVE PARAMETER EXTRACTION RESULTS.....	179
1.	Results for P1 Code.....	179
2.	Results for P2 Code.....	181
3.	Results for P3 Code.....	184
4.	Results for P4 Code.....	186
LIST OF REFERENCES	.....	189
INITIAL DISTRIBUTION LIST	.....	195

## LIST OF FIGURES

Figure 1.	Comparison of pulsed radar and CW radar (From [2]).	2
Figure 2.	Linear Frequency Modulated Waveform and the Doppler Shifted Return Signal (From [2]).	11
Figure 3.	Frank Code Phase Values for $M = 6, N_c = 36, cpp = 1$	14
Figure 4.	P1 Code Phase Values for $M = 6, N_c = 36, cpp = 1$	15
Figure 5.	P2 Code Phase Values for $M = 6, N_c = 36, cpp = 1$	16
Figure 6.	P3 Code Phase Values for $N_c = 36, cpp = 1$	17
Figure 7.	P4 Code Phase Values for $N_c = 36, cpp = 1$	18
Figure 8.	Stepped frequency waveform generating a T1(4) Code.	19
Figure 9.	Stepped frequency waveform generating a T2(4) Code.	20
Figure 10.	Stepped frequency waveform generating a T3(4) Code.	21
Figure 11.	Stepped frequency waveform generating a T4(4) Code.	22
Figure 12.	General FSK/PSK signal containing $N_F$ frequency subcodes each with duration $t_p$ s. Each frequency subcode is subdivided into $N_B$ phase slots each with duration $t_b$ (From [2]).	24
Figure 13.	Signal Folder Structure used for Detection and Classification.	25
Figure 14.	Detection, Classification and Parameter Extraction Architecture.	32
Figure 15.	Pseudo Wigner-Ville Distribution of a Frank Coded Signal with $N_c = 36$ .	34
Figure 16.	Choi-Williams Distribution of a Frank Coded Signal with $N_c = 36$ .	36
Figure 17.	Quadrature Mirror Filter Bank Tree (From [39]).	37
Figure 18.	QMFB Result for Layer $l = 5$ for a Frank Coded Signal with $N_c = 36$ .	38
Figure 19.	The Frequency Bands of Interests (a) PWVD (b) CWD (c) QMFB.	39
Figure 20.	T-F autonomous cropping and feature extraction algorithm (From [27]).	41
Figure 21.	Detect and Delete “No-signal region” Block.	41
Figure 22.	(a) T-F Image with No-Signal Region (b) Image after No-Signal Region Cropped.	42
Figure 23.	Frequency Rectangle Defined by Digital Frequencies.	43
Figure 24.	(a) 2-D FFT of image shown in Figure 22 (b) and (b) The zero frequency component is shifted to the center of spectrum.	44
Figure 25.	Frequency Domain Filtering Operations.	45
Figure 26.	Implementation of Filter Function (a) Desired Frequency Response, (b) Gaussian Window, (c) Gaussian Lowpass Filter, (d) Gaussian Lowpass Filter as an Image.	47
Figure 27.	(a) Frequency Domain Filtering, (b) Shift Back the Frequency Components, (c) 2-D Inverse FFT output.	48
Figure 28.	Determining the Frequency Band of Interest.	49
Figure 29.	Marginal Frequency Distribution (MFD) of a Frank Signal with $N_c = 36$ (From [27]).	49

Figure 30.	MFD Smoothing via Adaptive Filter & Moving-Average Filter. ....	50
Figure 31.	MFD of a Frank Coded Signal with $N_c = 36$ after Adaptive Filtering. ....	51
Figure 32.	Output of Moving Average Filter with a Window Length of 10. ....	52
Figure 33.	Threshold Determination by a Histogram. ....	53
Figure 34.	Frequency Band of Interest [27]. ....	54
Figure 35.	Autonomous Cropping and Feature Vector Generation Blockset. ....	54
Figure 36.	(a) LPF output (b) Cropped region (c) Contour Plot of the Cropped Region. ....	55
Figure 37.	Training Matrix Generation (From [27]). ....	57
Figure 38.	PCA Algorithm (From [27]). ....	59
Figure 39.	Block Diagram of Three-Layer Perceptron Neural Network (After [27]). ....	61
Figure 40.	Block Diagram of Radial Basis Function Neural Network with One Output (After [52]). ....	63
Figure 41.	Block Diagram of Probabilistic Neural Network (After [54]). ....	65
Figure 42.	Optimization of $\omega_1$ , $\omega_2$ and Bin Number for PWVD image classification with MLPNN. ....	68
Figure 43.	Optimization of $S_1$ , $S_2$ , $Th_\lambda$ and $\vee_i$ for PWVD image classification with MLPNN. ....	70
Figure 44.	Classification Results with MLPNN (Costas, Frank, FSK/PSK, FMCW, P1, P2 codes). ....	80
Figure 45.	Classification Results with MLPNN (P3, P4, T1, T2, T3, T4 codes). ....	81
Figure 46.	Classification Results with RBFNN (Costas, Frank, FSK/PSK, FMCW, P1, P2 codes). ....	83
Figure 47.	Classification Results with RBFNN (P3, P4, T1, T2, T3, T4 codes). ....	84
Figure 48.	Classification Results with PNN (Costas, Frank, FSK/PSK, FMCW, P1, P2 codes). ....	86
Figure 49.	Classification Results with PNN (P3, P4, T1, T2, T3, T4 codes). ....	87
Figure 50.	Classification Results using PWVD (Costas, Frank, FSK/PSK, FMCW, P1, P2 codes). ....	89
Figure 51.	Classification Results using PWVD (P3, P4, T1, T2, T3, T4 codes). ....	90
Figure 52.	Classification Results using CWD (Costas, Frank, FSK/PSK, FMCW, P1, P2 codes). ....	92
Figure 53.	Classification Results using CWD (P3, P4, T1, T2, T3, T4 codes). ....	93
Figure 54.	Classification Results using QMFB (Costas, Frank, FSK/PSK, FMCW, P1, P2 codes). ....	95
Figure 55.	Classification Results using QMFB (P3, P4, T1, T2, T3, T4 codes). ....	96
Figure 56.	Parameter Extraction Block Diagram for Polyphase Coded LPI Radar Waveforms using PWVD Images (From [28]). ....	100
Figure 57.	Carrier Frequency Determination by Finding the Maximum Intensity Level for PWVD. ....	101
Figure 58.	Geometry of the Radon Transform (From [56]). ....	102
Figure 59.	Parallel Beam Projection at Rotation Angle $\theta$ (From [56]). ....	103
Figure 60.	Radon Transform Geometry on PWVD image (From [28]). ....	104
Figure 61.	Normalized Radon Transform of a PWVD Image. ....	105

Figure 62.	Radon Transform and Projection Vector Cropping on an Angle $\theta_s$ (From [28]).	106
Figure 63.	(a) Filtered Projection Vector (b) Thresholded Projection Vector after Filtering (From [28]).	107
Figure 64.	Parameter Extraction Block Diagram for polyphase coded LPI radar modulations using CWD images.	109
Figure 65.	Carrier Frequency Determination by Finding the Maximum Intensity Level for CWD.	110
Figure 66.	(a) Gray Scale Plot of Enhanced Image after LPF (b) Contour Plot of Enhanced Image after LPF.	112
Figure 67.	(a) Time Slice Cropping (b) Time Slice Vector.	113
Figure 68.	Smoothed Time Slice Vector.	114
Figure 69.	Thresholded Time Slice Vector.	115
Figure 70.	Bandwidth Extraction after Smoothing and Thresholding the MFD.	116
Figure 71.	Carrier Frequency Error for Frank Code.	118
Figure 72.	Number of Subcode Error for Frank Code.	118
Figure 73.	Cycles per Subcode Error for Frank Code.	119
Figure 74.	Code Period Error for Frank Code.	119
Figure 75.	Bandwidth Error for Frank Code.	120
Figure 76.	Optimization of $\omega_1, \omega_2$ and Bin Number for CWD image classification with MLPNN.	127
Figure 77.	Optimization of $S_1, S_2, Th_\lambda$ and $\vee_i$ for CWD image classification with MLPNN.	128
Figure 78.	Optimization of $\omega_1, \omega_2$ and Bin Number for QMFB image classification with MLPNN (Test Modulation Results).	129
Figure 79.	Optimization of $S_1, S_2, Th_\lambda$ and $\vee_i$ for QMFB image classification with MLPNN.	130
Figure 80.	Optimization of $\omega_1, \omega_2$ and Bin Number for PWVD image classification with RBFNN.	131
Figure 81.	Optimization of $\sigma, Th_\lambda$ and $\vee_i$ for PWVD image classification with RBFNN.	132
Figure 82.	Optimization of $\omega_1, \omega_2$ and Bin Number for CWD image classification with RBFNN (Test Modulation Results).	133
Figure 83.	Optimization of $\sigma, Th_\lambda$ and $\vee_i$ for CWD image classification with RBFNN.	134
Figure 84.	Optimization of $\omega_1, \omega_2$ and Bin Number for QMFB image classification with RBFNN (Test Modulation Results).	135
Figure 85.	Optimization of $\sigma, Th_\lambda$ and $\vee_i$ for QMFB image classification with RBFNN.	136
Figure 86.	Optimization of $\omega_1, \omega_2$ and Bin Number for PWVD image classification with PNN (Test Modulation Results).	137
Figure 87.	Optimization of $\sigma, Th_\lambda$ and $\vee_i$ for PWVD image classification with PNN.	138

Figure 88.	Optimization of $\omega_1, \omega_2$ and Bin Number for CWD image classification with PNN (Test Modulation Results).....	139
Figure 89.	Optimization of $\sigma, Th_\lambda$ and $\vee_i$ for CWD image classification with PNN....	140
Figure 90.	Optimization of $\omega_1, \omega_2$ and Bin Number for QMFB image classification with PNN (Test Modulation Results).....	141
Figure 91.	Optimization of $\sigma, Th_\lambda$ and $\vee_i$ for QMFB image classification with PNN..	142
Figure 92.	Carrier Frequency Error for P1 Code.....	179
Figure 93.	Number of Subcode Error for P1 Code.....	179
Figure 94.	Cycles per Subcode Error for P1 Code.....	180
Figure 95.	Code Period Error for P1 Code.....	180
Figure 96.	Bandwidth Error for P1 Code.....	181
Figure 97.	Carrier Frequency Error for P2 Code.....	181
Figure 98.	Number of Subcode Error for P2 Code.....	182
Figure 99.	Cycles per Subcode Error for P2 Code.....	182
Figure 100.	Code Period Error for P2 Code.....	183
Figure 101.	Bandwidth Error for P2 Code.....	183
Figure 102.	Carrier Frequency Error for P3 Code.....	184
Figure 103.	Number of Subcode Error for P3 Code.....	184
Figure 104.	Cycles per Subcode Error for P3 Code.....	185
Figure 105.	Code Period Error for P3 Signal.....	185
Figure 106.	Bandwidth Error for P3 Code.....	186
Figure 107.	Carrier Frequency Error for P4 Code.....	186
Figure 108.	Number of Subcode Error for P4 Code.....	187
Figure 109.	Cycles per Subcode Error for P4 Code.....	187
Figure 110.	Code Period Error for P4 Code.....	188
Figure 111.	Bandwidth Error for P4 Code.....	188

## LIST OF TABLES

Table 1.	Signal Parameters for Training and Testing SNR (Test SNR). .....	27
Table 2.	Signal Parameters for Testing Modulations (Test Modulation). .....	29
Table 3.	Combinations of Neuron Numbers in the Hidden Layers. ....	69
Table 4.	Optimum Values for PWVD image classification with MLPNN. ....	69
Table 5.	Optimum Values for CWD image classification with MLPNN. ....	71
Table 6.	Optimum Values for QMFB image classification with MLPNN. ....	72
Table 7.	Optimum Values for PWVD image classification with RBFNN. ....	73
Table 8.	Optimum Values for CWD image classification with RBFNN. ....	74
Table 9.	Optimum Values for QMFB image classification with RBFNN. ....	75
Table 10.	Optimum Values for PWVD image classification with PNN. ....	76
Table 11.	Optimum Values for CWD image classification with PNN. ....	77
Table 12.	Optimum Values for QMFB image classification with PNN. ....	77
Table 13.	PWVD Classification Results with MLPNN ( $SNR = 10\text{ dB}$ ). ....	143
Table 14.	PWVD Classification Results with MLPNN ( $SNR = 6\text{ dB}$ ). ....	143
Table 15.	PWVD Classification Results with MLPNN ( $SNR = 3\text{ dB}$ ). ....	144
Table 16.	PWVD Classification Results with MLPNN ( $SNR = 0\text{ dB}$ ). ....	144
Table 17.	PWVD Classification Results with MLPNN ( $SNR = -3\text{ dB}$ ). ....	145
Table 18.	PWVD Classification Results with MLPNN ( $SNR = -6\text{ dB}$ ). ....	145
Table 19.	CWD Classification Results with MLPNN ( $SNR = 10\text{ dB}$ ). ....	146
Table 20.	CWD Classification Results with MLPNN ( $SNR = 6\text{ dB}$ ). ....	146
Table 21.	CWD Classification Results with MLPNN ( $SNR = 3\text{ dB}$ ). ....	147
Table 22.	CWD Classification Results with MLPNN ( $SNR = 0\text{ dB}$ ). ....	147
Table 23.	CWD Classification Results with MLPNN ( $SNR = -3\text{ dB}$ ). ....	148
Table 24.	CWD Classification Results with MLPNN ( $SNR = -6\text{ dB}$ ). ....	148
Table 25.	QMFB Classification Results with MLPNN ( $SNR = 10\text{ dB}$ ). ....	149
Table 26.	QMFB Classification Results with MLPNN ( $SNR = 6\text{ dB}$ ). ....	149
Table 27.	QMFB Classification Results with MLPNN ( $SNR = 3\text{ dB}$ ). ....	150
Table 28.	QMFB Classification Results with MLPNN ( $SNR = 0\text{ dB}$ ). ....	150
Table 29.	QMFB Classification Results with MLPNN ( $SNR = -3\text{ dB}$ ). ....	151
Table 30.	QMFB Classification Results with MLPNN ( $SNR = -6\text{ dB}$ ). ....	151
Table 31.	PWVD Classification Results with RBFNN ( $SNR = 10\text{ dB}$ ). ....	152
Table 32.	PWVD Classification Results with RBFNN ( $SNR = 6\text{ dB}$ ). ....	152
Table 33.	PWVD Classification Results with RBFNN ( $SNR = 3\text{ dB}$ ). ....	153
Table 34.	PWVD Classification Results with RBFNN ( $SNR = 0\text{ dB}$ ). ....	153
Table 35.	PWVD Classification Results with RBFNN ( $SNR = -3\text{ dB}$ ). ....	154
Table 36.	PWVD Classification Results with RBFNN ( $SNR = -6\text{ dB}$ ). ....	154
Table 37.	CWD Classification Results with RBFNN ( $SNR = 10\text{ dB}$ ). ....	155
Table 38.	CWD Classification Results with RBFNN ( $SNR = 6\text{ dB}$ ). ....	155

Table 39.	CWD Classification Results with RBFNN ( $SNR = 3\text{ dB}$ ).....	156
Table 40.	CWD Classification Results with RBFNN ( $SNR = 0\text{ dB}$ ). ....	156
Table 41.	CWD Classification Results with RBFNN ( $SNR = -3\text{ dB}$ ). ....	157
Table 42.	CWD Classification Results with RBFNN ( $SNR = -6\text{ dB}$ ). ....	157
Table 43.	QMFB Classification Results with RBFNN ( $SNR = 10\text{ dB}$ ).....	158
Table 44.	QMFB Classification Results with RBFNN ( $SNR = 6\text{ dB}$ ). ....	158
Table 45.	QMFB Classification Results with RBFNN ( $SNR = 3\text{ dB}$ ).....	159
Table 46.	QMFB Classification Results with RBFNN ( $SNR = 0\text{ dB}$ ). ....	159
Table 47.	QMFB Classification Results with RBFNN ( $SNR = -3\text{ dB}$ ). ....	160
Table 48.	QMFB Classification Results with RBFNN ( $SNR = -6\text{ dB}$ ). ....	160
Table 49.	PWVD Classification Results with PNN ( $SNR = 10\text{ dB}$ ). ....	161
Table 50.	PWVD Classification Results with PNN ( $SNR = 6\text{ dB}$ ). ....	161
Table 51.	PWVD Classification Results with PNN ( $SNR = 3\text{ dB}$ ). ....	162
Table 52.	PWVD Classification Results with PNN ( $SNR = 0\text{ dB}$ ). ....	162
Table 53.	PWVD Classification Results with PNN ( $SNR = -3\text{ dB}$ ). ....	163
Table 54.	PWVD Classification Results with PNN ( $SNR = -6\text{ dB}$ ). ....	163
Table 55.	CWD Classification Results with PNN ( $SNR = 10\text{ dB}$ ).....	164
Table 56.	CWD Classification Results with PNN ( $SNR = 6\text{ dB}$ ). ....	164
Table 57.	CWD Classification Results with PNN ( $SNR = 3\text{ dB}$ ).....	165
Table 58.	CWD Classification Results with PNN ( $SNR = 0\text{ dB}$ ). ....	165
Table 59.	CWD Classification Results with PNN ( $SNR = -3\text{ dB}$ ). ....	166
Table 60.	CWD Classification Results with PNN ( $SNR = -6\text{ dB}$ ). ....	166
Table 61.	QMFB Classification Results with PNN ( $SNR = 10\text{ dB}$ ).....	167
Table 62.	QMFB Classification Results with PNN ( $SNR = 6\text{ dB}$ ). ....	167
Table 63.	QMFB Classification Results with PNN ( $SNR = 3\text{ dB}$ ).....	168
Table 64.	QMFB Classification Results with PNN ( $SNR = 0\text{ dB}$ ). ....	168
Table 65.	QMFB Classification Results with PNN ( $SNR = -3\text{ dB}$ ).....	169
Table 66.	QMFB Classification Results with PNN ( $SNR = -6\text{ dB}$ ).....	169
Table 67.	Original Parameters vs. Extracted Parameters ( $SNR = 6\text{ dB}$ ). ....	171
Table 68.	Original Parameters vs. Extracted Parameters ( $SNR = 0\text{ dB}$ ). ....	172
Table 69.	Original Parameters vs. Extracted Parameters ( $SNR = -3\text{ dB}$ ). ....	173
Table 70.	Original Parameters vs. Extracted Parameters ( $SNR = -6\text{ dB}$ ). ....	174
Table 71.	Original Parameters vs. Extracted Parameters ( $SNR = 6\text{ dB}$ ). ....	175
Table 72.	Original Parameters vs. Extracted Parameters ( $SNR = 0\text{ dB}$ ). ....	176
Table 73.	Original Parameters vs. Extracted Parameters ( $SNR = -3\text{ dB}$ ). ....	177
Table 74.	Original Parameters vs. Extracted Parameters ( $SNR = -6\text{ dB}$ ). ....	178



## **ACKNOWLEDGMENTS**

I would like to express my sincere gratitude to my thesis advisors Professor Phillip E. Pace and Professor Roberto Cristi for their continuing support and guidance throughout this thesis work. I am also thankful to them as instructors who contributed my current knowledge the most.

I would like to thank my precious, my wife Dilek Acar Gulum, for her love, endless support, help and encouragement throughout my studies at NPS.

I am grateful to my parents; my father Husamettin Gulum and my mother Cemile Gulum. Their dedication, love and support have always encouraged me for the best. I am also grateful to my sister Kezban Yilmazer and brother Arif Gulum for always being there for me.

I would like to thank the Turkish Navy for giving me the opportunity to study at the Naval Postgraduate School.

This work was supported by the office at Naval Research Code 312, Arlington, VA. Much thanks to Dr. Peter Craig for his support.

THIS PAGE INTENTIONALLY LEFT BLANK

## EXECUTIVE SUMMARY

With the development of advanced electronic support (ES) receivers, radar warning receivers and electronic attack systems such as anti radiation missiles, the threat against high power pulsed radar systems has increased. The interception of radar transmissions may lead to significant vulnerability. To be able to survive and operate effectively, the radar systems need to deny signal interception and be invisible. Invisibility is the property of a radar which allows for it to see but not be seen. These radar systems are said to have low probability of intercept and are called LPI radar systems.

Modern intercept receivers must perform their tasks across a broad band and provide non-coherent integration capabilities. The intercept receiver can increase its processing gain by implementing time-frequency (T-F) detection techniques. T-F output images can provide detection and classification of frequency- and phase-modulated LPI modulations. The need for human interpretation of the T-F results however limits these techniques to non-real time electronic intelligence receivers.

Autonomous detection and classification of LPI modulations can eliminate the need for a human operator and enable near real-time coherent handling of the threat emitters being intercepted. Parameter extraction followed by correlation with existing emitters in a database (identification) can then aid in signal tracking and response management.

This thesis examines a pattern recognition technique for autonomous classification and parameter extraction of various LPI signal modulations. After a brief description of LPI radar properties, twelve LPI modulation techniques used in this thesis are described. The techniques include Frequency Modulation Continuous Wave (FMCW), Phase Shift Keying PSK (polyphase (Frank, P1, P2, P3, P4) and polytime (T1, T2, T3, T4) codes) and Frequency Shift Keying FSK (Costas, FSK/PSK codes).

A diverse database is developed that consists of twelve LPI modulation techniques each having 21 SNR levels (-10dB, -9dB... 9dB, 10dB). Two groups of

parameters are used for testing purposes. The first group of parameters (Data Group-1) is used for the testing of the effects of noise variations on the detection and classification algorithm and this test is referred to as Test SNR. There are 21 folders in Data Group-1, each one has a different SNR level. The training signals consist of 50 signals with SNR of 10 dB from the Data Group-1 with the same parameters. The second group (Data Group-2) of parameters is different from the parameters of training signals. Data Group-2 is used to test the detection and classification algorithms with different modulations and SNR levels where this test is referred to as Test Modulation. This is a potentially hard problem since the carrier cycles per subcode and modulation periods are different. There are also 21 folders in this group each with a different SNR level. Both training and testing signals consist of two carrier frequencies.

The detection techniques examined include the use of the T-F techniques. These include Wigner-Ville distribution (WVD), the Choi-Williams distribution (CWD) and a Quadrature Mirror Filter Bank (QMFB). The detection techniques provide an image output. The WVD is computed by correlating the signal with a time and frequency translated version of itself. The CWD simultaneously gives the representation of a signal in both time and frequency. This distribution is a bilinear time-frequency analysis techniques for signal processing. A QMFB tree consists of a number of layers of fully connected pairs of orthogonal wavelet filters (or basis functions) that linearly decompose the received waveform into tiles on the time-frequency plane.

Following the generation of T-F images a feature vector is generated by autonomously isolating and cropping the modulation energy from T-F images. First 2-D FFT of the images is taken and frequency domain low pass filter is applied to the transformed images. After the filtering, autonomous modulation energy cropping is performed using an adaptive threshold based on the marginal frequency distribution of the filtered images. Then the feature vectors are generated by resizing the new images and stacking the columns of the images onto each other.

The feature vectors are transformed into a lower dimensional feature space using the PCA prior to the classification networks. This is accomplished by first, generating the training matrix by stacking the feature vectors next to each other. Second, PCA is applied

to the training matrix where a projection matrix is obtained. Using this projection matrix the testing signals are also transformed into the lower dimensional feature space preserving their discriminating features. The dimension reduction of feature vectors prevents the classifiers to be overwhelmed by the complexity of high dimensional feature vectors.

Once the lower dimensional feature vectors are found, they are sent to the non-linear classifiers for classification. Non-linear classification techniques presented include the multi layer perceptron (MLP), radial basis function (RBF) and probabilistic neural networks (PNN). The MLP is a feed-forward interconnection of individual non-linear parallel computing units called neurons. In an MLP network the inputs propagate through the network in a forward direction, on a layer by layer basis. Global training of the MLP results in a non-linear mapping of the inputs at the output layer. Radial basis functions (RBFs) consist of three layer of nodes: the input layer where the inputs are applied, the output layer where the outputs are produced, and a hidden layer where the RBFs are applied to the input data. The argument of the activation function of each hidden unit computes the Euclidean norm (distance) between the input vector and the center of the unit. Using exponentially decaying localized nonlinearities, RBFs construct local approximations to nonlinear input-output mappings. PNN is a variant of the RBF network.

Before the classification tests are run, the best feature extraction and network parameters need to be determined. This is done by some iterative optimizations. After optimization is completed the final parameters are set and the classification tests are run.

Concerning the Test Modulation results, the best overall classification result is achieved with WVD technique. CWD results were very similar to WVD results. The QMFB technique on the other hand performed very poorly. The Test SNR results were very promising indicating that the autonomous modulation energy isolation and cropping performed well. Concerning the classifier performances, the PNN outperformed the RBFNN and MLPNN. The PNN and the RBFNN also outperformed the MLPNN concerning the training and classification speed.

The classification results of polyphase modulations (Frank, P1, P2, P3 and P4) were poor. The architecture could not perform to distinguish between polyphase modulations successfully. On the other hand the best results were obtained in the classification of the FMCW, Costas, FSK/PSK, P2 and T4 modulations. These modulations have distinctive T-F images which makes the classification process simpler.

Following the detection and classification algorithm two parameter extraction algorithms were investigated. First one was designed to extract the parameters from the PWVD images of polyphase coded LPI signals (Frank, P1, P2, P3, P4) based on the Radon transform of the PWVD images. The second algorithm was designed to extract the parameters from the CWD images of polyphase coded LPI signals (Frank, P1, P2, P3, P4) using frequency domain lowpass filter on the 2-D FFT of CWD images.

The test results obtained from both algorithms tend to coincide well with the actual values and the relative error depends on how closely results are examined. At  $SNR = -3\text{dB}$  the PWVD parameter extraction algorithm gave erroneous results, while the CWD parameter extraction algorithm still gave reasonable results. The PWVD parameter extraction algorithm performs without being affected from the cross terms present within the PWVD images.

## **I. INTRODUCTION**

### **A. LOW PROBABILITY OF INTERCEPT RADAR**

With the development of advanced electronic support (ES) receivers, radar warning receivers and electronic attack systems such as anti radiation missiles the threat against high power pulsed radar systems has increased. The interception of radar transmissions may lead to significant vulnerability. To be able to survive and operate effectively, the radar systems need to deny signal interception and be invisible. Invisibility is the property of a radar which allows it to see but not be seen. These radar systems are said to have low probability of intercept and are called LPI radar systems. Some of these properties are as follows [1, 2, 3]:

- Low sidelobe antennas with infrequent scan modulation,
- The use of broad non-scanning transmitting beam combined with a stationary set of receive beams,
- Reducing the radar power when tracking a closing target,
- Reducing peak power while maintaining the required average power,
- Making use of waveform coding to provide transmitting duty cycles approaching to one and using frequency hopping to force the interceptor to consider more of the spectrum to characterize the radar,
- Wideband continuous waveform (CW) emission,
- Atmospheric attenuation shielding at high frequencies,
- Very high receiver sensitivity,
- High processing gain,
- Coherent detection.

These techniques provide the ability for the LPI radar to detect and track targets without being detected by the intercepting receiver system. LPI radars take advantage of a large time-bandwidth product by reducing its transmitted peak power. The relation between peak power and duty cycle for pulse radar and CW radar is shown in Figure 1:

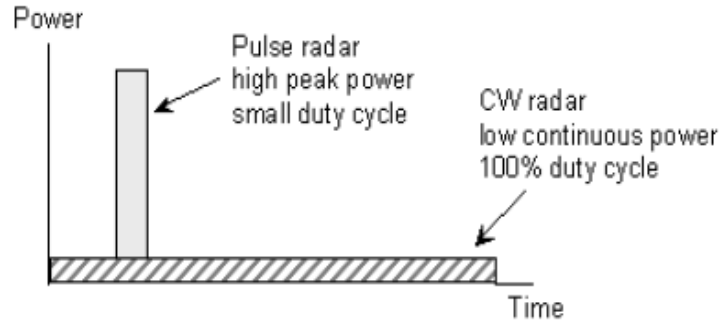


Figure 1. Comparison of pulsed radar and CW radar (From [2]).

Depending on the purpose or mission of the radar, the type of receiver that is trying to detect it and the engagement geometry, three levels of LPI can be defined as follows [4]:

- The radar is easily detectable but not easily identifiable-called a low probability of identification (LPID) radar,
- The radar can detect a target and is not detectable by an ES receiver at the same range but outside its main beam,
- The radar can detect a target and is not detectable by an ES receiver located on the target-a “quiet radar”.

The spread spectrum characteristic of an LPI radar is related to the waveform design. Pulse compression modulation techniques provide a wideband LPI CW transmit waveform which is spread over a wide frequency range in a manner that is initially unknown to a hostile receiver. The wide bandwidth makes the interception of the signal more difficult. Some of these wideband CW techniques include [2]:

- Linear and Non-Linear frequency modulation,
- Frequency hopping (frequency shift keying FSK), Costas arrays,
- Phase modulation (phase shift keying PSK),
- Combined phase modulation and frequency hopping (PSK/FSK),
- Random signal modulation.

The ratio of range at which the radar signal can be detected by an intercept receiver to the range at which it can detect a target is an example of the performance parameter for LPI radar [4]. This ratio is given as [2, 4]



$$\alpha = \frac{R_{I\max}}{R_{R\max}} \quad (1.1)$$

where  $R_{R\max}$  is the maximum range at which the LPI radar can detect a target and  $R_{I\max}$  is the maximum interception receiver detection range. If  $\alpha < 1$ , then the LPI radar can detect the targets at further ranges without being detected by the intercept receiver. If  $\alpha = 1$ , then the radar cannot be intercepted beyond the range at which it can detect targets. This also determines the maximum detection range of the LPI radar without being detected by the intercept receiver [2].

## **B. AUTONOMOUS CLASSIFICATION OF LPI RADAR CW MODULATIONS**

Reduced transmit power forces the intercept receiver into more sophisticated detection schemes. Modern intercept receivers must perform their tasks across a broad band and provide non-coherent integration capabilities [5]. This is a result of a point and counterpoint relationship that persists between the military radar and the electronic warfare (EW) receiving systems [6]. However, the intercept receiver can increase its processing gain by implementing time-frequency (T-F) detection techniques. These techniques necessitate usage of sophisticated signal processing algorithms. T-F output images can provide detection and classification of frequency- and phase-modulated LPI modulations. Following the classification, the modulation parameters can be extracted. The need for human interpretation of the T-F results however limits these techniques to non-real time electronic intelligence receivers.

Classification using T-F imaging has received considerable attention in such diverse fields as humpback whale signal recognition [7, 8], biomedical engineering [9, 10], underwater acoustic target detection [11], radar target classification [12], power grid analysis [13] and radar transmitter identification [14]. With the high degree of detail however, trainable autonomous classifiers can easily be overwhelmed by the complexity of the T-F input representation and many efforts have been presented to reduce this problem. A summary of these efforts is given next and for details the reader is referred to the references.

*Smoothing* the T-F images can be used to reduce the density of the features but will most often remove the class-distinction detail that the representation was intended to resolve. Quantizing the T-F representation in a class- or signal-dependent manner can also preserve the needed high resolution detail that highlights the differences between classes. A vector quantization technique that is a modified version of a Kohonen's self-organizing feature map is applied to the T-F representation in [15]. Class-dependent *smoothing* can also be accomplished by optimizing the T-F transformation kernel [14]. This approach eliminates the need to make *a priori* assumptions about the amount and type of smoothing needed and also allows for a direct classification without the need for preprocessing to reduce the dimensionality. Optimizing the T-F kernel parameters based on the *Fisher* criterion objective function is also examined in [7]. The Fisher criteria however, assume the classes have equal covariance. In [8], the T-F representation is used to construct a quadratic discriminant function which is evaluated at specific times to form a set of statistics that are then used in a multiple hypothesis test. The multiple hypotheses are treated simultaneously using a sequentially rejective Bonferroni test to control the probability of incorrect classification. A method based on T-F projection filtering is presented in [11]. In this approach the decision strategy about which a target is present depends on the comparison of a reference target and the filter output signal. In [12], a reduction in the feature vector dimensionality using the geometrical moments of the adaptive spectrogram is investigated. A principal components analysis is then used to further reduce the dimension of the feature space. This involves calculation of the covariance matrix and its eigenvectors. The feature vector is then formed using the eigenvectors associated to the highest eigenvalues, and then it is applied to a multi-layer perceptron for automatic recognition.

Automatic recognition of communication signal modulations has also been of interest for many years [16]. In particular, research on this topic is typically applicable to military systems. Now with the advent of software radios, research on autonomously recognizing communication signal modulations has resulted in the realization of reconfigurable and adaptive wireless transceivers. In general, there are two methods for autonomous classification of signal modulations: decision theoretic techniques and

pattern recognition techniques. A classification technique based on a hierarchical neural network in which a-priori knowledge is used to speed up the learning phase and improve the classification performance is presented in [17]. The a-priori knowledge (from a human expert) is incorporated so that similar classes can be grouped into metaclasses for subsequent preprocessing by a fast automatic neural classifier. Good classification results were obtained for signal-to-noise ratios  $\text{SNR} > 5$  dB. A wavelet transform approach using a Morlet wavelet to detect the phase changes in the signal is developed in [18]. The phase change rate is then used as a feature for the classification of the modulation schemes with good results for  $\text{SNR} > 0$  dB.

A set of decision criteria for quickly identifying different types of digital modulation is examined in [19]. The key features used in the identification algorithm are calculated using conventional signal processing methods with good success being achieved at  $\text{SNR} > 10$  dB. More recently, automatic modulation recognition was investigated using nonlinear transformations that when applied to the communication signal, generate unique spectral lines that are modulation dependent [20]. The spectral lines are then detected by periodogram analysis and a decision-tree used to classify the results in a white Gaussian noise (WGN) environment. Due to a large false alarm rate, the performance was later improved using a Hidden Markov Model [21] which showed superior performance to the decision-tree approach for  $\text{SNR} > 3$  dB. Both a decision-theoretic and a three-structure neural network approach are compared in [22]. At a  $\text{SNR} > 15$  dB, the decision-theoretic approach gave a 94% success rate while the neural network approach gave a success rate of 96%. A pattern recognition approach is investigated in [23] where feature extraction is achieved using the Margenau-Hill T-F distribution which preserves the signal's phase information. Classification is accomplished by combining the results with a decision-tree for good performance for  $\text{SNR} > 10$  dB. The use of multi-layer perceptron neural networks has been reported for recognition of ten different communication modulation types in [24]. In this work, a genetic algorithm is used to select the best feature subset from a combined statistical and spectral feature set in order to reduce the input dimension and increase the performance of the recognizer. This technique resulted in a 99% success at  $\text{SNR} = 0$  dB and 93% at  $\text{SNR} = -5$  dB.

Principal components analysis (PCA) has been used in many applications ranging from social science to space science, for the purpose of data compression and feature extraction [25]. In [25] PCA is used for automatic target recognition from synthetic aperture radar images and a comparison is presented with the conventional conditional Gaussian model based on Bayesian classifier. PCA is used in the frequency domain for neural identification of the radiated noise from ships in [26].

### **C. PRINCIPAL CONTRIBUTION**

Autonomous detection and classification of LPI modulations can eliminate the need for a human operator and enable near real-time coherent handling of the threat emitters being intercepted. Parameter extraction followed by correlation with existing emitters in a database (identification) can then aid in signal tracking and response management [27].

This thesis examines a pattern recognition technique for autonomous classification and parameter extraction of various LPI signal modulations. A diverse database is developed that consists of twelve LPI modulation techniques each having 21 SNR levels (-10dB, -9dB... 9dB, 10dB). The LPI modulation techniques include Frequency Modulation Continuous Wave (FMCW), Phase Shift Keying (PSK) and Frequency Shift Keying (FSK). PSK signals include polyphase (Frank, P1, P2, P3, P4) and polytime (T1, T2, T3, T4) codes and FSK signals include Costas and FSK/PSK codes.

The detection techniques examined include the use of the T-F techniques Wigner-Ville distribution (WVD), the Choi-Williams distribution (CWD) and a Quadrature Mirror Filter Bank (QMFB).

A feature vector is generated by autonomously cropping the modulation energy from T-F images. First a 2-D FFT of the images is taken and a frequency domain low pass filter is applied to the transformed images. Following the filtering, autonomous signal energy cropping is performed using an adaptive threshold based on the marginal

frequency distribution of the filtered images. After signal energy cropping, the feature vectors are generated by resizing the new images and stacking the columns of the images onto each other [27].

The feature vectors are transformed into a lower dimensional feature space using the PCA prior to the classification networks. This is accomplished by first, generating the training matrix by stacking the feature vectors next to each other. Second PCA is applied to the training matrix where a projection matrix is obtained. Using this projection matrix the testing signals are also transformed to the lower dimensional feature space preserving their discriminating features [27].

Once the lower dimensional feature vectors are found they are sent to the non-linear classifiers for classification. Non-linear classification techniques presented include the multi layer perceptron (MLP), radial basis function (RBF) and probabilistic neural networks (PNN).

Results indicate that the best overall classification result is achieved with WVD technique. CWD results were very similar to WVD results. QMFB technique on the other hand performed very poorly. The test results using the test signals having the same parameters with training signals were very promising indicating that the autonomous modulation energy isolation and cropping performed well. Concerning the classifier performances, the PNN outperformed the RBFNN and MLPNN. The PNN and the RBFNN also outperformed the MLPNN concerning the training and classification speed.

The classification results of polyphase modulations (Frank, P1, P2, P3 and P4) were poor. The architecture could not perform to distinguish between polyphase modulations successfully. On the other hand the best results were obtained in the classification of the FMCW, Costas, FSK/PSK, P2 and T4 modulations.

After classification autonomous extraction of the waveform parameters is accomplished using the images from the Wigner-Ville distribution and the Choi-Williams distribution for polyphase modulations. For the WVD images, radon transform is used and for the CWD images, 2-D FFT, frequency domain filtering and Marginal frequency distribution is used to extract the waveform parameters [28].

The test results obtained from both algorithms tend to coincide well with the actual values and the relative error depends on how closely results are examined. At  $SNR = -3\text{dB}$  the PWVD parameter extraction algorithm gave erroneous results, while the CWD parameter extraction algorithm still gave reasonable results.

#### **D. THESIS OUTLINE**

This thesis is organized as follows.

Chapter II presents a brief description of LPI signal modulations. Twelve LPI modulation techniques are described. The techniques include Frequency Modulation Continuous Wave (FMCW), Phase Shift Keying PSK (polyphase (Frank, P1, P2, P3, P4) and polytime (T1, T2, T3, T4) codes) and Frequency Shift Keying FSK (Costas, FSK/PSK codes).

Chapter III describes the structure of the database which is generated to test the detection, classification and parameter extraction system simulated in this work. The parameters used in the generation of LPI signal modulations are presented.

Chapter IV presents the detection and classification architecture. The T-F distributions used for detection are briefly described. These include Wigner-Ville distribution, Choi-Williams distribution and quadrature mirror filter bank. Feature extraction algorithm is presented which employs 2-D FFT, autonomous modulation energy cropping and PCA. Three different classifiers used to classify the LPI signals are also described. A multi-layer perceptron (MLP) network and two radial-basis function (RBF) networks are investigated. The classification results are presented and discussed.

Chapter V investigates two autonomous parameter extraction algorithms using the images from the Wigner-Ville distribution and the Choi-Williams distribution for polyphase modulations. The test results are presented for both algorithms.

Chapter VI concludes the thesis and recommends future work.

## II. REVIEW OF LPI RADAR SIGNAL MODULATIONS

This chapter describes the LPI signal modulation techniques used to simulate the detection, classification and parameter extraction algorithms in this thesis. In order to simulate a complex environment, a database which consists of twelve LPI signal modulation techniques was generated. The techniques include Frequency Modulation Continuous Wave (FMCW), Phase Shift Keying PSK (Frank, P1, P2, P3, P4, T1, T2, T3, T4 codes) and Frequency Shift Keying FSK (Costas, FSK/PSK codes).

### A. FREQUENCY MODULATION CONTINUOUS WAVE (FMCW)

One of the most important CW modulations utilized is the linear triangular FMCW emitter, since it can measure the target's range and range rate. Some of the properties which make FMCW waveforms still very effective are as follows [3, 29]:

- Resistance to jamming,
- It is simple to find range information using an FFT,
- Implementation of sensitivity time control (STC) to control dynamic range and prevent saturation in the receiver is easier in the frequency domain,
- The frequency modulation spreads the transmitted energy over a large modulation bandwidth,
- Interception of the emitter's signal is difficult because the power spectrum of the FMCW signal is nearly rectangular over the modulation bandwidth,
- The transmit waveform is deterministic and the transmit power is low,
- FMCW modulations are compatible with solid-state transmitters,
- FMCW is easier to implement than phase code modulation, as long as there is no strict demand on linearity specifications over the modulation bandwidth.

The waveform consists of two linear frequency modulation sections with positive and negative slopes. The frequency of the transmitted waveform for the first section is [2, 3, 30, 31]

$$f_1 = f_c - \frac{\Delta F}{2} + \frac{\Delta F}{t_m} t \quad (2.1)$$

for  $0 < t < t_m$  and zero elsewhere. Here  $f_c$  is the RF carrier frequency,  $\Delta F$  is the transmit modulation bandwidth, and  $t_m$  is the modulation period. The modulation (sweep) bandwidth  $\Delta F$  is chosen to provide the required *range resolution*

$$\Delta R = \frac{c}{2\Delta F} \text{ m} \quad (2.2)$$

The frequency of the transmitted waveform for the second section is similarly

$$f_2 = f_c + \frac{\Delta F}{2} - \frac{\Delta F}{t_m} t \quad (2.3)$$

for  $0 < t < t_m$ . The transmit signal for the first section is given by [2, 3, 29, 31]

$$s_1(t) = a_0 \sin 2\pi \left[ \left( f_c - \frac{\Delta F}{2} \right) t + \frac{\Delta F}{2t_m} t^2 \right] \quad (2.4)$$

where  $f_c$  is the RF carrier frequency,  $\Delta F$  is the transmit modulation bandwidth, and  $t_m$  is the modulation period with  $0 < t < t_m$ . The transmit baseband signal for the second section is given by

$$s_2(t) = a_0 \sin 2\pi \left[ \left( f_c + \frac{\Delta F}{2} \right) t - \frac{\Delta F}{2t_m} t^2 \right] \quad (2.5)$$

for  $t_m < t < 2t_m$ . FMCW signal characteristics are shown in Figure 2.



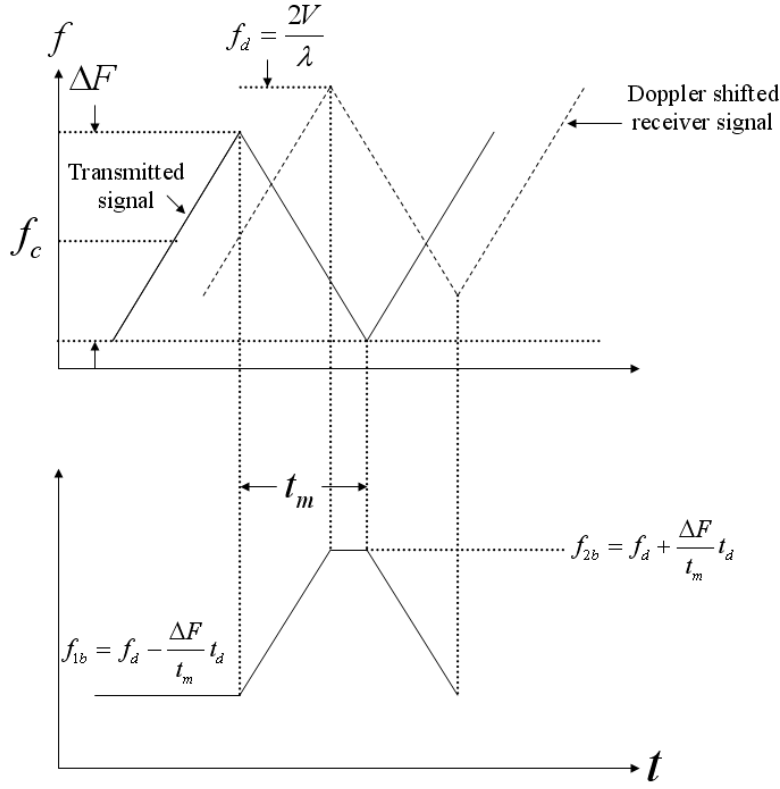


Figure 2. Linear Frequency Modulated Waveform and the Doppler Shifted Return Signal (From [2]).

Here  $f_{1b}$  and  $f_{2b}$  are the beat frequencies for the first and second segment respectively,  $t_d$  is the round-trip delay time and  $f_d$  is the Doppler frequency.

## B. PHASE SHIFT KEYING TECHNIQUES

PSK CW waveforms have recently been a topic of active investigation. They have wide bandwidth characteristics and inherently low periodic ambiguity function (PAF) side lobe levels. The PSK techniques can result in a high range resolution waveform, while also providing a large SNR processing gain for the radar. The average power of the CW transmission is responsible for extending the maximum detection range while improving the probability of target detection [2, 3].

In the PSK radar the phase shifting operation is performed in the radar's transmitter, with the timing information generated from the receiver-exciter. Within a single code period, the CW signal is phase shifted  $N_c$  (*code length*) times, with phase  $\phi_k$  every  $t_b$  (*subcode period*) seconds. The resulting code period is [2]

$$T = N_c t_b \quad \text{s} \quad (2.6)$$

and the *code rate* is

$$R_c = 1 / N_c t_b \quad \text{s}^{-1} \quad (2.7)$$

The *range resolution* of the phase coding CW radar is

$$\Delta R = \frac{c t_b}{2} \quad \text{m} \quad (2.8)$$

The *bandwidth* of the transmitted signal is

$$B = f_c / cpp = 1 / t_b \quad \text{Hz} \quad (2.9)$$

where *cpp* is the number of cycles of the carrier frequency per subcode.

## 1. Polyphase Codes

Polyphase coding refers to phase modulation of the CW carrier, with a polyphase sequence consisting of a number of discrete phases. These codes are developed by approximating a stepped frequency or linear frequency modulation waveform, where the phase steps vary as needed to approximate the underlying waveform, and the time spent at any given phase state is a constant. The sequence elements are taken from an alphabet of size  $N_c > 2$  [2].

Low range-time side lobes, ease of implementation, compatibility with digital implementation, and low cross-correlation between codes are some of the useful features provided by polyphase codes [3]. By increasing the alphabet size  $N_c$ , the autocorrelation side lobes can be decreased significantly while providing a larger processing gain [2]. The

major disadvantage of this kind of code is that as the phase increment becomes smaller, the equipment needed to generate them becomes more complex and therefore more costly. [3].

*a. Frank Code*

The Frank code is well documented and has recently been used successfully in LPI radars (such as the Omnidirectional LPI) [30]. These codes are characterized by having a perfect autocorrelation function and minimum side lobes [29, 33].

The Frank code is derived from a step approximation to a linear frequency modulation waveform using  $M$  frequency steps and  $M$  samples per frequency. The Frank code has a length or processing gain of  $N_c = M^2$ . The phase of the  $i$ th sample of the  $j$ th frequency is [2]

$$\phi_k = \phi_{i,j} = \frac{2\pi}{M}(i-1)(j-1) \quad (2.10)$$

where  $i$  ( $i=1,2,\dots,M$ ) is the number of the sample in a given frequency,  $j$  ( $j=1,2,\dots,M$ ) is the number of the frequency and  $M=1,2,3,\dots$ . Figure 3 (a) illustrates the discrete phase values and Figure 3 (b) illustrates the signal phase modulo  $2\pi$  and demonstrates that the Frank code has the largest phase increments from sample to sample in the center of the code.

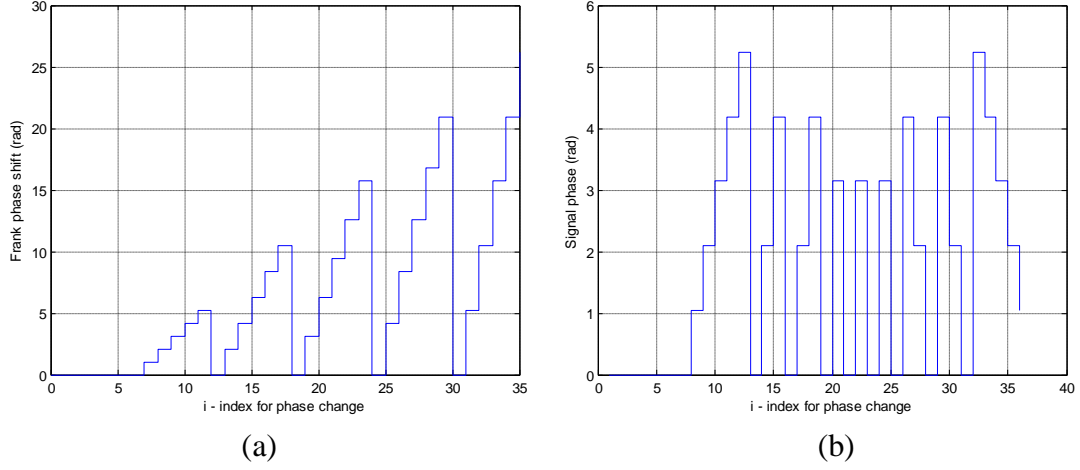


Figure 3. Frank Code Phase Values for  $M = 6$ ,  $N_c = 36$ ,  $c_{pp} = 1$ .

**b. P1 Phase Code**

This code is generated using a step approximation to a linear frequency modulation waveform.  $M$  frequency steps and  $M$  samples per frequency result in a compression ratio of  $N_c = M^2$ . The phase of the  $i$ th sample of the  $j$ th frequency is [2]

$$\phi_k = \phi_{i,j} = \frac{-\pi}{M} [M - (2j - 1)][(j - 1)M + (i - 1)] \quad (2.11)$$

where  $i$  ( $i = 1, 2, \dots, M$ ) is the number of the sample in a given frequency,  $j$  ( $j = 1, 2, \dots, M$ ) is the number of the frequency and  $M = 1, 2, 3, \dots$ . P1 codes have the largest phase changes at the ends of the code which makes it more Doppler tolerant than the Frank code [29, 34].

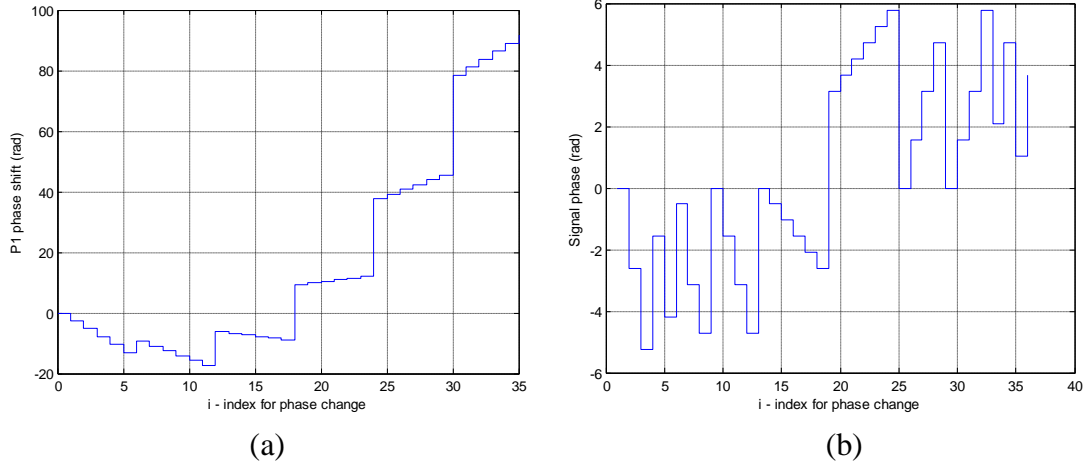


Figure 4. P1 Code Phase Values for  $M = 6$ ,  $N_c = 36$ ,  $c_{pp} = 1$ .

Figure 4 (a) illustrates the discrete phase values and Figure 4 (b) illustrates the signal phase modulo  $2\pi$  and demonstrates that the P1 code has the largest phase increments from sample to sample at the ends of the code.

### c. P2 Phase Code

The P2 code is valid for  $M$  even, and each group of the code is symmetric about 0 phase. The requirement for  $M$  to be even in this code stems from the desire for low autocorrelation side lobes. An odd value for  $M$  results in high autocorrelation side lobes. The phase increment within each phase group is the same as the P1 code, except that the starting phases are different [34]. P2 code length is also  $N_c = M^2$ . The phase of the  $i$ th sample of the  $j$ th frequency is [2]

$$\phi_k = \phi_{i,j} = \frac{-\pi}{2M} [2i-1-M][2j-1-M] \quad (2.12)$$

where  $i$  ( $i=1,2,\dots,M$ ) is the number of the sample in a given frequency,  $j$  ( $j=1,2,\dots,M$ ) is the number of the frequency,  $k=1,2,\dots,N_c$  and  $M=2,4,6,\dots$

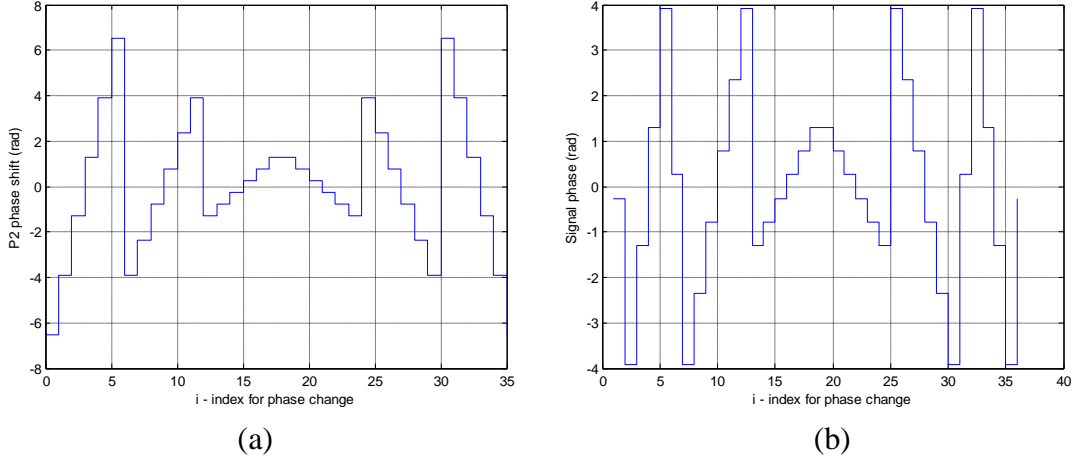


Figure 5. P2 Code Phase Values for  $M = 6$ ,  $N_c = 36$ ,  $c_{pp} = 1$ .

Figure 5 (a) illustrates the discrete phase values and Figure 5 (b) illustrates the signal phase modulo  $2\pi$  and demonstrates that the P2 code has the largest phase increments toward the end of the code. The P2 PAF has also an opposite slope compared to the other PSK sequences [2].

The Frank, P1 and P2 polyphase codes have the same response to Doppler as the step frequency modulation code in that grating lobes begin to appear with Doppler and maximize every odd multiple of a half frequency step [34].

#### *d. P3 Phase Code*

The P3 code is conceptually derived by converting a linear frequency modulation waveform to baseband, by using a synchronous oscillator on one end of the frequency sweep, and sampling the  $I$  and  $Q$  video at the Nyquist rate [2, 32]. The phase sequence of a P3 signal is described by [2]

$$\phi_k = \frac{\pi}{N_c} (k-1)^2 \quad (2.13)$$

for  $k = 1, 2, \dots, N_c$  where  $N_c$  is the processing gain.

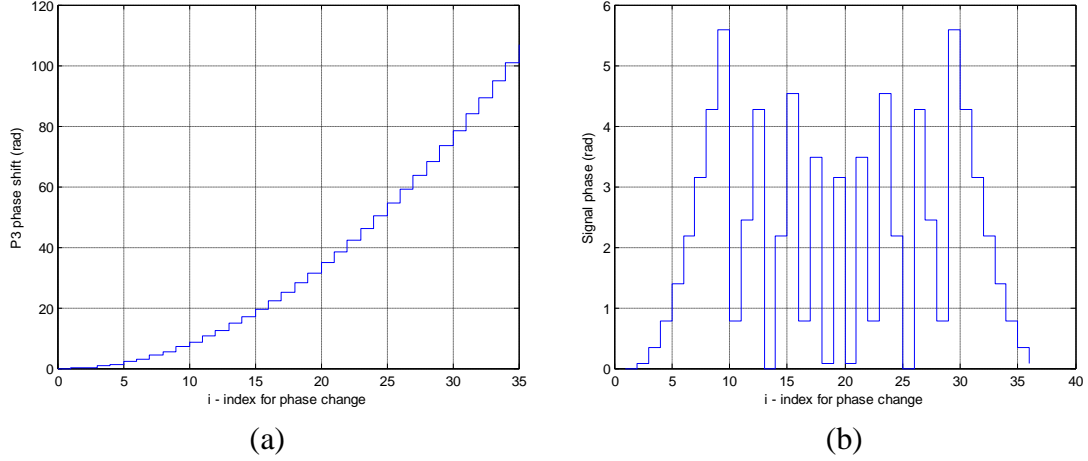


Figure 6. P3 Code Phase Values for  $N_c = 36, cpp = 1$ .

Figure 6 (a) illustrates the discrete phase values and Figure 6 (b) illustrates the signal phase modulo  $2\pi$  and demonstrates that the P3 code has the largest phase increments at the center of the code.

#### *e. P4 Phase Code*

The P4 code is conceptually derived from a linear frequency modulation waveform and consists of the discrete phases of the linear chirp waveform (sub-codes) taken at specific, uniformly spaced, time intervals. The P4 code exhibits the same range Doppler coupling associated with the chirp waveform; however, the peak side lobe levels are lower than those of the unweighted chirp waveform. The phase sequence of a P4 signal is described by [2]

$$\phi_k = \frac{\pi}{N_c} (k-1)^2 - \pi(k-1) \quad (2.14)$$

for  $k = 1, 2, \dots, N_c$  where  $N_c$  is the processing gain.

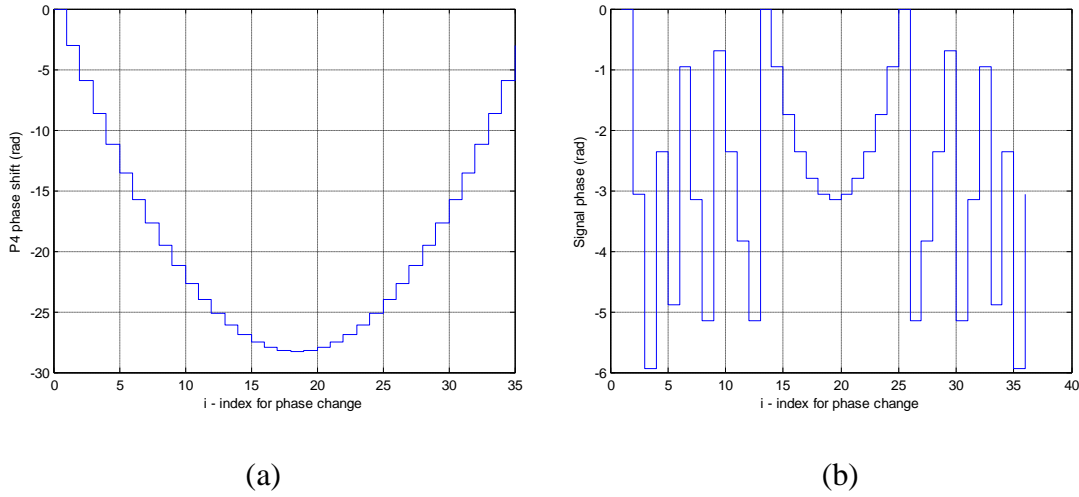


Figure 7. P4 Code Phase Values for  $N_c = 36, cpp = 1$ .

Figure 7 (a) illustrates the discrete phase values and Figure 7 (b) illustrates the signal phase modulo  $2\pi$  and demonstrates that the P4 code has the largest phase increments from sample to sample on the ends of the code.

The most significant difference between the P3 or P4 code compressed pulses and that of a Frank code is in the peak side lobes with those of the P3 and P4 codes being on the order of 3dB higher than the Frank code [34].

## 2. Polytime Codes

Another approach to approximate a stepped frequency or linear frequency modulation waveform is polytime coding. In this case, the time spent at each phase state changes throughout the duration of the code period  $T$ . That is, the code sequences use fixed phase states with varying time periods at each phase state [35].

Four types of polytime sequences are defined. The T1(n) and T2(n) polytime sequences can be generated from the stepped frequency model where n is the number of phase states used to approximate the underlying waveform. The T3(n) and T4(n) polytime sequences are approximations to a linear frequency modulation waveform. The quality of the polytime approximation to the underlying waveform can be increased by increasing the number of phase states. The phase state (or subcode) durations change as a



function of time. The minimum subcode duration sets the waveform bandwidth. Polytime coding also has the advantage that arbitrary time-bandwidth waveforms can be generated with only a few phase states [2].

**a. Polytime Code T1(n)**

The T1(n) sequence is generated using the stepped frequency waveform that is zero beat at the leading segment. The expression for the wrapped phase versus time for the T1(n) polytime sequence is [35]

$$\phi_{T1}(t) = \text{mod} \left\{ \frac{2\pi}{n} \text{INT} \left[ (kt - jT) \frac{jn}{T} \right], 2\pi \right\} \quad (2.15)$$

where  $j = 0, 1, 2, \dots, k-1$  is the segment number in the stepped frequency waveform,  $k$  is the number of segments in the T1 code sequence,  $t$  is time, and  $T$  is the code period.

An example of how a stepped frequency waveform is converted into a T1(4) polytime waveform with  $k = 4$  segments and  $n = 4$  phase states is shown in Figure 8 (one period with length  $T = 16$  ms). Figure 8(a) shows the unwrapped phase change in the time domain. Figure 8(b) shows the wrapped phase.

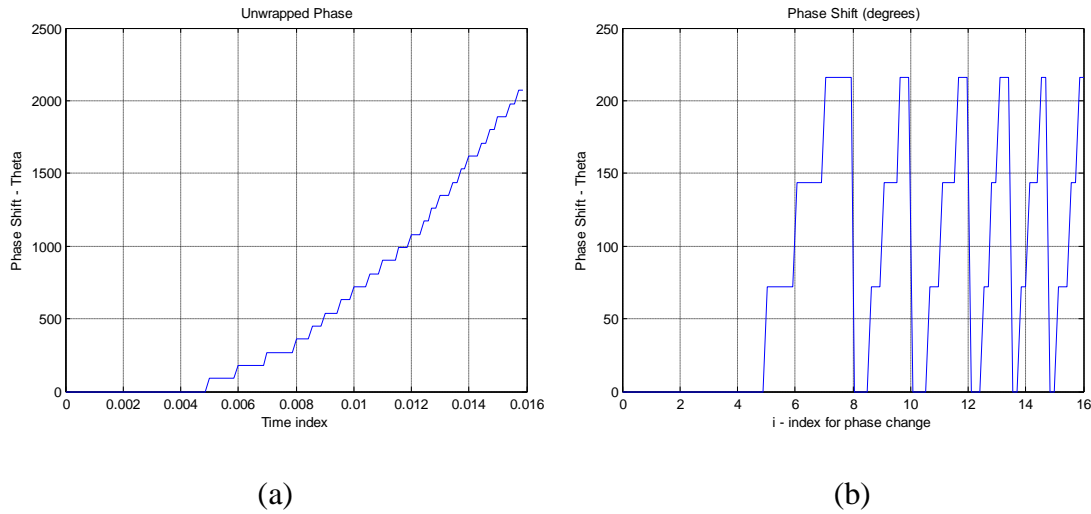


Figure 8. Stepped frequency waveform generating a T1(4) Code.

**b. Polytime Code T2(n)**

The T2(n) sequence is generated by approximating a stepped-frequency waveform that is zero at its center frequency. For stepped frequency waveforms with an odd number of segments, the zero frequency is the frequency of the center segment. If an even number of segments are used, the zero frequency is the frequency halfway between the two center most segments. The expression for the wrapped phase versus time for the T2(n) polytime sequence is [2]

$$\phi_{T_2}(t) = \text{mod} \left\{ \frac{2\pi}{n} \text{INT} \left[ (kt - jT) \left( \frac{2j - k + 1}{T} \right) \frac{n}{2} \right], 2\pi \right\} \quad (2.15)$$

where  $j = 0, 1, 2, \dots, k-1$  is the segment number in the stepped frequency waveform,  $k$  is the number of segments in the T2 code sequence,  $t$  is time, and  $T$  is the code period.

An example of how a stepped frequency waveform is converted into a T2(4) polytime waveform with  $k = 4$  segments and  $n = 4$  phase states is shown in Figure 9 (one period with length  $T = 16$  ms). Figure 9(a) shows the unwrapped phase change in the time domain. Figure 9(b) shows the wrapped phase.

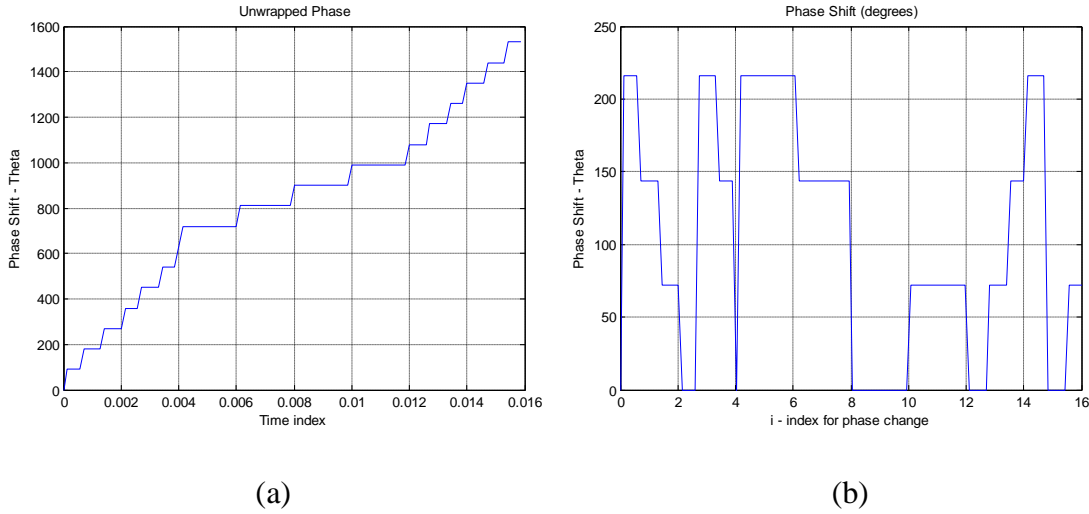


Figure 9. Stepped frequency waveform generating a T2(4) Code.

**c. Polytime Code T3(n)**

The T3 Polytime sequence is an approximation to a linear FM underlying model. A linear FM waveform that is zero beat at its beginning generates a T3 waveform [35]. The equation for the wrapped phase versus time for a T3 polytime sequence is [2]

$$\phi_{T3}(t) = \text{mod} \left\{ \frac{2\pi}{n} \text{INT} \left[ \frac{n\Delta F t^2}{2t_m} \right], 2\pi \right\} \quad (2.17)$$

where  $t_m$  is the modulation period and  $\Delta F$  is the modulation bandwidth.

An example T3(4) polytime waveform with  $n = 4$  phase states is shown in Figure 10 (one period with length  $t_m = 16$  ms and  $\Delta F = 250$  Hz). Figure 10(a) shows the unwrapped phase change in the time domain. Figure 10(b) shows the wrapped phase.

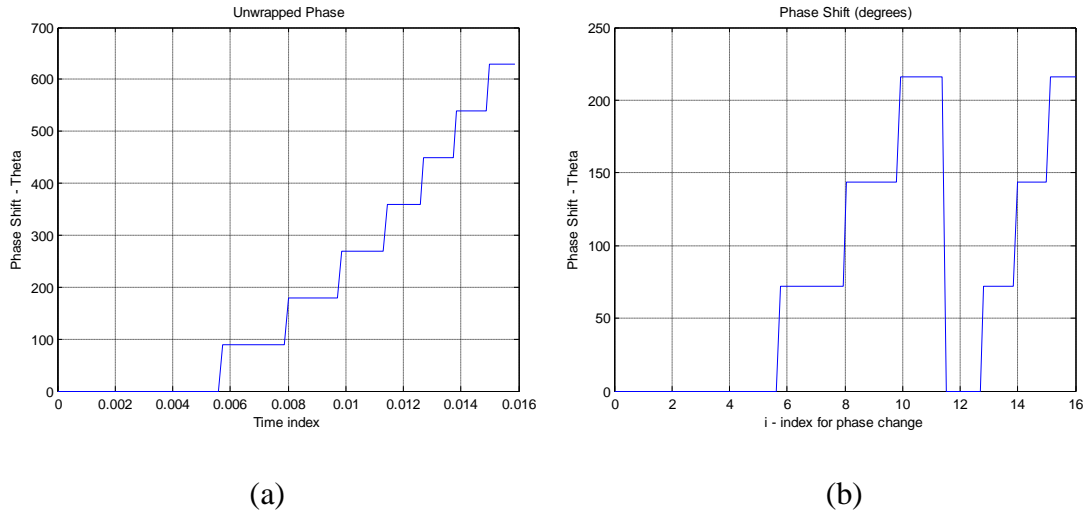


Figure 10. Stepped frequency waveform generating a T3(4) Code.

**d. Polytime Code T4(n)**

The T4 Polytime sequence is also an approximation to a linear FM underlying model. A linear FM waveform that is zero beat at its center and is quantized into  $n$  discrete phases generates a T4 waveform. The equation for the wrapped phase versus time for a T4 polytime sequence is [2]

$$\phi_{T4}(t) = \text{mod} \left\{ \frac{2\pi}{n} \text{INT} \left[ \frac{n\Delta F t^2}{2t_m} - \frac{n\Delta F t}{2} \right], 2\pi \right\} \quad (2.18)$$

where  $t_m$  is the modulation period and  $\Delta F$  is the modulation bandwidth.

An example of a T4(4) polytime waveform with  $n = 4$  phase states is shown in Figure 11 (one period with length  $t_m = 16$  ms and  $\Delta F = 250$  Hz). Figure 11(a) shows the unwrapped phase change in the time domain. Figure 11(b) shows the wrapped phase.

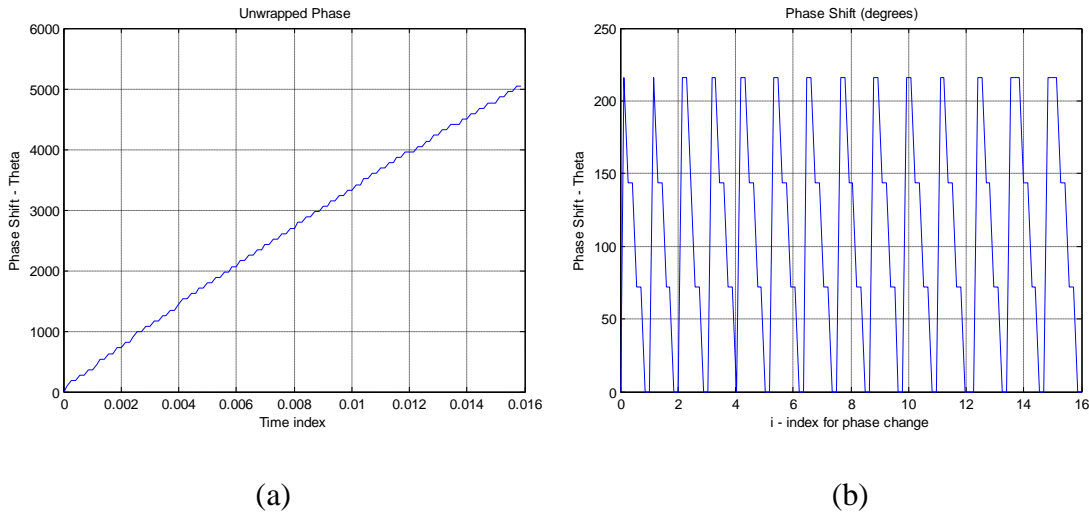


Figure 11. Stepped frequency waveform generating a T4(4) Code.

### C. FREQUENCY SHIFT KEYING TECHNIQUES

Frequency hopping (FH) techniques require hopping or changing the transmitting frequency in time over a wide bandwidth in order to prevent an unintended receiver from intercepting the waveform. FH is an important FSK technique for coding CW waveforms. The frequency slots used are chosen from a FH sequence and this unknown sequence gives the radar the advantage in terms of processing gain. A major advantage of the FH radar is the simplicity of the FSK architecture especially for track processing and generating large bandwidth signals. Also the range resolution is independent of the bandwidth and depends only on the hop rate [2].

In a FSK radar, the transmitted frequency  $f_j$  is chosen from the FH sequence  $f_1, f_2, \dots, f_{N_F}$  of available frequencies for transmission at a set of consecutive time intervals  $t_1, t_2, \dots, t_{N_F}$ . The frequencies are placed in the various time slots corresponding to a *binary time-frequency matrix*. Each frequency is used once within the code period with one frequency per time slot and one time slot per frequency. The transmitted waveform has  $N_F$  contiguous frequencies within a band  $B$  with each frequency lasting  $t_p$  s in duration.

## 1. Costas Codes

The Costas sequence of frequencies provide a FH code that produce peak side lobes in the PAF that are down from the main lobe response by a factor of  $1/N$  for all regions in the delay-Doppler frequency plane. A Costas frequency sequence  $f_1, f_2, \dots, f_{N_F}$  is a sequence that is a permutation of the integers  $t_1, t_2, \dots, t_{N_F}$  satisfying the property [2]

$$f_{k+i} - f_k \neq f_{j+i} - f_j \quad (2.19)$$

for every  $i, j$  and  $k$  such that  $1 \leq k < i < i + j \leq N_F$ . An array that results from a Costas sequence in this way is called a Costas array. Most construction methods to produce a large number of Costas arrays of equal length are based on the properties of primitive roots. For a detailed Costas array construction theory see [2].

## 2. Hybrid FSK/PSK Technique

The hybrid LPI radar technique discussed in this section combines the technique of FSK (FH using Costas sequences) with that of a PSK modulation that uses binary phase modulation using Barker sequences of varying length. The hybrid FSK/PSK signal subdivides each sub-period  $t_p$  of  $N_F$  contiguous frequencies within a band  $B$  into  $N_B$  phase slots each of duration  $t_b$  as shown in Figure 12. The total number of phase slots in the FSK/PSK waveform is then [2]

$$N_T = N_F N_B \quad (2.20)$$

with the total code period  $T = t_b N_F N_B$ .

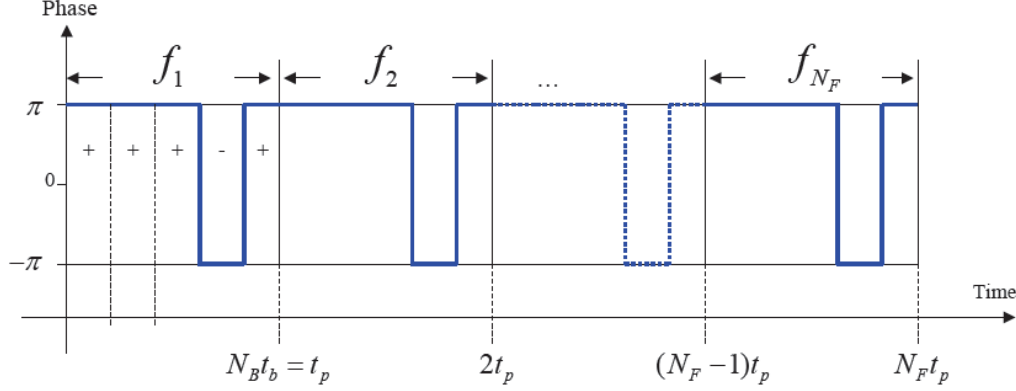


Figure 12. General FSK/PSK signal containing  $N_F$  frequency subcodes each with duration  $t_p$  s. Each frequency subcode is subdivided into  $N_B$  phase slots each with duration  $t_b$  (From [2]).

Figures 3 through 12 presented in this chapter are generated by the low probability of intercept toolbox (LPIT) provided with [2].

#### D. SUMMARY

Basic characteristics of three LPI radar signal modulation techniques (FMCW, PSK and FSK) covering several coding types associated with these techniques are briefly explained. Overall twelve different modulation types are explained which are used in the LPI signal databank generated to test the detection and classification system presented in this thesis. With implementing as many modulation types as possible it is intended to resemble the real environmental.

The next chapter presents a brief description of the LPI radar signal databank. The signal parameters and folder structure used throughout the simulation is shown.

### III. DATABASE DESCRIPTION

Selection of the LPI signal modulation types constitutes an important part for classification studies. The modulations should be selected carefully so that providing a resemblance of the real environmental conditions. For the purpose of this thesis environmental conditions phrase is used to express the various LPI signal modulation types which may be used in the battlefield during an operation.

A database consists of twelve LPI modulation techniques each having 21 SNR levels (-10dB, -9dB... 9dB, 10dB) is generated with a sampling frequency of 7000 Hz to test the detection and classification system. The parameter values have been chosen so that the classification techniques can be easily simulated. A sampling frequency of 7000 Hz can provide ease of computation concerning the sample size while accomplishes the test of the detection and classification system.

The LPI modulation techniques include Frequency Modulation Continuous Wave (FMCW), Phase Shift Keying (Frank, P1, P2, P3, P4, T1(n), T2(n), T3(n), T4(n) codes) and Frequency Shift Keying (Costas, FSK/PSK codes). The derivation of these signals sometimes causes similarities between the T-F representations of these modulation types which makes the database complex. The folder structure used in the detection and classification algorithm is shown in Figure 13.

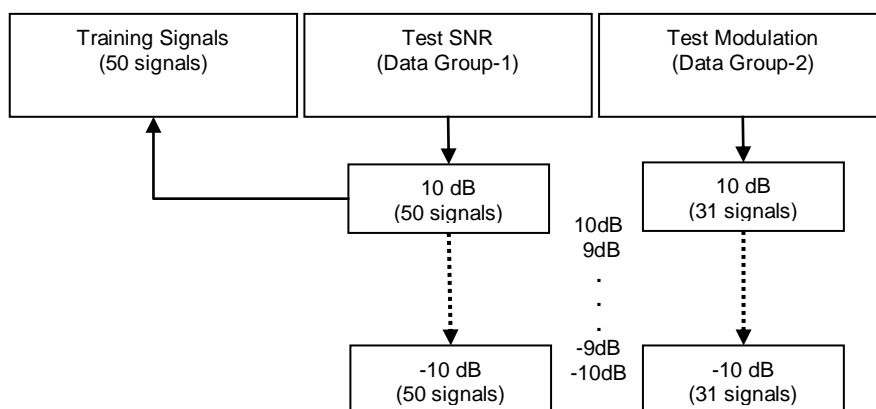


Figure 13. Signal Folder Structure used for Detection and Classification.

Two groups of parameters are used for testing purposes. The first group of parameters (Data Group-1) is used for the testing of the effects of noise variations on the detection and classification algorithm. There are 21 folders in Data Group-1, each has a different SNR level. Each folder consists of 50 signals. Data Group-1 consists of 1050 signals in total. The testing of these parameters will be represented by the “Test SNR” term. The training signals consist of 50 signals with SNR of 10 dB from the Data Group-1 with the same parameters.

The second group (Data Group-2) of parameters is different from the parameters of training signals as shown in Table 2. Data Group-2 is used to test the detection and classification algorithms with different modulations and SNR levels. Note that this is a potentially hard problem since the carrier cycles per subcode and modulation periods are different. This set of results is referred to as “Test Modulation”. There are also 21 folders in this group each with a different SNR level. Each folder consists of 31 signals. Data Group-2 consists of 651 signals in total. The test results of these parameters will be referred to as “Test Modulation”. Both training and testing signals consist of two carrier frequencies; 1495 Hz and 2195 Hz. The LPI radar signals presented below are generated by the low probability of intercept toolbox (LPIT) provided with [2].



Table 1. Signal Parameters for Training and Testing SNR (Test SNR).

SIGNAL TYPE	$f_s$ (Hz) (Sampling freq.)	$f_c$ (Hz) (Carrier freq.)	SNR −10:10dB (1 dB increments)	
			$\Delta F$ (Hz) (Modulation bandwidth)	$t_m$ (ms) (Modulation period)
FMCW	7000	1495	250	15
		2195	800	15

SIGNAL TYPE	$f_s$ (Hz) (Sampling freq.)	$f_c$ (Hz) (Carrier freq.)	SNR −10:10dB (1 dB increments)	
			$N_c$ (Code length)	$c_{pp}$ (Cycles per subcode)
FRANK	7000	1495	9	5
			25	2
			36	1
		2195	16	6
			25	3
P1	7000	1495	9	5
			25	2
			36	1
		2195	16	4
				5
P2	7000	1495	16	3
			36	1
			16	5
		2195	36	3
				3
P3	7000	1495	9	4
			36	5
				1
		2195	16	6
			25	3
P4	7000	1495	9	5
			25	2
			36	1
		2195	16	4
				5

SIGNAL TYPE	$f_s$ (Hz) (Sampling freq.)	$f_c$ (Hz) (Carrier freq.)	$T$ (ms) (Overall code period)	$t_m$ (ms) (Modulation period)	SNR −10:10dB (1 dB increments)		
					$\Delta F$ (Hz) (Modulation bandwidth)	$n$ (Number of phase states)	$k$ (Segment number in the stepped frequency waveform)
T1	7000	1495	30	N/A	N/A	2	5
						3	4
		2195	30	N/A	N/A	2	3
						4	4
T2	7000	1495	30	N/A	N/A	4	3
						8	4
		2194	30	N/A	N/A	4	3
						6	4
T3	7000	1495	N/A	25	300	4	N/A
				30	900	9	
		2195	N/A	25	400	2	
				30	1000	7	
				35	800	6	
T4	7000	1495	N/A	25	400	2	N/A
			N/A	30	550	3	
		2194	N/A	30	850	7	
					600	5	
					900	9	

SIGNAL TYPE	$f_s$ (Hz) (Sampling freq.)	Frequency Choices	$t_m$ (ms) (Modulation period)	$t_p$ (ms) (Sub code-period)	SNR −10:10dB (1 dB increments)
					Barker Frequency
FSK/PSK Costas	7000	(3 2 6 4 5 1)x150 Hz	N/A	1	5
		(5 4 6 2 3 1)x300Hz	N/A	0.3	13
Costas	7000	(3 2 6 4 5 1)x200Hz	5	N/A	N/A
		(2 4 8 5 10 9 7 3 6 1)x150Hz	3	N/A	

Table 2. Signal Parameters for Testing Modulations (Test Modulation).

SIGNAL TYPE	$f_s$ (Hz) (Sampling freq.)	$f_c$ (Hz) (Carrier freq.)	SNR −10:10dB (1 dB increments)	
			$\Delta F$ (Hz) (Modulation bandwidth)	$t_m$ (ms) (Modulation period)
FMCW	7000	1495	500	20
		2195	400	20

SIGNAL TYPE	$f_s$ (Hz) (Sampling freq.)	$f_c$ (Hz) (Carrier freq.)	SNR −10:10dB (1 dB increments)	
			$N_c$ (Code length)	$c_{pp}$ (Cycles per subcode)
FRANK	7000	1495	9	4
		2195	16	4
				5
P1	7000	1495	9	4
		2195	16	6
			25	3
P2	7000	1495	16	2
		2195	16	4
P3	7000	1495	25	2
		2195	16	4
				5
P4	7000	1495	9	4
		2195	16	6
			25	3

SIGNAL TYPE	$f_s$ (Hz) (Sampling freq.)	$f_c$ (Hz) (Carrier freq.)	$T$ (ms) (Overall code period)	$t_m$ (ms) (Modulation period)	SNR −10:10dB (1 dB increments)		
					$\Delta F$ (Hz) (Modulation Bandwidth)	$n$ (Number of phase states)	$k$ (Segment number in the stepped frequency waveform)
T1	7000	1495	30	N/A	N/A	4	4
				N/A	N/A	6	3
		2195	30	N/A	N/A	3	3
T2	7000	1495	30	N/A	N/A	6	4
				N/A	N/A	4	5
		2194	30	N/A	N/A	8	3
T3	7000	1495	N/A	30	500	5	N/A
				35	700	8	
		2195	N/A	30	600	3	
T4	7000	1495	N/A	35	700	6	N/A
				N/A	450	4	
		2194	N/A	35	750	8	

SIGNAL TYPE	$f_s$ (Hz) (Sampling freq.)	Frequency Choices	$t_m$ (ms) (Modulati on period)	$t_p$ (ms) (Sub code- period)	SNR −10:10dB (1 dB increments)
					Barker Frequency
FSK/PSK Costas	7000	(3 2 6 4 5 1)x200 Hz	N/A	0.4	11
		(5 4 6 2 3 1)x250Hz	N/A	0.7	7
Costas	7000	(5 4 6 2 3 1)x400Hz	5	N/A	N/A

## A. SUMMARY

The database used for the testing of pre-processing, classification and parameter extraction algorithms is explained. The folder configuration based on twenty one SNR levels is shown. The parameters of twelve modulation types used in this work are presented.

The next chapter discusses the detection and classification architecture used in this work. Four detection techniques including the Wigner-Ville distribution (WVD), the Choi-Williams distribution (CWD), Quadrature Mirror Filter Bank (QMFB), and Cyclostationary Spectral Analysis (CYCL) are briefly explained. The pre-processing algorithms both for T-F and B-F detection techniques are described. The subjects include 2-D Discrete Fourier transform, frequency domain filtering, autonomous signal cropping and principal component analysis. Three classification networks (multi layer perceptron, radial basis function and probabilistic neural network) used in this work are explained.

#### IV. DETECTION AND CLASSIFICATION ARCHITECTURE

The autonomous detection, classification and parameter extraction system block diagram used in this work is illustrated in Figure 14. The system contains T-F (the Wigner-Ville distribution , the Choi-Williams distribution and Quadrature mirror filter bank ) detection techniques. The detection techniques provide an image output. The output image from each detection method is preprocessed to form a feature vector. An autonomous image cropping and feature extraction algorithm based on two-dimensional Fast Fourier Transform (2-D FFT) and PCA is applied to the T-F images.

Later the extracted features are used as input to a non-linear classifier. In this work an MLP neural network, an RBF neural network and a PNN are used as classifiers. The output of the classifiers generates a confusion matrix (CM) which shows the detection results as a probability of correct classification (Pcc) for each trial. The columns of the CM represent the input vector modulation type while the rows indicate the assignment by the classifier and the sum of all values should be one. The diagonals of the CM indicate the Pcc, and are the percentage of correct assignments by the network. Once the modulation is classified, the parameters can be extracted using the T-F images.

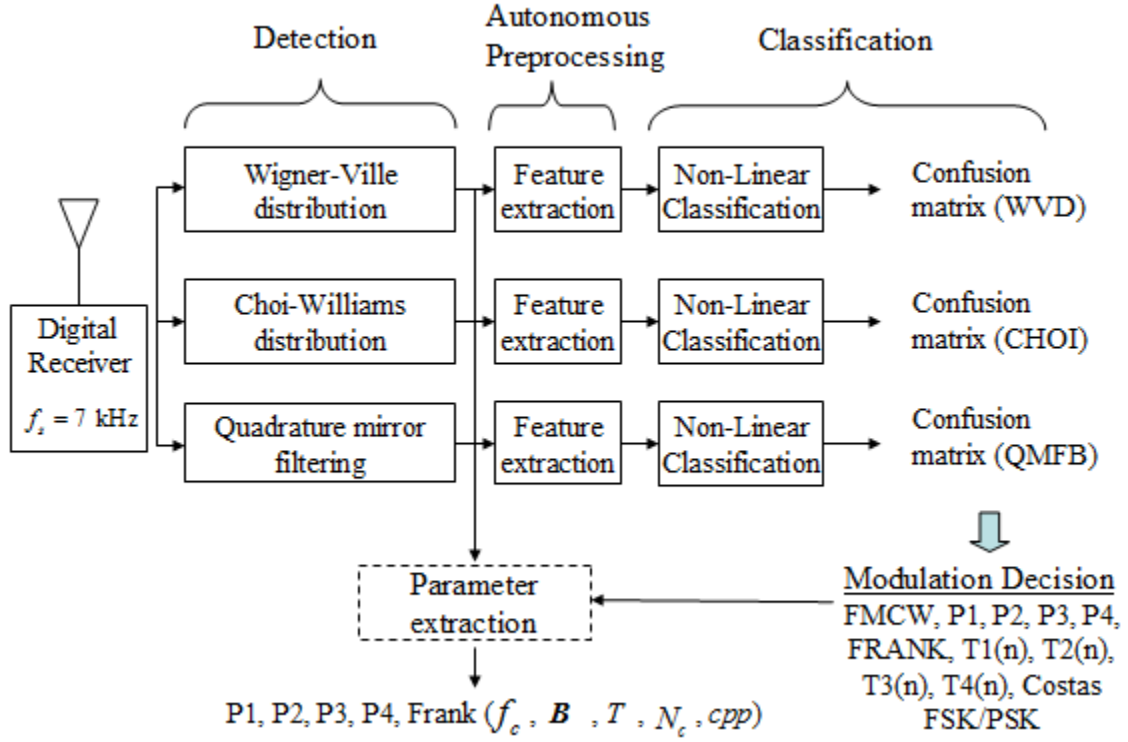


Figure 14. Detection, Classification and Parameter Extraction Architecture.

## A. DETECTION TECHNIQUES

### 1. Wigner-Ville Distribution

One of the most prominent members of T-F energy density functions is the Wigner-Ville distribution (WVD). The WVD is computed by correlating the signal with a time and frequency translated version of itself. The time and frequency marginal properties are preserved for any signal [36]. The WVD exhibits the highest signal energy concentration in the T-F plane for linearly modulated signals. The WVD also contains interfering *cross terms* between every pair of signal components which limits its applications. Although several formulations can be used to reduce the amplitude of the

cross terms, since the cross terms contain additional T-F information, it is of interest to determine if they facilitate the classification process in comparison to the CWD and QMFB [2].

The WVD of a continuous one-dimensional function  $x(t)$  is defined as [2]

$$W_x(t, \omega) = \int_{-\infty}^{\infty} x(t + \frac{\tau}{2}) x^*(t - \frac{\tau}{2}) e^{-j\omega\tau} d\tau \quad (4.1)$$

where  $t$  is the time variable,  $\omega$  is the angular frequency variable ( $2\pi f$ ), and the  $*$  indicates complex conjugate. Let  $x(l)$  be a sampled time series representing the digitized signal where  $l$  is a discrete time index from  $-\infty$  to  $\infty$ . The discrete WVD is

$$W(l, \omega) = 2 \sum_{n=-\infty}^{\infty} x(l+n) x^*(l-n) e^{-j2\omega n} \quad (4.2)$$

Windowing the data results in the pseudo WVD (PWVD)

$$W(l, \omega) = 2 \sum_{n=-N+1}^{N-1} x(l+n) x^*(l-n) w(n) w(-n) e^{-j2\omega n} \quad (4.3)$$

where  $w(n)$  is a length  $2N-1$  real window function with  $w(0) = 1$ . Using  $f_l(n)$  to represent the kernel function

$$f_l(n) = x(l+n) x^*(l-n) w(n) w(-n) \quad (4.4)$$

the PWVD becomes

$$W(l, \omega) = 2 \sum_{n=-N+1}^{N-1} f_l(n) e^{-j2\omega n} \quad (4.5)$$

where  $\omega = \pi k / (2N)$ . The choice of  $N$  (usually a power of 2) greatly affects the computational cost as well as the time frequency resolution of the output. Once  $N$  is chosen, the kernel function can be generated. Since  $f_l(n) = f_l^*(-n)$ , only  $f_l(n)$  needs to be computed for  $n \geq 0$  [2]. For a detailed analysis of WVD refer to [2, 34].

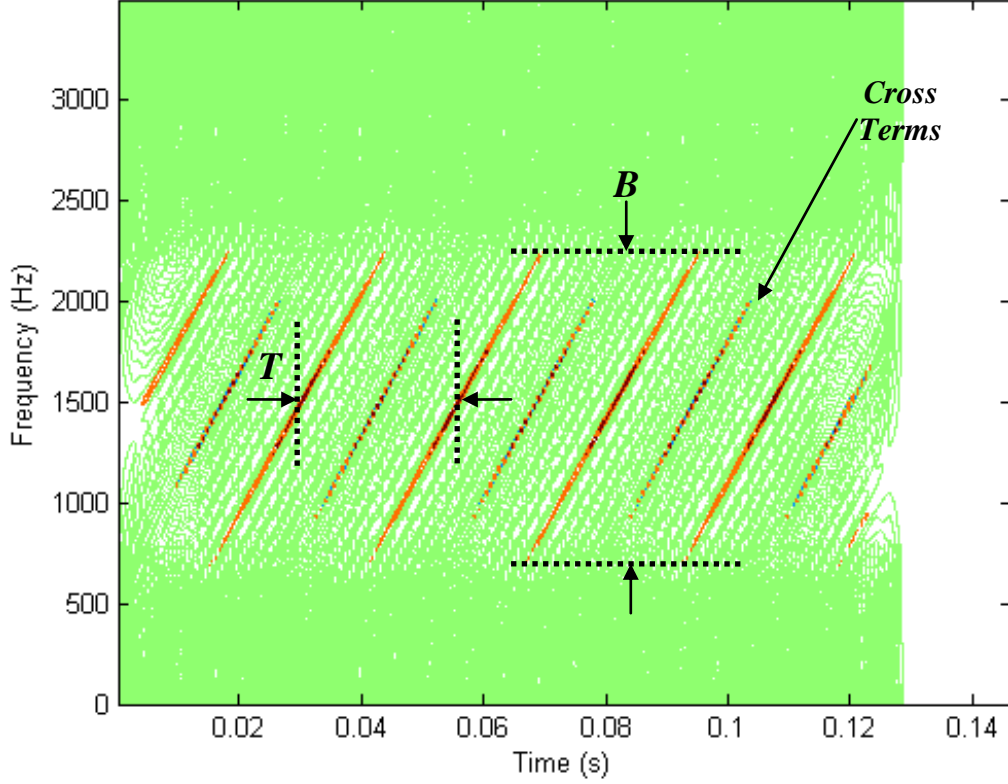


Figure 15. Pseudo Wigner-Ville Distribution of a Frank Coded Signal with  $N_c = 36$ .

Figure 15 shows the PWVD results for a Frank coded signal with  $N_c = 36$  subcodes, a carrier frequency of  $f_c = 1495$  Hz with a sampling frequency of  $f_s = 7$  kHz in a contour plot. With the number of carrier frequency cycles within a subcode of  $c_{pp} = 1$ , the transmitted bandwidth  $B = f_c / c_{pp} = 1495$  Hz and the code period is  $T = 24.1$  ms. Note the presence of the characteristic cross terms. Note also that with the PWVD time-frequency information, the signal parameters can be measured accurately including the number of subcodes  $N_c = T/B$ . The frequency resolution of the WVD  $\Delta f_w = f_s / 2N$  and the time resolution  $\Delta t_w = 1/f_s$ . For efficiency the implementation of the Wigner-Ville distribution used in this work was made by [37].



## 2. Choi-Williams Distribution

The Choi-Williams Distribution (CWD) simultaneously gives the representation of a signal in both time and frequency. The Choi-Williams distribution has been noted as one of the more useful in the Cohen's class of distributions since it reduces the amplitude of the cross terms [27]. This distribution is a bilinear time-frequency analysis techniques for signal processing and has been used in many fields of engineering.

The Choi-Williams distribution is given as [38]

$$C_x(t, \nu; f) = \iiint_{\infty} e^{j2\pi\xi(s-t)} f(\xi, \tau) x(s + \tau/2) x^*(s - \tau/2) e^{-j2\pi\nu\tau} d\xi ds d\tau \quad (4.6)$$

where  $f(\xi, \tau)$  is a 2-D function called the *parameterization function*. A natural choice for the kernel is to consider a Gaussian function

$$f(\xi, \tau) = e^{-(\pi\xi\tau)^2 / 2\sigma^2} \quad (4.7)$$

resulting in

$$CW_x(t, \nu) = \sqrt{\frac{2}{\pi}} \iint_{\infty} \frac{\sigma}{|\tau|} e^{-2\sigma^2(s-t)^2 / \tau^2} x(s + \tau/2) x^*(s - \tau/2) e^{-j2\pi\nu\tau} ds d\tau \quad (4.8)$$

The frequency-resolution and the suppression of the cross-terms can be controlled by varying the  $\sigma$ . The smaller the parameter  $\sigma$ , the more the cross-terms are suppressed. But this also will affect the auto-terms. Therefore, there is trade-off for the selection of the parameter  $\sigma$  [36]. Note that as  $\sigma \rightarrow \infty$ , the corresponding distribution converges to the the Wigner-Ville distribution. Note that this means to set the parameterization function to one,  $f(\xi, \tau) = 1$ .

Figure 16 shows the Choi-Williams results for a Frank coded signal with  $N_c = 36$  subcodes, a carrier frequency of  $f_c = 1495$  Hz with a sampling frequency of  $f_s = 7$  kHz in a contour plot. With the number of carrier frequency cycles within a subcode of  $c_{pp} = 1$ , the transmitted bandwidth  $B = f_c / c_{pp} = 1495$  Hz and the code period is  $T = 24.1$  ms. Note that with the CWD time-frequency information, the signal parameters can

also be measured accurately including the number of subcodes  $N_c = T/B$ . Note that the cross-terms are suppressed. The implementation of the Choi-Williams distribution used in this work was made by [37].

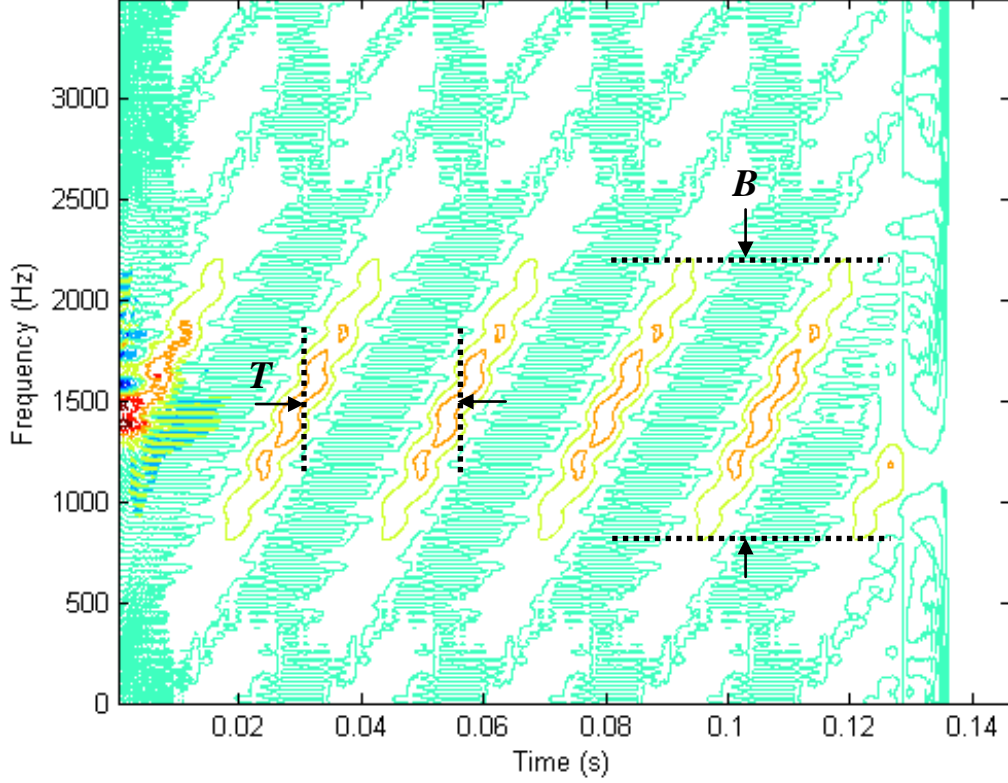


Figure 16. Choi-Williams Distribution of a Frank Coded Signal with  $N_c = 36$ .

### 3. Quadrature Mirror Filter Bank Tree

A QMFB tree consists of a number of layers of fully connected pairs of orthogonal wavelet filters (or basis functions) that linearly decompose the received waveform into tiles on the time-frequency plane. A modified sinc filter is used and every filter output is connected to a filter pair in the next layer, as shown in Figure 17 [39]. Figure 17 also illustrates the implementation of the QMFB tree used in this thesis work.

The tiles are used to refer to the rectangular regions of the time-frequency plane containing the basis function's energy. Each filter pair divides the digital input waveform

into its high-frequency and low-frequency components, with a transition centered at  $\pi$ . Within the series of time-frequency layers, each subsequent layer provides a trade-off in time and frequency resolution. By examining the energy within the tiles, parameters such as bandwidth, center frequency, phase modulation, signal duration and location in the time-frequency plane can be determined [2].

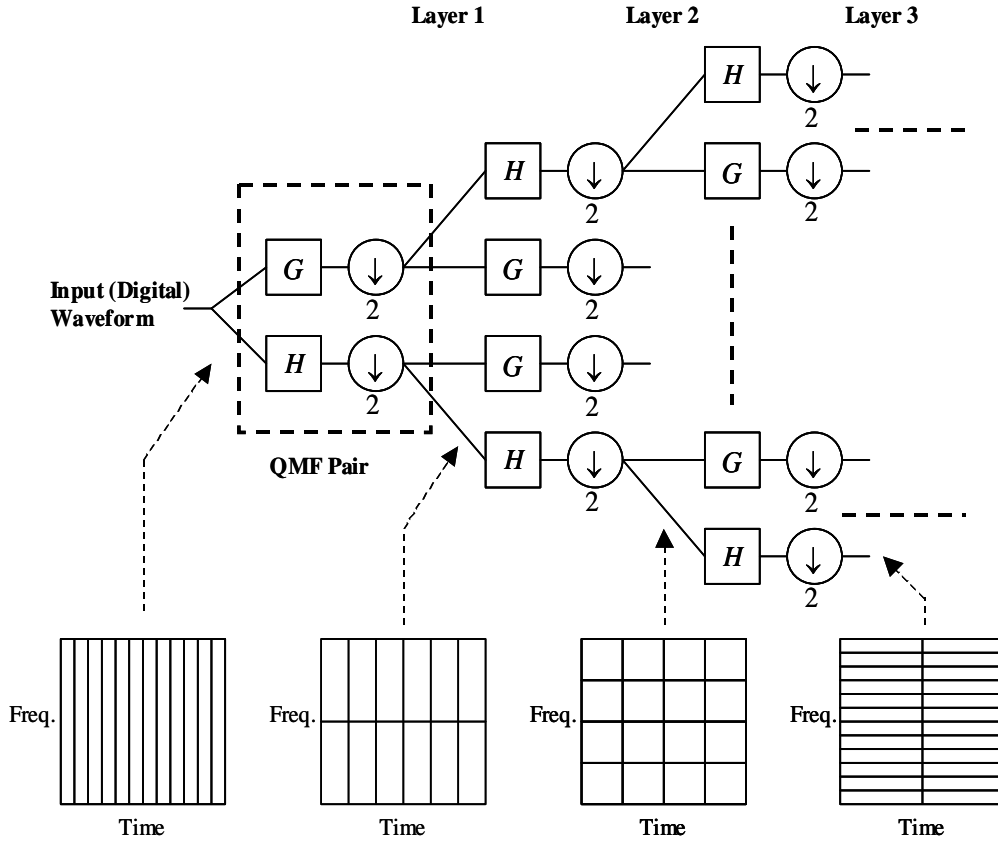


Figure 17. Quadrature Mirror Filter Bank Tree (From [39]).

The received signal is first padded with zeros to contain  $N_p = 2^L$  samples where  $L$  is the number of layers within the tree. A normalized input of one sample per second is assumed, with a signal bandwidth of  $[0, \pi]$  radians, with  $\pi$  corresponding to half the sampling frequency. Since each filter's output signal has half the bandwidth, only half the samples are required to meet the Nyquist criteria; therefore, these sequences are

downsampled by two and the same number of output samples is returned [40]. The  $l \leq \lfloor L/2 \rfloor$  layer provides a good compromise in time and frequency resolution. The frequency resolution of a QMFB layer  $l$  is [2]

$$\Delta f = \frac{f_s}{2(2^l - 1)} \quad (4.9)$$

where  $f_s$  is the sampling frequency. The resolution in time is determined by how many samples are used within the QMFB and is

$$\Delta t = \frac{2^L}{f_s(2^{L-l} - 1)} \quad (4.10)$$

where  $L$  is the total number of layers. In this work layer  $l = 5$  is used which provides an output with  $32 \times 32$  points. In this work QMFB is implemented using LPIT provided with [2].

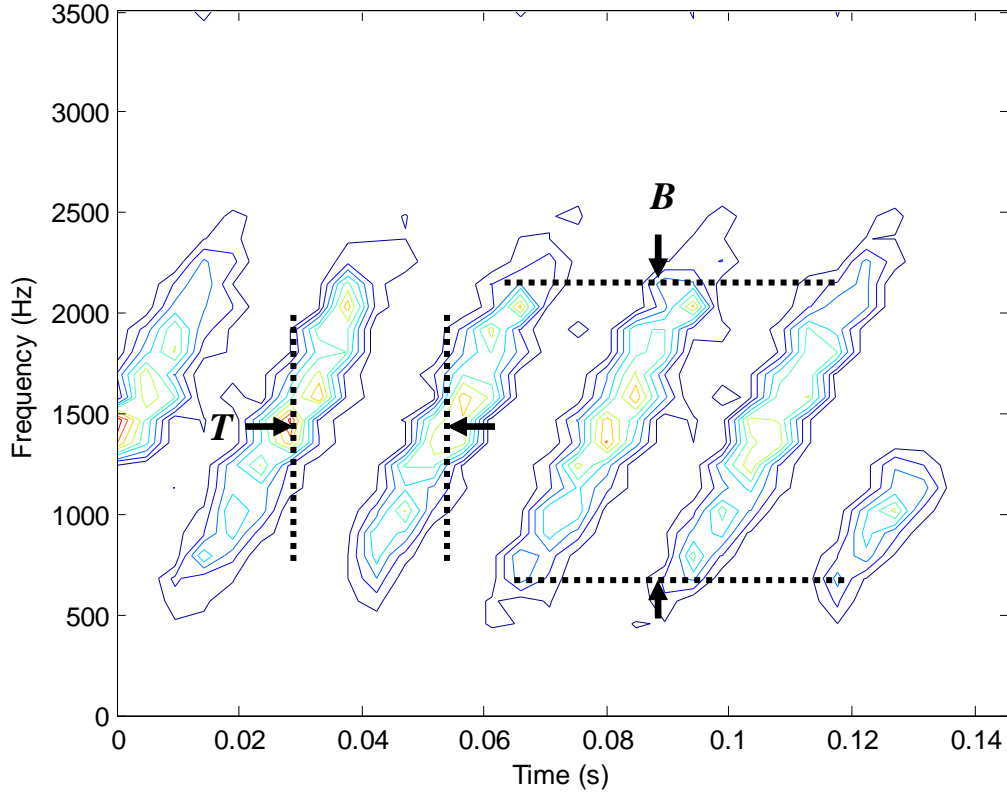


Figure 18. QMFB Result for Layer  $l = 5$  for a Frank Coded Signal with  $N_c = 36$ .

Figure 18 shows the QMFB result for layer  $l = 5$  for a Frank coded signal with  $N_c = 36$  subcodes, a carrier frequency of  $f_c = 1495$  Hz with a sampling frequency of  $f_s = 7$  kHz in a contour plot. With the number of carrier frequency cycles within a subcode of  $c_{pp} = 1$ , the transmitted bandwidth  $B = f_c / c_{pp} = 1495$  Hz and the code period is  $T = 24.1$  ms. Here  $L = 10$ ,  $\Delta t = 0.0047$  s and  $\Delta f = 112.9$  Hz.

## B. AUTONOMOUS PREPROCESSING

Autonomous preprocessing is performed in order to generate a feature vector from the T-F images to be used in the classification networks. The first goal of the algorithm is to autonomously crop a part of the image where the signal is present. This is the part of the image within the frequency band of interest. The frequency bands of interests are illustrated in Figure 19 between the dashed lines.

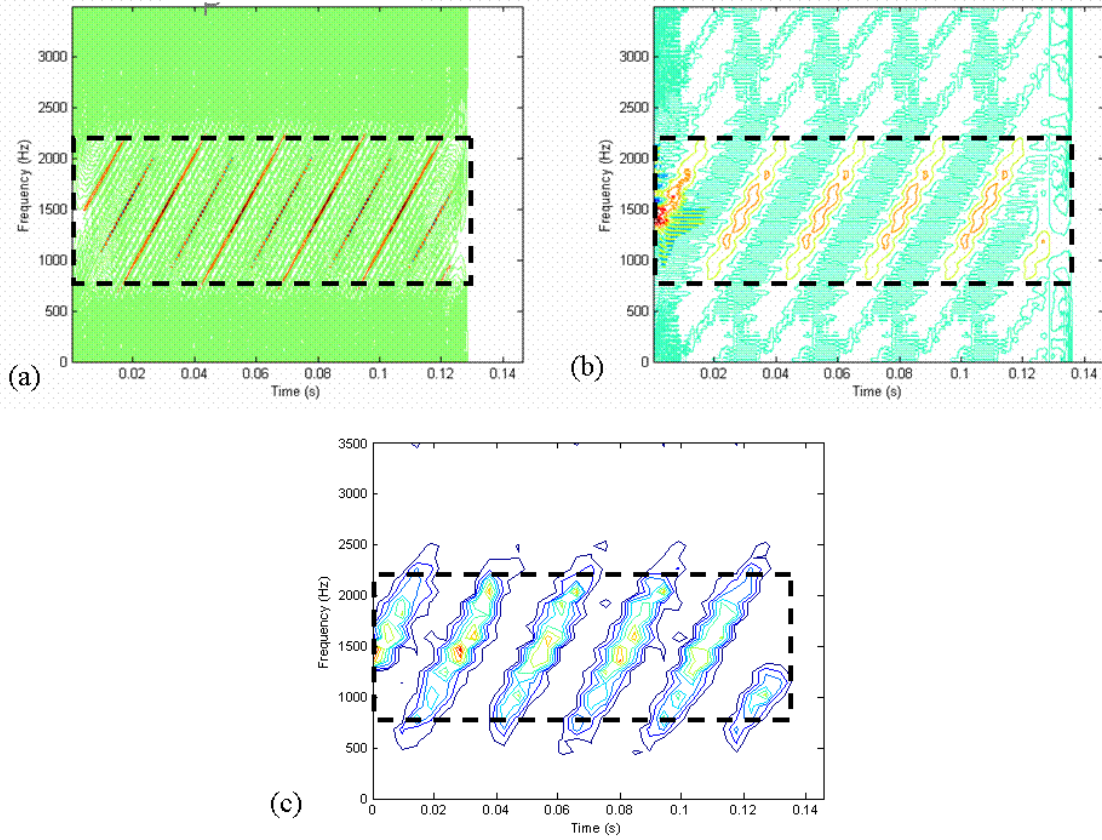


Figure 19. The Frequency Bands of Interests (a) PWVD (b) CWD (c) QMFB.

The sensitivity of the cropping is very important since the noise level present in the signal may easily distort the algorithm. The less the cropping algorithm is affected by the SNR changes the more accurate the expected classification results.

The second goal is to process the images with minimum interference (for instance thresholding, binarization, morphological operations, etc.). Any operation on the images either adds new information to the image or results in some information loss. Third goal is to reduce the dimension of the feature vectors while preserving their discriminating properties.

T-F representations are processed as images throughout this work. Let the dimension of an image be  $M \times N$ . In this work for the PWVD and CWD images  $M, N$  depend on the length of the intercepted signal sequence, which is the sample size. For the QMFB images  $M = N = 32$  depend on the selected layer  $l = 5$ . Following sections briefly explain each step taken through T-F autonomous cropping and feature extraction operations.

### **1. T-F Autonomous Cropping and Feature Extraction Algorithm**

Block diagram of the T-F autonomous cropping and feature extraction algorithm used in this work is shown in Figure 20.

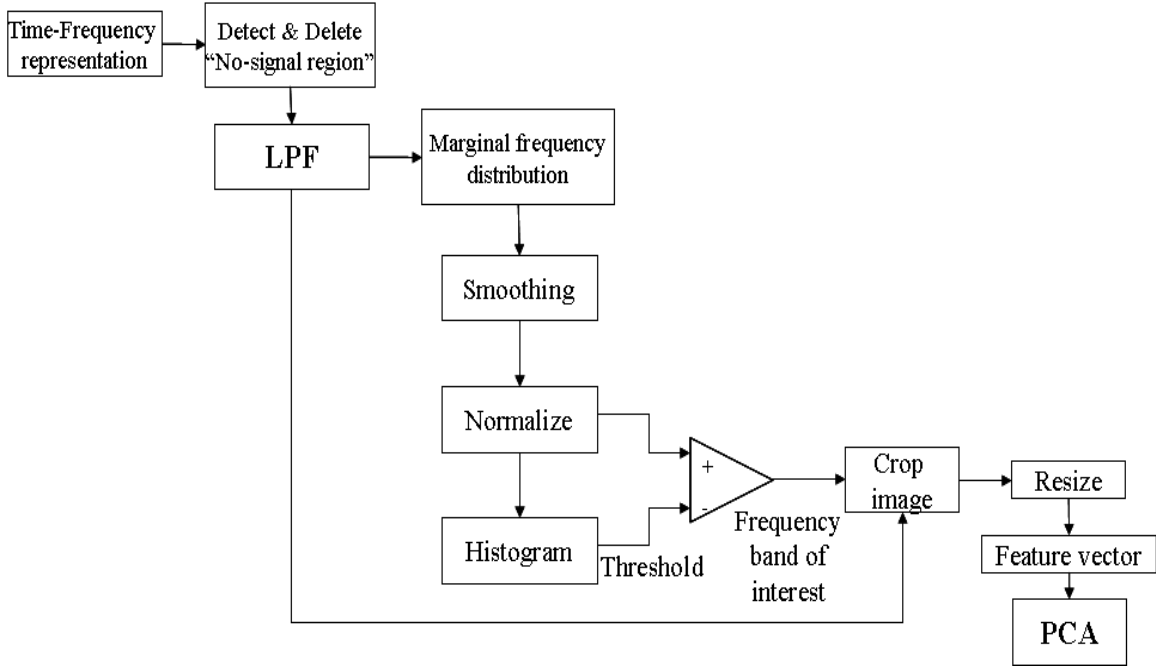


Figure 20. T-F autonomous cropping and feature extraction algorithm (From [27]).

The first step of the algorithm is to detect and delete the region where no signal is present. No signal regions may occur if the duration of the LPI signal is smaller than the time interval processed. The block corresponds to this step is shown in Figure 21. This step is performed as defined in [29].

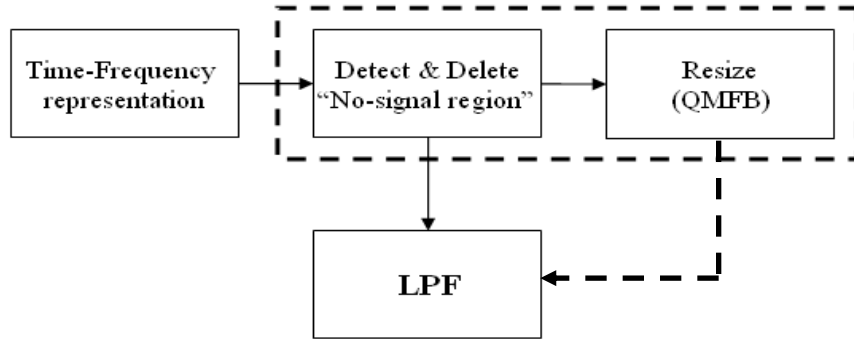


Figure 21. Detect and Delete "No-signal region" Block.

Figure 22 shows an illustration of this operation. The image is obtained by WVD representation of a Frank code signal with  $f_s = 7kHz$ ,  $f_c = 1495Hz$ ,  $N_c = 36$ , and  $c_{pp} = 1$  ( $B = 1495$  Hz) with an  $SNR = 0dB$ . Figure 22 (a) shows the original output of the WVD, and Figure 22 (b) shows the new image after the no-signal region is deleted.

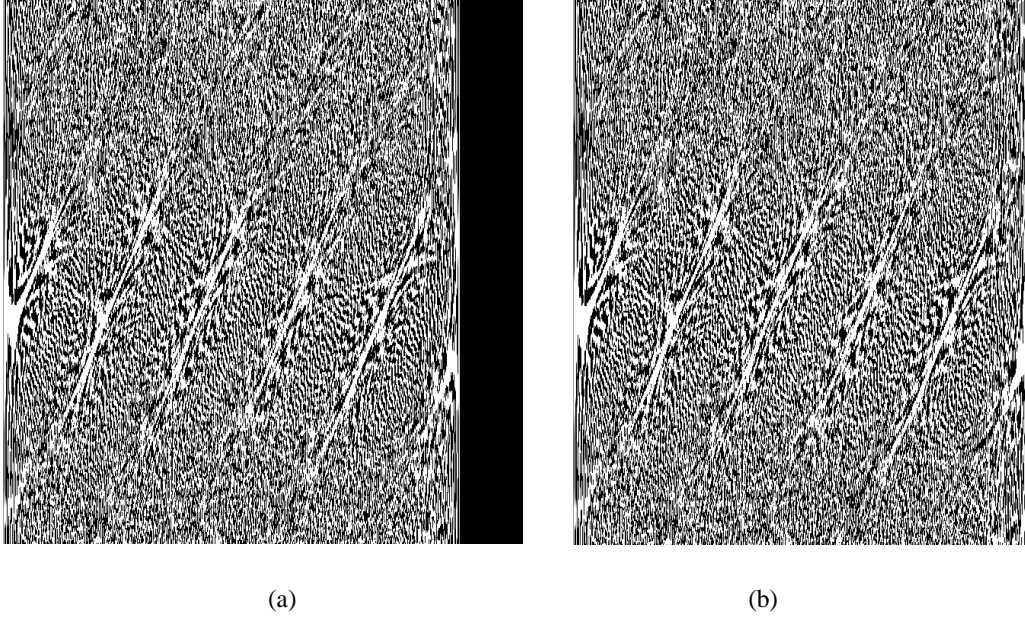


Figure 22. (a) T-F Image with No-Signal Region (b) Image after No-Signal Region Cropped.

Followed by the deletion of the no-signal region, the image is lowpass filtered (LPF). Assuming that the additive noise has high frequency components and the LPI modulation energy is preserved in the low frequencies, after filtering only the modulation energy should be preserved. The filtering can be performed in the frequency domain [27].

The following section briefly explains the 2-D Discrete Fourier Transform (2-D DFT) and the implementation of frequency domain filtering. Since QMFB images have very small dimensions ( $32 \times 32$ ) compared to the PWVD and CWD images, they are resized and enlarged by 10 times of their original sizes after the no signal region is cropped (prior to the filtering).



**a. The 2-D Discrete Fourier Transform and Frequency Domain Filtering**

Let  $f(k_1, k_2)$ , for  $k_1 = 0, 1, 2, \dots, M-1$  and  $k_2 = 0, 1, 2, \dots, N-1$ , denote an  $M \times N$  image. The 2-D DFT of  $f$ , denoted by  $F(u, v)$ , is given by equation [41]

$$F(u, v) = \sum_{k_1=0}^{M-1} \sum_{k_2=0}^{N-1} f(k_1, k_2) e^{-j2\pi(uk_1/M + vk_2/N)} \quad (4.11)$$

for  $u = 0, 1, 2, \dots, M-1$  and  $v = 0, 1, 2, \dots, N-1$ . The frequency domain is simply the coordinate system spanned by  $F(u, v)$  with  $u$  and  $v$  as variables. The  $M \times N$  rectangular region defined by  $u$  and  $v$  is often referred as the frequency rectangle and of the same size as the input image. Note that frequency rectangle can also be defined by digital frequencies as shown in Figure 23.

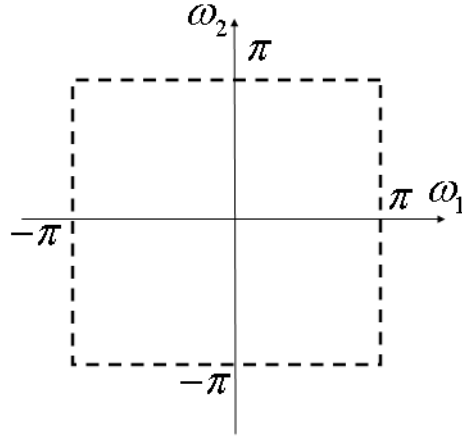


Figure 23. Frequency Rectangle Defined by Digital Frequencies.

where  $\omega_1 = u2\pi/M$  and  $\omega_2 = v2\pi/N$ .

Given  $F(u, v)$ ,  $f(k_1, k_2)$  can be obtained by means of the inverse DFT. Both DFT and inverse DFT are obtained in practice using a fast Fourier transform (FFT) algorithm [41]. If  $f(k_1, k_2)$  is the image obtained by WVD representation of a Frank

signal with  $f_s = 7\text{kHz}$ ,  $f_c = 1495\text{Hz}$ ,  $N_c = 36$ , and  $c_{pp} = 1$  ( $B = 1495\text{ Hz}$ ), with an  $SNR = 0\text{dB}$ , the 2-D FFT of  $f(k_1, k_2)$  is shown in Figure 24 (a) and the zero frequency component shifted to the center of spectrum is shown in Figure 24 (b).

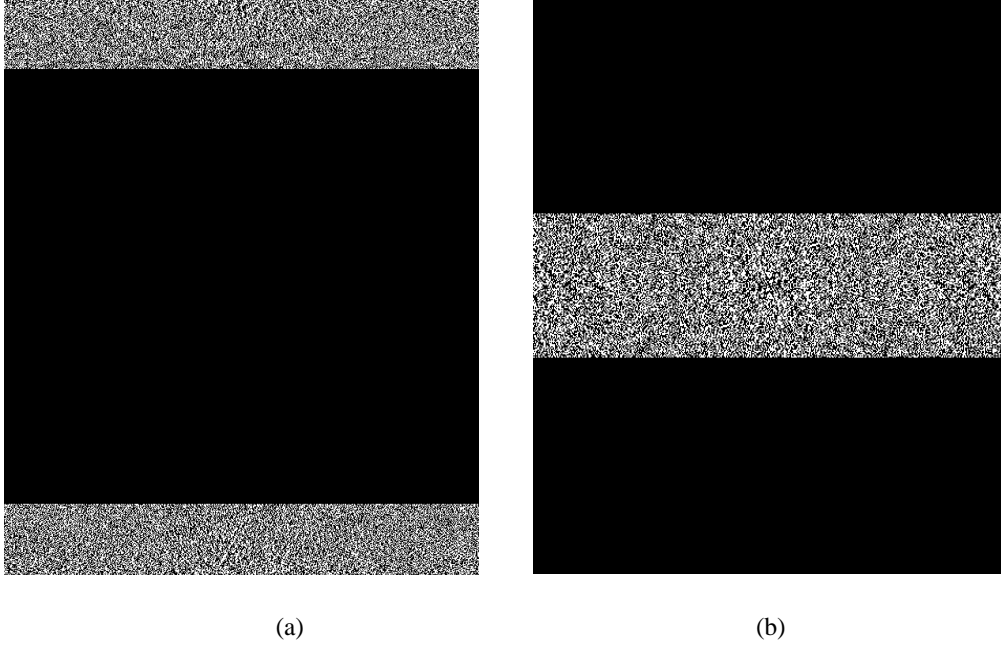


Figure 24. (a) 2-D FFT of image shown in Figure 22 (b) and (b) The zero frequency component is shifted to the center of spectrum.

The convolution theorem which is the foundation for linear filtering in both spatial and frequency domains can be written as follows [41]

$$f(k_1, k_2) * h(k_1, k_2) \Leftrightarrow H(u, v) F(u, v) \quad (4.12)$$

and conversely,

$$f(k_1, k_2) h(k_1, k_2) \Leftrightarrow H(u, v) * F(u, v) \quad (4.13)$$

Filtering in the spatial domain consists of convolving an image  $f(k_1, k_2)$  with a filter mask,  $h(k_1, k_2)$ . According to the convolution theorem, the same result can be obtained in the frequency domain by multiplying  $F(u, v)$  by  $H(u, v)$  which can also be referred as the *filter transfer function* [41]. The frequency domain filtering used in this work is shown in Figure 25.

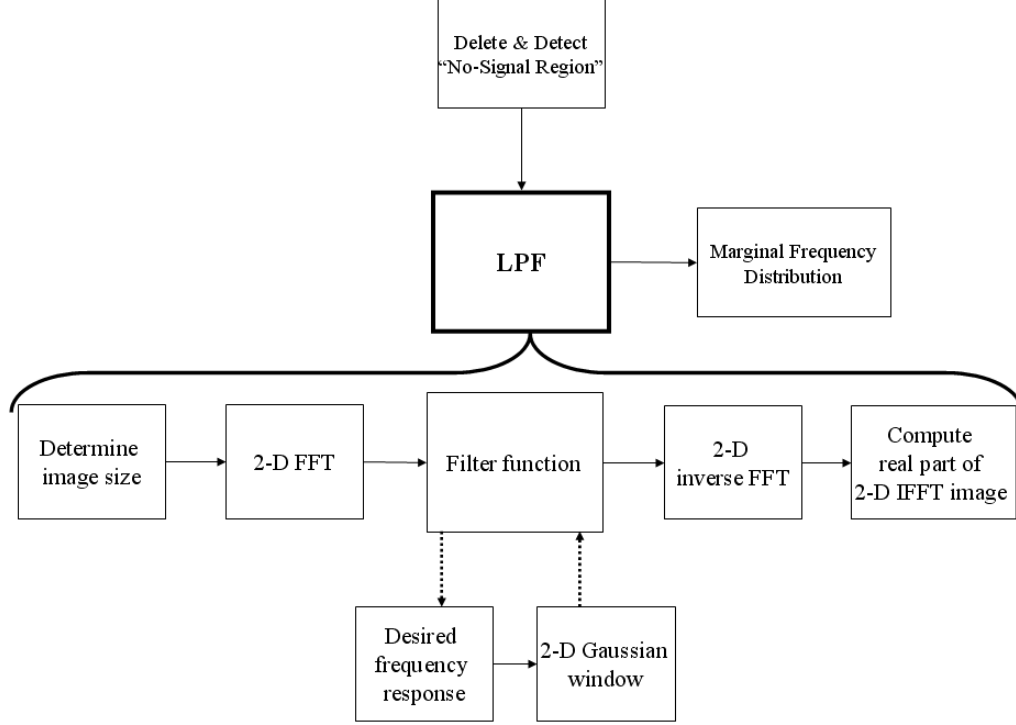


Figure 25. Frequency Domain Filtering Operations.

In this work  $H(u, v)$  is obtained in three steps. First, the desired frequency response (ideal lowpass filter)  $H_d(u, v)$  is created as a matrix. An ideal lowpass filter has the transfer function [41]

$$H_d(u, v) = \begin{cases} 1 & \text{if } D(u, v) \leq D_0 \\ 0 & \text{if } D(u, v) \geq D_0 \end{cases} \quad (4.14)$$

where  $D_0$  (cutoff parameter) is a specified nonnegative number and  $D(u, v)$  is the distance from point  $(u, v)$  to the center of the filter.  $D_0$  can also be defined as the normalized value of digital frequencies  $\omega_1, \omega_2$  by  $\pi$ .

Second, a two dimensional Gaussian window is created with a standard deviation

$$\sigma = N \times D_0 / 8 \quad (4.15)$$

where  $N$  is the number of columns in the image. Since the standard deviation of the window is related to  $D_0$ , the structure becomes adaptive to the changes in the desired frequency responses. In this application both the frequency response matrix and the Gaussian window have dimensions of  $M \times N$  which is equal to the image dimension ( $f(k_1, k_2)$ ) and the 2-D FFT output dimension ( $F(u, v)$ ). The last step is to multiply  $H_d(u, v)$  by the Gaussian window.

The transfer function of the Gaussian lowpass filter obtained by this multiplication process is then given by [41]

$$H(u, v) = e^{D^2(u, v)/2\sigma^2} \quad (4.16)$$

These steps are illustrated in Figure 26. Figure 26 (a) shows the desired frequency response with  $D_0 = 0.3$  (where  $|D_0| \in [0, 1]$ ) or  $\omega_1 = \omega_2 = 0.3\pi$ , Figure 26 (b) shows the Gaussian window with  $\sigma = N \times D_0 / 8 = 33.825$ . The dimension of both the frequency response matrix and Gaussian window is  $M = 1024, N = 902$ . Figure 26 (c) shows the resultant Gaussian lowpass Filter and Figure 26 (d) shows the Gaussian lowpass filter as an image. Several values of  $\omega_1, \omega_2$  are tested during the simulation to find an optimum value for each distribution. For each trial the digital cutoff frequencies are set to be  $\omega_1 = \omega_2$ .

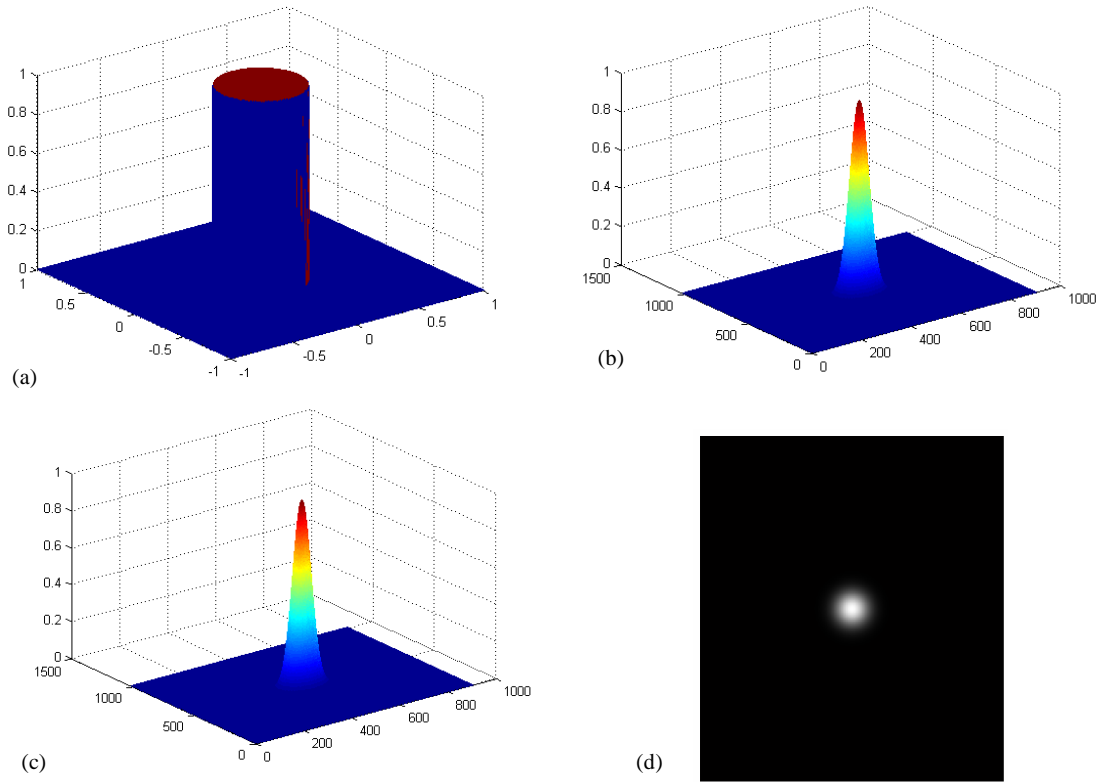


Figure 26. Implementation of Filter Function (a) Desired Frequency Response, (b) Gaussian Window, (c) Gaussian Lowpass Filter, (d) Gaussian Lowpass Filter as an Image.

After obtaining the lowpass filter, the frequency domain filtering can be implemented by multiplying  $F(u,v)$  by  $H(u,v)$ . This operation is followed by shifting back of the frequency components and taking the inverse FFT of the filtered domain. The last step is obtaining the real part of the inverse FFT. Figure 27 illustrates these steps. Figure 27 (a) shows the result after the frequency domain filtering of Figure 22 (b), Figure 27 (b) shows decentering of the frequency components and Figure 27 (c) shows the real part of the 2-D inverse FFT.

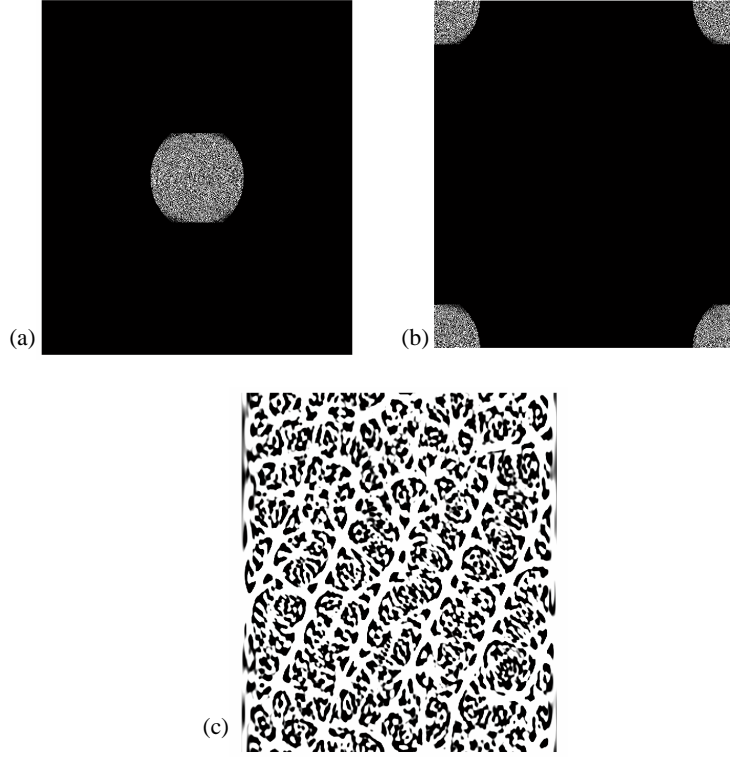


Figure 27. (a) Frequency Domain Filtering, (b) Shift Back the Frequency Components, (c) 2-D Inverse FFT output.

#### ***b. Determination of the Frequency Band of Interest***

The steps for determining the frequency band of interest from the T-F plane is shown in Figure 28. The operations are applied to the marginal frequency distribution (MFD) of the T-F plane. The MFD gives the instantaneous energy of the signal as a function of frequency. This is obtained by integrating the time values for each frequency in the T-F image resulting  $M \times 1$  values **A**.

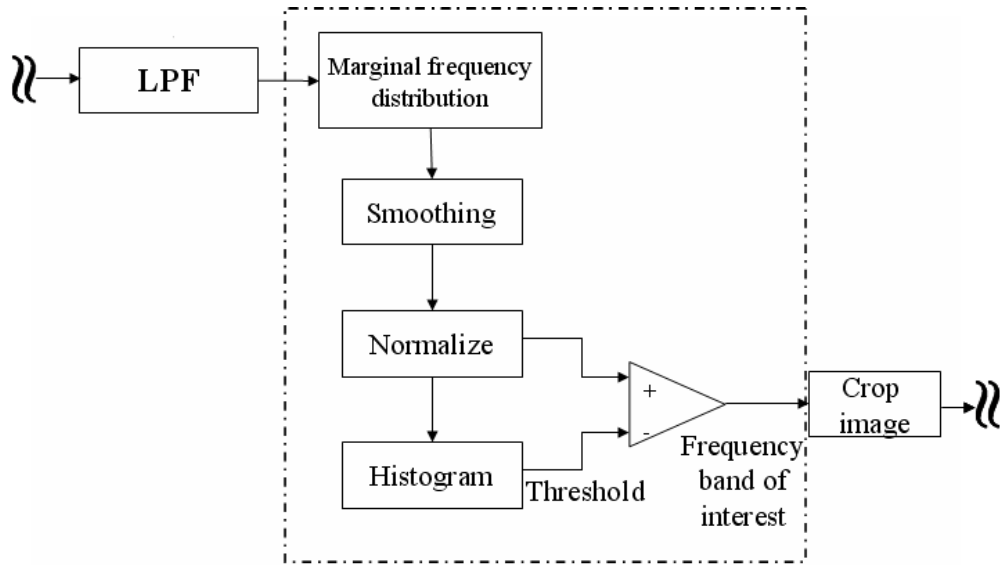


Figure 28. Determining the Frequency Band of Interest.

The MFD of a Frank coded signal with  $f_s = 7\text{kHz}$ ,  $f_c = 1495\text{Hz}$ ,  $N_c = 36$ , and  $c_{pp} = 1$  ( $B = 1495\text{ Hz}$ ) with an  $SNR = 0\text{dB}$  is shown in Figure 29.

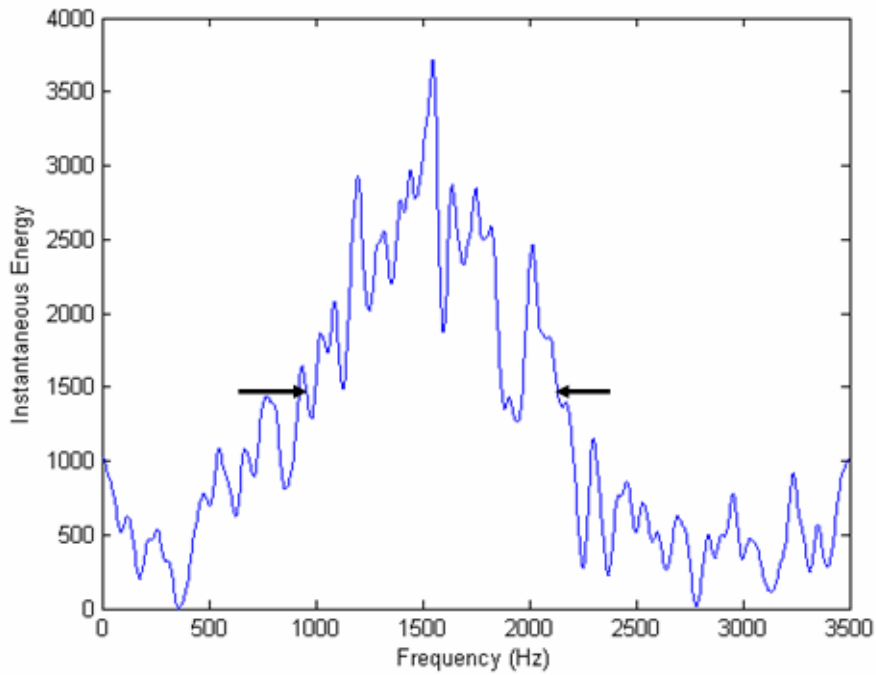


Figure 29. Marginal Frequency Distribution (MFD) of a Frank Signal with  $N_c = 36$  (From [27]).

As it can be seen from the Figure 29 the higher energy interval corresponds to the frequency band of interest which preserves the modulation energy. The goal is to isolate and crop the region of interest as accurately as possible. This is done by setting a threshold. The instantaneous energy values above the threshold can be collected and cropped. But one problem will emerge as the noise level changes; the actual position set by the threshold may change from one SNR level to another. In order to minimize this effect, a *smoothing* operation is applied on  $\mathbf{A}$  [27].

The *smoothing* is applied in two steps as shown in Figure 30. In the first step an adaptive filter is applied to attenuate the noise. In the second step a moving average filter is applied to smooth the edges and local peaks.

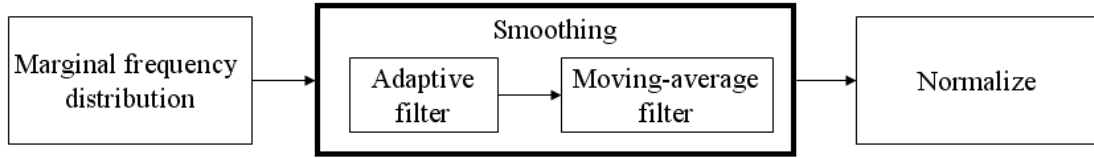


Figure 30. MFD Smoothing via Adaptive Filter & Moving-Average Filter.

An adaptive filter is a filter that changes behavior based on the statistical characteristics of the input signal within the filter. In this work a Wiener filter is applied to  $\mathbf{A}$  using the local neighborhood of size  $m$ -by-1 to estimate the local image mean and standard deviation. The filter estimates the local mean and variance around each vector element. The local mean is estimated as [42],

$$\mu = \frac{1}{m} \sum_{n \in \eta} \mathbf{A}(n) \quad (4.17)$$

and the local variance is estimated as

$$\sigma^2 = \frac{1}{m} \sum_{n \in \eta} \mathbf{A}^2(n) - \mu^2 \quad (4.18)$$



where  $\eta$  is the  $m$ -by-1 local neighborhood of each element in the vector  $\mathbf{A}$ . The Wiener filter is created element wise using these estimates. The processed image within the local neighborhood can be expressed as

$$b(n) = \mu + \frac{\sigma^2 - \nu^2}{\sigma^2} (\mathbf{A}(n) - \mu) \quad (4.19)$$

where  $\nu^2$  is the noise variance estimated using the average of all the local estimated variances. When the variance is large, the filter performs little smoothing and when the variance is small, it performs more smoothing.

For PWVD and CWD images a local neighborhood of  $\eta = 10$  is used and for QMFB images  $\eta = 4$  is used. Figure 31 shows the output of the adaptive filter for the input MFD of Frank signal with  $N_c = 36$  previously shown in Figure 29 with  $\eta = 10$ . Note that there is considerable noise attenuation.

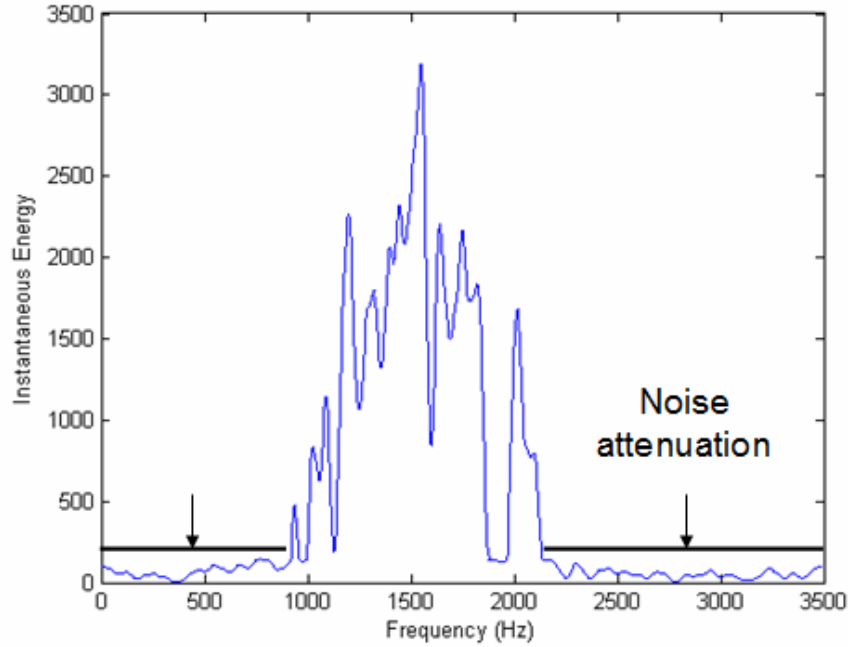


Figure 31. MFD of a Frank Coded Signal with  $N_c = 36$  after Adaptive Filtering.

Although the adaptive noise attenuation gives promising results, the threshold determination may be affected by the local noise peaks that could not be reduced by the adaptive filter. To avoid this problem a moving average filter is applied to the output of the adaptive filter. As a generalization of the average filter, averaging over  $N + M + 1$  neighboring points can be considered. The moving average filter is represented by the following difference equation [43]:

$$y(n) = \frac{1}{N + M + 1} \sum_{k=-N}^M x(n-k) \quad (4.20)$$

where  $x(n)$  is the input and  $y(n)$  is the output. The corresponding impulse response is a rectangular pulse. For PWVD and CWD images a window length of  $N + M + 1 = 10$  is used and for QMFB images  $N + M + 1 = 4$  is used. Figure 32 shows  $\tilde{\mathbf{A}}_{avg}$ , the output vector of the moving average filter with  $N + M + 1 = 10$ .

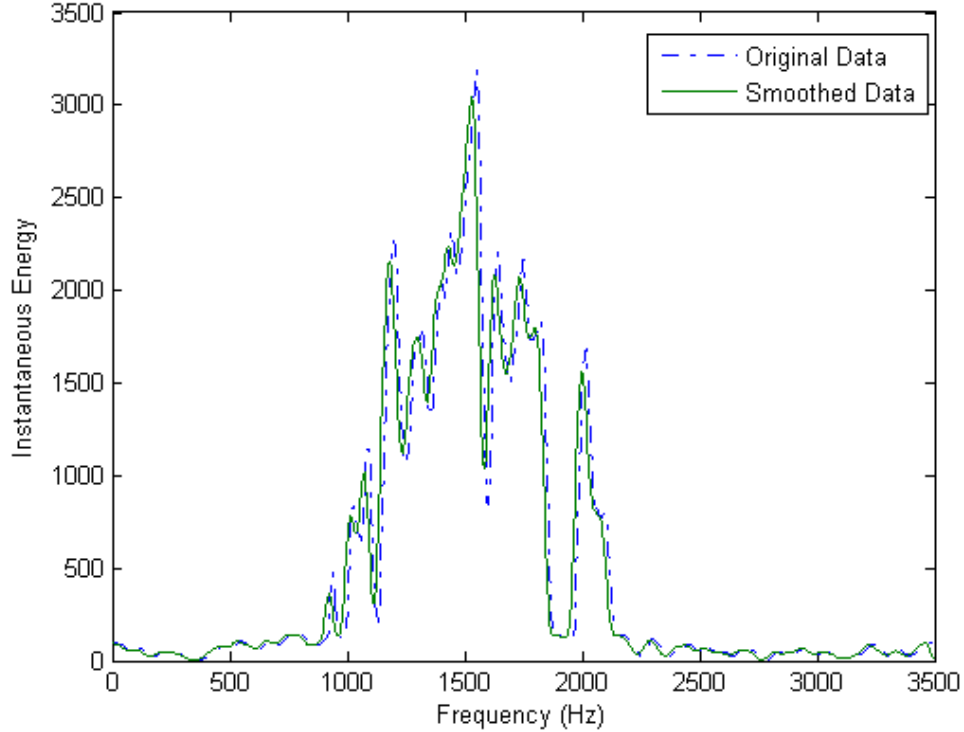


Figure 32. Output of Moving Average Filter with a Window Length of 10.

After moving average filtering, the output is normalized by the maximum value of  $\tilde{\mathbf{A}}_{avg}$  as follows,

$$\mathbf{A}_n = \frac{\tilde{\mathbf{A}}_{avg}}{\max(\tilde{\mathbf{A}}_{avg})} \quad (4.21)$$

where  $\mathbf{A}_n$  is the normalized smoothed MFD. After normalization a histogram of 100 bins is generated for PWVD and CWD images and a histogram of 30 bins is generated for QMFB images. Using these histogram bins a threshold is determined [27]. Threshold determination is illustrated in Figure 33 using the histogram of  $\mathbf{A}_n$  for the 30th bin. Note that the value corresponding to the 30th bin,  $T_h = 0.2954$  is selected as the threshold. For simulation purposes the histogram bin numbers are optimized using a range of values for each detection technique and each network. The bin number which provides the best Pcc is selected.

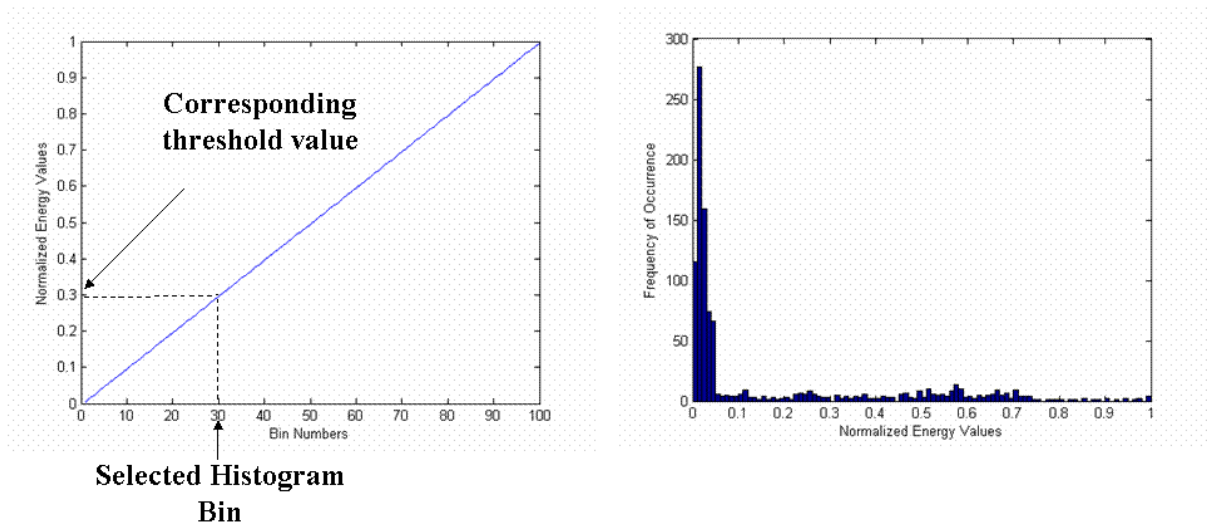


Figure 33. Threshold Determination by a Histogram.

Once the threshold is determined, the values of  $\mathbf{A}_n$  below the threshold are set to zero. Then the beginning and ending frequencies of the frequency band of interest is determined as shown in Figure 34. Using the lowest and highest frequency values from the frequency band of interest the modulation energy can now be cropped from the image.

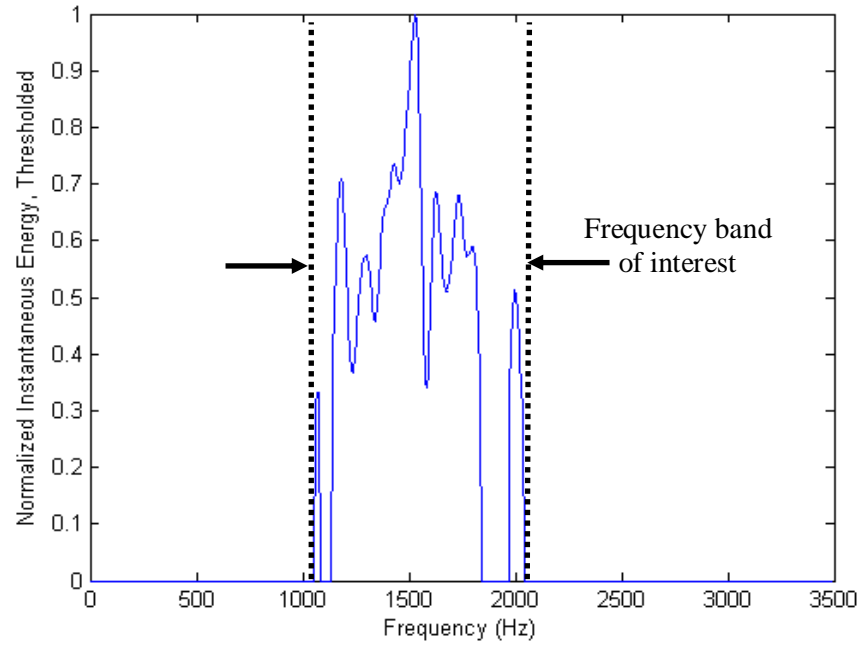


Figure 34. Frequency Band of Interest [27].

*c. Cropping and Feature Vector Generation*

The steps for cropping and feature vector generation are shown in Figure 35.

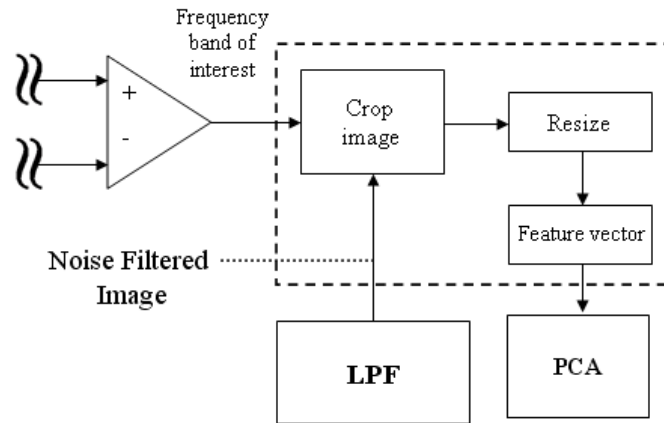


Figure 35. Autonomous Cropping and Feature Vector Generation Blockset.

After the determination of the frequency band of interest the modulation energy is autonomously cropped from the LPF output containing the noise filtered image. The cropping is illustrated in Figure 36. Figure 36 (a) shows the LPF output which is obtained previously, Figure 36 (b) shows the cropped region and Figure 36 (c) shows the contour plot where the signal energy can easily be seen. Note also the absence of the cross terms.

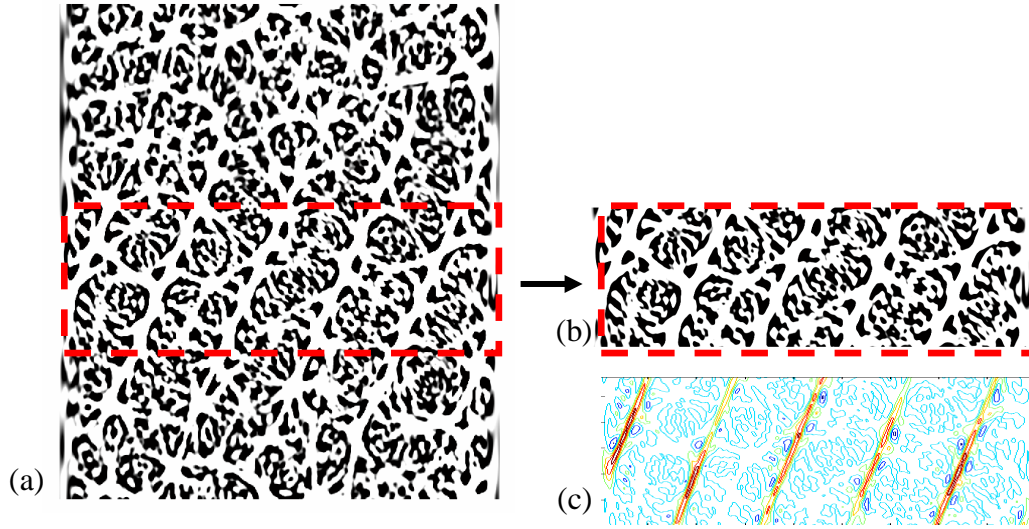


Figure 36. (a) LPF output (b) Cropped region (c) Contour Plot of the Cropped Region.

Once the LPF output is cropped, the new image is resized to  $50 \times 400$  pixels for the PWVD and CWD images. The QMFB images are resized to  $30 \times 120$  pixels. Resizing is done in order to obtain as much similarity as possible between the same modulation types. Following the resizing operation the columns of the resized image are formed the feature vector of size  $50 \times 400 = 20000$  for PWVD and CWD images, and of size  $30 \times 120 = 3600$  for QMFB images.

## 2. Principal Components Analysis

PCA is one possible approach to reduce the dimensionality of the class features. The method projects high-dimensional data vectors onto a lower dimensional space by using a projection which best represents the data in a mean square sense [44]. PCA can be viewed as a rotation of the existing axes to new positions in the space defined by the

original variables, where there is no correlation between the new variables defined by the rotation [45]. Using PCA the given data vector is represented as a linear combination of the eigenvectors obtained from the data covariance matrix. As a result, lower dimensional data vectors may be obtained by projecting the high-dimensional data vectors onto a number of dominant eigenvectors [44].

The PCA maps an ensemble of  $P$   $N$ -dimensional vectors  $\mathbf{X} = [\underline{x}_1, \underline{x}_2, \dots, \underline{x}_p]$  onto an ensemble of  $P$   $D$ -dimensional vectors  $\mathbf{Y} = [\underline{y}_1, \underline{y}_2, \dots, \underline{y}_p]$ , where  $D < N$ , using a linear transformation. This linear transformation can be represented by a rectangular matrix  $\mathbf{A}$  so that [44]

$$\mathbf{Y} = \mathbf{A}^H \mathbf{X} \quad (4.22)$$

where  $\mathbf{A}$  has orthogonal column vectors,  $i = 1, 2, \dots, P$ , and  $H$  is the Hermitian operation. For PCA, the matrix  $\mathbf{A}$  is selected as the  $P \times D$  matrix containing the  $D$  eigenvectors associated with the larger eigenvalues of the data covariance matrix  $\mathbf{X}^H \mathbf{X}$ . With such a choice of transformation matrix  $\mathbf{A}$ , the transformed data vectors  $\mathbf{Y}$  have uncorrelated components [44]

In this work the  $\mathbf{X}$  matrix is obtained first to form the training data set. The feature extraction algorithm is applied to the images in the “Training Signals” folder for each detection technique. The cropped images are resized and a column vector is formed to represent the signal modulation. These column vectors are stacked together to form the training data set matrix. Later the mean of the training matrix is calculated column wise and the mean is subtracted from the training data set matrix giving the matrix  $\mathbf{X}$ . This operation is illustrated in Figure 37.

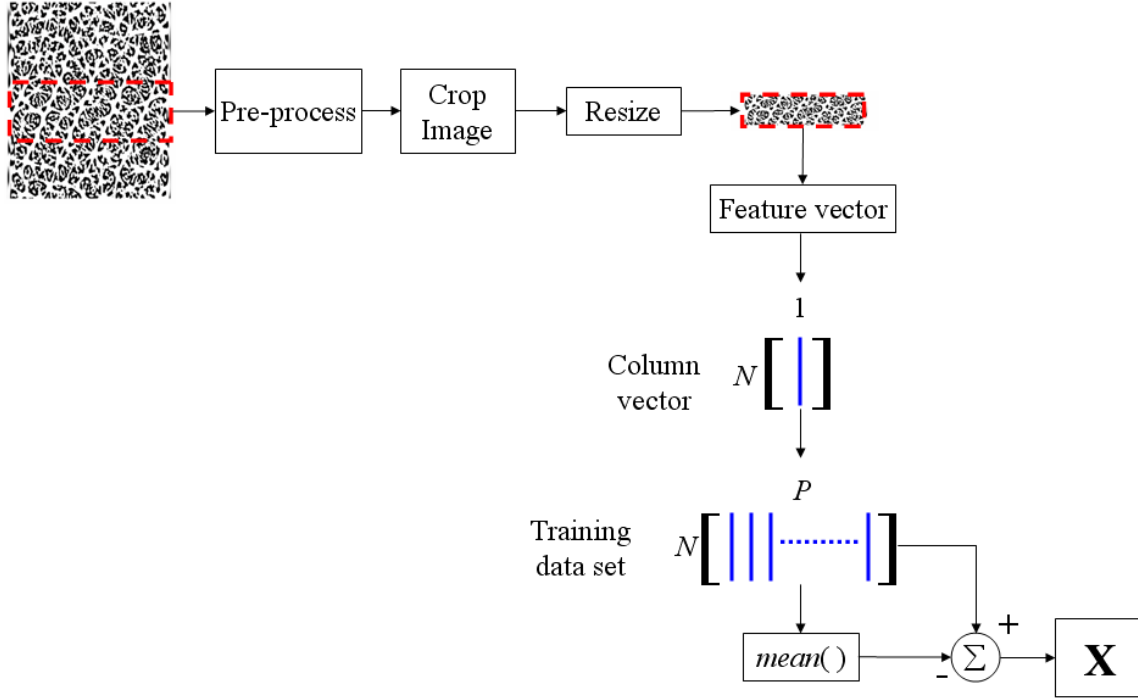


Figure 37. Training Matrix Generation (From [27]).

where  $P$  is the number of training signals which is 50 in this work, and  $N$  is the length of the feature vectors. For PWVD and CWD  $\mathbf{X}$  is of dimension  $20000 \times 50$  (50 training signals) and for QMFB  $\mathbf{X}$  is of dimension  $3600 \times 50$ .

In order to obtain the non-zero eigenvectors of  $\mathbf{X}$ , singular value decomposition (SVD) may be performed. SVD states that any  $N \times P$  matrix  $\mathbf{X}$  can be decomposed as [46]

$$\mathbf{X} = \mathbf{U} \mathbf{\Sigma} \mathbf{V}^H \quad (4.23)$$

where  $\mathbf{U}$  is the  $N \times N$  unitary matrix,  $\mathbf{V}$  is the  $P \times P$  unitary matrix and  $\mathbf{\Sigma}$  is the  $N \times P$  matrix of non-negative real singular values. Note that

$$\mathbf{X}^H \mathbf{X} = \mathbf{V} \mathbf{\Sigma}^H (\mathbf{U})^H \mathbf{U} \mathbf{\Sigma} \mathbf{V}^H = \mathbf{V} (\mathbf{\Sigma}^H \mathbf{\Sigma}) \mathbf{V}^H \quad (4.24)$$

equation (4.24) indicates that the eigenvectors of  $\mathbf{X}^H \mathbf{X}$  is contained in the  $\mathbf{V}$  matrix and the eigenvalues of  $\mathbf{X}^H \mathbf{X}$  are the squared singular values of  $\mathbf{X}$  which are the diagonal elements of the matrix  $\Sigma^H \Sigma$ . It can similarly be shown that the eigenvectors of  $\mathbf{X} \mathbf{X}^H$  are contained in the  $\mathbf{U}$  matrix.

If  $p = \min(P, N)$ , both  $\mathbf{X} \mathbf{X}^H$  and  $\mathbf{X}^H \mathbf{X}$  will have the same  $p$  non-zero eigenvalues [45]. The product of  $\mathbf{X}$  and  $\mathbf{V}$  gives

$$\mathbf{X} \mathbf{V} = \mathbf{U} \Sigma \mathbf{V}^H \mathbf{V} = \mathbf{U} \Sigma \quad (4.25)$$

since  $\mathbf{V}$  is unitary, and the eigenvectors associated with non-zero eigenvalues can be extracted by

$$\mathbf{U} = \mathbf{X} \mathbf{V} \Sigma^{-1} \quad (4.26)$$

As a result the non-zero eigenvalues of the higher dimensional covariance matrix  $\mathbf{X} \mathbf{X}^H$  may be computed by computing SVD of smaller dimensional covariance matrix [45]

$$\mathbf{X}^H \mathbf{X} \quad (4.27)$$

Following the SVD of the data matrix and determination of the eigenvector matrix  $\mathbf{U}$ , dimensionality reduction is performed using the projection (transformation) matrix  $\mathbf{A}$ . The matrix  $\mathbf{A}$  is composed of  $D$  eigenvectors selected from the eigenvector matrix  $\mathbf{U}$  corresponding to  $D$  largest eigenvalues. In order to find the  $D$  largest eigenvalues, the biggest eigenvalue is multiplied by a threshold constant and the eigenvalues above the product are taken. Let the threshold be  $Th_\lambda$  and named as *eigenvalue selection threshold constant*. Three values of  $Th_\lambda = [0.001, 0.005, 0.01]$  are used in this work. For each case, once the eigenvalues are found, four variations of eigenvector selection are used. Let these variations be  $\vee_i$ , where  $i = 0, 1, 2, 3$ . The variations are defined by the  $i$  index as follows:

$\vee_0 \rightarrow$  All the eigenvectors corresponding to the eigenvalues above  $Th_\lambda$  are used to form the matrix  $\mathbf{A}$ .



$\forall_1 \rightarrow$  All the eigenvectors corresponding to the eigenvalues above  $Th_\lambda$  are selected initially; all of them except the eigenvector corresponding to the eigenvalue with the highest value are used to form the matrix  $\mathbf{A}$ .

$\forall_2 \rightarrow$  All the eigenvectors corresponding to the eigenvalues above  $Th_\lambda$  are selected initially; all of them except the two eigenvectors corresponding to the two eigenvalues with the highest values are used to form the matrix  $\mathbf{A}$ .

$\forall_3 \rightarrow$  All the eigenvectors corresponding to the eigenvalues above  $Th_\lambda$  are selected initially; all of them except the three eigenvectors corresponding to the three eigenvalues with the highest values are used to form the matrix  $\mathbf{A}$ .

Once the projection matrix  $\mathbf{A}$  is generated, both the training matrix  $\mathbf{X}$  and the testing signals are projected onto a smaller dimensional feature space. The dataset is reduced in dimension to  $D$  using the projection process. The projected data is used later for classification.

The MATLAB functions which perform PCA is derived from [45] and implemented in the classification routines presented in this work. The PCA algorithm is shown below.

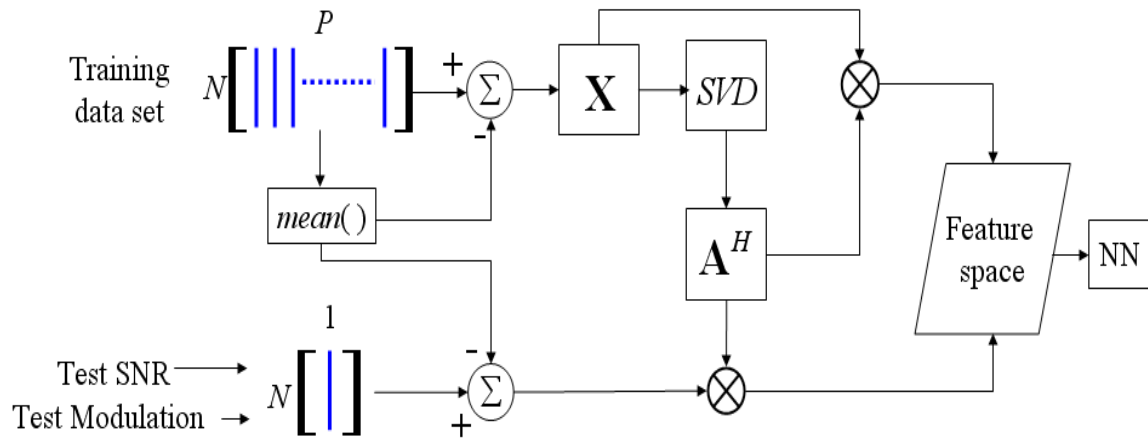


Figure 38. PCA Algorithm (From [27]).

## C. CLASSIFICATION NETWORKS

This section describes three types of non-linear classification networks. These include the multi layer perceptron (MLP), radial basis function (RBF) and probabilistic neural networks (PNN).

### 1. MLP Classifiers

The MLP is a feed-forward interconnection of individual non-linear parallel computing units called neurons [24]. A neuron is an information-processing unit that is fundamental to the operation of a neural network. Three basic elements of a neuron can be identified [47]:

1. A set of synapses or connecting links, each of which is characterized by a weight of its own.
2. An adder for summing the input signals, weighted by the respective synapses of the neuron.
3. An activation function for limiting the amplitude of the output of a neuron. The neuron may also include an externally applied bias which has the effect of increasing or lowering the net input of the activation function, depending on whether it is positive or negative, respectively.

An MLP has three distinctive characteristics [47]:

1. The model of each neuron in the network includes a nonlinear activation function.
2. The network contains one or more layers of hidden neurons that are not part of the input or output of the network.
3. The network exhibits a high degree of connectivity, determined by the synapses of the network.

In an MLP network the inputs propagate through the network in a forward direction, on a layer by layer basis. Global training of the MLP results in a non-linear mapping of the inputs at the output layer. The MLP can be described in general as [24]

$$y_k(l) = \phi \left( \sum_{h=1}^H w_{kh} \phi \left( \sum_{i=1}^I w_{hi} x_i(l) \right) \right) \quad (4.28)$$

where  $y_k$  is the output,  $x_i$  is the input,  $l$  is the sample number,  $i$  is the number of input nodes,  $h$  is the number of hidden layers and  $k$  is the output node index. Here  $w_{kh}$  and  $w_{hi}$

represent the weight value from neuron  $h$  to  $k$  and from neuron  $i$  to  $h$  respectively and  $\phi$  represents the activation function. All weight values  $w$  in the MLP are determined at the same time in a single, global (non-linear) training strategy involving supervised learning.

The activation functions  $\phi$  are monotonic and may vary for different layers of neurons. The activation function can be any type of function that fits the action desired from the respective neuron and is a design choice which depends on the specific problem. Log sigmoid and hyperbolic tangent sigmoid functions are commonly used in multi-layer neural networks with a backpropagation algorithm since they are differentiable and can form arbitrary nonlinear decision surfaces [48]. The network activation function,  $\phi$ , used in this work is a log-sigmoid defined as;

$$\phi(x) = 1/(1 + e^{-x}) \quad (4.29)$$

In this work a three-layer feed-forward neural network with  $h = 2$  hidden layers is used. The output layer has 12 neurons each of which corresponds to a modulation type. A block diagram of the three-layer feed-forward neural network is shown in Figure 39.

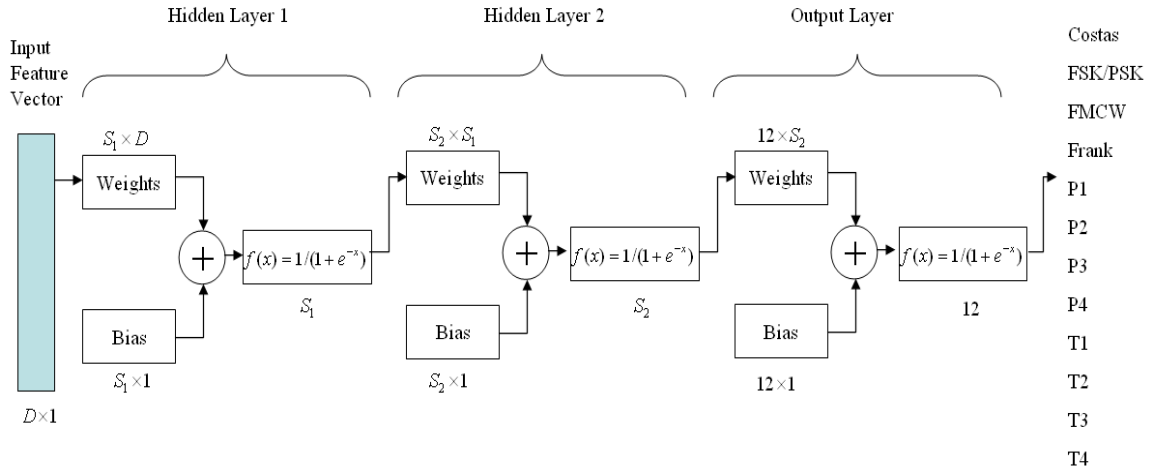


Figure 39. Block Diagram of Three-Layer Perceptron Neural Network (After [27]).

The input feature vector is the preprocessed image as described in the previous sections. The feature vector dimension  $D \times 1$  is determined after several optimizations on PCA for each detection method. Several neuron numbers for each of the hidden layers ( $h = 2$ ) are also tested to determine an optimum combination for the selected detection type.

It is shown in [49] that such an architecture can separate classes resulting from any union of polyhedral regions. This is performed by forming the hyperplanes in the first layer, forming the regions in the second layer and forming the classes in the output layer.

The supervised training of this feed-forward MLP network uses the gradient of the performance function to determine how to adjust the weights. The gradient is determined using a technique called backpropagation [50]. The backpropagation algorithm is a generalization of the least mean square algorithm used for linear networks, where the performance index is the mean square error. Basically, a training sequence is passed through the multi-layer network, the error between the target output and the actual output is computed, and the error is then propagated back through the hidden layers from the output to the input in order to update weights and biases in all layers [48].

Different modifications of training algorithms may improve the convergence speed of the network. One of these modifications is the variable learning rate which is also used in this work. With standard steepest descent, the learning rate held constant throughout training. The performance of the algorithm is very sensitive to the proper setting of the learning rate. The performance of the steepest descent algorithm is improved when the learning rate is allowed to change during the training process which is a variable learning rate [50].

To improve the network generalization, regularization was used. The network regularization  $R$  was measured using

$$R = gM_{SE} + (1 - g)M_{SW} \quad (4.30)$$

where  $g$  is a performance ratio ( $g = 0.7$ ),  $M_{se}$  is the mean sum of squares of the network errors and  $M_{sw}$  is the mean sum of squares of the network weights and biases. The regularization performance goal was set to  $R = 7 \times 10^{-10}$ . For each training set, several training iterations (*epochs*) are tested to find an optimum value.

## 2. RBF Classifier

Radial basis functions (RBFs) consist of three layer of nodes: the input layer where the inputs are applied, the output layer where the outputs are produced, and a hidden layer where the RBFs are applied on the input data. RBFs are so named because they have radial symmetry. Gaussian functions at the hidden layer with appropriate mean and autocovariance matrices are popular choice of RBFs [51].

The hidden layer of an RBF neural network (RBFNN) is nonlinear, whereas the output layer is linear. The argument of the activation function of each hidden unit computes the Euclidean norm (distance) between the input vector and the center of the unit. Using exponentially decaying localized nonlinearities, RBFs construct local approximations to nonlinear input-output mappings [47].

The structure of RBFNN for D-dimensional input and one output is shown in Figure 40.

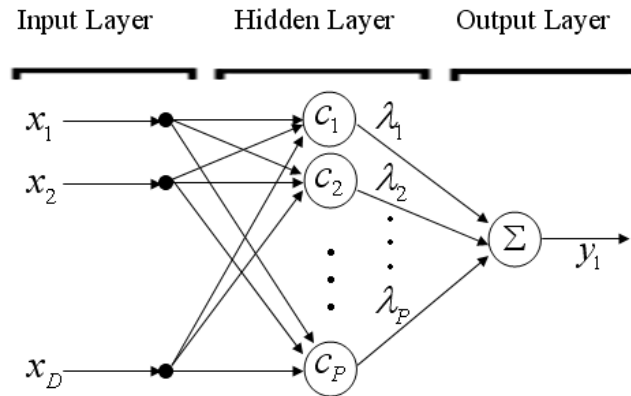


Figure 40. Block Diagram of Radial Basis Function Neural Network with One Output (After [52]).

where the input-output relations are implemented as follows [52]:

$$F(\boldsymbol{\lambda}; \mathbf{C}; \mathbf{x}) = \sum_{j=1}^P \lambda_j \phi(\|\mathbf{x} - \mathbf{c}_j\|) \quad (4.31)$$

where  $j=1, \dots, P$ ,  $\mathbf{x}$  is the input vector,  $\boldsymbol{\lambda}$  is the linear weight matrix between the radial basis layer and the output layer,  $\phi$  is the radial basis function and  $\mathbf{C}$  is a center matrix whose columns are the centers of RBFNN with its spread predetermined. These columns  $\mathbf{c}_j$  are also called the center vectors. Note that the center vectors are also the weight vectors of the radial basis layer. The radial basis function is given by the Gaussian function:

$$\phi(\|\mathbf{x} - \mathbf{c}\|) = e^{-\left(\frac{\|\mathbf{x} - \mathbf{c}\|}{\sigma}\right)^2} \quad (4.32)$$

where  $\sigma$  is the spread of the basis function. The basis function described above indicates that the center vectors  $\mathbf{C}$  are fixed points in  $D$ -dimensional input space.

In this work two approaches of RBFNNs are used. In the first approach an efficient design is implemented by iteratively creating the RBFNN one neuron at a time. Neurons are added to the network until the sum-squared error falls beneath an error goal or a maximum number of neurons has been reached [50].

Two design parameters need to be optimized to obtain a better classification probability. These are the *goal* and *spread*  $\sigma$ . The spread constant should be larger than the distance between adjacent input vectors, so as to get a good generalization, but smaller than the distance across the whole input space [50]. This network is implemented in MATLAB using the function *newrb*.

In the second approach a probabilistic neural network (PNN) is used which is a variant of RBFNN. The radial basis layer of the PNN is identical with the RBFNNs. The weight vectors in the radial basis layer of the RBFNN are equal to center vectors  $\mathbf{c}_j (j=1, \dots, P)$  in radial basis function. Note that  $P$  is the node number in the radial basis hidden layer [53].

The difference between the PNN and the RBFNN is that the nodes in the second layer make a sum calculation and form a link with the selective nodes of the first layer. The weight matrix  $\lambda$  is set to the matrix  $\mathbf{T}$  of target vectors. Each vector has a one only in the row associated with that particular class of input, and zeros elsewhere. The output is later found by finding the maximum of  $y_i (i = 1, \dots, K)$  where  $K$  is the total number of input classes as shown in Figure 41.

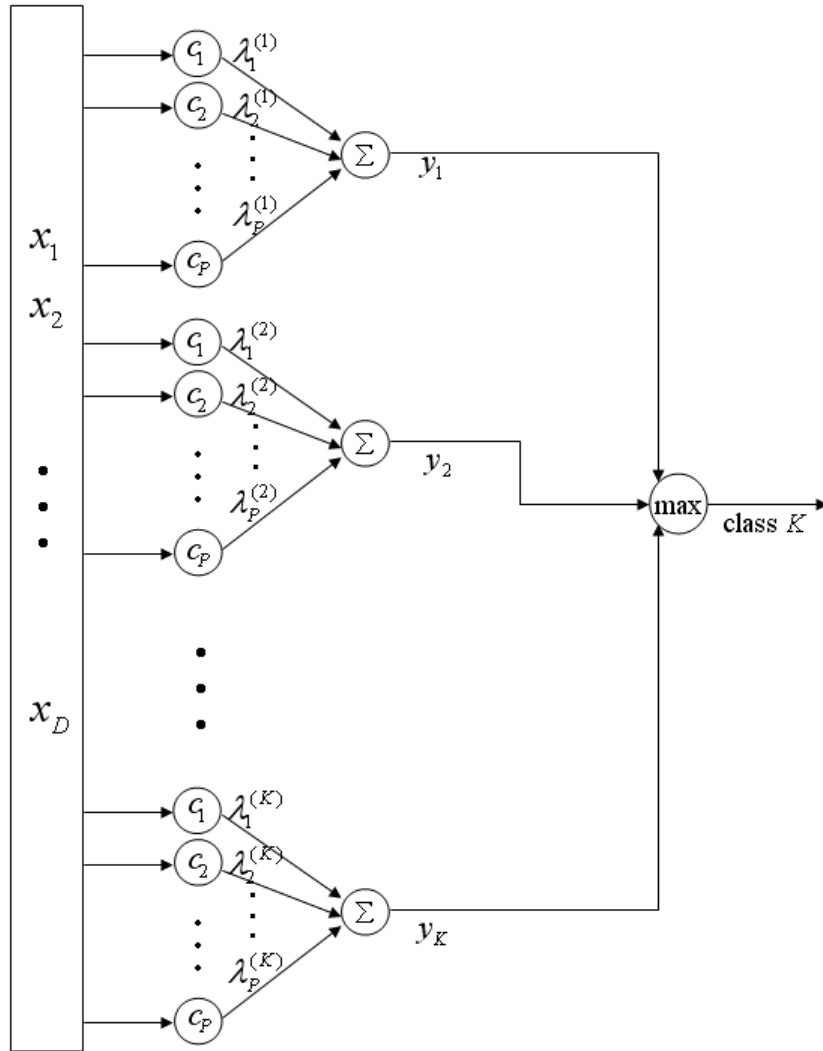


Figure 41. Block Diagram of Probabilistic Neural Network (After [54]).

Thus, the network classifies the input vector into a specific one of  $K$  classes because that class had the maximum probability of being correct [50]. The design parameter *spread*  $\sigma$ , needs to be optimized for a higher  $P_{cc}$ . This network is implemented in MATLAB using the function *newpnn*.

Two major differences between RBFNNs and MLP neural networks (MLPNN) are [51]

- RBFs provide a nonzero output for portions of the input space that is closely concentrated around the center of RBF while this is not true for the activation functions used in the hidden layers of the MLPNN.
- If the parameters of the RBFs are chosen a priori, then the learning of the weights can focus only on the weight parameters converging to the output layer of the RBFNN. Hence, the convergence to a solution for such an RBFNN can be very fast than the MLP.

The only disadvantage of RBF network is that the number of weights increases exponentially with the number of inputs and outputs. It often requires as many hidden nodes as the number of data sets used for learning. This may lead to the problem of being overdetermined [52].

#### **D. CLASSIFICATION RESULTS**

This section presents the classification results for T-F detection techniques with three classifier networks. Using initial network parameters two feature extraction parameters, the LPF cutoff frequencies and histogram bin, are optimized. Later using the optimum LPF cutoff frequency and histogram bin the PCA network parameters are optimized. The simulation is performed with the final optimum values. The optimization is performed using the test signals with an SNR of 10 dB. The optimum parameter selection is based on the highest average probability of correct classification.

Two tests were run for each classifier. The first test uses the signals presented in Table 1 which are referred as to *Test SNR*. These signals have the same modulation parameters with the signals used for training purpose but their *SNR* is varied as  $-10\text{dB} \leq \text{SNR} \leq 10\text{ dB}$ .



The second test uses the signals shown in Table 2. These signals have different modulation parameters from the training signals which are referred as to *Test Modulation*. Note that this test is more important and more difficult than the first test. The *SNR* is also varied as  $-10\text{dB} \leq \text{SNR} \leq 10\text{ dB}$  for these signals.

To build the classification statistics 100 test runs were used. Before each test, networks were reinitialized with the optimum network parameters to randomize the weight matrices. Two CMs were created for each classification test for each *SNR* level. One of the CMs shows the results for Test SNR and the other shows the results for Test Modulation.

## 1. Optimization of Feature Extraction and Network Parameters

### a. Optimization for MLPNN

For each detection technique, first the network is set using initial values for the parameters of *epochs*, number of neurons in the first hidden layer  $S_1$ , number of neurons in the second hidden layer  $S_2$ , eigenvalue selection threshold constant  $Th_\lambda$  and eigenvector selection variations  $\vee_i$ . Once the initial values are set, an optimization is performed to determine optimum values for 2-D FFT frequency domain LPF digital frequencies  $\omega_1, \omega_2$  (it is selected so that  $\omega_1 = \omega_2$ ) and histogram bin number. After these two values are found and set, another optimization for *epochs*,  $S_1$ ,  $S_2$ ,  $Th_\lambda$  and  $\vee_i$  is performed. Once all the values are found and set the classification network is tested.

For the classification of PWVD images the initial values used are  $Th_\lambda = 0.001$ ,  $\vee_0$ , *epochs* = 6000,  $S_1 = 50$  and  $S_2 = 50$ . Figure 42 shows the average *Pcc* results for five digital frequency ( $\omega_1, \omega_2$ ) values between  $0.1\pi$  and  $0.5\pi$  and fourteen bin numbers between 5 and 70 for each digital frequency value. Both Test Modulation and Test SNR classification results are evaluated. The optimum values are determined as  $\omega_1 = \omega_2 = 0.1\pi$  and *bin number* = 45.

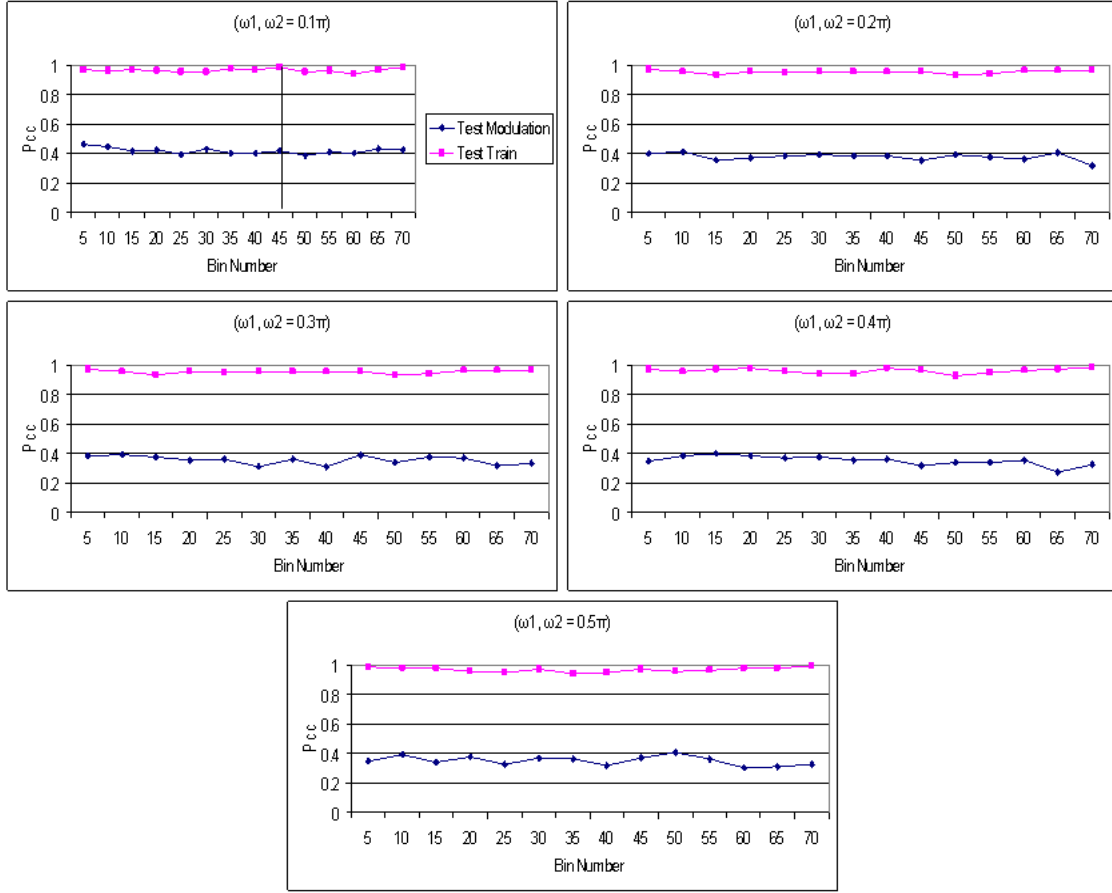


Figure 42. Optimization of  $\omega_1$ ,  $\omega_2$  and Bin Number for PWVD image classification with MLPNN.

Using the values  $\omega_1 = \omega_2 = 0.1\pi$  and  $bin\ number = 45$   $S_1$ ,  $S_2$ ,  $Th_\lambda$  and  $\vee_i$  are optimized. Figure 43 shows the average  $Pcc$  results for three values of eigenvalue selection threshold constant  $Th_\lambda$ , four values of eigenvector selection variations  $\vee_i$  for each  $Th_\lambda$  value and 10 combinations of hidden layer variations for each  $\vee_i$  value. The hidden layer combinations are shown in Table 3. This combination set is also used for the initialization of MLPNN for CWD and QMFB image classification.

Table 3. Combinations of Neuron Numbers in the Hidden Layers.

	<b>Combination</b>									
<b>Hidden Layers</b>	1	2	3	4	5	6	7	8	9	10
$S_1$ (# of neurons)	40	40	50	50	60	60	70	70	80	80
$S_2$ (# of neurons)	35	40	45	50	55	60	65	70	75	80

As shown in Figure 43 the combination 10 gave the optimum result with  $S_1 = 80$ ,  $S_2 = 80$ ,  $Th_\lambda = 0.001$  and  $\vee_1$ . Using these parameters the MLPNN is set again and the network is tested for five epoch values where  $epochs = 2000, 3000, 4000, 5000, 6000$  are used. The best result is obtained with  $epochs = 5000$ . Final optimum values for PWVD image classification with MLPNN is shown in Table 4.

Table 4. Optimum Values for PWVD image classification with MLPNN.

$\omega_1 = \omega_2$	<i>Bin number</i>	$S_1$	$S_2$	$Th_\lambda$	$\vee_i$	<i>epochs</i>
$0.1\pi$	45	80	80	0.001	$\vee_1$	5000

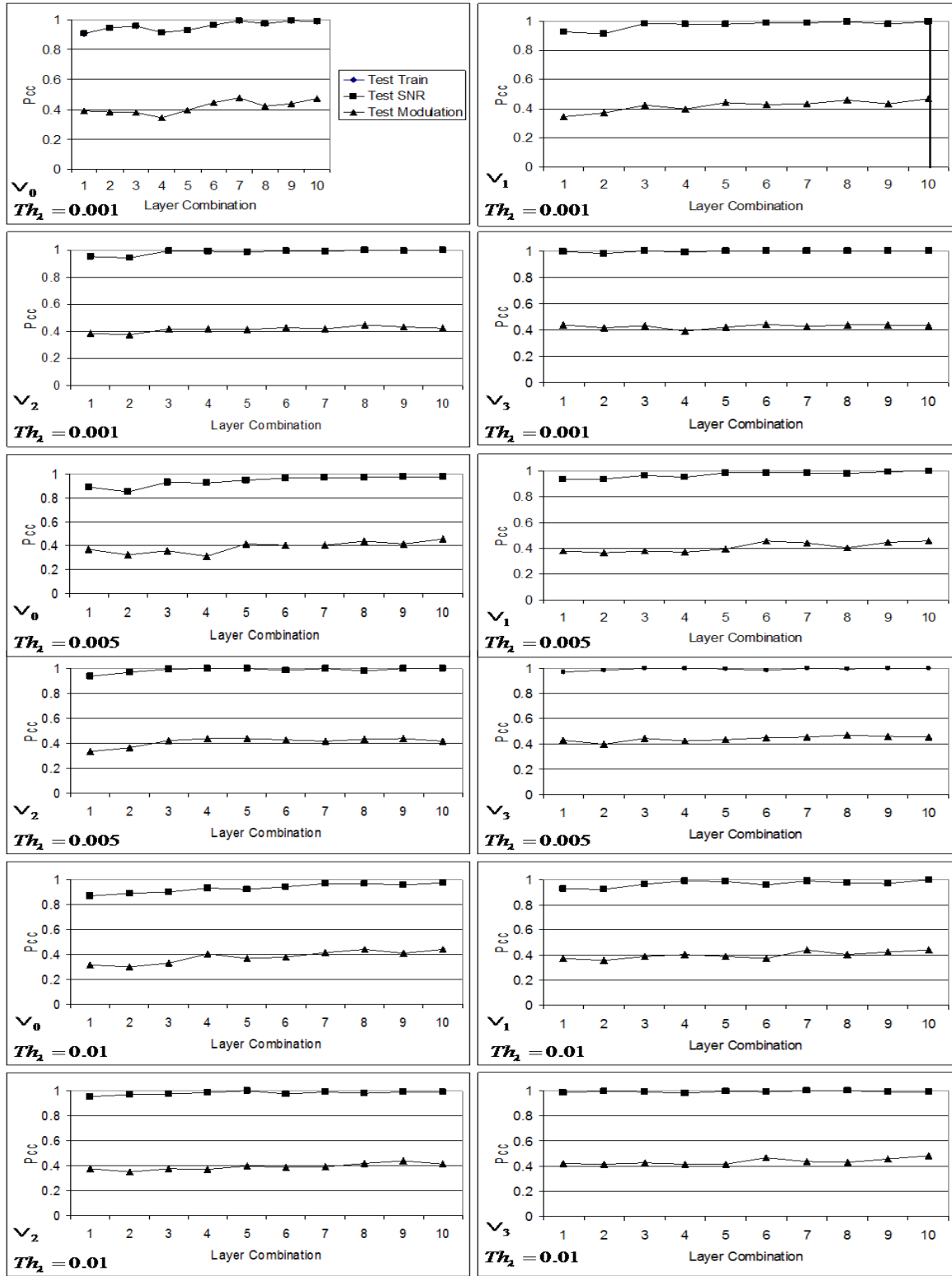


Figure 43. Optimization of  $S_1$ ,  $S_2$ ,  $Th_\lambda$  and  $v_i$  for PWVD image classification with MLPNN.

For the classification of CWD images the initial values used are  $Th_\lambda = 0.001$ ,  $\vee_0$ ,  $epochs = 5000$ ,  $S_1 = 60$  and  $S_2 = 60$ . The optimization charts for the rest of the networks are presented in Appendix A, Section A, Figure 69 shows the average  $Pcc$  results for five digital frequency  $(\omega_1, \omega_2)$  values between  $0.1\pi$  and  $0.5\pi$  and fourteen bin numbers between 5 and 70 for each digital frequency value for the classification of CWD images with MLPNN. The optimum values are determined as  $\omega_1 = \omega_2 = 0.1\pi$  and  $bin\ number = 15$ .

Using the values  $\omega_1 = \omega_2 = 0.1\pi$  and  $bin\ number = 15$ ,  $S_1$ ,  $S_2$ ,  $Th_\lambda$  and  $\vee_i$  are optimized. Appendix A, Section A, Figure 70 shows the average  $Pcc$  results for three values of eigenvalue selection threshold constant  $Th_\lambda$ , four values of eigenvector selection variations  $\vee_i$  for each  $Th_\lambda$  value and 10 combinations of hidden layer variations for each  $\vee_i$  value. As shown in Appendix A, Section A, Figure 70 the combination 10 gave the optimum result with  $S_1 = 80$ ,  $S_2 = 80$ ,  $Th_\lambda = 0.001$  and  $\vee_0$ . Using these parameters the MLPNN is set again and the network is tested for five epoch values where  $epochs = 2000, 3000, 4000, 5000, 6000$  are used. The best result is obtained with  $epochs = 6000$ . Final optimum values for CWD image classification with MLPNN is shown in Table 5.

Table 5. Optimum Values for CWD image classification with MLPNN.

$\omega_1 = \omega_2$	<i>Bin number</i>	$S_1$	$S_2$	$Th_\lambda$	$\vee_i$	<i>epochs</i>
$0.1\pi$	15	80	80	0.001	$\vee_0$	6000

For the classification of QMFB images the initial values used are  $Th_\lambda = 0.001$ ,  $\vee_0$ ,  $epochs = 5000$ ,  $S_1 = 60$  and  $S_2 = 60$ . Appendix A, Section A, Figure 71 shows the average  $Pcc$  results for five digital frequency  $(\omega_1, \omega_2)$  values between  $0.4\pi$  and  $0.8\pi$  and twelve bin numbers between 2 and 24 for each digital frequency value for the classification of QMFB images with MLPNN. Note that the digital frequency range

for QMFB is different from WVD and CWD and it has higher values. LPF with a small cutoff frequency cause very high information losses in the QMFB images. Since QMFB images are partially filtered from noise at the output of the filter bank, when the filter cutoff frequency is small, the filtering is mostly applied on the modulation information within the QMFB image. Another reason is that QMFB images have a small dimension which affects the filtering process. Due to the small dimensionality, filtering causes much information loss than the PWVD and CWD images which have very high dimensional images compared to the QMFB images. As it can be seen from Appendix A, Section A, Figure 71 the optimum values are determined as  $\omega_1 = \omega_2 = 0.4\pi$  and  $bin\ number = 18$ .

Using the values  $\omega_1 = \omega_2 = 0.4\pi$  and  $bin\ number = 18$ ,  $S_1$ ,  $S_2$ ,  $Th_\lambda$  and  $\vee_i$  are optimized. Appendix A, Section A, Figure 72 shows the average  $Pcc$  results for three values of eigenvalue selection threshold constant  $Th_\lambda$ , four values of eigenvector selection variations  $\vee_i$  for each  $Th_\lambda$  value and 10 combinations of hidden layer variations for each  $\vee_i$  value. As shown in Appendix A, Section A, Figure 72 the combination 6 gave the optimum result with  $S_1 = 60$ ,  $S_2 = 60$ ,  $Th_\lambda = 0.005$  and  $\vee_0$ . Using these parameters the MLPNN is set again and the network is tested for five epoch values where  $epochs = 2000, 3000, 4000, 5000, 6000$  are used. The best result is obtained with  $epochs = 5000$ . Final optimum values for QMFB image classification with MLPNN is shown in Table 6.

Table 6. Optimum Values for QMFB image classification with MLPNN.

$\omega_1 = \omega_2$	<i>Bin number</i>	$S_1$	$S_2$	$Th_\lambda$	$\vee_i$	<i>epochs</i>
$0.4\pi$	18	60	60	0.005	$\vee_0$	5000

#### ***b. Optimization for RBFNN***

For each detection technique, first the network is set using initial values for the parameters *spread*  $\sigma$ , *goal*,  $Th_\lambda$  and  $\vee_i$ . Once the initial values are set, an optimization is performed to determine optimum values for 2-D FFT frequency domain

LPF digital frequencies  $\omega_1, \omega_2$  (it is selected so that  $\omega_1 = \omega_2$ ) and histogram bin number. After these two values are found and set, another optimization for  $\sigma$ ,  $goal$ ,  $Th_\lambda$  and  $\vee_i$  is performed. Once all the values are found and set the classification network is tested.

For the classification of PWVD images the initial values used are  $Th_\lambda = 0.001$ ,  $\vee_0$ ,  $\sigma = 2000$  and  $goal = 1$ . Appendix A, Section B, Figure 73 shows the average  $Pcc$  results for five digital frequency ( $\omega_1, \omega_2$ ) values between  $0.1\pi$  and  $0.5\pi$  and fourteen bin numbers between 5 and 70 for each digital frequency value for the classification of PWVD images with RBFNN. The optimum values are determined as  $\omega_1 = \omega_2 = 0.2\pi$  and  $bin\ number = 55$ .

Using the values  $\omega_1 = \omega_2 = 0.2\pi$  and  $bin\ number = 55$   $\sigma$ ,  $goal$ ,  $Th_\lambda$  and  $\vee_i$  are optimized. Appendix A, Section B, Figure 74 shows the average  $Pcc$  results for three values of eigenvalue selection threshold constant  $Th_\lambda$ , four values of eigenvector selection variations  $\vee_i$  for each  $Th_\lambda$  value and 8 values of  $\sigma$  between 500 and 4000 for each  $\vee_i$  value. As shown in Appendix A, Section B, Figure 74 the spread constant  $\sigma = 2000$  gave the optimum result with  $Th_\lambda = 0.001$  and  $\vee_0$ . Using these parameters the RBFNN is set again and the network is tested for  $goal$  values between 0.2 and 2. The best result is obtained with  $goal = 0.9$ . Final optimum values for PWVD image classification with MLPNN is shown in Table 7.

Table 7. Optimum Values for PWVD image classification with RBFNN.

$\omega_1 = \omega_2$	<i>Bin number</i>	$\sigma$	<i>goal</i>	$Th_\lambda$	$\vee_i$
$0.2\pi$	55	2000	0.9	0.001	$\vee_0$

For the classification of CWD images the initial values used are  $Th_\lambda = 0.001$ ,  $\vee_0$ ,  $\sigma = 4000$  and  $goal = 1$ . Appendix A, Section B, Figure 75 shows the average  $Pcc$  results for five digital frequency ( $\omega_1, \omega_2$ ) values between  $0.1\pi$  and  $0.5\pi$

and fourteen bin numbers between 5 and 70 for each digital frequency value for the classification of CWD images with RBFNN. The optimum values are determined as  $\omega_1 = \omega_2 = 0.5\pi$  and  $bin\ number = 55$ .

Using the values  $\omega_1 = \omega_2 = 0.5\pi$  and  $bin\ number = 55$   $\sigma$ ,  $goal$ ,  $Th_\lambda$  and  $\vee_i$  are optimized. Appendix A, Section B, Figure 76 shows the average  $Pcc$  results for three values of eigenvalue selection threshold constant  $Th_\lambda$ , four values of eigenvector selection variations  $\vee_i$  for each  $Th_\lambda$  value and 8 values of  $\sigma$  between 2500 and 6000 for each  $\vee_i$  value. As shown in Appendix A, Section B, Figure 76 the spread constant  $\sigma = 3500$  gave the optimum result with  $Th_\lambda = 0.001$  and  $\vee_0$ . Using these parameters the RBFNN is set again and the network is tested for  $goal$  values between 0.2 and 2. The best result is obtained with  $goal = 0.9$ . Final optimum values for CWD image classification with MLPNN is shown in Table 8.

Table 8. Optimum Values for CWD image classification with RBFNN.

$\omega_1 = \omega_2$	$Bin\ number$	$\sigma$	$goal$	$Th_\lambda$	$\vee_i$
$0.5\pi$	55	3500	0.9	0.001	$\vee_0$

For the classification of QMFB images the initial values used are  $Th_\lambda = 0.001$ ,  $\vee_0$ ,  $\sigma = 30$  and  $goal = 1$ . Appendix A, Section B, Figure 77 shows the average  $Pcc$  results for five digital frequency ( $\omega_1, \omega_2$ ) values between  $0.4\pi$  and  $0.8\pi$  and 12 bin numbers between 2 and 24 for each digital frequency value for the classification of QMFB images with RBFNN. The optimum values are determined as  $\omega_1 = \omega_2 = 0.6\pi$  and  $bin\ number = 4$ .

Using the values  $\omega_1 = \omega_2 = 0.6\pi$  and  $bin\ number = 4$   $\sigma$ ,  $goal$ ,  $Th_\lambda$  and  $\vee_i$  are optimized. Appendix A, Section B, Figure 78 shows the average  $Pcc$  results for three values of eigenvalue selection threshold constant  $Th_\lambda$ , four values of eigenvector



selection variations  $\vee_i$  for each  $Th_\lambda$  value and 14 values of  $\sigma$  between 5 and 70 for each  $\vee_i$  value. As shown in Appendix A, Section B, Figure 78 the spread constant  $\sigma = 25$  gave the optimum result with  $Th_\lambda = 0.001$  and  $\vee_0$ . Using these parameters the RBFNN is set again and the network is tested for *goal* values between 0.2 and 2. The best result is obtained with 0.8. Final optimum values for QMFB image classification with MLPNN is shown in Table 9.

Table 9. Optimum Values for QMFB image classification with RBFNN.

$\omega_1 = \omega_2$	<i>Bin number</i>	$\sigma$	<i>goal</i>	$Th_\lambda$	$\vee_i$
$0.6\pi$	4	25	0.8	0.001	$\vee_0$

### c. Optimization for PNN

For each detection technique, first the network is set using initial values for the parameters *spread*  $\sigma$ ,  $Th_\lambda$  and  $\vee_i$ . Once the initial values are set, an optimization is performed to determine optimum values for 2-D FFT frequency domain LPF digital frequencies  $\omega_1, \omega_2$  (it is selected so that  $\omega_1 = \omega_2$ ) and histogram bin number. After these two values are found and set, another optimization for  $\sigma$ ,  $Th_\lambda$  and  $\vee_i$  is performed. Once all the values are found and set the classification network is tested.

For the classification of PWVD images the initial values used are  $Th_\lambda = 0.001$ ,  $\vee_0$  and  $\sigma = 50$ . Appendix A, Section C, Figure 79 shows the average *Pcc* results for five digital frequency ( $\omega_1, \omega_2$ ) values between  $0.1\pi$  and  $0.5\pi$  and fourteen bin numbers between 5 and 70 for each digital frequency value for the classification of PWVD images with PNN. The optimum values are determined as  $\omega_1 = \omega_2 = 0.2\pi$  and *bin number* = 50.

Using the values  $\omega_1 = \omega_2 = 0.2\pi$  and *bin number* = 50  $\sigma$ ,  $Th_\lambda$  and  $\vee_i$  are optimized. Appendix A, Section C, Figure 80 shows the average *Pcc* results for three values of eigenvalue selection threshold constant  $Th_\lambda$ , four values of eigenvector

selection variations  $\vee_i$  for each  $Th_\lambda$  value and 20 values of  $\sigma$  between 10 and 200 for each  $\vee_i$  value. As shown in Appendix A, Section C, Figure 80 the spread constant  $\sigma = 70$  gave the optimum result with  $Th_\lambda = 0.001$  and  $\vee_0$ . Final optimum values for PWVD image classification with PNN is shown in Table 10.

Table 10. Optimum Values for PWVD image classification with PNN.

$\omega_1 = \omega_2$	<i>Bin number</i>	$\sigma$	$Th_\lambda$	$\vee_i$
$0.2\pi$	50	70	0.001	$\vee_0$

For the classification of CWD images the initial values used are  $Th_\lambda = 0.001$ ,  $\vee_0$  and  $\sigma = 100$ . Appendix A, Section C, Figure 81 shows the average *Pcc* results for five digital frequency ( $\omega_1, \omega_2$ ) values between  $0.1\pi$  and  $0.5\pi$  and fourteen bin numbers between 5 and 70 for each digital frequency value for the classification of CWD images with PNN. The optimum values are determined as  $\omega_1 = \omega_2 = 0.3\pi$  and *bin number* = 70.

Using the values  $\omega_1 = \omega_2 = 0.3\pi$  and *bin number* = 70  $\sigma$ ,  $Th_\lambda$  and  $\vee_i$  are optimized. Appendix A, Section C, Figure 82 shows the average *Pcc* results for three values of eigenvalue selection threshold constant  $Th_\lambda$ , four values of eigenvector selection variations  $\vee_i$  for each  $Th_\lambda$  value and 20 values of  $\sigma$  between 10 and 200 for each  $\vee_i$  value. As shown in Appendix A, Section C, Figure 82 the spread constant  $\sigma = 130$  gave the optimum result with  $Th_\lambda = 0.001$  and  $\vee_0$ . Final optimum values for CWD image classification with PNN is shown in Table 11.

Table 11. Optimum Values for CWD image classification with PNN.

$\omega_1 = \omega_2$	<i>Bin number</i>	$\sigma$	$Th_\lambda$	$\vee_i$
$0.3\pi$	70	130	0.001	$\vee_0$

For the classification of QMFB images the initial values used are  $Th_\lambda = 0.001$ ,  $\vee_0$  and  $\sigma = 2$ . Appendix A, Section C, Figure 83 shows the average *Pcc* results for five digital frequency ( $\omega_1, \omega_2$ ) values between  $0.4\pi$  and  $0.8\pi$  and 12 bin numbers between 2 and 24 for each digital frequency value for the classification of QMFB images with PNN. The optimum values are determined as  $\omega_1 = \omega_2 = 0.8\pi$  and *bin number* = 16.

Using the values  $\omega_1 = \omega_2 = 0.8\pi$  and *bin number* = 16  $\sigma$ ,  $Th_\lambda$  and  $\vee_i$  are optimized. Appendix A, Section C, Figure 84 shows the average *Pcc* results for three values of eigenvalue selection threshold constant  $Th_\lambda$ , four values of eigenvector selection variations  $\vee_i$  for each  $Th_\lambda$  value and 14 values of  $\sigma$  between 0.25 and 3.5 for each  $\vee_i$  value. As shown in Appendix A, Section C, Figure 84 the spread constant  $\sigma = 2$  gave the optimum result with  $Th_\lambda = 0.005$  and  $\vee_0$ . Final optimum values for QMFB image classification with PNN is shown in Table 12.

Table 12. Optimum Values for QMFB image classification with PNN.

$\omega_1 = \omega_2$	<i>Bin number</i>	$\sigma$	$Th_\lambda$	$\vee_i$
$0.8\pi$	16	2	0.005	$\vee_0$

The following sections present the test results for the detection and classification architecture. The results are presented using two approaches. In the first approach the results are presented under a classification network showing the differences between the detection techniques and in the second approach the results are presented under a

detection technique showing the differences between classification networks. These approaches help the comparative relationship to better be seen. Both Test SNR and Test Modulation results are shown in charts for each LPI modulation type.

Test SNR results provide an understanding on the performance of autonomous modulation energy isolation and cropping and the performance of noise reduction as well. On the other hand Test Modulation results provide an understanding on the performance of feature extraction algorithm such as its modulation discriminative ability.

## 2. Classification Results with MLPNN

The classification results for each LPI radar waveform with three detection techniques are shown in Figures 44 and 45. The CMs which include more details about the MLPNN classification results are presented in Appendix B.A for  $SNR = 10, 6, 3, 0, -3, -6$  dB (Tables 13-30).

All the detection techniques show similar results on Test SNR case. Most of the modulations are classified with more than 80% classification rate for  $SNR > 0$  dB. There is a considerable stability in classification of signals with  $SNR > 0$  dB. This stability states that the autonomous modulation energy isolation and cropping becomes more sensitive to noise variations below  $SNR = 0$  dB. The  $P_{cc}$  of Frank, FSK/PSK, FMCW, T1, T2 and T4 modulations with PWVD and CWD techniques exhibit 100% for most of the SNR levels above 0 dB.

Concerning the Test Modulation case, the best results are obtained in the classification of FMCW, Costas, FSK/PSK, P2 and T2 modulations while the worst results are obtained in the classification of polyphase codes. Note that most of the results for Frank, P1, P3 and P4 modulations are below  $P_{cc} = 0.4$ . Classification of Costas, FSK/PSK, FMCW, P2, P4, T1, T2, T3 and T4 modulations with PWVD and CWD techniques exhibit similar results. Overall, the classification results with the PWVD technique outperform the other detection techniques.

While the QMFB technique performs worse than the other techniques it outperforms the other techniques in the classification of T2 and T4 modulations for  $SNR > 5\text{dB}$ . Recall that the QMFB images have a very low resolution than the PWVD and CWD images which becomes a disadvantage for modulation discrimination.

One interesting result is observed on Costas modulation classification. While the  $P_{cc}$  for Test Modulation is 100% with all detection techniques, the  $P_{cc}$  for Test SNR is not. This is an unexpected result. It is expected that the Test SNR results to outperform the Test Modulation results since the signals used in Test SNR have the same parameters with the training signals. In this sense the Test SNR results can be used as a measure of reliability. This shows that, although the Costas results seem very good for Test Modulation case, they may not be reliable. Concerning that, it can be seen that the classification of Costas code is best performed with CWD detection technique for  $SNR > 4\text{dB}$ . Note also that, it is not necessarily true that the Test Modulation results perform better if the Test SNR results perform well. The  $P_{cc}$  for Test Modulation depends on the modulation discriminative power of the feature extraction algorithm implemented.

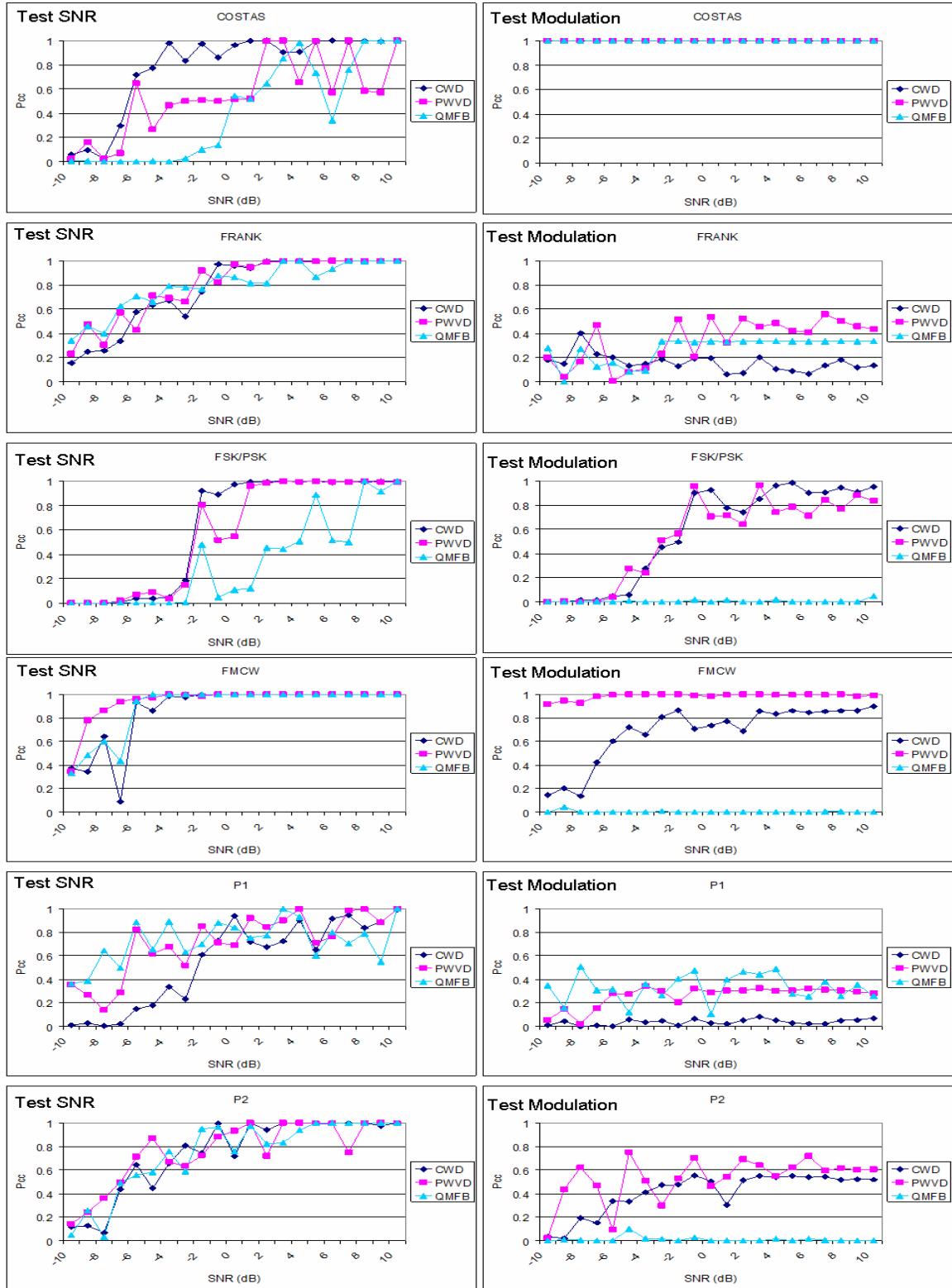


Figure 44. Classification Results with MLPNN (Costas, Frank, FSK/PSK, FMCW, P1, P2 codes).

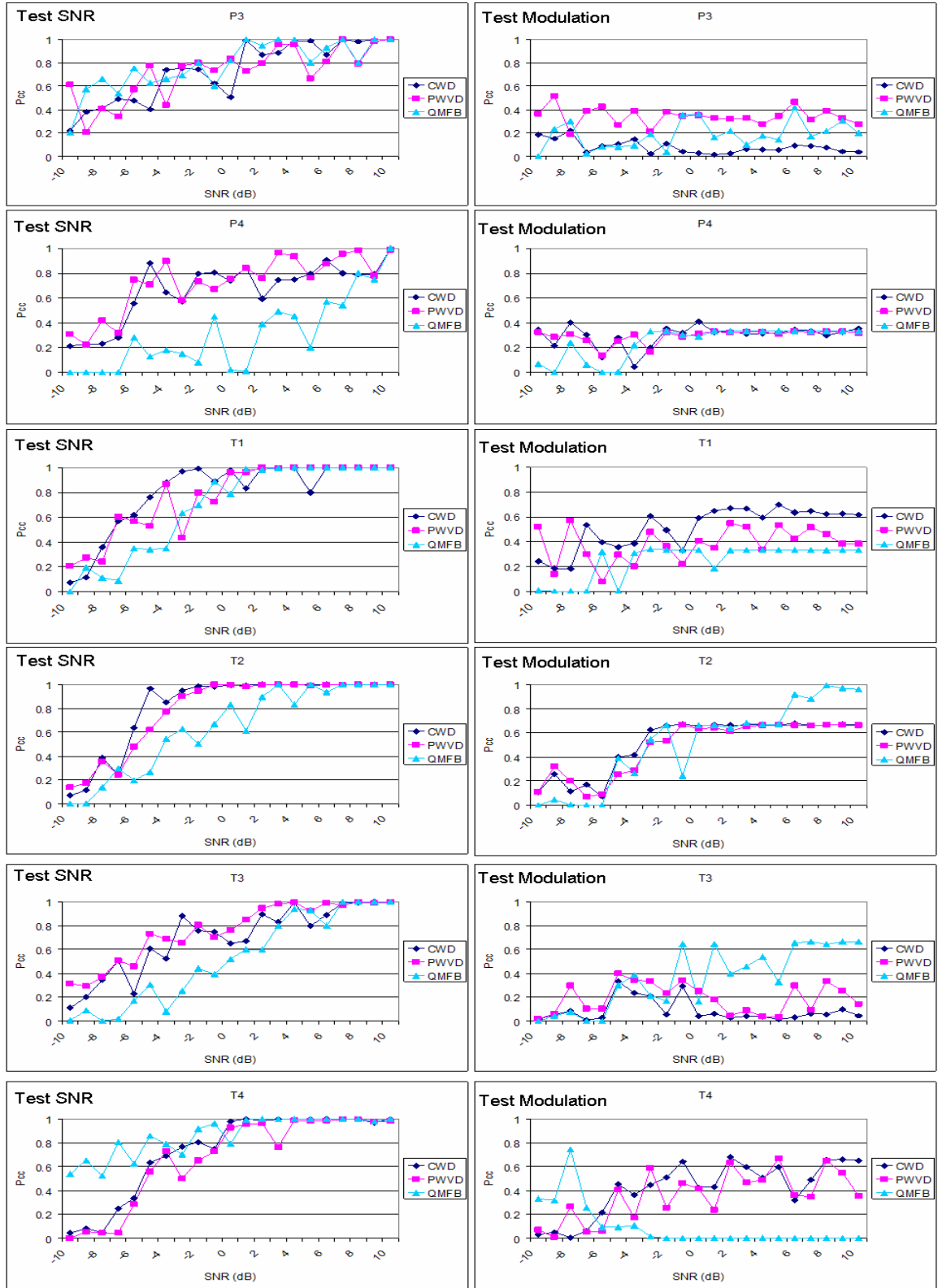


Figure 45. Classification Results with MLPNN (P3, P4, T1, T2, T3, T4 codes).

### 3. Classification Results with RBFNN

The classification results for each LPI radar waveform with three detection techniques are shown in Figures 46 and 47. The CMs are presented in Appendix B.B for  $SNR = 10, 6, 3, 0, -3, -6$  dB (Tables 31-48).

Note that the classification results with RBFNN are not as smooth as in the MLPNN case. This is due to the fact that RBFNN has one solution for a test signal which does not change from one test to another. For instance, if the first test result is  $P_{cc} = 0.75$ , that continues for all tests. As a result, the  $P_{cc}$  for a modulation type with four test signals can be 0, 0.25, 0.5, 0.75 or 1. Note also that the PNN results exhibit the same behavior since it is a variant of RBFNN.

All the detection techniques show similar results on Test SNR case. Frank, FMCW, P2, T1, T2, T3 and T4 modulations are mostly classified with more than 80% classification rate for  $SNR > 2$  dB. The autonomous modulation energy isolation and cropping becomes more sensitive to noise variations below  $SNR = 2$  dB. The FMCW modulation is classified with 100% for  $SNR > 4$  dB, and P2 modulation is classified with 100% for  $SNR > 5$  dB with all detection techniques.

Concerning the Test Modulation case, the best results are obtained in the classification of FMCW, Costas, P1, P2 and T2 modulations while the worst results are obtained in the classification of P4, T1 and T3 modulations. The FMCW modulation is classified 100% with PWVD detection technique for  $SNR > -10$  dB and 100% with CWD detection technique for  $SNR > -1$  dB. The T4 modulation is classified 100% with PWVD detection for  $SNR > 2$  dB. The P2 modulation is classified 100% with CWD detection for  $SNR > -3$  dB. Overall, the classification results with the PWVD technique outperform the other detection techniques.

The QMFB technique performs worse than the other two techniques. However, it outperforms the other techniques in the classification of P1 modulation with a classification rate above 66%.



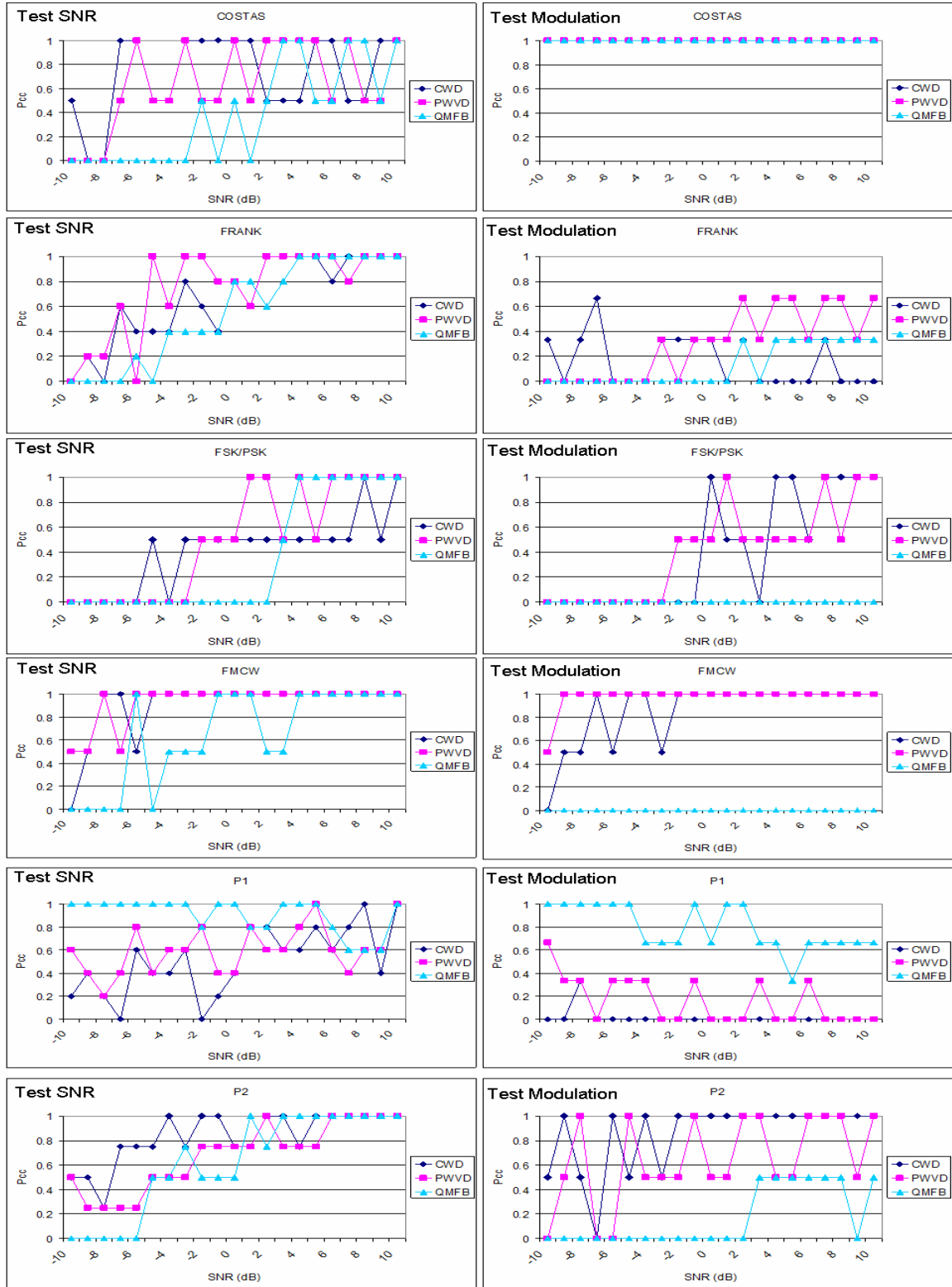


Figure 46. Classification Results with RBFNN (Costas, Frank, FSK/PSK, FMCW, P1, P2 codes).

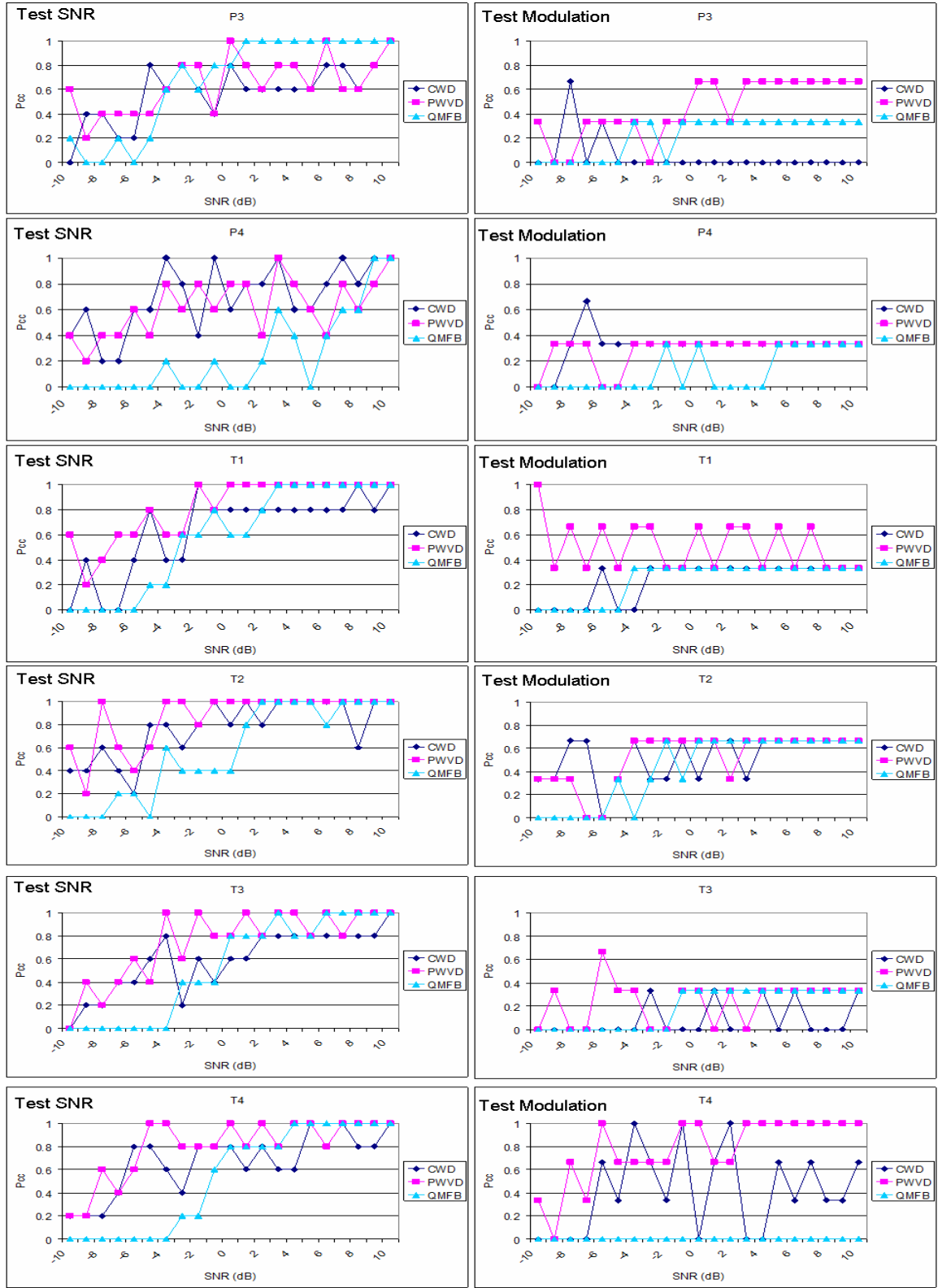


Figure 47. Classification Results with RBFNN (P3, P4, T1, T2, T3, T4 codes).

#### 4. Classification Results with PNN

The classification results for each LPI radar waveform with three detection techniques are shown in Figures 48 and 49. The CMs are presented in Appendix B.C for  $SNR = 10, 6, 3, 0, -3, -6$  dB (Tables 49-66).

All the detection techniques show similar results on Test SNR case. The best results are obtained in the classification of Frank, FSK/PSK, FMCW, T1, T2 and T4 modulations. For these modulations the classification rate reaches 100% for  $SNR > 1$  dB. The autonomous modulation energy isolation and cropping becomes more sensitive to noise variations below  $SNR = 1$  dB.

Concerning the Test Modulation case, the best results are obtained in the classification of FSK/PSK, FMCW, Costas, P2, T2 and T4 modulations while the worst results are obtained in the classification of Frank, P1 and P4 modulations. The FMCW, FSK/PSK, Costas and P2 modulations are classified 100% with PWVD detection technique for different  $SNR$  levels as shown in Figure 48. But note that the Test SNR result for Costas and P2 modulations are not stable for the same SNR levels. So the results for Test Modulation of Costas and P2 modulations may not be reliable. The FMCW modulation is classified 100% for  $SNR > -4$  dB and the FSK/PSK modulation is classified 100% for  $SNR > 3$  dB with CWD detection technique. The T1 modulation is classified 66% with CWD detection technique for  $SNR > 4$  dB. The T2 modulation is classified 66% with PWVD detection technique for  $SNR > -5$  dB and 66% with QMFB detection technique for  $SNR > -1$  dB. The T4 modulation is classified 66% with CWD detection technique for  $SNR > -1$  dB.

Overall, the classification results with the PWVD technique outperform the other detection techniques. Still the QMFB technique performs worse than the other two techniques.

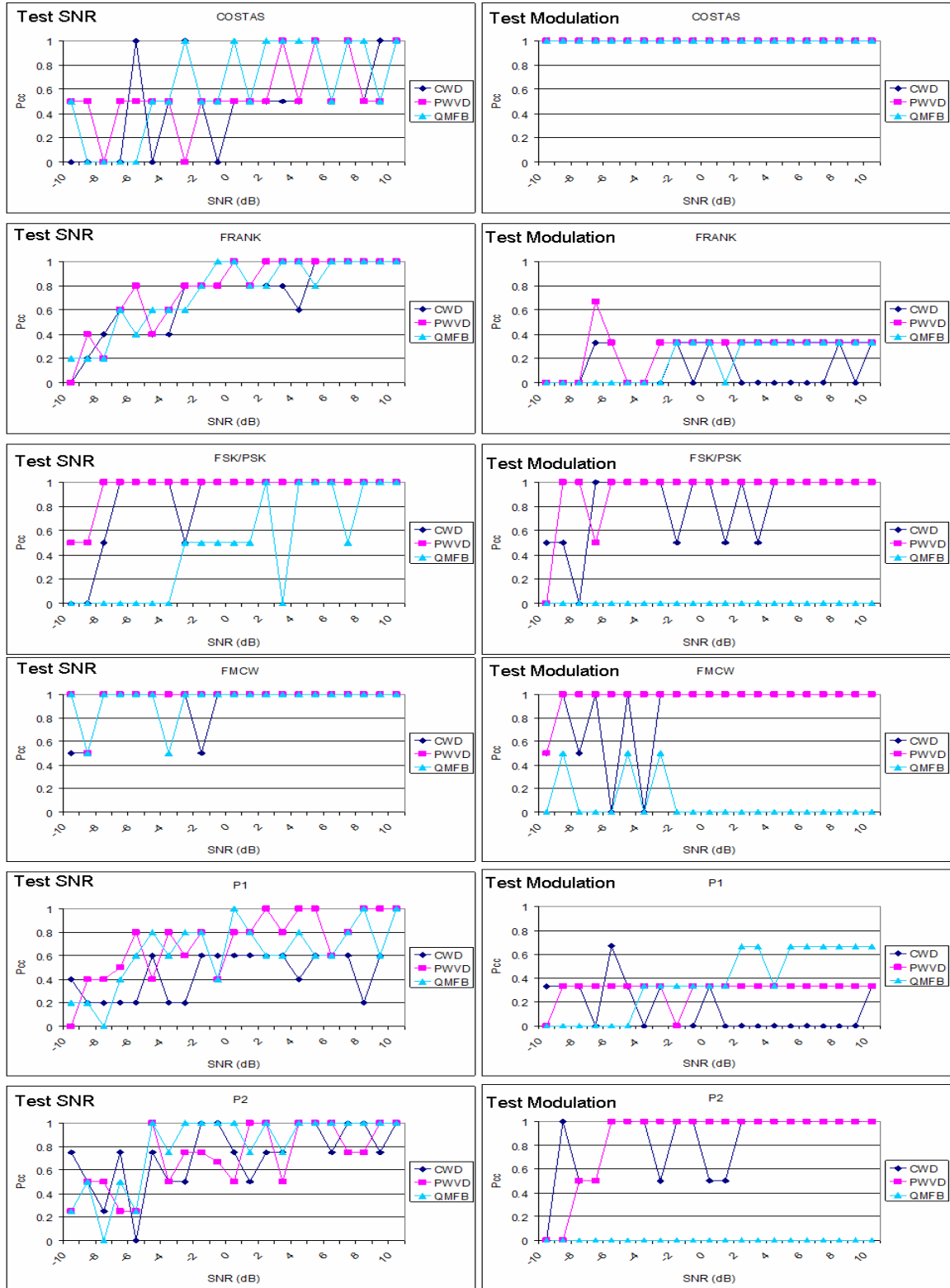


Figure 48. Classification Results with PNN (Costas, Frank, FSK/PSK, FMCW, P1, P2 codes).

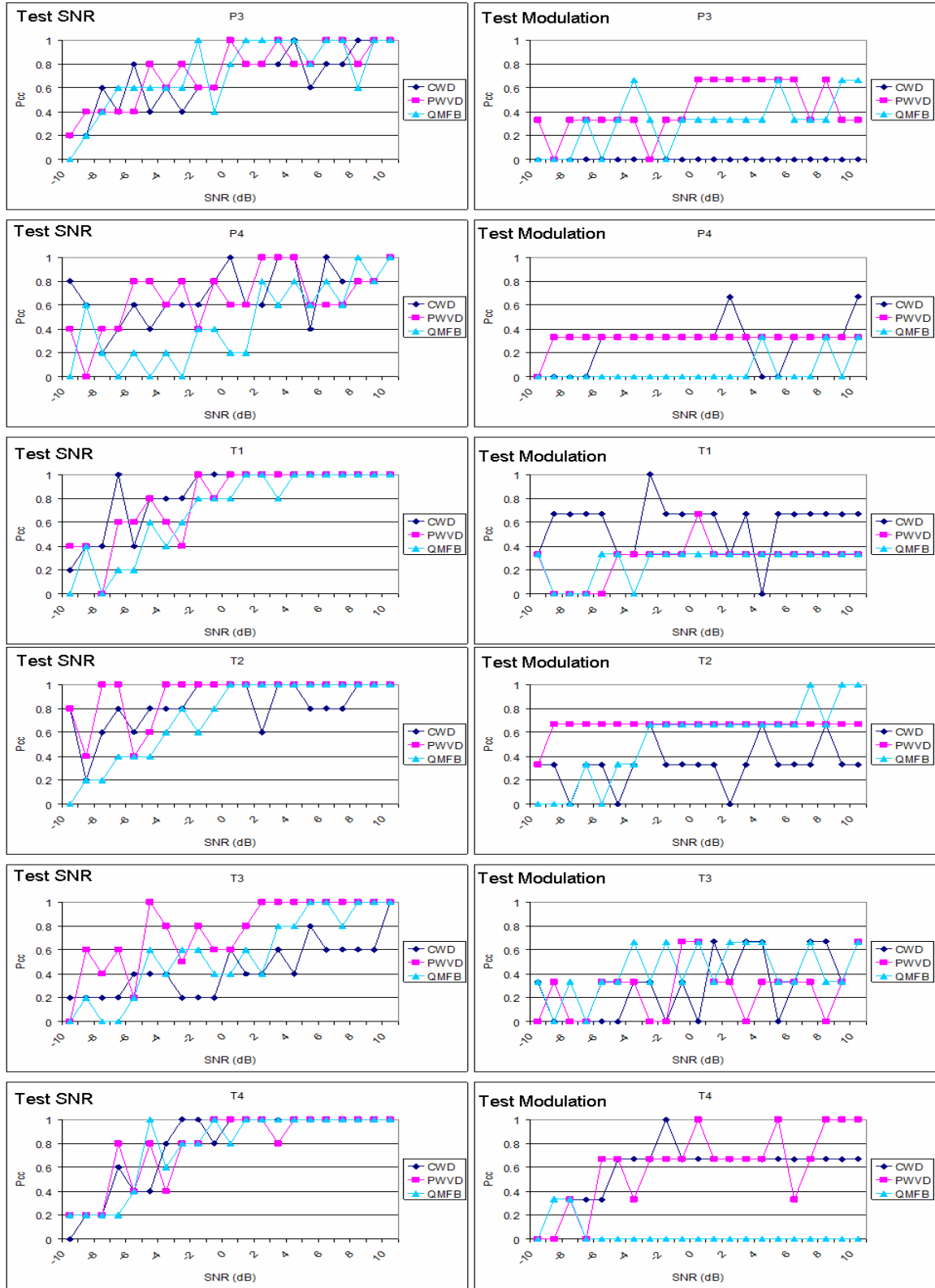


Figure 49. Classification Results with PNN (P3, P4, T1, T2, T3, T4 codes).

## 5. Classification Results using PWVD

The classification results for each LPI radar waveform with three classification networks are shown in Figures 50 and 51. The CMs are presented in Appendix B.A, B.C for  $SNR = 10, 6, 3, 0, -3, -6$  dB (Tables 13-18, 31-36, 49-54).

All the classification networks show similar results on Test SNR case. The best results are obtained in the classification of Frank, FSK/PSK, FMCW, T1, T2, T3 and T4 modulations. For these modulations stable classification regions can be identified as shown in Figures 50 and 51. Note that the classification results for Costas, P1, P2, P3 and P4 modulations are unstable which informs that the Test Modulation results may be unreliable.

Concerning the Test Modulation case, the best results are obtained in the classification of FSK/PSK, FMCW, Costas, P2, T2 and T4 modulations while the worst results are obtained in the classification of Frank, P1, P4, T1 and T3 modulations. The Costas, FMCW, FSK/PSK and P2 modulations are classified 100% with PNN for  $SNR > -7$  dB. But note that the Test SNR results for Costas and P2 modulations indicate that the Test Modulation results may not be reliable. The FMCW modulation is classified 100% for  $SNR > -8$  dB with all classification networks. The FSK/PSK modulation is classified 100% for  $SNR > -7$  dB with PNN and classified above 66% for  $SNR > -2$  dB with MLPNN. The T2 modulation is classified 66% with all three networks for  $SNR > 3$  dB. The T4 modulation is classified 100% with RBFNN for  $SNR > 2$  dB.

Overall, the classification results with radial basis function based networks outperform the MLP network. Among the radial basis function based networks, PNN exhibits better results than RBFNN.

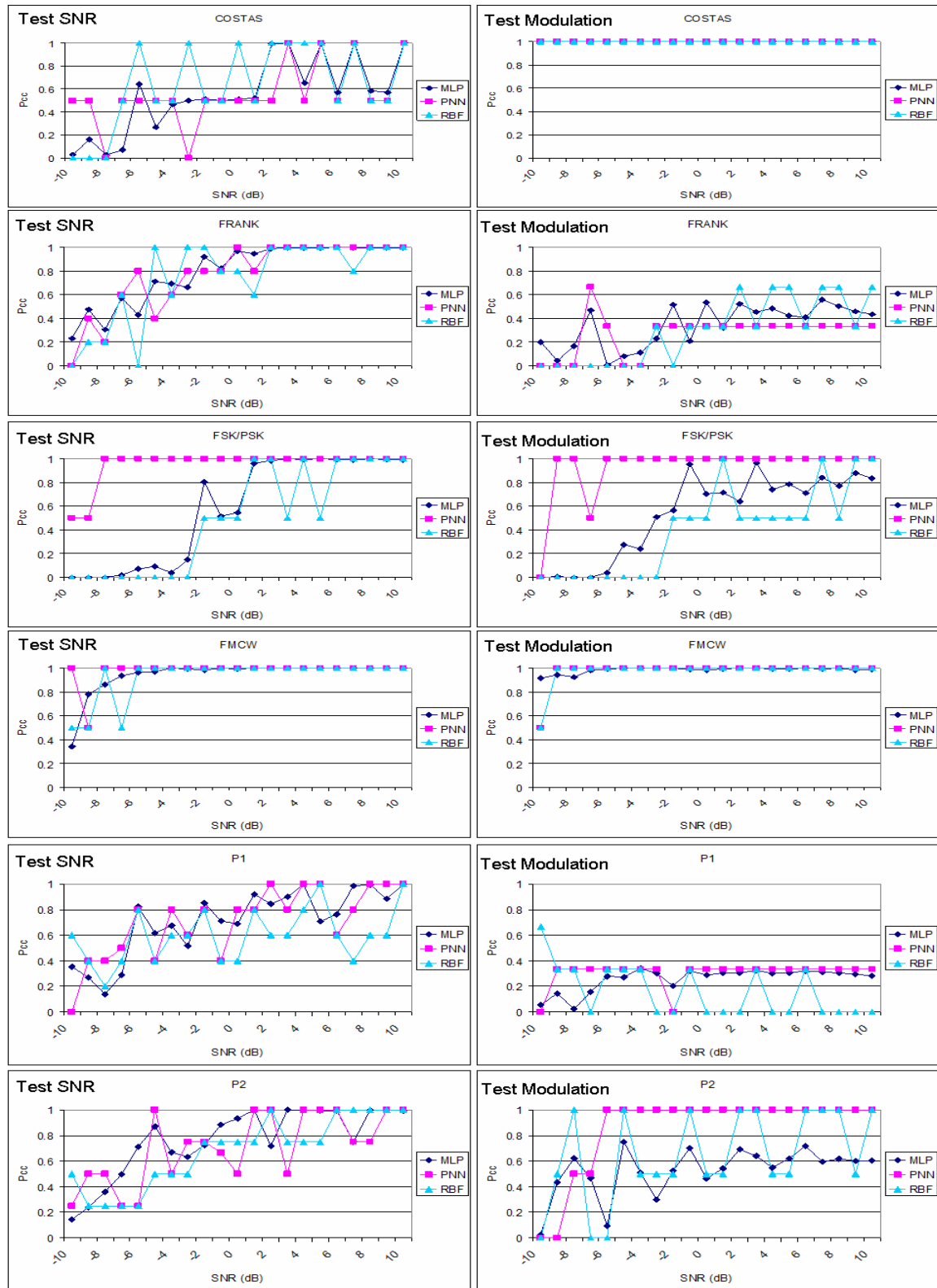


Figure 50. Classification Results using PWVD (Costas, Frank, FSK/PSK, FMCW, P1, P2 codes).

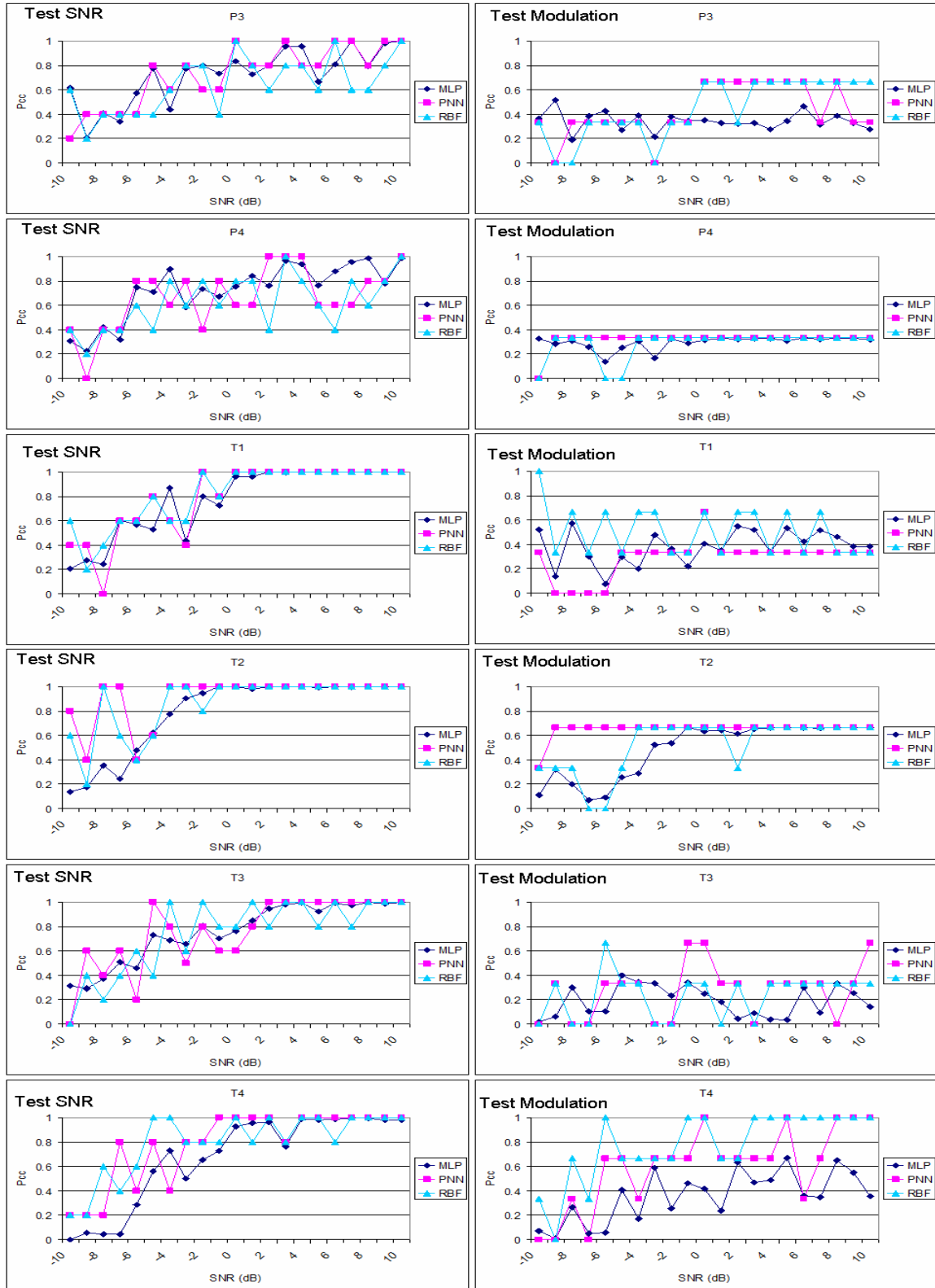


Figure 51. Classification Results using PWVD (P3, P4, T1, T2, T3, T4 codes).



## 6. Classification Results Using CWD

The classification results for each LPI radar waveform with three classification networks are shown in Figures 52 and 53. The CMs are presented in Appendix B.A, B.C for  $SNR = 10, 6, 3, 0, -3, -6$  dB (Tables 19-24, 37-42, 55-60).

For the CWD images all the classification networks show similar results on Test SNR case. The best results are obtained in the classification of Frank, FSK/PSK, FMCW, T1, T2, and T4 modulations. For these modulations stable classification regions can be identified as shown in Figures 52 and 53. Note that the classification results for Costas, P1, P2, P3, P4 and T3 modulations are unstable which informs that the Test Modulation results may be unreliable.

The results of the Test Modulation case indicates that the classification results of FSK/PSK, FMCW, Costas, P2, T2 and T4 modulations are better than the classification results of Frank, P1, P4, T1 and T3 modulations. The Costas, FMCW, FSK/PSK and P2 modulations are classified 100% with PNN and RBFNN for different  $SNR$  levels as shown in Figure 52. For Costas modulation a reliable classification region can be defined for  $SNR > 4$  dB with MLPNN and for P2 modulation a reliable classification region can also be defined for  $SNR > 4$  dB with RBFNN. The T1 and T2 modulations are classified above 60% with MLPNN for  $SNR > -1$  dB. Overall, the classification results with radial basis function based networks outperform the MLP network. The PNN and the RBFNN results are very similar.

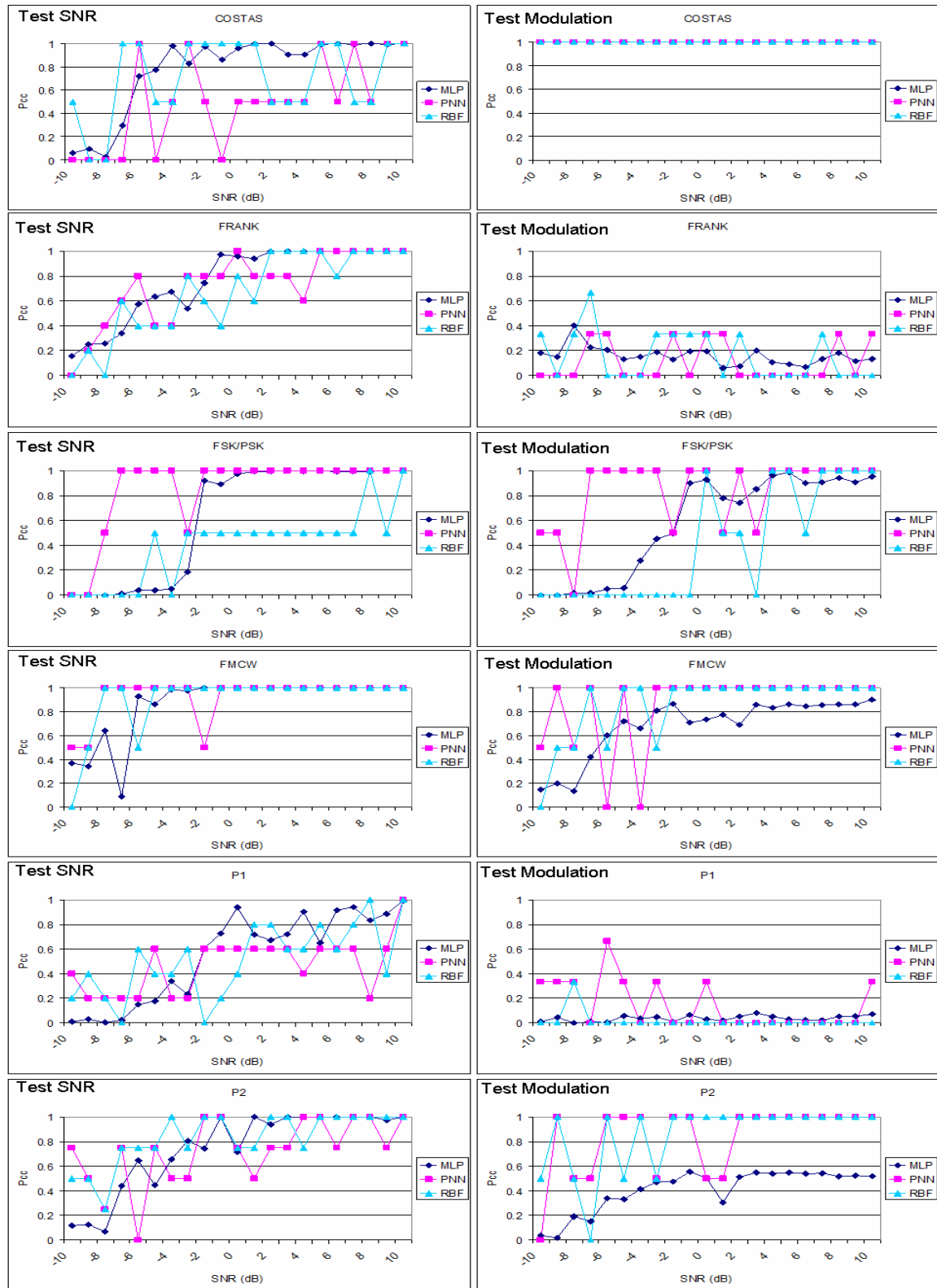


Figure 52. Classification Results using CWD (Costas, Frank, FSK/PSK, FMCW, P1, P2 codes).

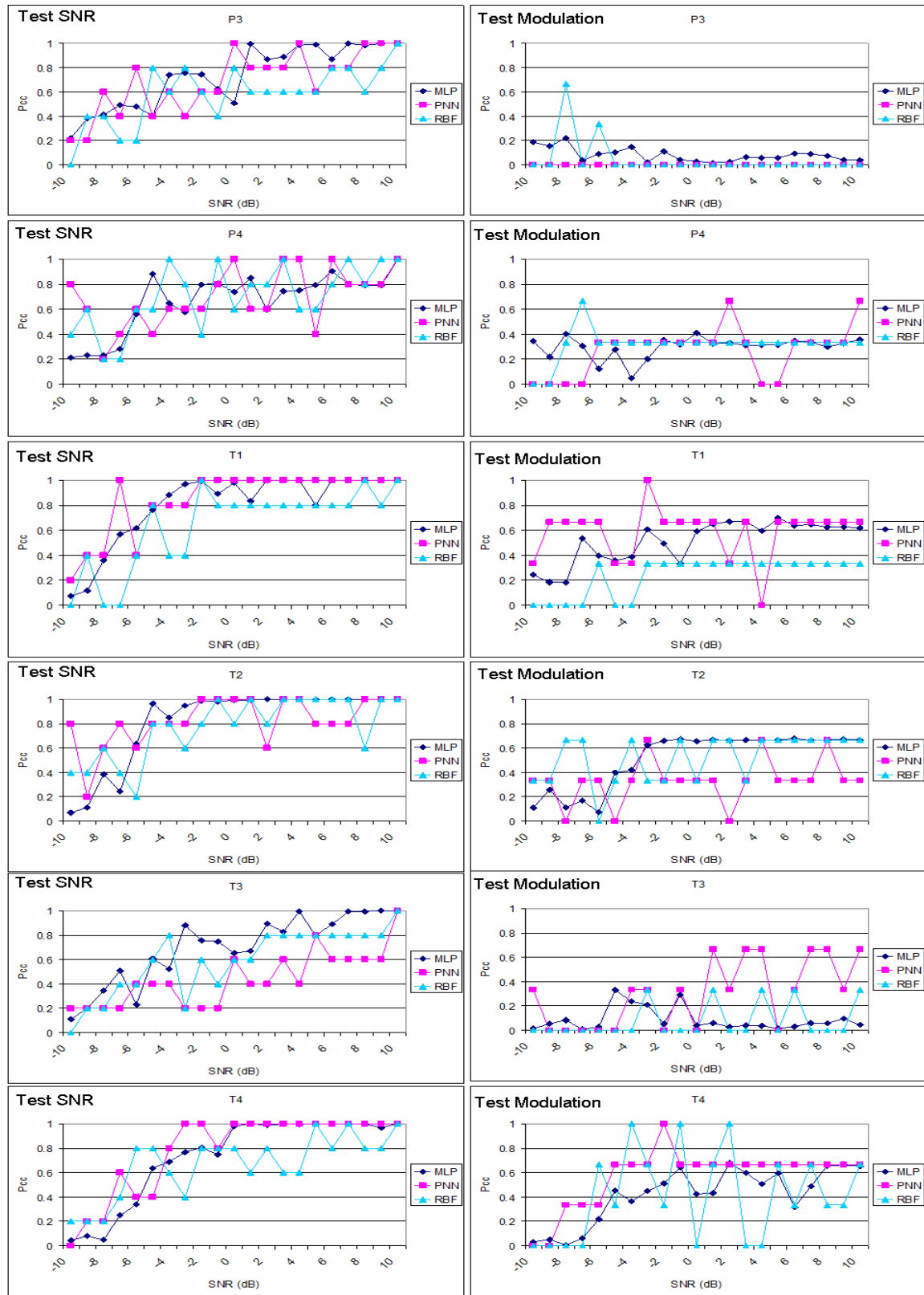


Figure 53. Classification Results using CWD (P3, P4, T1, T2, T3, T4 codes).

## 7. Classification Results using QMFB

The classification results for each LPI radar waveform with three classification networks are shown in Figures 54 and 55. The CMs are presented in Appendix B.A, B.C for  $SNR = 10, 6, 3, 0, -3, -6$  dB (Tables 25-30, 43-48, 61-66).

For the Test SNR case the best results are obtained in the classification of Frank, FSK/PSK, P2, P3, T1, T2, T3 and T4 modulations for  $SNR > 4$  dB. FMCW modulation also gives good result for  $SNR > -4$  dB with MLPNN and PNN. Concerning the Test Modulation case, for most of the modulations the classification results are very poor. None of the classifiers improves the classification results significantly.

The results indicate that the QMFB images could not provide class distinctive information when the T-F feature extraction algorithm defined in this work is applied. One of the reasons for this problem is the QMFB image resolution. The QMFB images had small dimensions and due to this fact they did not contain as much class distinctive information as PWVD and CWD images.

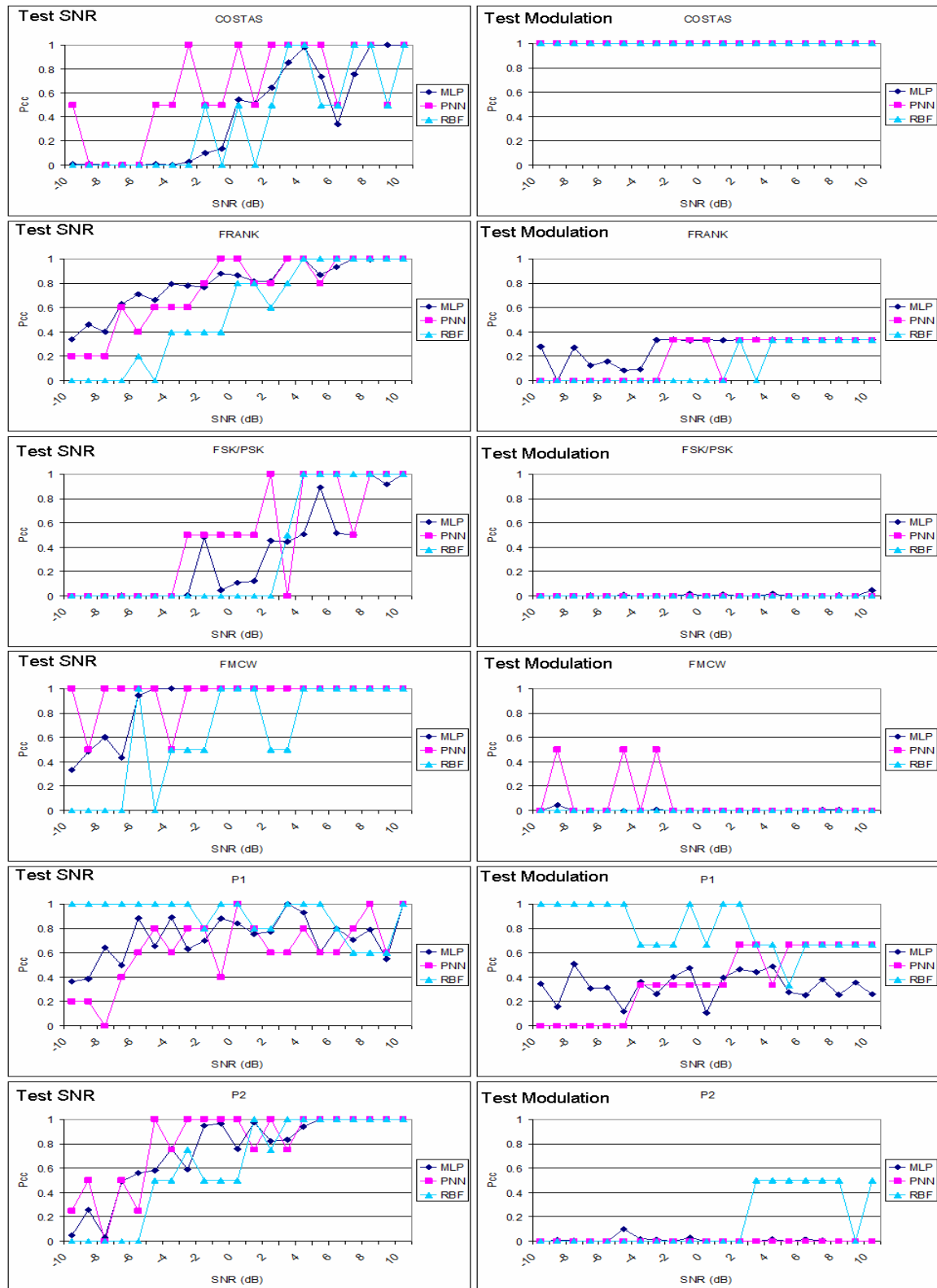


Figure 54. Classification Results using QMFB (Costas, Frank, FSK/PSK, FMCW, P1, P2 codes).

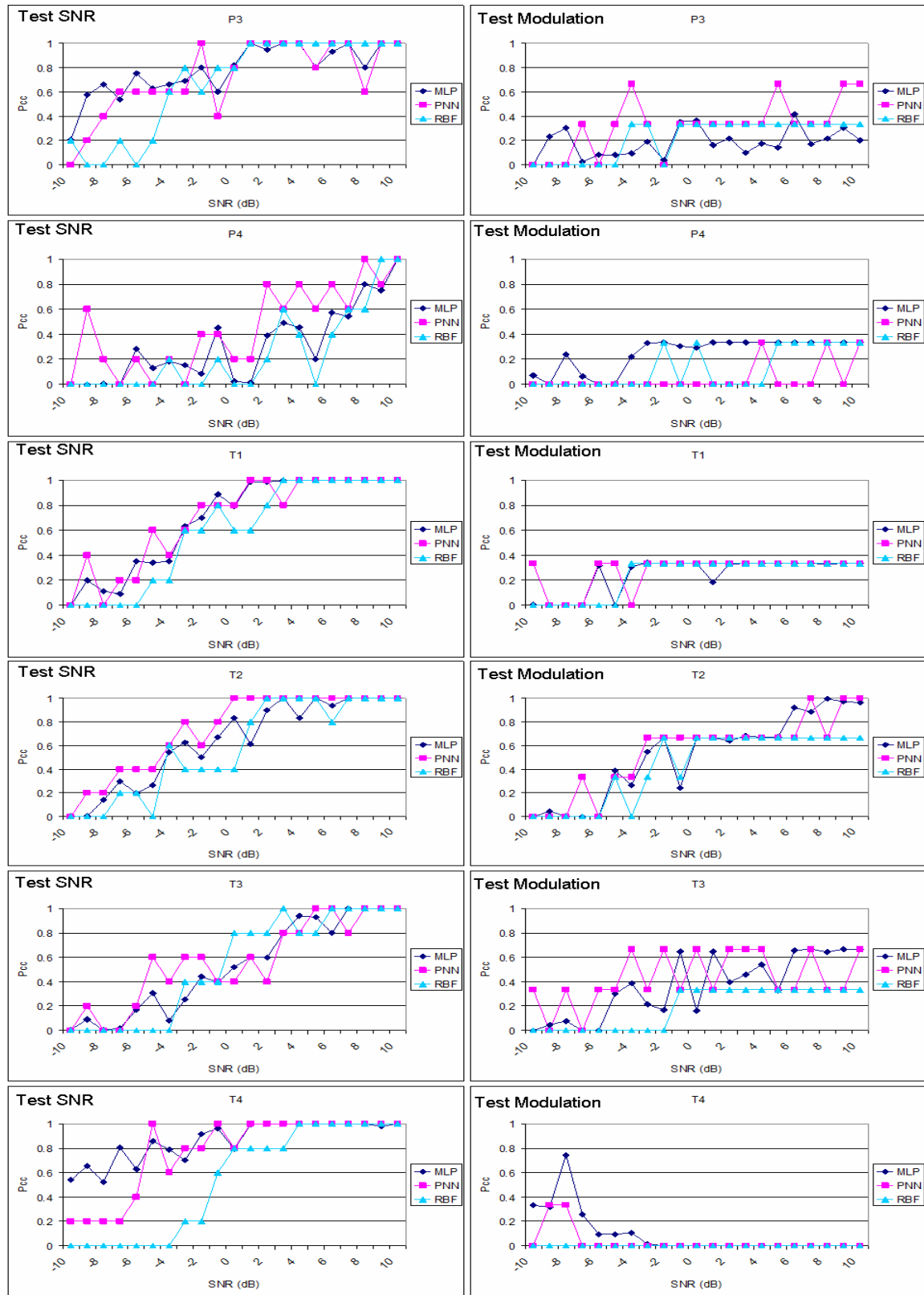


Figure 55. Classification Results using QMFB (P3, P4, T1, T2, T3, T4 codes).

## **E. SUMMARY**

The autonomous detection and classification algorithms used in this work are described. The detection techniques include the Wigner-Ville distribution, the Choi-Williams distribution and quadrature mirror filter bank. An autonomous image cropping and feature extraction algorithm based on two dimensional Fast Fourier Transform (2-D FFT) and PCA is presented. MLPNN, RBFNN and PNN are described as the non-linear classifiers used in this work. The simulation results of classification networks are presented.

The next chapter presents the two parameter extraction algorithms investigated. First one is designed to extract the parameters from the PWVD images of polyphase coded LPI signals using the Radon transform of the PWVD images and the second one is designed to extract the parameters from the CWD images of polyphase coded LPI signals using frequency domain lowpass filter on the 2-D FFT of CWD images. The algorithms are tested with the polyphase signals shown in Table 1 and Table 2 and the results are also presented.

THIS PAGE INTENTIONALLY LEFT BLANK



## V. PARAMETER EXTRACTION ALGORITHMS

Parameter extraction is the last phase of autonomous LPI signal detection and classification algorithm. Once the signal modulation is identified the parameters of the signal should be extracted to counter attack the transmitting systems.

In this work two parameter extraction algorithms are investigated. The first algorithm extracts the parameters of polyphase coded LPI modulations (Frank, P1, P2, P3, P4) using the PWVD images. The second algorithm extracts the parameters of polyphase coded LPI modulations using the CWD images. The extracted parameters are the carrier frequency  $f_c$ , bandwidth  $B$ , code period  $T$ , code length  $N_c$  and cycles of the carrier frequency per subcode  $c_{pp}$ .

The illustrations presented in this section are based on a Frank coded signal with  $N_c = 36$  subcodes, a carrier frequency of  $f_c = 1495$  Hz with a sampling frequency of  $f_s = 7$  kHz at an SNR level of 0 dB. With the number of carrier frequency cycles within a subcode of  $c_{pp} = 1$ , the transmitted bandwidth  $B = f_c / c_{pp} = 1495$  Hz and the code period is  $T = 24.1$  ms.

### A. PARAMETER EXTRACTION OF POLYPHASE CODED LPI RADAR MODULATIONS USING PWVD IMAGES

The parameter extraction algorithm for polyphase coded LPI radar waveforms using PWVD images is shown in Figure 56.

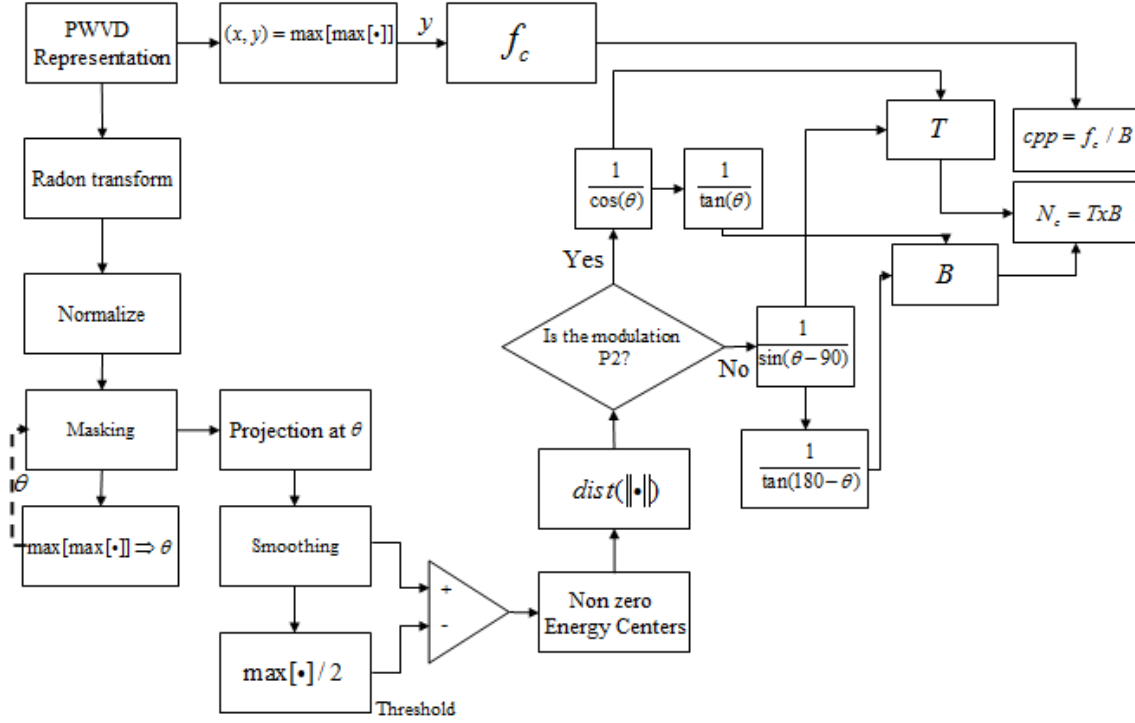


Figure 56. Parameter Extraction Block Diagram for Polyphase Coded LPI Radar Waveforms using PWVD Images (From [28]).

The algorithm carrier frequency  $f_c$  is extracted directly from the PWVD image without any pre-processing. This is performed by finding the location of the maximum intensity level in the image. The corresponding frequency at this location gives  $f_c$  [28]. This is illustrated in Figure 57 on a grayscale PWVD image. Note that with the PWVD, this maximum sometimes occurs at a cross term but not all the times.

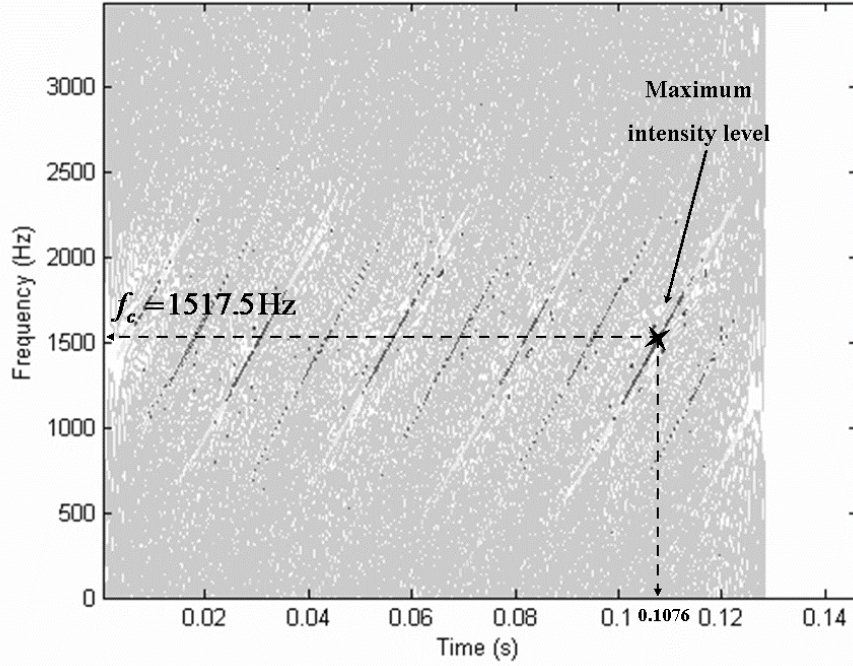


Figure 57. Carrier Frequency Determination by Finding the Maximum Intensity Level for PWVD.

In order to extract the code length  $T$  and bandwidth  $B$  the Radon transform of the image is computed [28]. The Radon transform is the projection of the image intensity along a radial line oriented at a specific angle. It transforms a 2-D image with lines (line-trends) into a domain of the possible line parameters  $\rho$  and  $\theta$ , where  $\rho$  is the smallest distance from the origin and  $\theta$  is its angle with the x-axis. In this form, a line is defined as [55].

$$\rho = x \cos \theta + y \sin \theta \quad (5.1)$$

Using this definition of a line, the Radon transform of a 2-D image  $f(x, y)$  can then be defined as follows

$$R(\rho, \theta) = \int_{-\infty}^{+\infty} f(\rho \cos \theta - s \sin \theta, \rho \sin \theta + s \cos \theta) ds \quad (5.2)$$

where the  $s$ -axis lies along the line perpendicular to  $\rho$  as shown in Figure 58. Here  $s$  can be calculated from

$$s = y \cos \theta - x \sin \theta \quad (5.3)$$

Note  $\rho$  and  $s$  can be calculated from  $x$ ,  $y$  and  $\theta$  using equations (5.1) and (5.3).

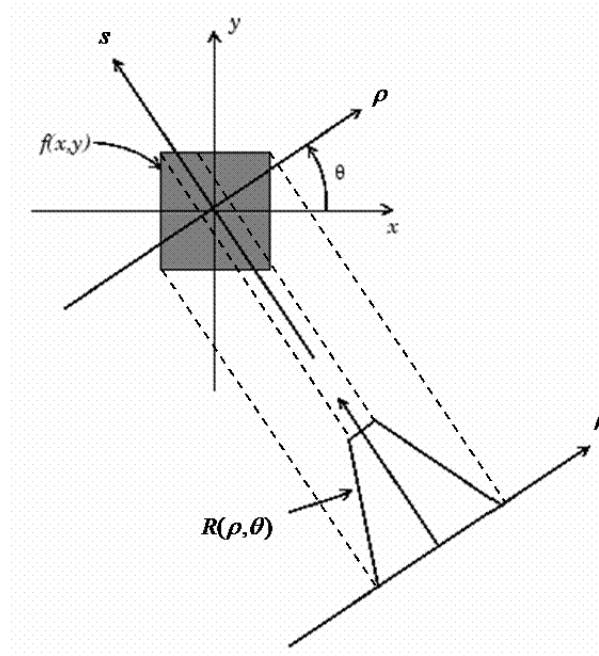


Figure 58. Geometry of the Radon Transform (From [56]).

In this work the projection of the images are computed as line integrals from multiple sources along parallel paths in a certain direction. The beams are spaced 1 pixel unit apart. This is illustrated in Figure 59 for a single projection at a specified rotation angle  $\theta$  [56].

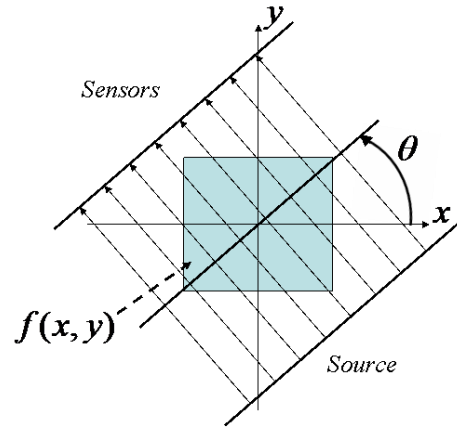


Figure 59. Parallel Beam Projection at Rotation Angle  $\theta$  (From [56]).

Figure 60 shows the grayscale PWVD image illustrating the extraction goal for the bandwidth and the code period. The algorithm aims to measure the indicated regions by implementing the Radon transform to find  $\theta$  and  $d$ . Here  $d$  is the distance between consecutive linear energy lines of the modulation at angle  $\theta$ . To prevent confusion the angle  $\theta$  which is equal to the slope of the modulation energy lines will be referred as  $\theta_s$  for the rest of the section. The expectation is to obtain maximum intensity levels in the transformed image at angle  $\theta_s$ . Once  $\theta_s$  and  $d$  is determined,  $B$  and  $T$  can be calculated using geometrical relations as shown below [28].

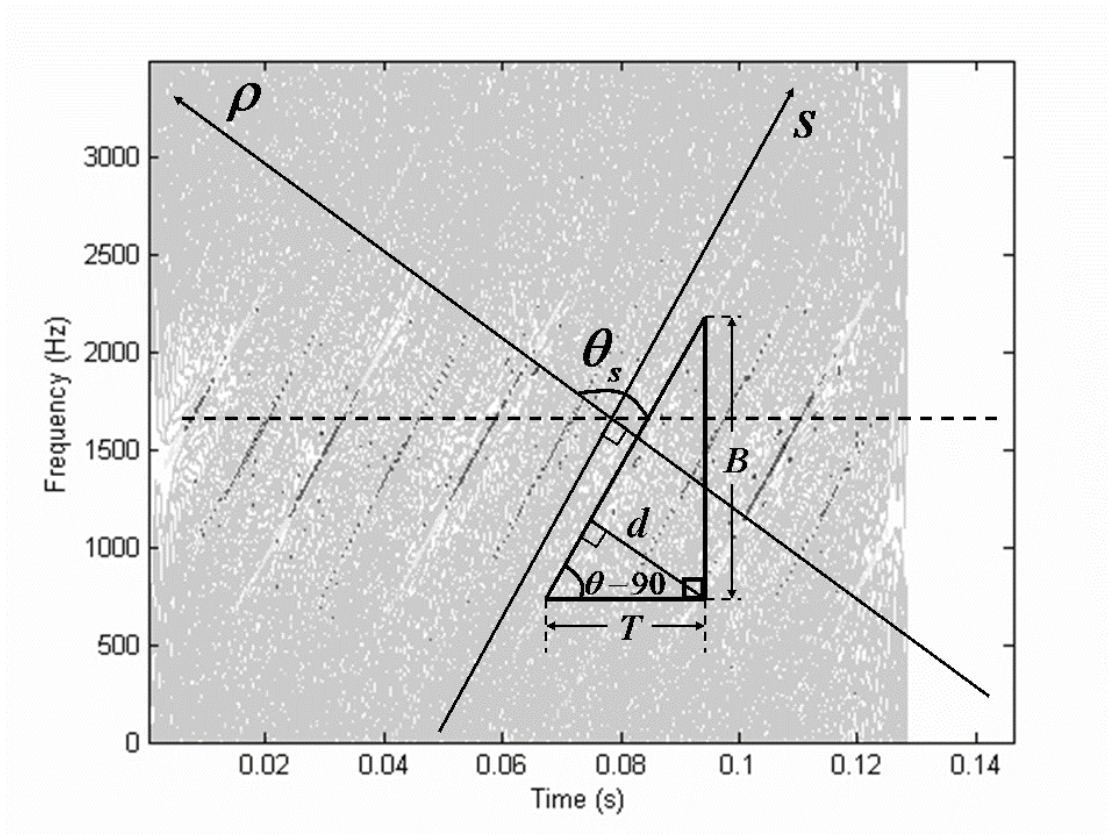


Figure 60. Radon Transform Geometry on PWVD image (From [28]).

The Radon transform is implemented so that the parallel-beam projections of the image are taken between  $[0^\circ, 179^\circ]$ . Once the transform is completed it is normalized [28]. The normalized radon transform of the PWVD image is shown in Figure 61 on a contour plot.

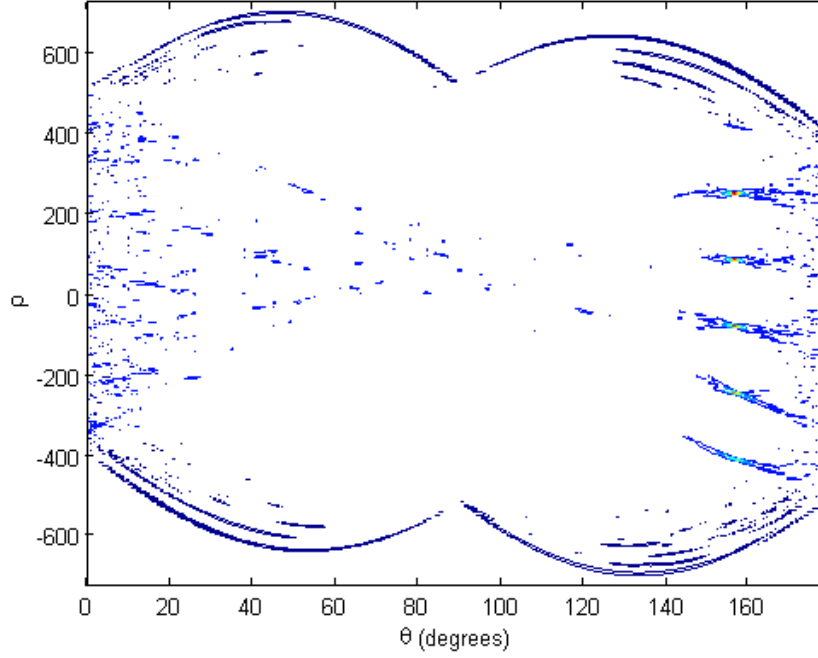


Figure 61. Normalized Radon Transform of a PWVD Image.

In some cases the maximum intensity on the transform may occur around  $\theta = 90^\circ$  which corresponds to the MFD. Since we do not want to detect the angle corresponding to the MFD, we assume that the slope of linear energy lines are not between  $10^\circ$  and  $-10^\circ$  and the projections on angles between  $\theta = [80^\circ, 100^\circ]$  are masked, and set to zero. After masking, the location of the maximum intensity level of the transform is found. The corresponding projection angle at this location gives  $\theta_s$  [28].

Once  $\theta_s$  is found the projection at angle  $\theta_s$  is cropped from the masked Radon transform and a projection vector is obtained. Figure 62 illustrates the cropping of the projection at angle  $\theta_s$  from the masked Radon transform.

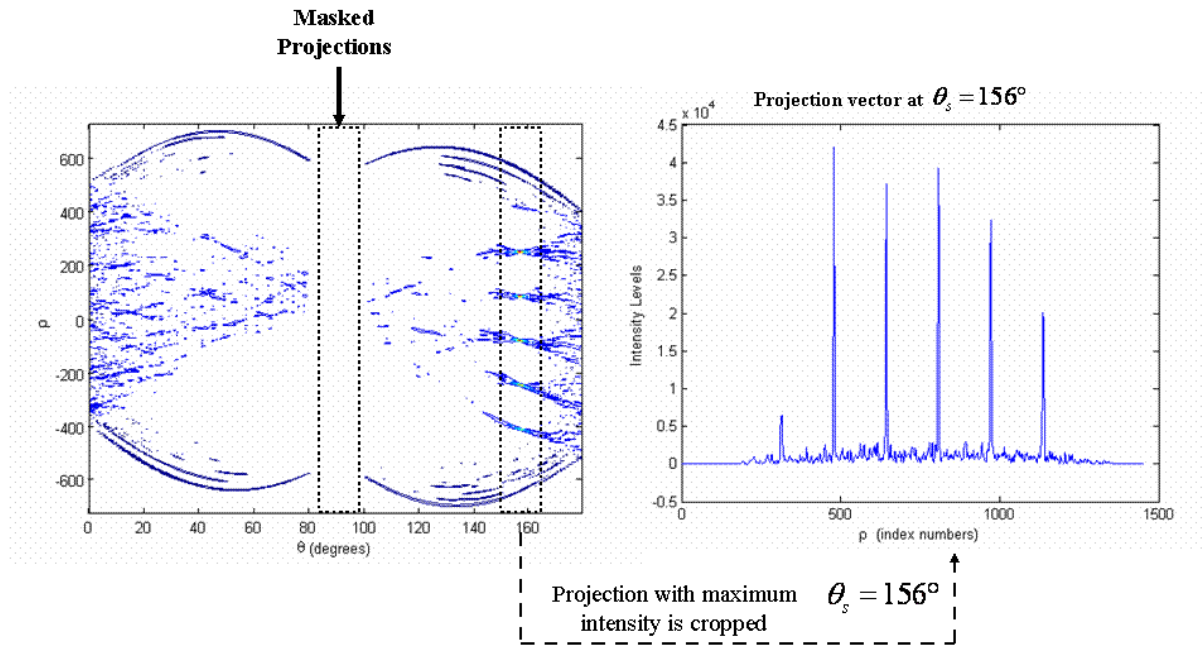


Figure 62. Radon Transform and Projection Vector Cropping on an Angle  $\theta_s$  (From [28]).

From Figure 62 the number of modulation energy lines contained in the WVD image can easily be detected from both the Radon transform and the projection vector at angle  $\theta_s$ . The ripples between each modulation energy component correspond to the noise and cross term integration at angle  $\theta_s$ . As noise increases, these ripples also increase. High levels of noise may affect the thresholding process described below. Due to this fact the projection vector is smoothed with an adaptive filter using the same algorithm as in the T-F autonomous cropping and feature extraction algorithm described previously in section Chapter IV-B-1. A local neighborhood of  $\eta=10$  is used in the adaptive filter [28].

Following smoothing, the projection vector is thresholded with a threshold equal to one half of the maximum value of the projection vector. Figure 63 (a) shows the filtered projection vector and Figure 63 (b) shows the thresholded projection vector after filtering.



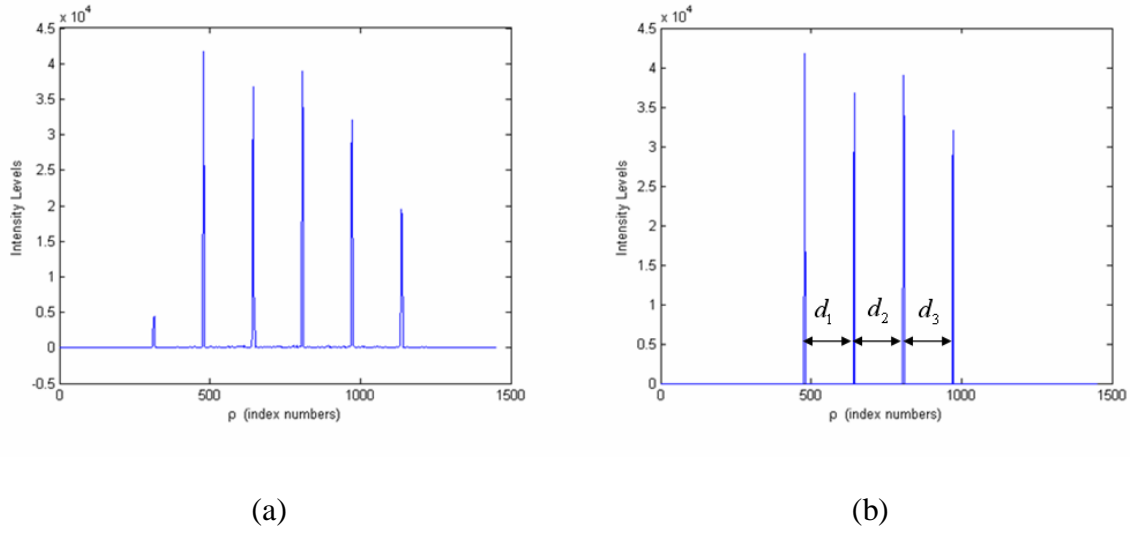


Figure 63. (a) Filtered Projection Vector (b) Thresholded Projection Vector after Filtering (From [28]).

After thresholding the distances can be found between the nonzero values in the projection vector which correspond to the consecutive modulation energy components. Several distances can be found between consecutive modulation energy components. And the final distance  $d$  can be determined by finding the mean value of these distances. Recall Figure 60 , once  $d$  is found the code period can also be found using the relation [28]

$$T = \frac{1}{f_s} \left( \frac{d}{\sin(\theta_s - \frac{\pi}{2})} \right) \quad (5.4)$$

and the bandwidth can be found using the relation

$$B = \Delta f \left( \frac{d}{\sin(\theta_s - \frac{\pi}{2})} \right) / \tan(\pi - \theta_s) \quad (5.5)$$

where  $\Delta f$  is the frequency resolution of the PWVD image. Note that (5.4) and (5.5) are not applied to P2 coded signals since it has an opposite slope. For P2 coded signals the following relations apply:

$$T = \frac{1}{f_s} \left( \frac{d}{\cos \theta} \right) \quad (5.6)$$

$$B = \Delta f \left( \frac{d}{\cos \theta} \right) / \tan \theta \quad (5.7)$$

Once  $f_c$ ,  $T$  and  $B$  are obtained the code length  $N_c$  can be obtained using the relation  $N_c = T \times B$  and the cycles of the carrier frequency per subcode  $c_{pp}$  can be obtained using the relation  $c_{pp} = f_c / B$ .

## **B. PARAMETER EXTRACTION OF POLYPHASE CODED LPI RADAR MODULATIONS USING CWD IMAGES**

The parameter extraction algorithm for polyphase coded LPI radar modulations using CWD images is shown in Figure 64.



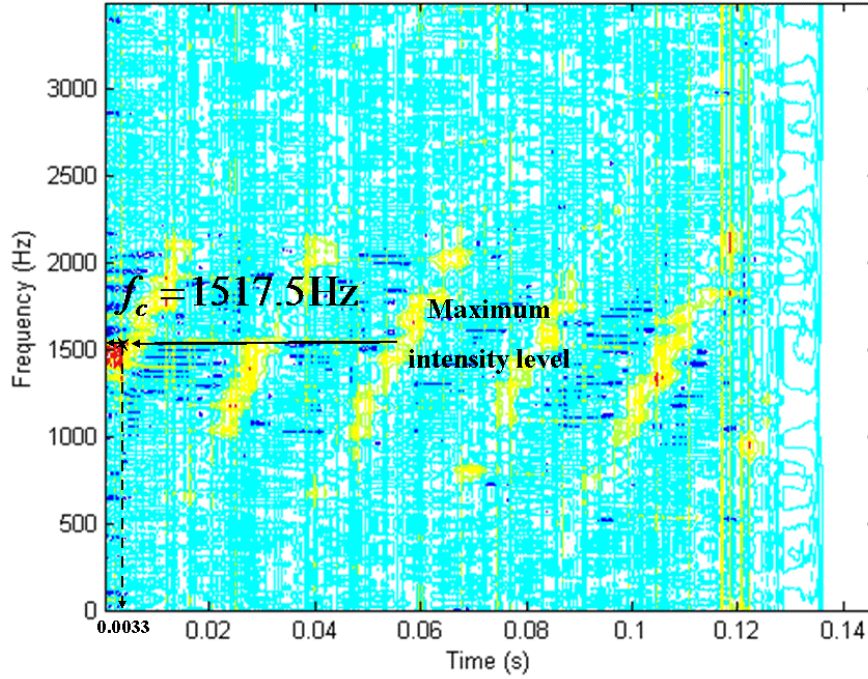


Figure 65. Carrier Frequency Determination by Finding the Maximum Intensity Level for CWD.

The goal behind the extraction of the bandwidth and the code period from the image can be recalled from Figure 16. The algorithm aims to measure the indicated regions in Figure 16.

In order to extract the code length  $T$  and bandwidth  $B$ , several pre-processing operations are performed on the image. First step is to detect and delete the region where no signal is present. Followed by the deletion of the no-signal region, the image is lowpass filtered (LPF). These two steps are performed as in the T-F autonomous cropping and feature extraction algorithm described previously in this work. Here  $\omega_1 = \omega_2 = 0.2\pi$  is used in the frequency domain LPF.

Following the lowpass filtering, an absolute value operation is performed on the image and the intensity values are scaled to the range  $[0,1]$  which is shown as the Gray scaling block.

The image is later enhanced using a sharpening filter. The sharpening filter can be obtained from the negative of the Laplacian filter with parameter  $\alpha$ . The parameter  $\alpha$  controls the shape of the Laplacian which allows fine tuning of the enhancement results. The parameter  $\alpha$  must be in the range  $[0,1]$  and in this work  $\alpha = 0.2$  is used.

Enhancement using the negative of the Laplacian filter is based on the equation [41]

$$g(x, y) = f(x, y) + [-\nabla^2 f(x, y)] \quad (5.8)$$

where  $f(x, y)$  is the input image and  $g(x, y)$  is the sharpened image.

The negative Laplacian of an image  $-\nabla^2 f$  can be implemented at all points  $(x, y)$  in an image by convolving the image with the following spatial mask  $m$  [41];

$$m = \frac{1}{\alpha + 1} \begin{bmatrix} -\alpha & \alpha - 1 & -\alpha \\ \alpha - 1 & \alpha + 5 & \alpha - 1 \\ -\alpha & \alpha - 1 & -\alpha \end{bmatrix} \quad (5.9)$$

Figure 52 (a) shows the enhanced image in a gray scale plot and Figure 52 (b) shows the enhanced image in a contour plot following the low pass filtering.

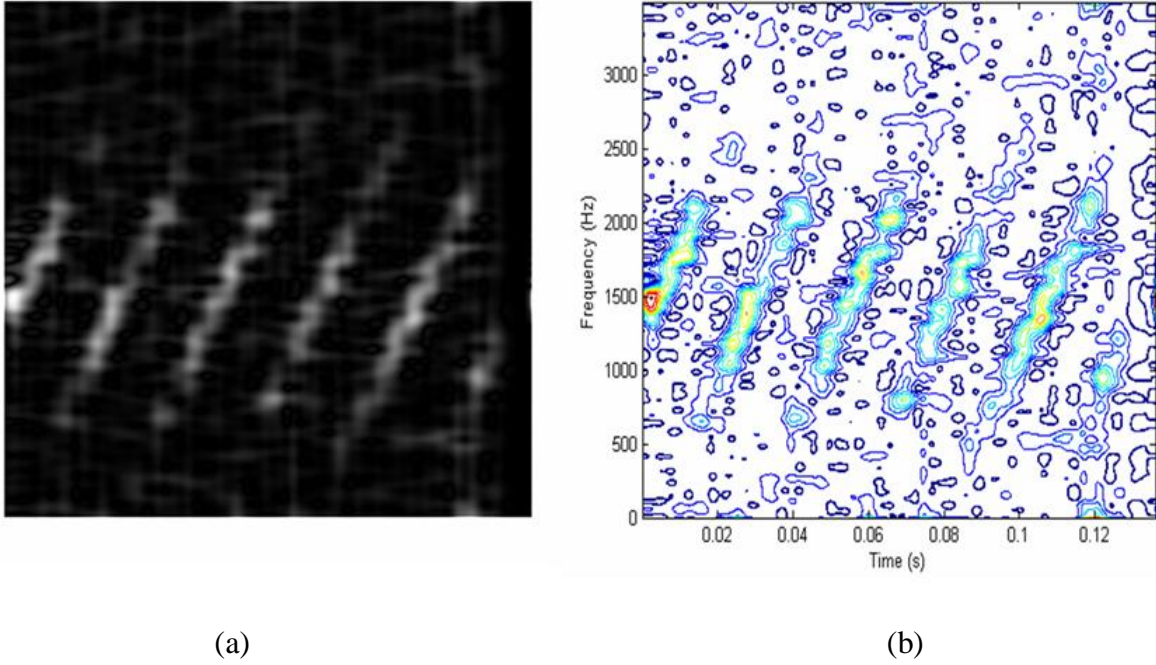


Figure 66. (a) Gray Scale Plot of Enhanced Image after LPF (b) Contour Plot of Enhanced Image after LPF.

The CWD may generate high energy regions at the edges of the time axis. These regions affect an accurate time marginal calculation. Without affecting the overall image and the algorithm the first and the last 5 time indices are masked. That is, the intensity values within these regions are set to zero.

After the time masking, the algorithm follows two directions. One of the directions lead to the extraction of the code period and the other leads to the extraction of the bandwidth. In order to extract the code period a time slice is cut from the time masked image at  $f = f_c$  and the later operations are performed on this time slice vector. The goal of time slice cropping is to find the peak values where the distance between the peak values provide the code period. This operation is illustrated in Figure 53.

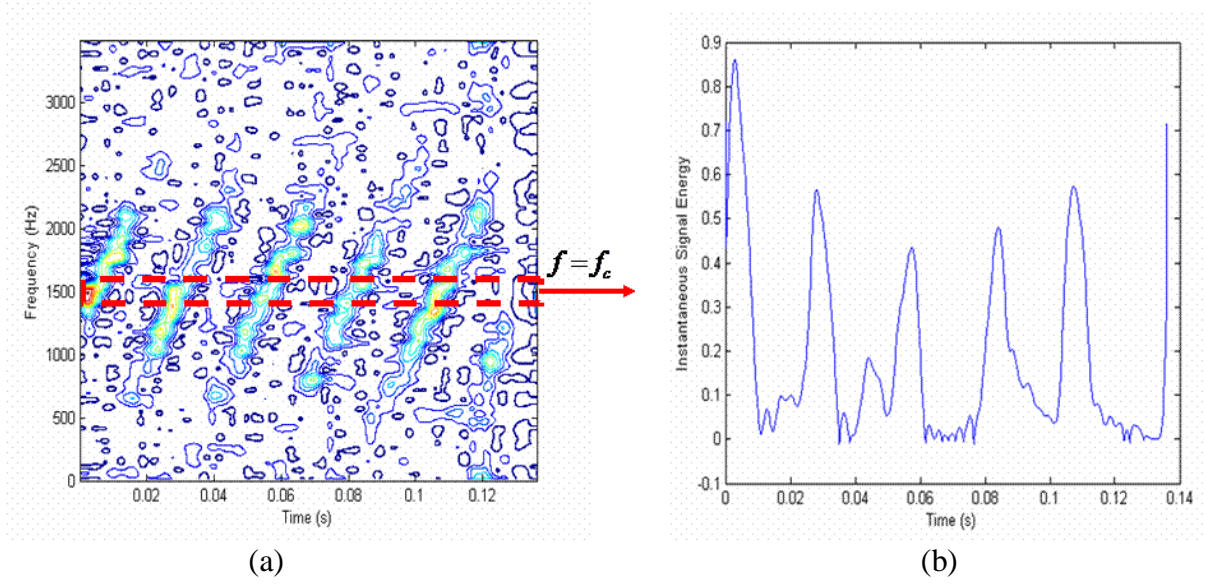


Figure 67. (a) Time Slice Cropping (b) Time Slice Vector.

The time slice vector is smoothed using the same algorithm as in the T-F autonomous cropping and feature extraction algorithm described previously in section Chapter IV.B.1. A local neighborhood of  $\eta=10$  is used in the adaptive filter and a window length of  $m=5$  is used in the moving average filter. Figure 54 shows the smoothed time slice vector vs. original time slice vector. Note that due to the low pass filtering the effect of smoothing is very slight. But since the ripples caused by noise are expected to be high at low SNR levels smoothing acts as a buffer which offers stability to the thresholding operation.

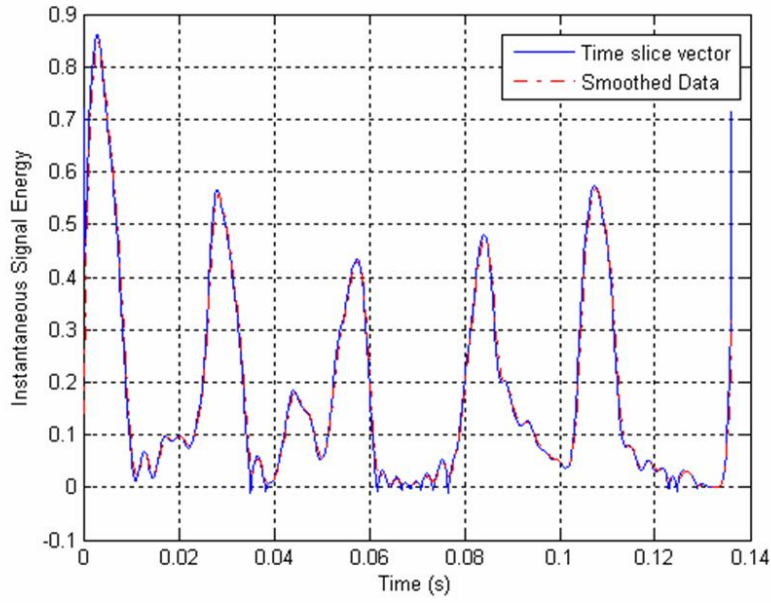


Figure 68. Smoothed Time Slice Vector.

Followed by the smoothing operation a histogram of 100 bins is generated. Using this histogram bins a threshold is determined as described in the T-F autonomous cropping and feature extraction algorithm previously. The value corresponding to the 35<sup>th</sup> bin is used as the threshold. Once the threshold is determined, the values below the threshold are set to zero. The obtained vector provides nonzero values grouped around the center of code periods. Since thresholding may result in gaps within a group of nonzero values another average filtering is applied to this vector. The aim is to obtain continuous zero sections between the nonzero groups, which will provide a code period measurement. Later using the nonzero groups and the zero sections an average code period is obtained as described in the previous section. This is illustrated in Figure 55.



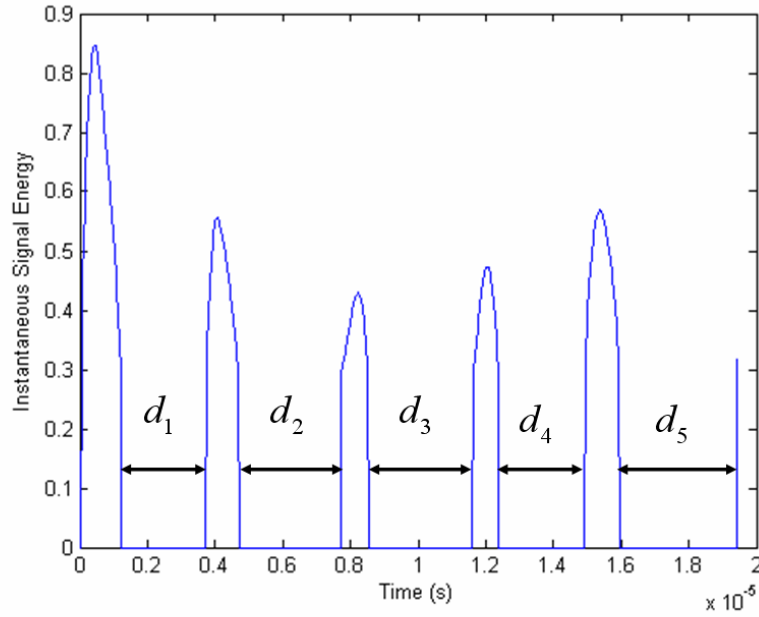


Figure 69. Thresholded Time Slice Vector.

The bandwidth measurement is very close to the technique used in the T-F autonomous cropping and feature extraction algorithm previously to obtain the frequency band of interest. First the marginal frequency distribution (MFD) is found. MFD is smoothed using a local neighborhood of  $\eta=10$  in the adaptive filter and a window length of  $m=20$  in the moving average filter. Followed by the smoothing operation a histogram of 100 bins is generated and the value corresponds to the 20<sup>th</sup> bin is used as the threshold. After the determination of the threshold the values below the threshold are set to zero. The frequency band found between the first and last nonzero value is expected to provide the bandwidth. Figure 56 shows the steps to obtain the bandwidth.

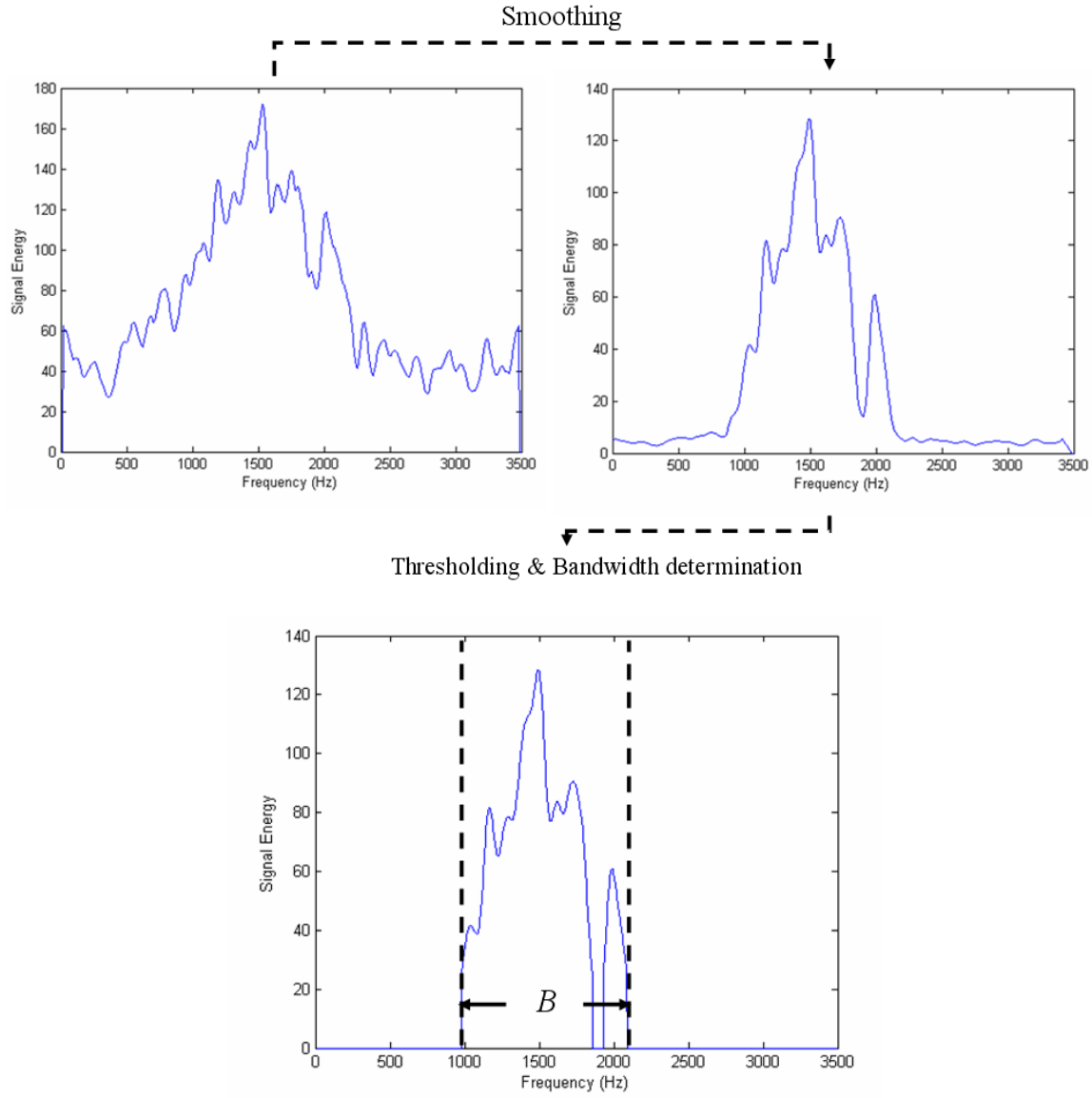


Figure 70. Bandwidth Extraction after Smoothing and Thresholding the MFD.

Once  $f_c$ ,  $T$  and  $B$  are obtained, the code length  $N_c$  can be obtained using the relation  $N_c = T \times B$  and the cycles of the carrier frequency per subcode  $c_{pp}$  can be obtained using the relation  $c_{pp} = f_c / B$ .

### C. PARAMETER EXTRACTION TEST RESULTS

The results of the parameter extraction algorithms are presented in Appendix C.A and C.B. Tables 67 through 74 include the actual parameters used to generate the polyphase signals, the extracted parameters by using the algorithms and the absolute value of the relative error which is denoted as *error*. If  $a^*$  is a measurement value of a quantity whose exact value is  $a$ , then the absolute value of the relative error  $\varepsilon_r$  is defined by [2]

$$\varepsilon_r = \left| \frac{a^* - a}{a} \right| = \left| \frac{\text{Error}}{\text{True value}} \right| \quad (5.10)$$

Both algorithms designed to extract the parameters of polyphase coded LPI modulations (Frank, P1, P2, P3, P4). The testing signals include all the Frank, P1, P2, P3 and P4 signals presented in Tables 1-2 at SNR levels of 6 dB, 0dB, -3dB and -6dB. The results are presented both in detailed tables (Appendix C.A, B) and in error charts (Appendix C.C). The extraction results from CWD images are denoted as CWD and the extraction results from PWVD images are denoted as PWVD on the error charts. Error charts are obtained for SNR levels of 6 dB, 0dB, -3dB for each parameter extracted. The signal parameters corresponding to the signal number shown in error charts can be found in Appendix C.A and C.B Tables 67 through 74.

The test results for Frank signals are presented below. The test results show that both algorithms provide very similar results and both algorithms have reasonably small errors. The carrier frequency error is very small for all SNR levels and for both algorithms. Note that if the frequency resolution of the PWVD and CWD images are increased the carrier frequency error may decrease.

The number of subcode error is related to  $T$  and  $B$  since  $N_c$  is found using the relation  $N_c = T \times B$ , and cycles per subcode error is related to the  $f_c$  and  $B$  since  $c_{pp}$  is found using the relation  $c_{pp} = f_c / B$ . Note that the high cycles per subcode error for the first signal at  $SNR = -3\text{dB}$  in Figure 73. Although the carrier frequency error is very

small; the bandwidth error increases the cycles per subcode error dramatically. For the Frank code overall results show that the error rate slightly increases with the decrease in the SNR.

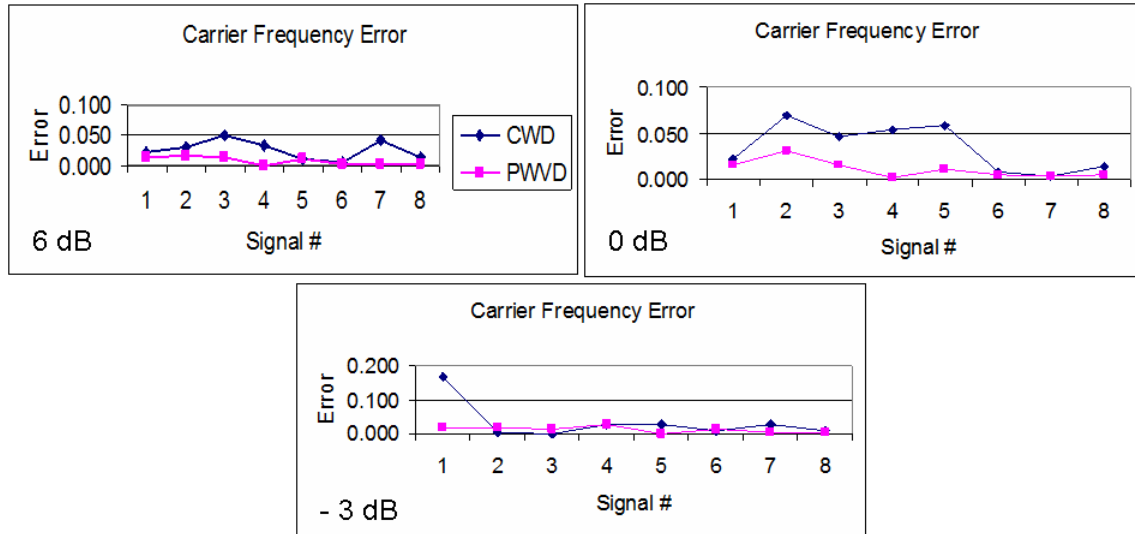


Figure 71. Carrier Frequency Error for Frank Code.

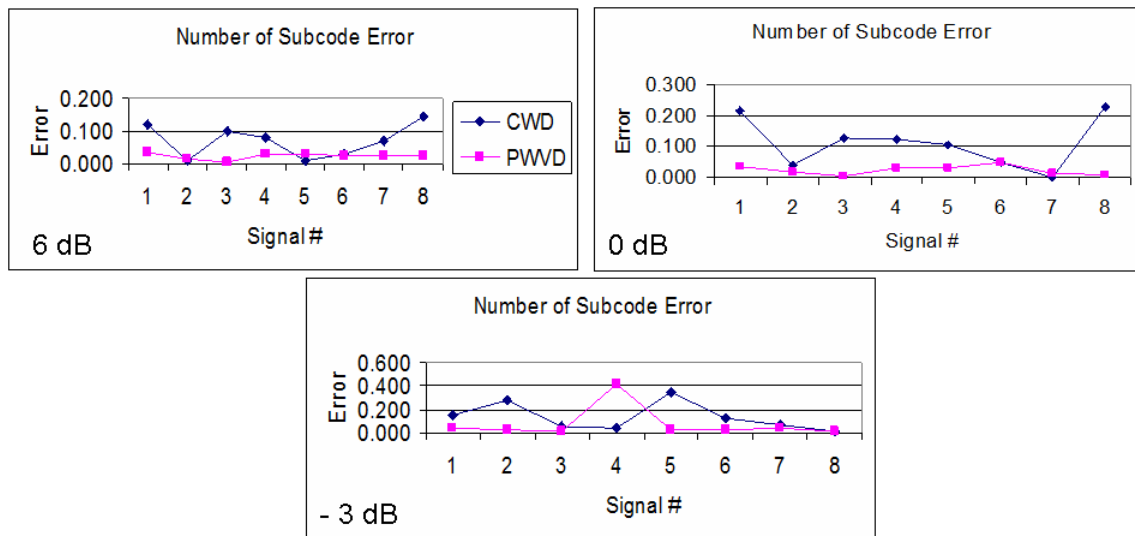


Figure 72. Number of Subcode Error for Frank Code.

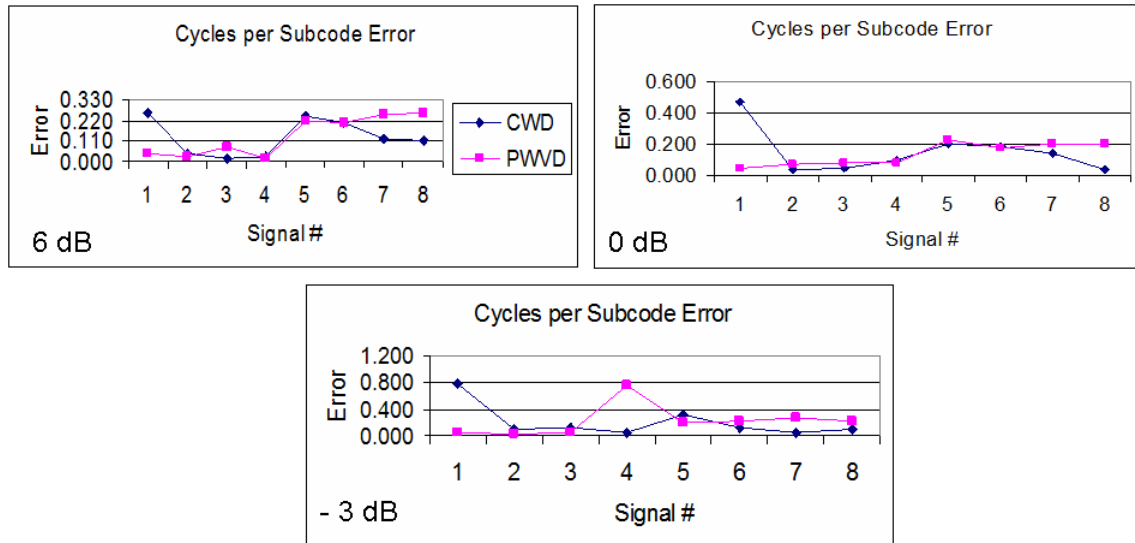


Figure 73. Cycles per Subcode Error for Frank Code.

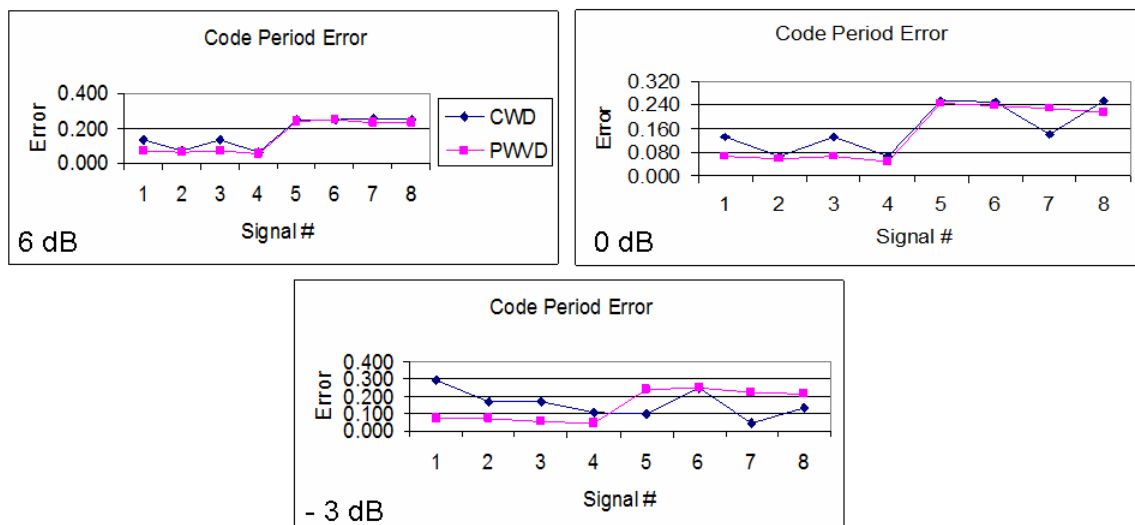


Figure 74. Code Period Error for Frank Code.

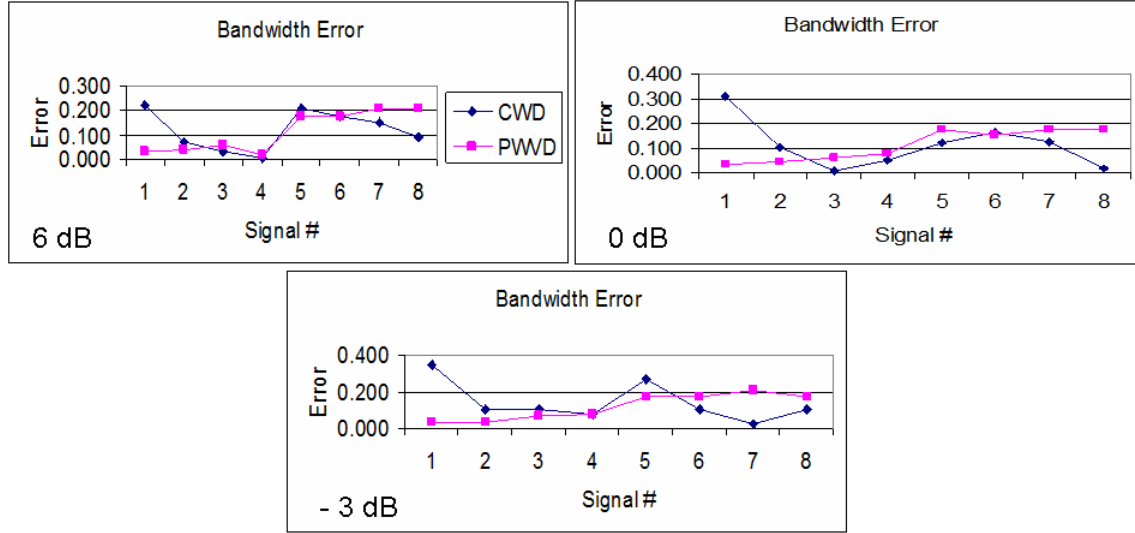


Figure 75. Bandwidth Error for Frank Code.

The parameter extraction test results for P1, P2, P3 and P4 codes are presented for PWVD images in Appendix C.A and for CWD images in Appendix C.B. The error charts providing comparison between two approaches are presented in Appendix C.C.

The overall error rates are reasonably small. The carrier frequency error slightly increases from  $SNR = 6\text{ dB}$  to  $SNR = -3\text{ dB}$ . The bandwidth and code period extraction results from PWVD images exhibit several high error rates for P1, P2 and P3 codes at  $SNR = 0$  and  $SNR = -3\text{ dB}$ . This exhibits one of the drawbacks of the algorithm. As the  $SNR$  level decrease below  $0\text{ dB}$  the maximum intensity level occurs at a very small projection angle  $\theta_s$ . This corresponds to the marginal time distribution and produce erroneous results.

The CWD parameter extraction algorithm slightly outperforms the PWVD algorithm as the  $SNR$  decreases. The results obtained from both algorithms tend to coincide well with the actual values and the relative error depends on how closely results are examined. Note also that the PWVD algorithm is not affected from the cross terms present within the PWVD images.

#### **D. SUMMARY**

Two parameter extraction algorithms are investigated. First one is designed to extract the parameters from the PWVD images of polyphase coded LPI signals (Frank, P1, P2, P3, P4) based on the Radon transform of the PWVD images. The second algorithm is designed to extract the parameters from the CWD images of polyphase coded LPI signals (Frank, P1, P2, P3, P4) using frequency domain lowpass filter on the 2-D FFT of CWD images.

The algorithms are tested with the Frank, P1, P2, P3 and P4 signals presented in Tables 1-2 at SNR levels of 6 dB, 0dB, -3dB and -6dB.

The next chapter presents the conclusion of this thesis and recommendations for further research.

THIS PAGE INTENTIONALLY LEFT BLANK



## VI. CONCLUSIONS AND RECOMMENDATIONS

In this thesis an autonomous detection and classification architecture was investigated. The architecture contained T-F detection techniques which provide image outputs of LPI radar waveforms. A diverse database was generated including twelve LPI modulation techniques each having 21 SNR levels. The use of T-F detection techniques provides an efficient method for the extraction of a composite feature vector to classify LPI modulations. An autonomous image cropping and feature extraction algorithm based on 2-D FFT and PCA was applied to the T-F images. The extracted features were used as input to a non-linear classifier. In this work an MLPNN, an RBFNN and a PNN were used as classifiers.

The feature extraction and network parameter optimization work showed that there is not a unique solution for each detection technique or each classifier concerning the optimum parameters. Each variable used within the algorithms need to be optimized for the best result. For MLPNN, it is shown that the classification performance has increased as the number of hidden layer neurons was increased.

Applying the PCA, the high dimensional feature vectors can be reduced to a smaller dimensional feature vector by preserving most of their information. In this work, the training matrix and feature vectors of testing signals were reduced in dimension successfully by applying the PCA. This prevents the classifiers to be overwhelmed by the complexity of high dimensional feature vectors. In this way the need for resizing the T-F images to a smaller dimension to generate the feature vector can be eliminated. An optimization is also applied in order to analyze the amount of principal components needed for the best classification rate. The concern arises from the fact that the minor components do not necessarily consist of noise and they may contain important information. The results showed that for PWVD and CWD images the use of minor components improve the classification results.

Concerning the Test Modulation results, the best overall classification result is achieved with PWVD technique. This might be due to the presence of the cross-terms

within the PWVD images. Since cross-terms may preserve additional information about the modulation type, they might have improved the classification results. CWD results were very similar to PWVD results. QMFB technique on the other hand performed very poorly. The choice of a particular QMFB layer which determines the dimension of the QMFB image influences the results significantly. The smaller dimensional images are expected to contain less class distinctive information. The Test SNR results were very promising indicating that the autonomous modulation energy isolation and cropping performed well.

Concerning the classifier performances, the PNN outperformed the RBFNN and MLPNN. The training and classification speed is also one of the most important considerations. The PNN and the RBFNN outperformed the MLPNN concerning the training and classification speed. The classification results of polyphase modulations (Frank, P1, P2, P3 and P4) were poor. The architecture could not perform to distinguish between polyphase modulations successfully. On the other hand the best results were obtained in the classification of the FMCW, Costas, FSK/PSK, P2 and T4 modulations. These modulations have distinctive T-F images which makes the classification process simpler.

Following the detection and classification algorithm two parameter extraction algorithms were investigated. First one was designed to extract the parameters from the PWVD images of polyphase coded LPI signals (Frank, P1, P2, P3, P4) based on the Radon transform of the PWVD images. The second algorithm was designed to extract the parameters from the CWD images of polyphase coded LPI signals (Frank, P1, P2, P3, P4) using frequency domain lowpass filter on the 2-D FFT of CWD images. The results obtained from both algorithms tend to coincide well with the actual values and the relative error depends on how closely results are examined. At  $SNR = -3\text{dB}$  the PWVD parameter extraction algorithm gave erroneous results, while the CWD parameter extraction algorithm still gave reasonable results. The PWVD parameter extraction algorithm performs without being affected from the cross terms present within the PWVD images.

In order to enhance the feature extraction and classification algorithm and to increase its robustness and reliability, there are still some issues that should be addressed. Future efforts may include expanding the database of LPI CW radar modulations. The training matrix may be increased in dimension in order to include more diverse parameters. The optimization process might be conducted in more detail. The use of bi-frequency detection techniques may also be investigated for LPI waveform classification and parameter extraction. Other feature extraction methods might be investigated such as Fisher Linear Discriminant Analysis which might improve the extraction of class discriminating information better. The information theoretic feature selection algorithms might also be investigated to select the best features from a potential feature set of a T-F image. The performance of other classification networks such as self-organizing networks and adaptive resonance networks might also be investigated.

THIS PAGE INTENTIONALLY LEFT BLANK

## APPENDIX A.

### A. INITIALIZATION OF MLPNN

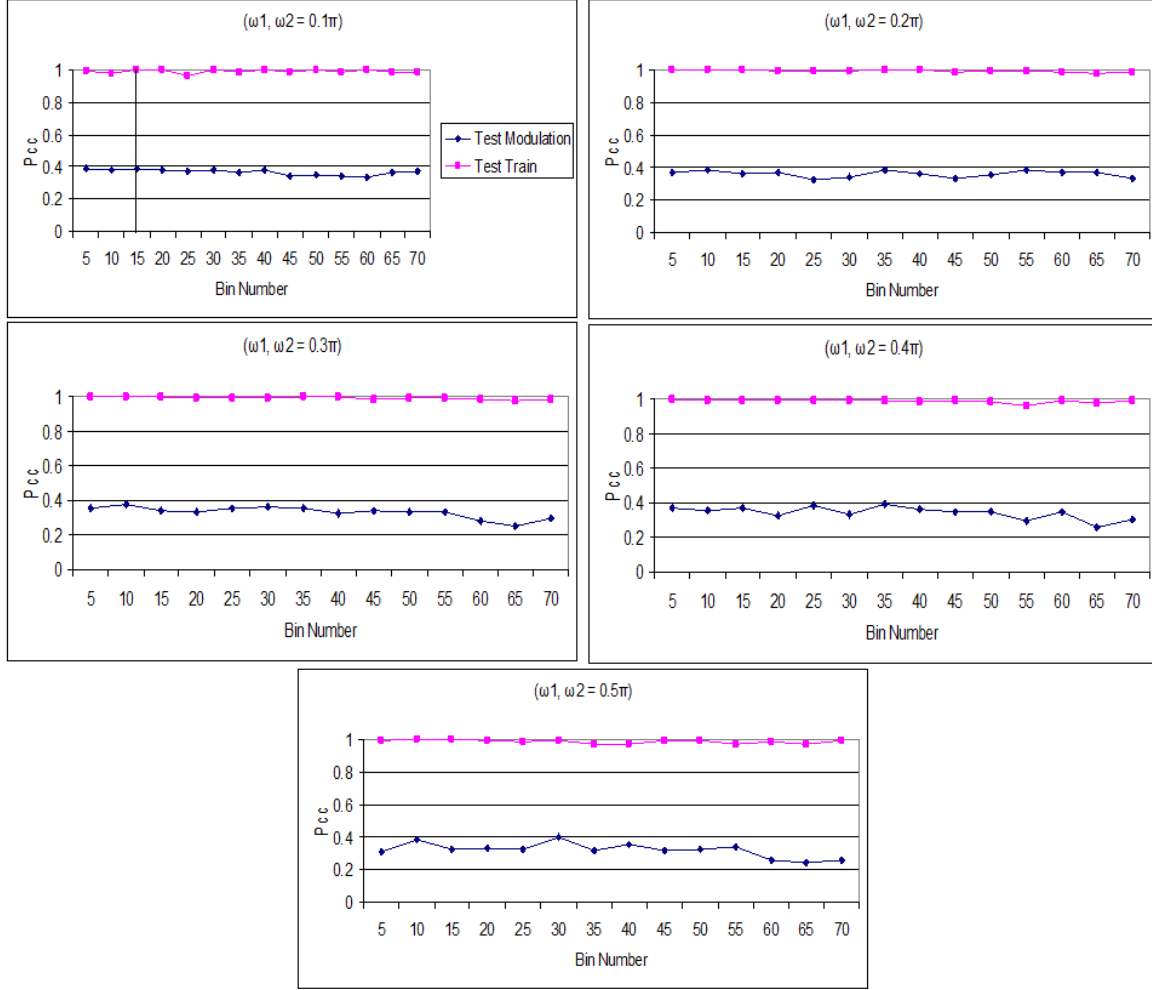


Figure 76. Optimization of  $\omega_1$ ,  $\omega_2$  and Bin Number for CWD image classification with MLPNN.

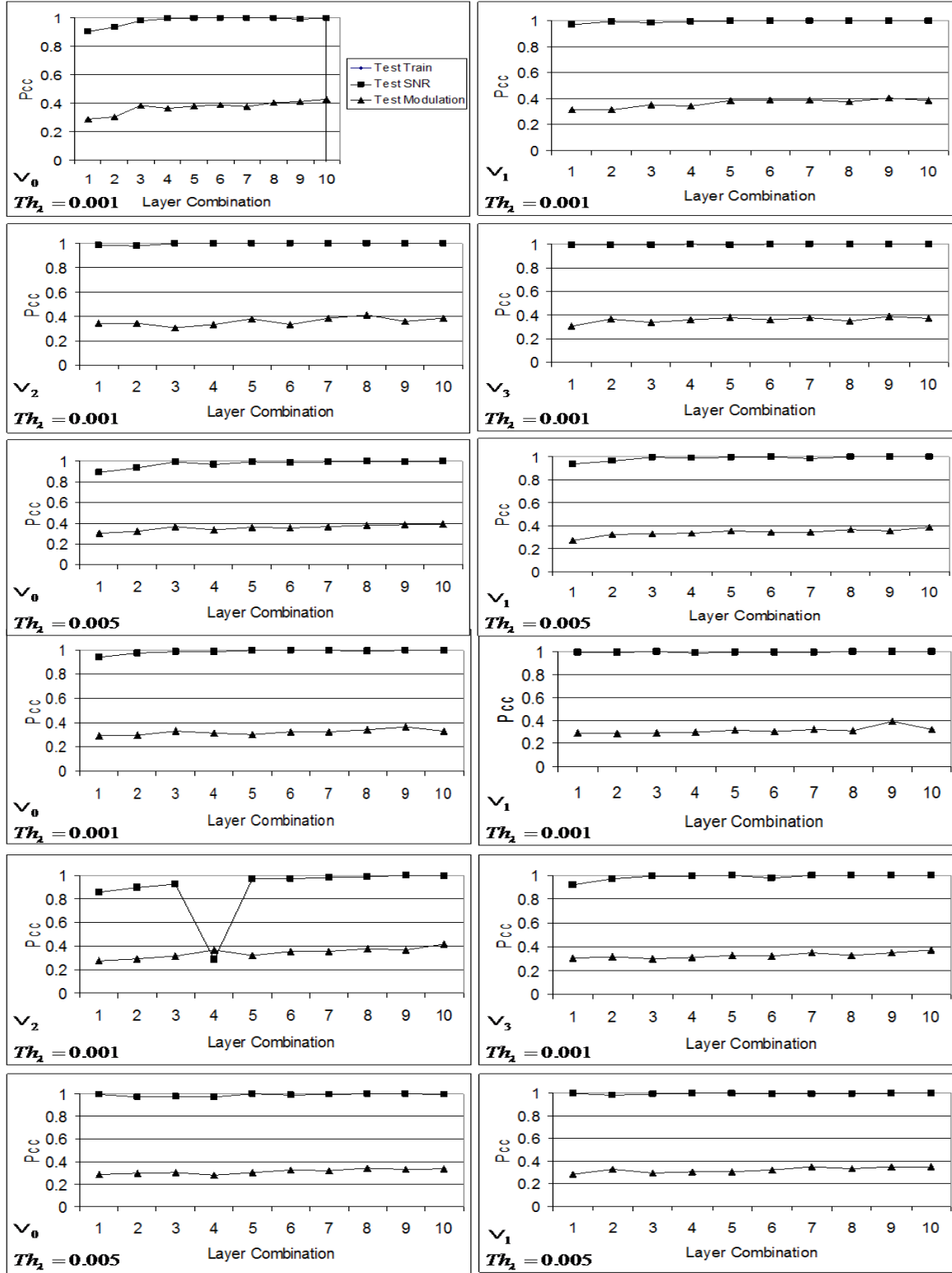


Figure 77. Optimization of  $S_1$ ,  $S_2$ ,  $Th_\lambda$  and  $v_i$  for CWD image classification with MLPNN.

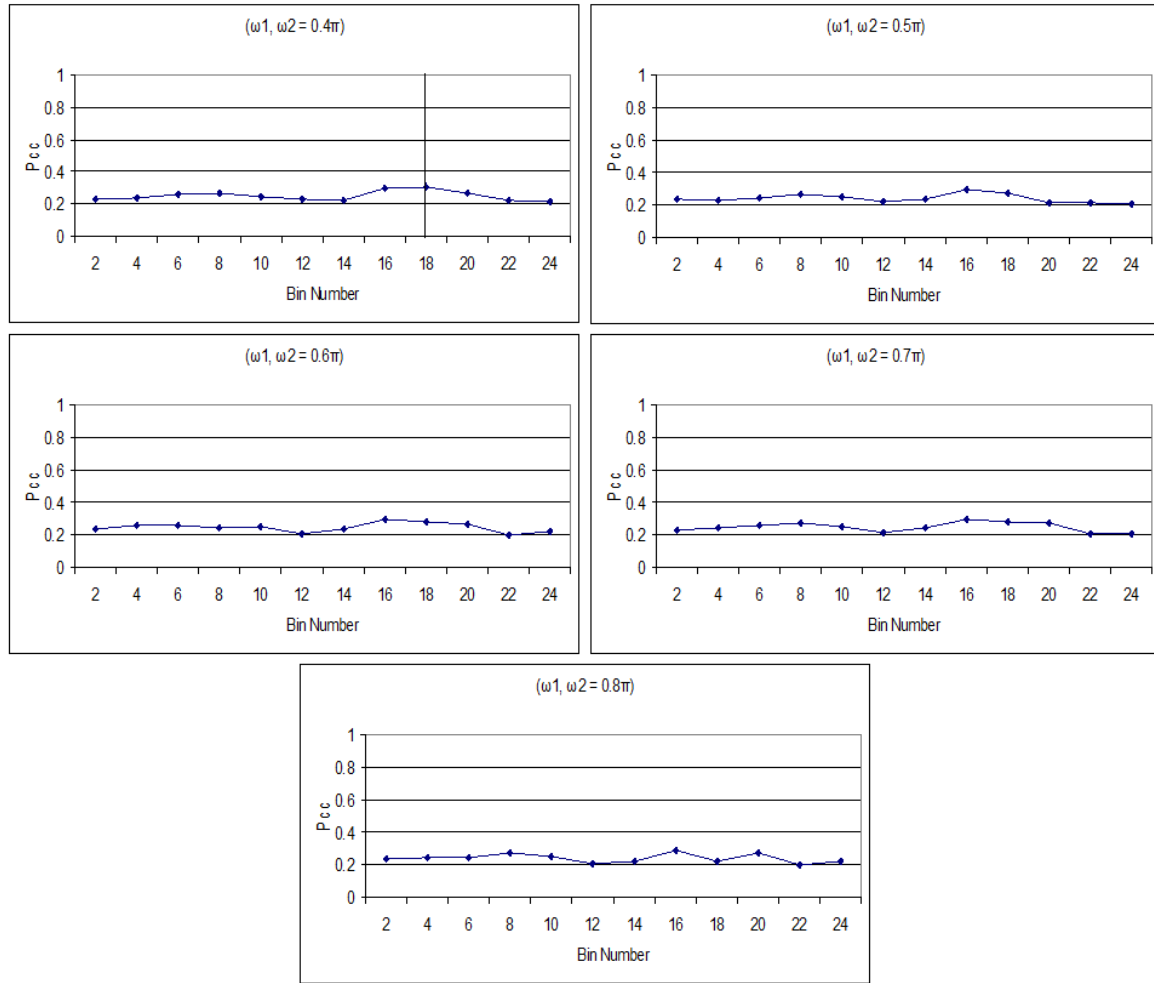


Figure 78. Optimization of  $\omega_1$ ,  $\omega_2$  and Bin Number for QMFB image classification with MLPNN (Test Modulation Results).

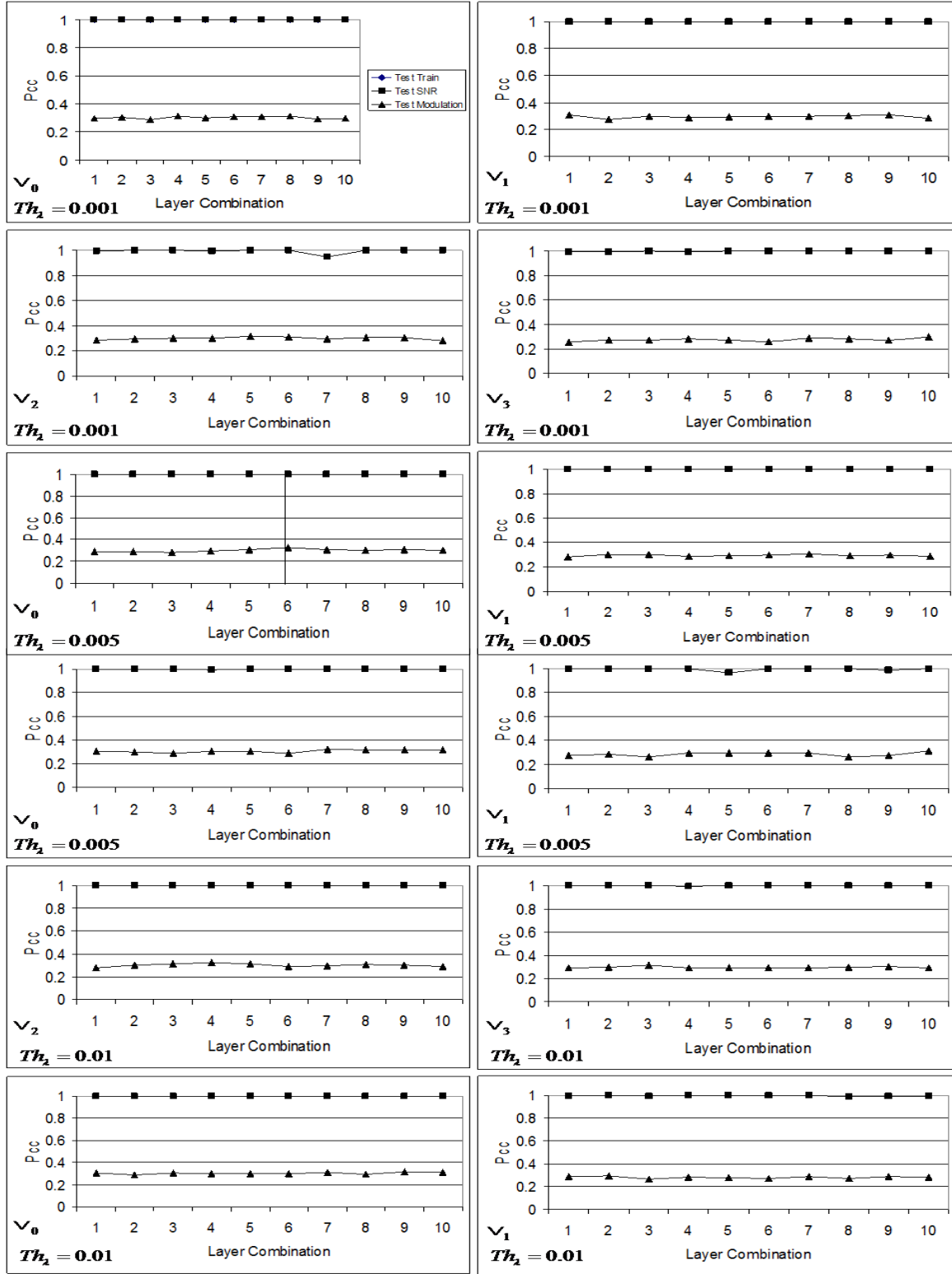


Figure 79. Optimization of  $S_1$ ,  $S_2$ ,  $Th_\lambda$  and  $v_i$  for QMFB image classification with MLPNN.



## B. INITIALIZATION OF RBFNN

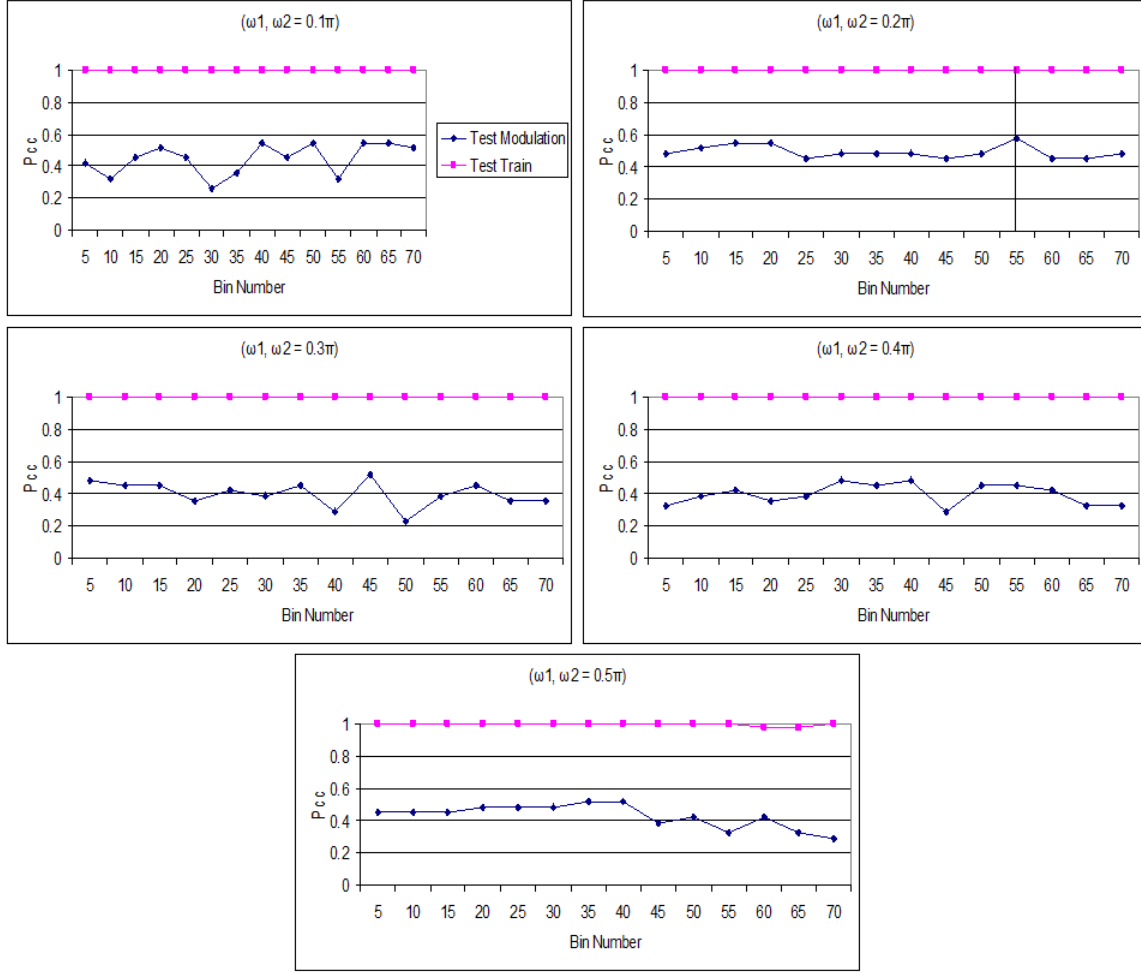


Figure 80. Optimization of  $\omega_1$ ,  $\omega_2$  and Bin Number for PWVD image classification with RBFNN.

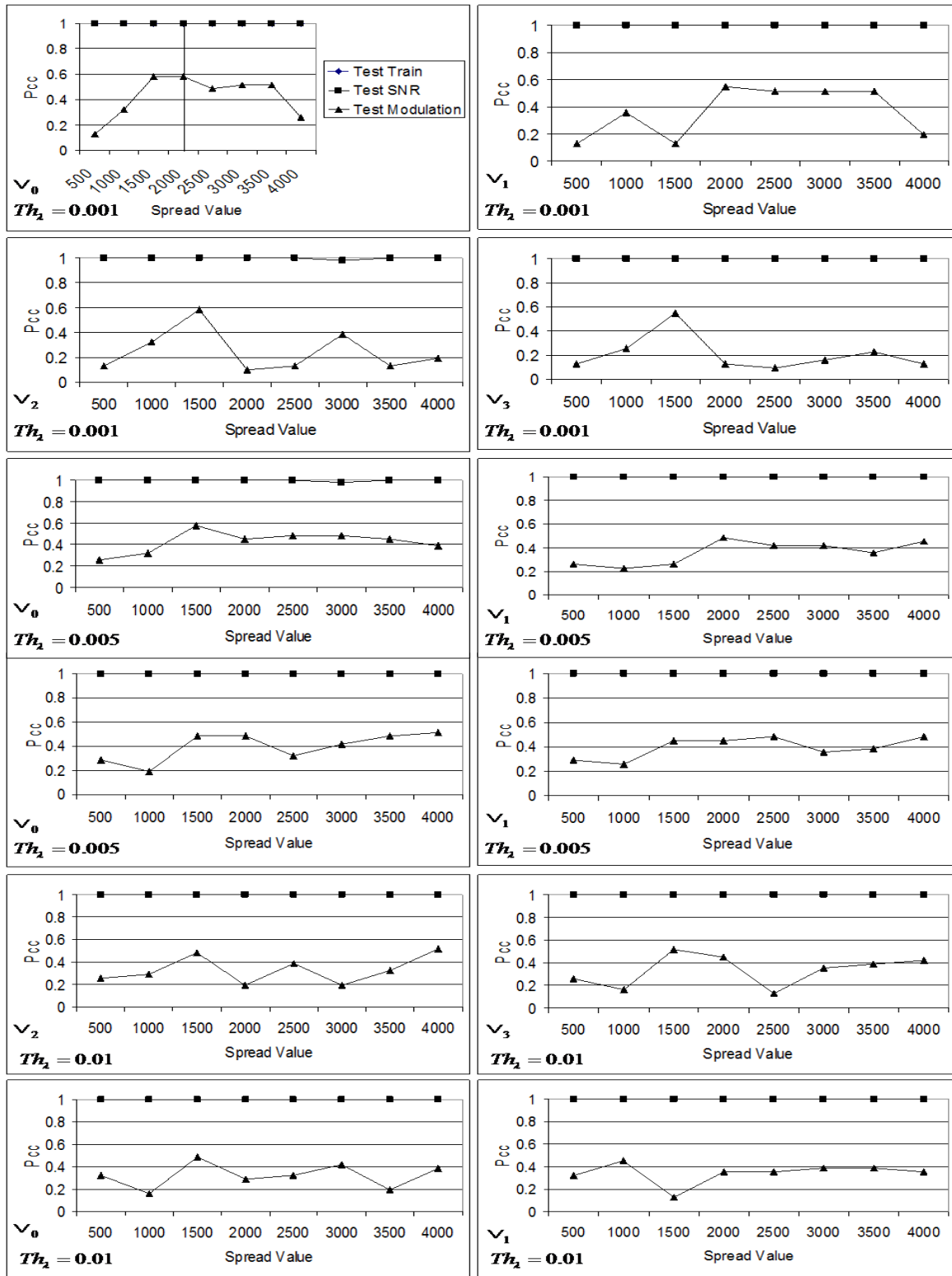


Figure 81. Optimization of  $\sigma$ ,  $Th_i$  and  $v_i$  for PWVD image classification with RBFNN

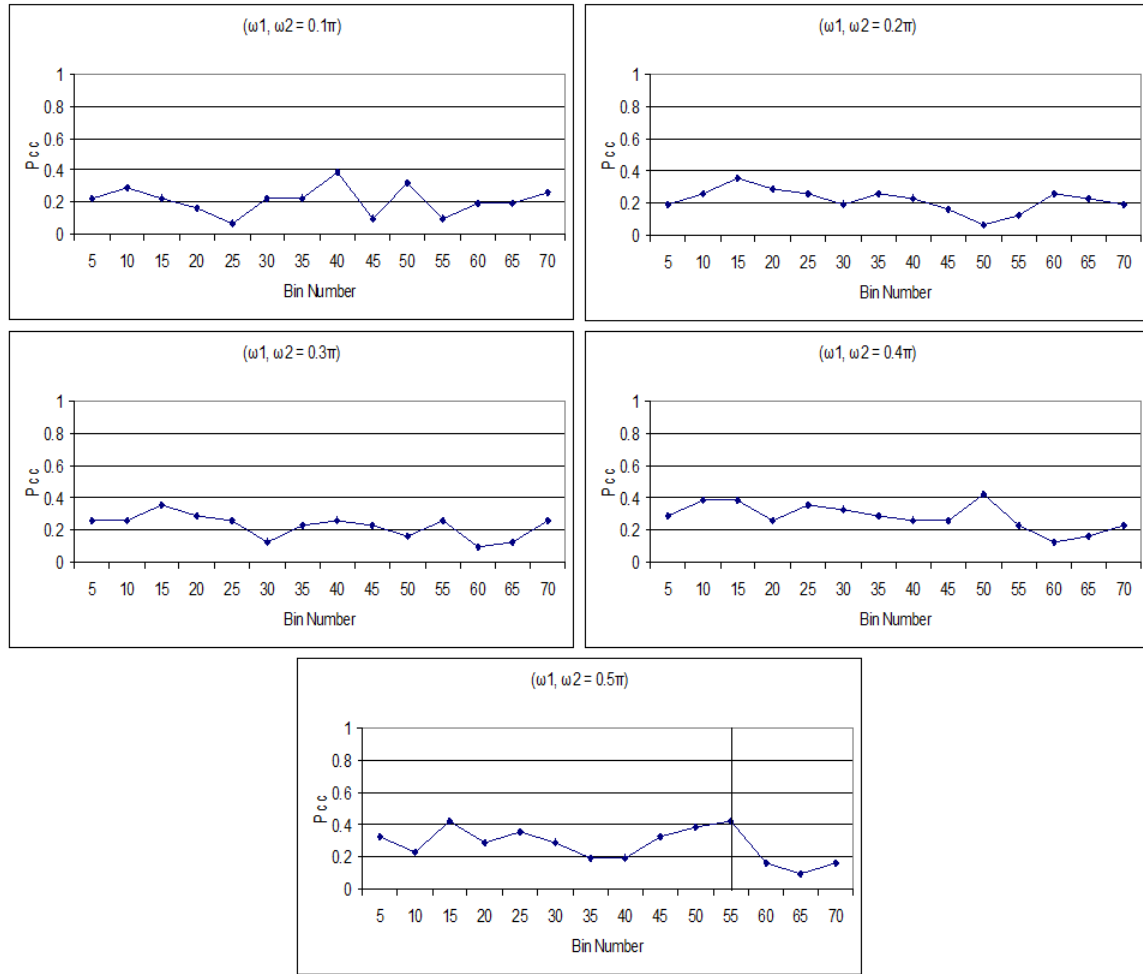


Figure 82. Optimization of  $\omega_1$ ,  $\omega_2$  and Bin Number for CWD image classification with RBFNN (Test Modulation Results).

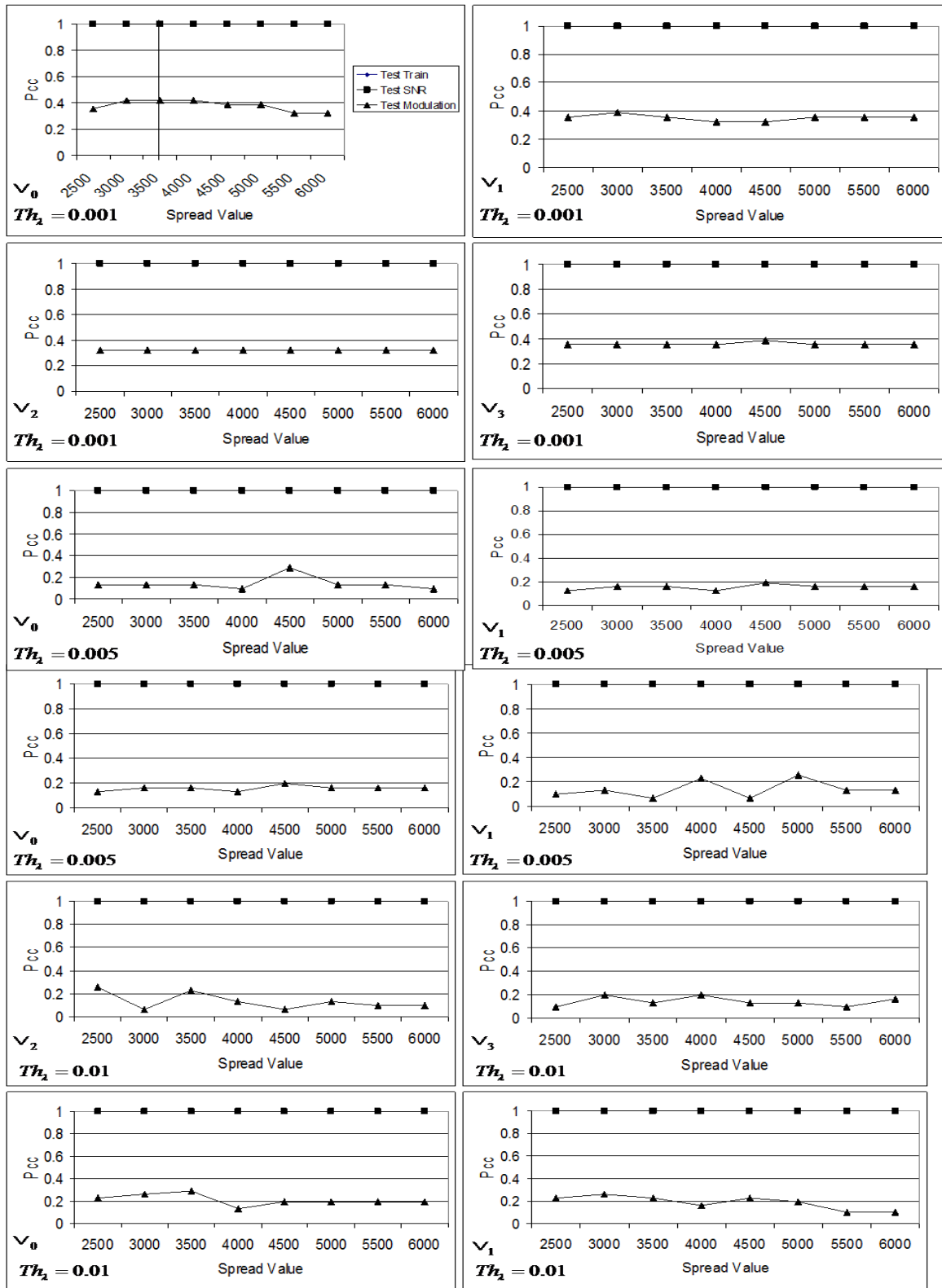


Figure 83. Optimization of  $\sigma$ ,  $Th_\lambda$  and  $v_i$  for CWD image classification with

## RBFNN

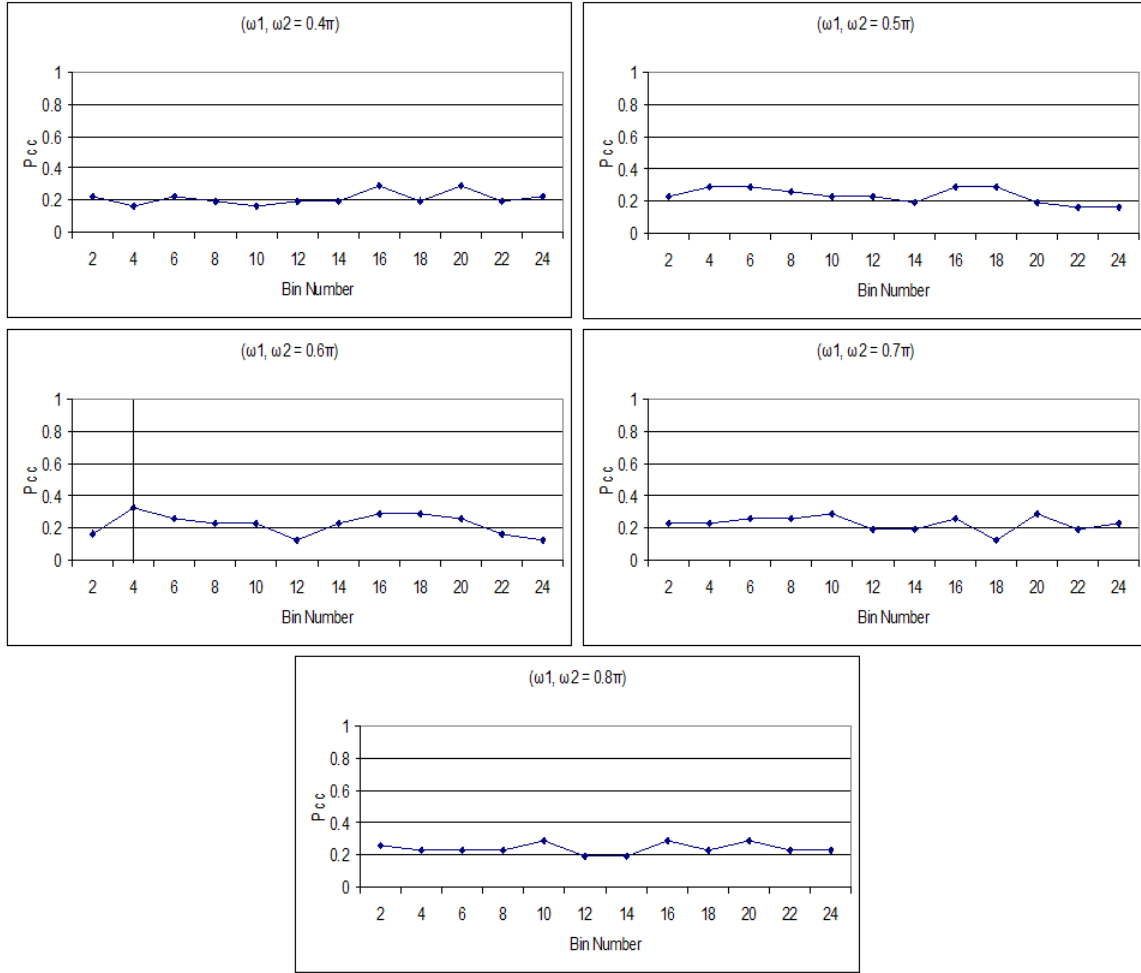


Figure 84. Optimization of  $\omega_1, \omega_2$  and Bin Number for QMFB image classification with RBFNN (Test Modulation Results).

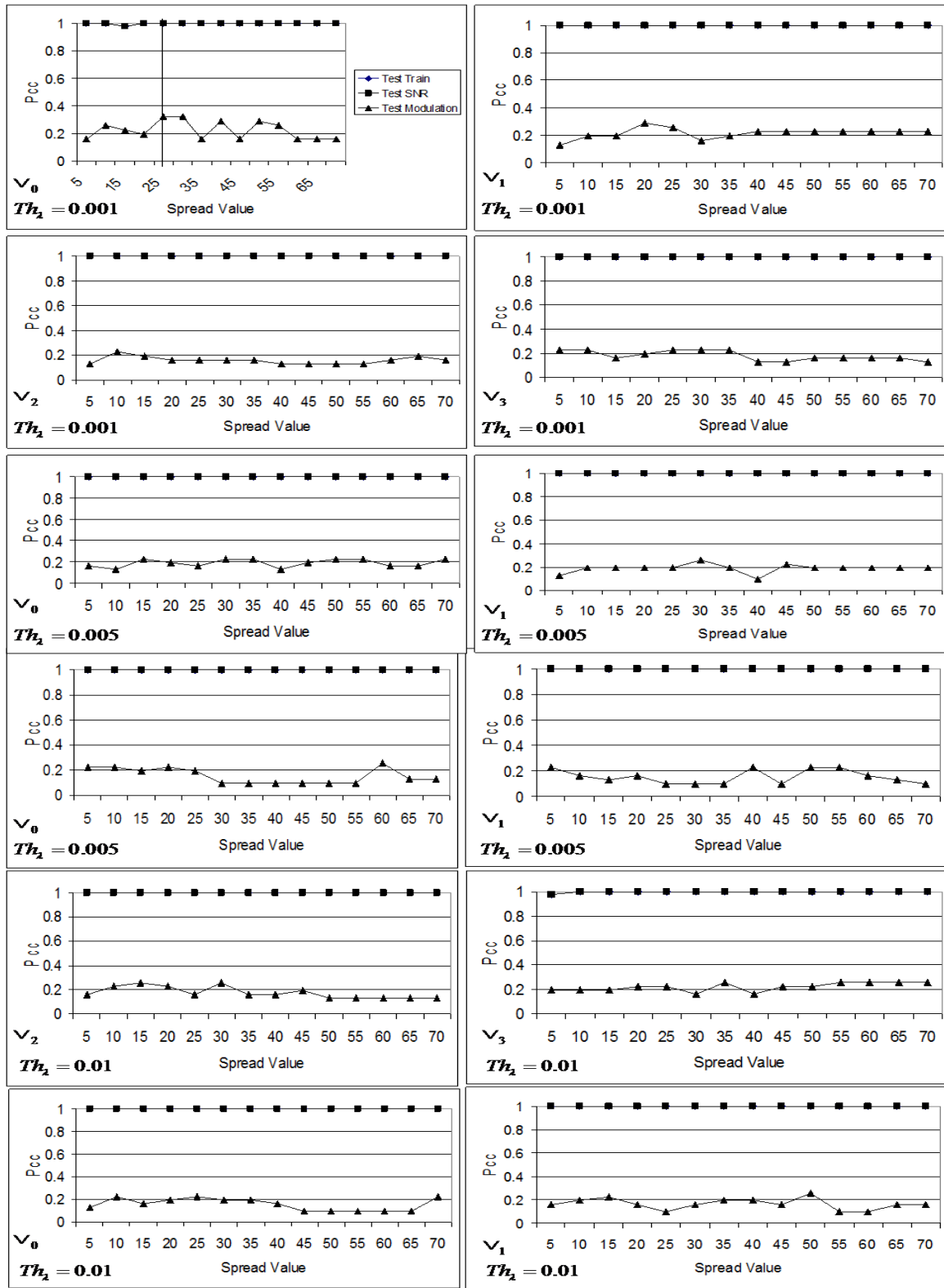


Figure 85. Optimization of  $\sigma$ ,  $Th_\lambda$  and  $v_i$  for QMFB image classification with

## C. INITIALIZATION OF PNN

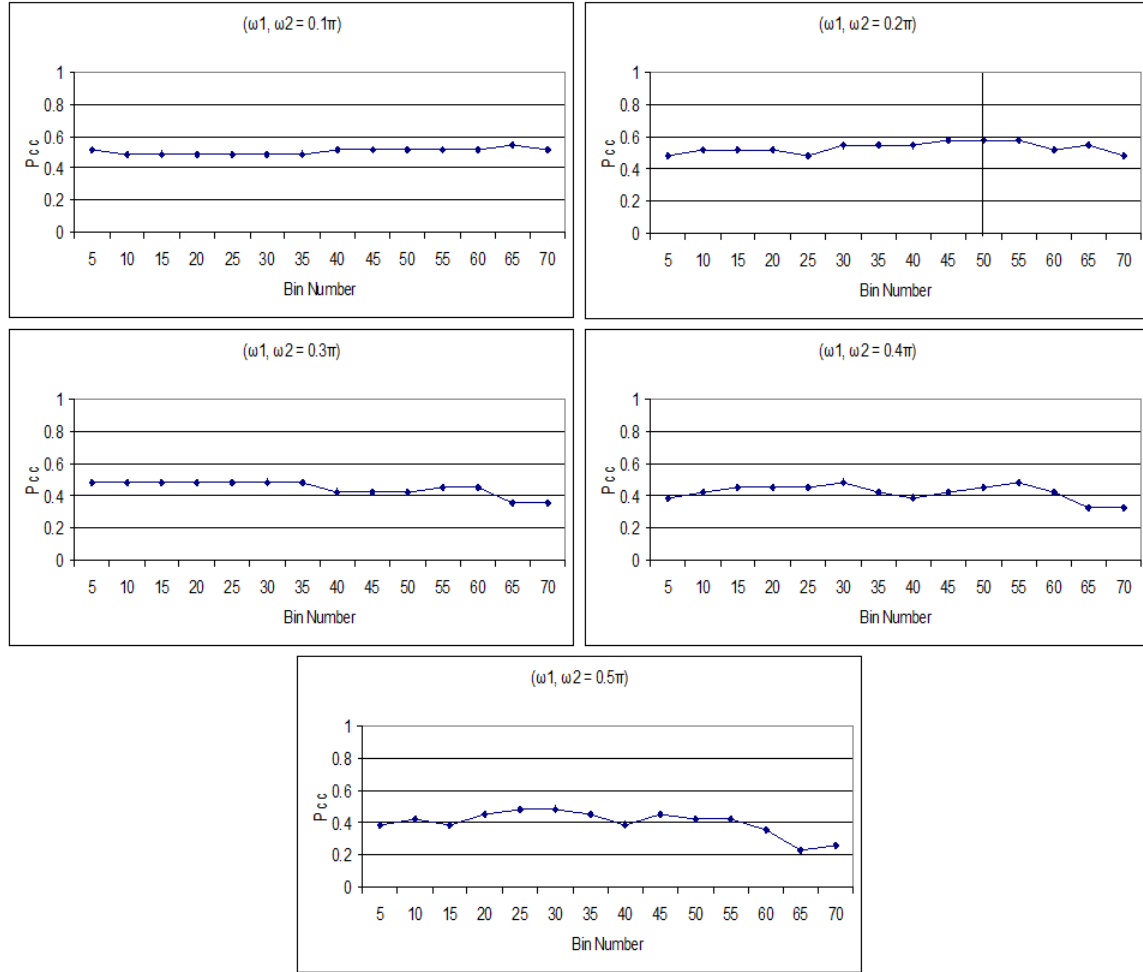


Figure 86. Optimization of  $\omega_1$ ,  $\omega_2$  and Bin Number for PWVD image classification with PNN (Test Modulation Results).

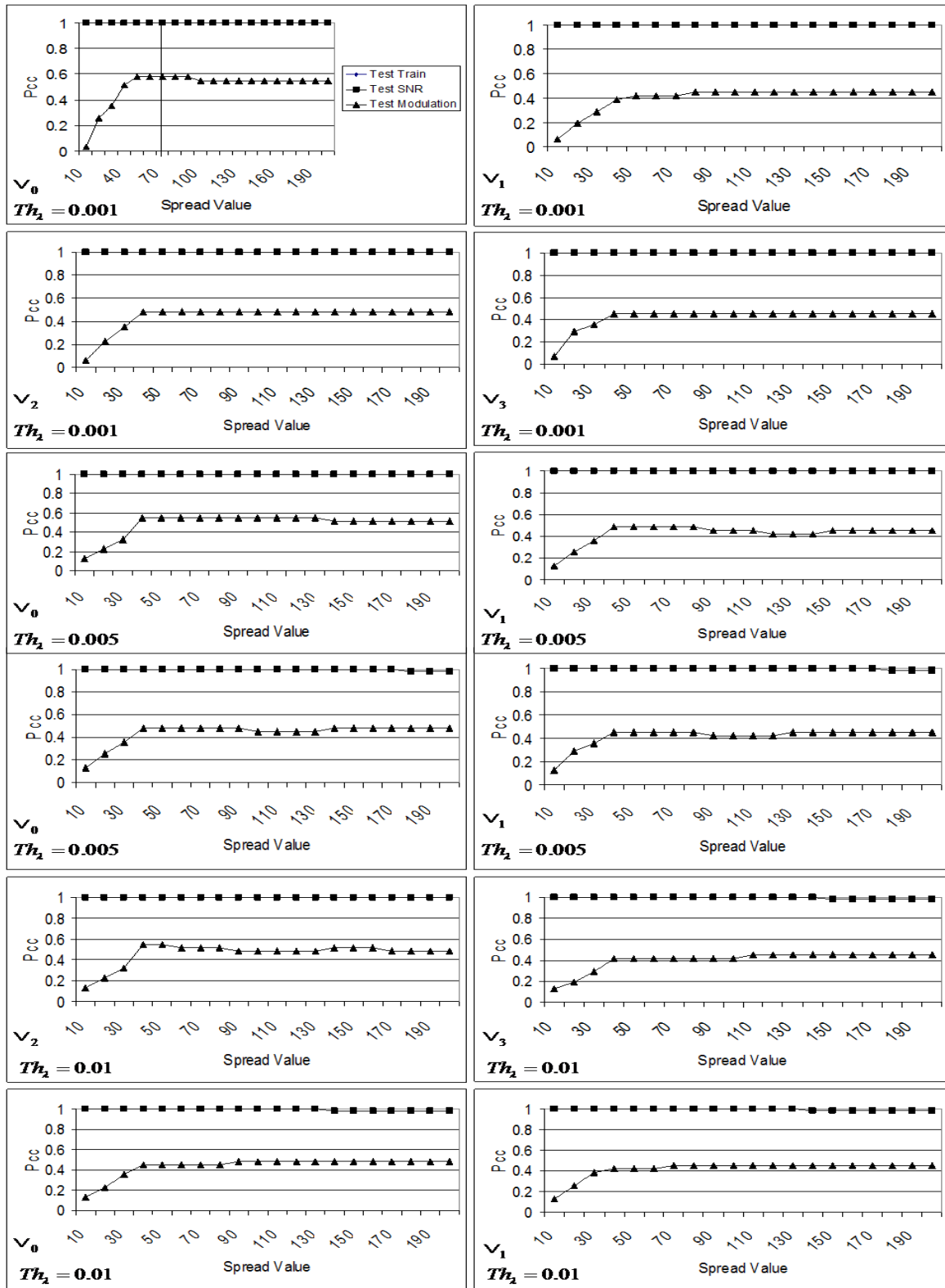


Figure 87. Optimization of  $\sigma$ ,  $Th_i$  and  $v_i$  for PWVD image classification with PNN.



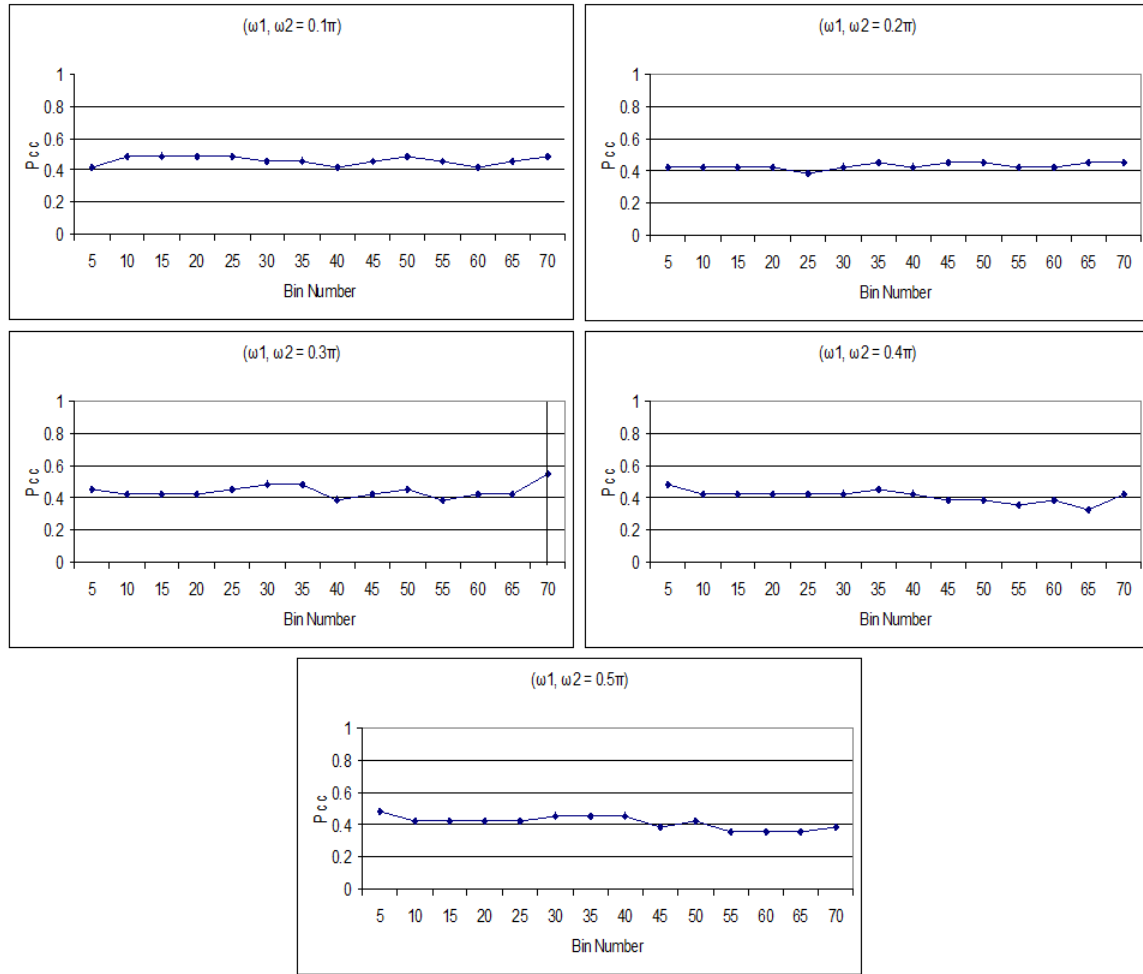


Figure 88. Optimization of  $\omega_1$ ,  $\omega_2$  and Bin Number for CWD image classification with PNN (Test Modulation Results).

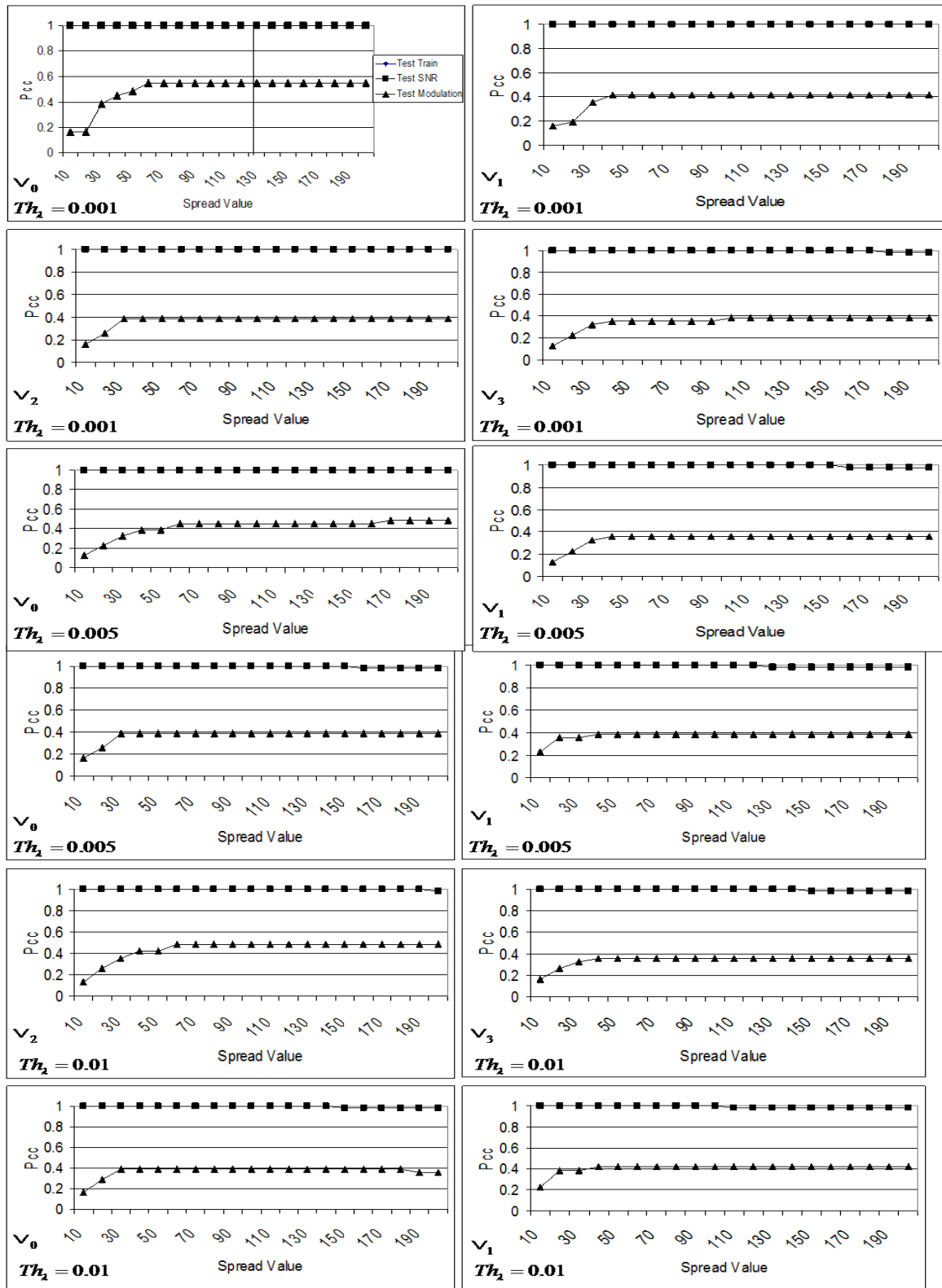


Figure 89. Optimization of  $\sigma$ ,  $Th_i$  and  $v_i$  for CWD image classification with PNN.

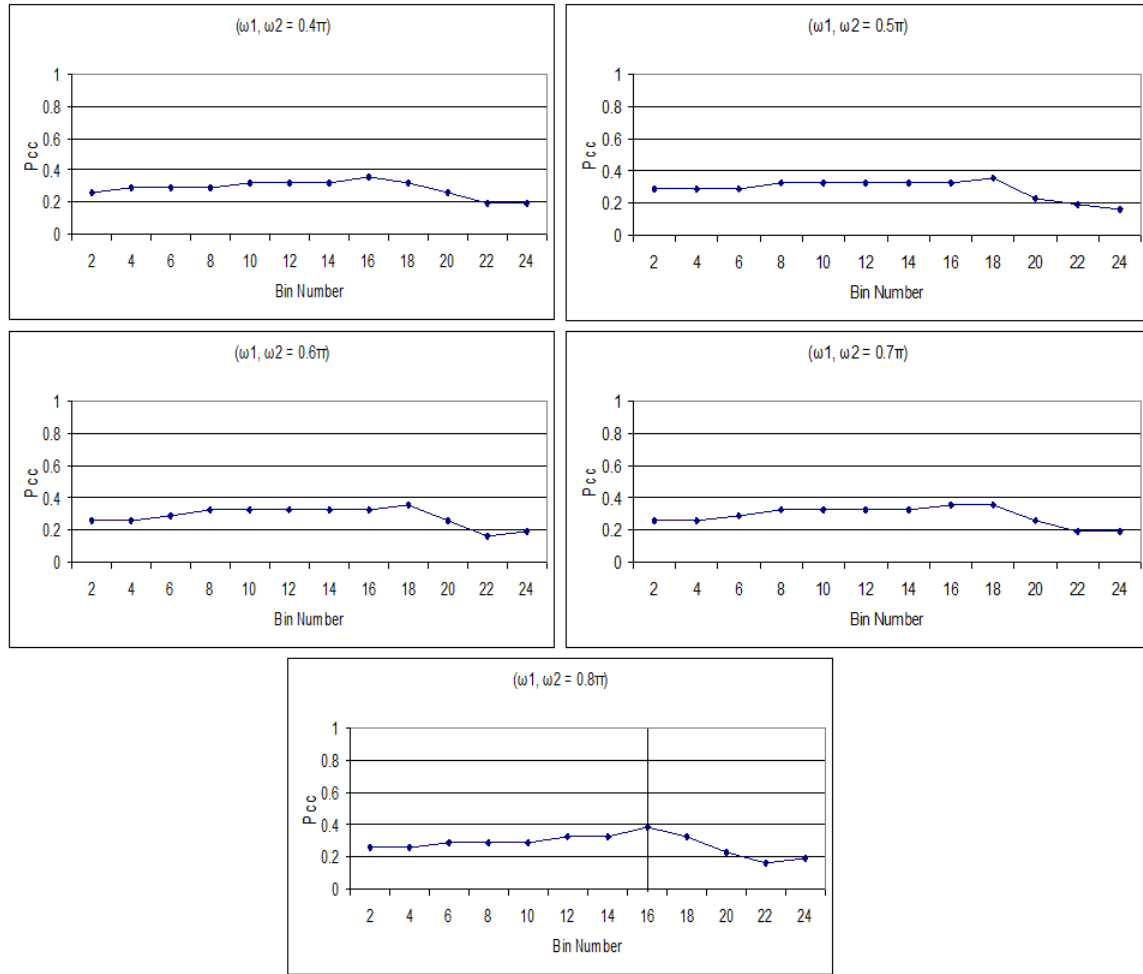


Figure 90. Optimization of  $\omega_1$ ,  $\omega_2$  and Bin Number for QMFB image classification with PNN (Test Modulation Results).

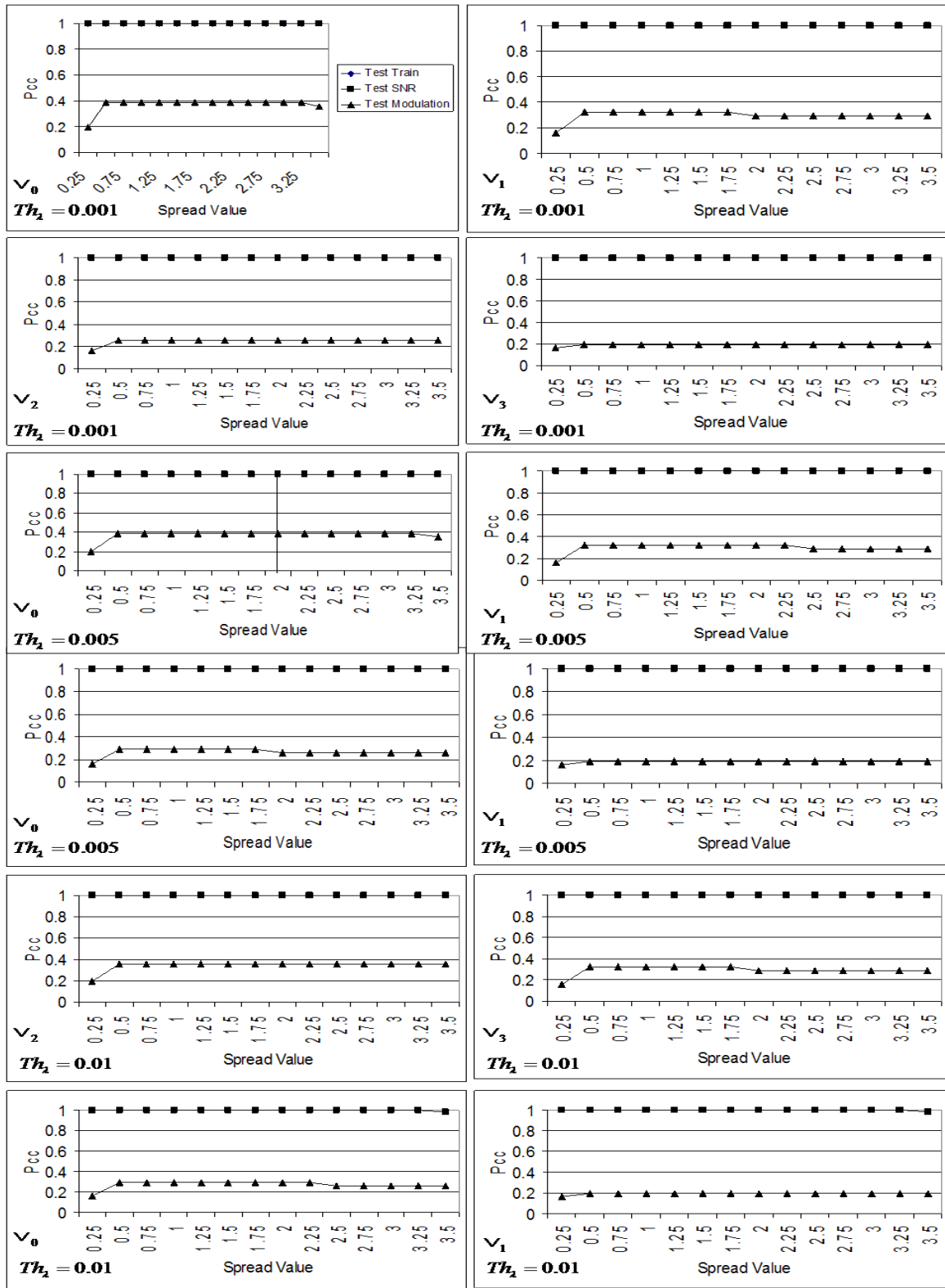


Figure 91. Optimization of  $\sigma$ ,  $Th_i$  and  $v_i$  for QMFB image classification with PNN.

## APPENDIX B.

### A. MLPNN CLASSIFICATION CONFUSION MATRICES

Table 13. PWVD Classification Results with MLPNN (  $SNR = 10\text{dB}$  ).

TEST SNR	COSTAS	FRANK	FSK/PSK	FMCW	P1	P2	P3	P4	T1(n)	T2(n)	T3(n)	T4(n)
COSTAS	<b>1.00</b>	0.00	0.01	0.00	0.00	0.00	0.00	0.00	0.00	0.00	0.00	0.00
FRANK	0.00	<b>1.00</b>	0.00	0.00	0.00	0.00	0.00	0.00	0.00	0.00	0.00	0.00
FSK/PSK	0.00	0.00	<b>0.99</b>	0.00	0.00	0.00	0.00	0.00	0.00	0.00	0.00	0.00
FMCW	0.00	0.00	0.00	<b>1.00</b>	0.00	0.00	0.00	0.00	0.00	0.00	0.00	0.00
P1	0.00	0.00	0.00	0.00	<b>1.00</b>	0.00	0.00	0.01	0.00	0.00	0.00	0.00
P2	0.00	0.00	0.00	0.00	0.00	<b>0.99</b>	0.00	0.00	0.00	0.00	0.00	0.00
P3	0.00	0.00	0.00	0.00	0.00	0.00	<b>1.00</b>	0.00	0.00	0.00	0.00	0.00
P4	0.00	0.00	0.00	0.00	0.00	0.00	0.00	<b>0.99</b>	0.00	0.00	0.00	0.00
T1(n)	0.00	0.00	0.00	0.00	0.00	0.00	0.00	0.00	<b>1.00</b>	0.00	0.00	0.00
T2(n)	0.00	0.00	0.00	0.00	0.00	0.01	0.00	0.00	0.00	<b>1.00</b>	0.00	0.00
T3(n)	0.00	0.00	0.00	0.00	0.00	0.00	0.00	0.00	0.00	0.00	<b>1.00</b>	0.02
T4(n)	0.00	0.00	0.01	0.00	0.00	0.00	0.00	0.00	0.00	0.00	0.00	<b>0.98</b>
TEST MODULATION	COSTAS	FRANK	FSK/PSK	FMCW	P1	P2	P3	P4	T1(n)	T2(n)	T3(n)	T4(n)
COSTAS	<b>1.00</b>	0.02	0.02	0.00	0.00	0.00	0.01	0.01	0.01	0.00	0.02	0.00
FRANK	0.00	<b>0.43</b>	0.02	0.00	0.34	0.33	0.57	0.31	0.00	0.00	0.09	0.00
FSK/PSK	0.00	0.01	<b>0.84</b>	0.00	0.00	0.00	0.00	0.01	0.00	0.00	0.03	0.00
FMCW	0.00	0.00	0.00	<b>0.99</b>	0.01	0.01	0.00	0.01	0.00	0.00	0.01	0.00
P1	0.00	0.01	0.00	0.01	<b>0.28</b>	0.00	0.00	0.01	0.01	0.00	0.02	0.01
P2	0.00	0.06	0.01	0.00	0.05	<b>0.60</b>	0.02	0.02	0.00	0.00	0.03	0.01
P3	0.00	0.08	0.00	0.00	0.22	0.02	<b>0.28</b>	0.27	0.21	0.00	0.11	0.00
P4	0.00	0.00	0.01	0.00	0.06	0.01	0.00	<b>0.32</b>	0.01	0.00	0.00	0.02
T1(n)	0.00	0.04	0.00	0.00	0.02	0.00	0.05	0.03	<b>0.38</b>	0.00	0.04	0.00
T2(n)	0.00	0.00	0.00	0.00	0.00	0.04	0.00	0.00	0.04	<b>0.66</b>	0.01	0.00
T3(n)	0.00	0.11	0.00	0.01	0.01	0.00	0.07	0.01	0.19	0.00	<b>0.14</b>	0.60
T4(n)	0.00	0.22	0.12	0.00	0.00	0.00	0.00	0.00	0.14	0.33	0.48	<b>0.35</b>

Table 14. PWVD Classification Results with MLPNN (  $SNR = 6\text{dB}$  ).

TEST SNR	COSTAS	FRANK	FSK/PSK	FMCW	P1	P2	P3	P4	T1(n)	T2(n)	T3(n)	T4(n)
COSTAS	<b>0.57</b>	0.00	0.00	0.00	0.00	0.00	0.00	0.00	0.00	0.00	0.00	0.00
FRANK	0.29	<b>1.00</b>	0.00	0.00	0.02	0.00	0.01	0.00	0.00	0.00	0.00	0.00
FSK/PSK	0.05	0.00	<b>1.00</b>	0.00	0.00	0.01	0.00	0.00	0.00	0.00	0.00	0.00
FMCW	0.00	0.00	0.00	<b>1.00</b>	0.00	0.00	0.00	0.00	0.00	0.00	0.00	0.00
P1	0.00	0.00	0.00	0.00	<b>0.76</b>	0.00	0.00	0.02	0.00	0.00	0.00	0.00
P2	0.00	0.00	0.00	0.00	0.00	<b>0.99</b>	0.00	0.00	0.00	0.00	0.00	0.00
P3	0.01	0.00	0.00	0.00	0.00	0.00	<b>0.81</b>	0.02	0.00	0.00	0.00	0.00
P4	0.00	0.00	0.00	0.00	0.21	0.00	0.18	<b>0.88</b>	0.00	0.00	0.00	0.00
T1(n)	0.00	0.00	0.00	0.00	0.00	0.00	0.00	0.00	<b>1.00</b>	0.00	0.00	0.00
T2(n)	0.00	0.00	0.00	0.00	0.00	0.00	0.00	0.00	0.00	<b>1.00</b>	0.00	0.00
T3(n)	0.00	0.00	0.00	0.00	0.00	0.00	0.00	0.00	0.00	0.00	<b>0.99</b>	0.02
T4(n)	0.09	0.00	0.01	0.00	0.00	0.00	0.00	0.08	0.00	0.00	0.01	<b>0.98</b>
TEST MODULATION	COSTAS	FRANK	FSK/PSK	FMCW	P1	P2	P3	P4	T1(n)	T2(n)	T3(n)	T4(n)
COSTAS	<b>1.00</b>	0.04	0.01	0.00	0.00	0.00	0.03	0.01	0.00	0.00	0.00	0.00
FRANK	0.00	<b>0.41</b>	0.11	0.00	0.19	0.22	0.30	0.34	0.00	0.00	0.16	0.00
FSK/PSK	0.00	0.04	<b>0.71</b>	0.00	0.05	0.00	0.04	0.00	0.00	0.00	0.01	0.00
FMCW	0.00	0.01	0.00	<b>1.00</b>	0.00	0.01	0.01	0.00	0.00	0.00	0.02	0.00
P1	0.00	0.02	0.00	0.00	<b>0.32</b>	0.00	0.00	0.01	0.00	0.00	0.01	0.00
P2	0.00	0.05	0.00	0.00	0.05	<b>0.72</b>	0.03	0.02	0.00	0.00	0.01	0.00
P3	0.00	0.10	0.02	0.00	0.25	0.01	<b>0.46</b>	0.27	0.22	0.00	0.09	0.00
P4	0.00	0.00	0.02	0.00	0.02	0.00	0.00	<b>0.33</b>	0.00	0.00	0.00	0.01
T1(n)	0.00	0.03	0.00	0.00	0.03	0.00	0.02	0.02	<b>0.43</b>	0.00	0.01	0.00
T2(n)	0.00	0.02	0.00	0.00	0.05	0.04	0.02	0.00	0.01	<b>0.66</b>	0.02	0.00
T3(n)	0.00	0.06	0.00	0.00	0.01	0.01	0.09	0.00	0.03	0.00	<b>0.30</b>	0.63
T4(n)	0.00	0.22	0.15	0.00	0.01	0.01	0.00	0.00	0.30	0.33	0.35	<b>0.36</b>

Table 15. PWVD Classification Results with MLPNN (  $SNR = 3\text{ dB}$  ).

TEST SNR	COSTAS	FRANK	FSK/PSK	FMCW	P1	P2	P3	P4	T1(n)	T2(n)	T3(n)	T4(n)
COSTAS	<b>1.00</b>	0.00	0.00	0.00	0.00	0.00	0.00	0.00	0.00	0.00	0.00	0.00
FRANK	0.00	<b>1.00</b>	0.00	0.00	0.02	0.00	0.00	0.02	0.00	0.00	0.00	0.00
FSK/PSK	0.00	0.00	<b>1.00</b>	0.00	0.00	0.00	0.00	0.00	0.00	0.00	0.00	0.00
FMCW	0.00	0.00	0.00	<b>1.00</b>	0.00	0.00	0.00	0.00	0.00	0.00	0.00	0.00
P1	0.00	0.00	0.00	0.00	<b>0.90</b>	0.00	0.00	0.02	0.00	0.00	0.00	0.01
P2	0.00	0.00	0.00	0.00	0.00	<b>1.00</b>	0.00	0.00	0.00	0.00	0.00	0.00
P3	0.00	0.00	0.00	0.00	0.00	0.00	<b>0.96</b>	0.00	0.00	0.00	0.01	0.00
P4	0.00	0.00	0.00	0.00	0.07	0.00	0.02	<b>0.96</b>	0.00	0.00	0.00	0.21
T1(n)	0.00	0.00	0.00	0.00	0.00	0.00	0.00	0.00	<b>0.99</b>	0.00	0.00	0.00
T2(n)	0.00	0.00	0.00	0.00	0.00	0.00	0.00	0.00	0.00	<b>1.00</b>	0.00	0.00
T3(n)	0.00	0.00	0.00	0.00	0.00	0.00	0.00	0.00	0.00	0.00	<b>0.98</b>	0.01
T4(n)	0.00	0.00	0.00	0.00	0.00	0.00	0.02	0.00	0.00	0.00	0.01	<b>0.76</b>
TEST MODULATION	COSTAS	FRANK	FSK/PSK	FMCW	P1	P2	P3	P4	T1(n)	T2(n)	T3(n)	T4(n)
COSTAS	<b>1.00</b>	0.02	0.00	0.00	0.01	0.00	0.00	0.00	0.01	0.00	0.03	0.00
FRANK	0.00	<b>0.45</b>	0.04	0.00	0.30	0.25	0.60	0.32	0.00	0.00	0.12	0.00
FSK/PSK	0.00	0.02	<b>0.97</b>	0.00	0.01	0.01	0.00	0.00	0.00	0.00	0.02	0.00
FMCW	0.00	0.00	0.00	<b>1.00</b>	0.01	0.00	0.00	0.00	0.00	0.00	0.00	0.00
P1	0.00	0.02	0.00	0.00	<b>0.32</b>	0.00	0.00	0.01	0.00	0.01	0.00	0.01
P2	0.00	0.07	0.00	0.00	0.03	<b>0.64</b>	0.01	0.01	0.00	0.00	0.04	0.01
P3	0.00	0.12	0.00	0.00	0.24	0.02	<b>0.33</b>	0.27	0.14	0.00	0.12	0.00
P4	0.00	0.00	0.00	0.00	0.02	0.01	0.00	<b>0.33</b>	0.00	0.00	0.00	0.01
T1(n)	0.00	0.01	0.00	0.00	0.04	0.00	0.02	0.04	<b>0.52</b>	0.00	0.02	0.00
T2(n)	0.00	0.01	0.00	0.00	0.00	0.08	0.00	0.00	0.04	<b>0.65</b>	0.03	0.01
T3(n)	0.00	0.11	0.00	0.00	0.01	0.02	0.04	0.02	0.21	0.02	<b>0.09</b>	0.50
T4(n)	0.00	0.17	0.00	0.00	0.00	0.00	0.00	0.00	0.07	0.31	0.52	<b>0.47</b>

Table 16. PWVD Classification Results with MLPNN (  $SNR = 0\text{ dB}$  ).

TEST SNR	COSTAS	FRANK	FSK/PSK	FMCW	P1	P2	P3	P4	T1(n)	T2(n)	T3(n)	T4(n)
COSTAS	<b>0.51</b>	0.00	0.06	0.00	0.00	0.02	0.00	0.00	0.00	0.00	0.01	0.00
FRANK	0.08	<b>0.97</b>	0.20	0.00	0.00	0.00	0.01	0.00	0.00	0.00	0.00	0.00
FSK/PSK	0.18	0.00	<b>0.55</b>	0.00	0.00	0.00	0.00	0.00	0.00	0.00	0.00	0.00
FMCW	0.00	0.00	0.00	<b>1.00</b>	0.00	0.00	0.00	0.00	0.00	0.00	0.02	0.00
P1	0.07	0.01	0.03	0.00	<b>0.69</b>	0.03	0.02	0.08	0.00	0.00	0.01	0.00
P2	0.00	0.00	0.01	0.00	0.00	<b>0.93</b>	0.00	0.01	0.01	0.00	0.00	0.00
P3	0.00	0.00	0.14	0.00	0.01	0.00	<b>0.83</b>	0.08	0.02	0.00	0.03	0.00
P4	0.01	0.01	0.01	0.00	0.28	0.00	0.13	<b>0.75</b>	0.00	0.00	0.02	0.01
T1(n)	0.13	0.00	0.00	0.00	0.00	0.00	0.00	0.00	<b>0.96</b>	0.00	0.00	0.00
T2(n)	0.00	0.00	0.00	0.01	0.00	0.00	0.00	0.00	0.00	<b>1.00</b>	0.00	0.00
T3(n)	0.01	0.00	0.02	0.00	0.00	0.01	0.00	0.00	0.01	0.00	<b>0.76</b>	0.06
T4(n)	0.01	0.00	0.01	0.00	0.01	0.01	0.00	0.07	0.00	0.00	0.14	<b>0.92</b>
TEST MODULATION	COSTAS	FRANK	FSK/PSK	FMCW	P1	P2	P3	P4	T1(n)	T2(n)	T3(n)	T4(n)
COSTAS	<b>1.00</b>	0.02	0.03	0.00	0.02	0.00	0.01	0.01	0.01	0.00	0.02	0.00
FRANK	0.00	<b>0.54</b>	0.20	0.00	0.00	0.44	0.30	0.10	0.00	0.00	0.16	0.01
FSK/PSK	0.00	0.01	<b>0.71</b>	0.00	0.01	0.00	0.01	0.05	0.00	0.00	0.01	0.00
FMCW	0.00	0.01	0.00	<b>0.99</b>	0.00	0.00	0.01	0.00	0.00	0.00	0.02	0.01
P1	0.00	0.04	0.00	0.00	<b>0.29</b>	0.00	0.00	0.02	0.00	0.02	0.02	0.03
P2	0.00	0.08	0.01	0.00	0.07	<b>0.47</b>	0.04	0.03	0.00	0.00	0.02	0.00
P3	0.00	0.06	0.00	0.01	0.23	0.03	<b>0.35</b>	0.25	0.19	0.00	0.05	0.02
P4	0.00	0.00	0.01	0.00	0.06	0.00	0.02	<b>0.31</b>	0.00	0.00	0.00	0.15
T1(n)	0.00	0.06	0.00	0.00	0.05	0.00	0.09	0.05	<b>0.41</b>	0.01	0.02	0.00
T2(n)	0.00	0.03	0.00	0.01	0.04	0.07	0.01	0.02	0.00	<b>0.63</b>	0.03	0.00
T3(n)	0.00	0.04	0.00	0.00	0.15	0.00	0.15	0.15	0.11	0.01	<b>0.25</b>	0.37
T4(n)	0.00	0.12	0.06	0.00	0.08	0.00	0.00	0.00	0.28	0.33	0.39	<b>0.42</b>

Table 17. PWVD Classification Results with MLPNN (  $SNR = -3\text{dB}$  ).

TEST SNR	COSTAS	FRANK	FSK/PSK	FMCW	P1	P2	P3	P4	T1(n)	T2(n)	T3(n)	T4(n)
COSTAS	<b>0.50</b>	0.00	0.01	0.00	0.01	0.03	0.00	0.00	0.02	0.00	0.03	0.01
FRANK	0.33	<b>0.66</b>	0.36	0.00	0.01	0.03	0.01	0.05	0.08	0.01	0.04	0.00
FSK/PSK	0.03	0.00	<b>0.15</b>	0.00	0.00	0.03	0.01	0.00	0.00	0.00	0.00	0.00
FMCW	0.00	0.00	0.00	<b>1.00</b>	0.01	0.01	0.01	0.01	0.01	0.00	0.00	0.00
P1	0.01	0.04	0.03	0.00	<b>0.52</b>	0.13	0.03	0.08	0.00	0.02	0.00	0.02
P2	0.00	0.00	0.07	0.00	0.03	<b>0.63</b>	0.01	0.00	0.04	0.02	0.15	0.00
P3	0.01	0.01	0.01	0.00	0.16	0.02	<b>0.77</b>	0.20	0.03	0.00	0.04	0.03
P4	0.04	0.05	0.04	0.00	0.23	0.05	0.05	<b>0.58</b>	0.00	0.04	0.00	0.39
T1(n)	0.08	0.20	0.01	0.00	0.00	0.00	0.00	0.00	<b>0.43</b>	0.00	0.00	0.00
T2(n)	0.00	0.02	0.08	0.01	0.01	0.04	0.01	0.01	0.01	<b>0.90</b>	0.00	0.00
T3(n)	0.01	0.00	0.02	0.00	0.01	0.04	0.01	0.01	0.36	0.00	<b>0.66</b>	0.05
T4(n)	0.01	0.02	0.25	0.00	0.02	0.01	0.08	0.06	0.00	0.00	0.07	<b>0.50</b>
TEST MODULATION	COSTAS	FRANK	FSK/PSK	FMCW	P1	P2	P3	P4	T1(n)	T2(n)	T3(n)	T4(n)
COSTAS	<b>1.00</b>	0.08	0.02	0.00	0.00	0.00	0.00	0.01	0.02	0.01	0.02	0.00
FRANK	0.00	<b>0.23</b>	0.03	0.00	0.29	0.57	0.48	0.15	0.01	0.01	0.10	0.00
FSK/PSK	0.00	0.01	<b>0.51</b>	0.00	0.00	0.00	0.00	0.02	0.00	0.00	0.00	0.00
FMCW	0.00	0.01	0.00	<b>1.00</b>	0.01	0.02	0.03	0.04	0.01	0.01	0.02	0.00
P1	0.00	0.01	0.01	0.00	<b>0.30</b>	0.00	0.02	0.18	0.01	0.01	0.00	0.01
P2	0.00	0.06	0.01	0.00	0.05	<b>0.30</b>	0.05	0.04	0.00	0.00	0.01	0.01
P3	0.00	0.28	0.01	0.00	0.24	0.05	<b>0.21</b>	0.29	0.08	0.04	0.06	0.04
P4	0.00	0.02	0.01	0.00	0.04	0.00	0.02	<b>0.17</b>	0.11	0.01	0.00	0.00
T1(n)	0.00	0.09	0.37	0.00	0.04	0.00	0.08	0.03	<b>0.48</b>	0.09	0.28	0.04
T2(n)	0.00	0.01	0.02	0.00	0.00	0.05	0.00	0.01	0.00	<b>0.52</b>	0.00	0.00
T3(n)	0.00	0.06	0.03	0.00	0.03	0.02	0.07	0.04	0.26	0.27	<b>0.33</b>	0.31
T4(n)	0.00	0.16	0.00	0.00	0.00	0.00	0.03	0.02	0.03	0.02	0.16	<b>0.59</b>

Table 18. PWVD Classification Results with MLPNN (  $SNR = -6\text{dB}$  ).

TEST SNR	COSTAS	FRANK	FSK/PSK	FMCW	P1	P2	P3	P4	T1(n)	T2(n)	T3(n)	T4(n)
COSTAS	<b>0.65</b>	0.00	0.01	0.01	0.00	0.00	0.00	0.00	0.00	0.01	0.02	0.01
FRANK	0.26	<b>0.43</b>	0.16	0.00	0.04	0.07	0.05	0.10	0.01	0.04	0.03	0.03
FSK/PSK	0.01	0.00	<b>0.07</b>	0.00	0.00	0.03	0.00	0.00	0.00	0.00	0.00	0.00
FMCW	0.01	0.00	0.01	<b>0.97</b>	0.00	0.01	0.02	0.01	0.01	0.03	0.01	0.01
P1	0.01	0.05	0.04	0.00	<b>0.82</b>	0.00	0.05	0.10	0.00	0.03	0.18	0.01
P2	0.00	0.01	0.04	0.00	0.00	<b>0.71</b>	0.08	0.00	0.00	0.00	0.06	0.00
P3	0.00	0.16	0.19	0.02	0.01	0.02	<b>0.57</b>	0.03	0.03	0.12	0.19	0.02
P4	0.00	0.11	0.20	0.01	0.12	0.00	0.10	<b>0.75</b>	0.00	0.03	0.04	0.24
T1(n)	0.04	0.03	0.04	0.00	0.00	0.01	0.03	0.01	<b>0.57</b>	0.11	0.02	0.02
T2(n)	0.00	0.02	0.01	0.00	0.00	0.08	0.01	0.00	0.00	<b>0.48</b>	0.00	0.00
T3(n)	0.04	0.16	0.12	0.01	0.00	0.07	0.03	0.00	0.39	0.15	<b>0.46</b>	0.38
T4(n)	0.01	0.01	0.14	0.00	0.00	0.01	0.06	0.00	0.00	0.00	0.01	<b>0.29</b>
TEST MODULATION	COSTAS	FRANK	FSK/PSK	FMCW	P1	P2	P3	P4	T1(n)	T2(n)	T3(n)	T4(n)
COSTAS	<b>1.00</b>	0.00	0.00	0.00	0.05	0.00	0.00	0.01	0.01	0.01	0.00	0.01
FRANK	0.00	<b>0.01</b>	0.50	0.00	0.01	0.72	0.36	0.24	0.02	0.04	0.08	0.03
FSK/PSK	0.00	0.01	<b>0.04</b>	0.00	0.00	0.00	0.00	0.01	0.00	0.00	0.01	0.00
FMCW	0.00	0.02	0.00	<b>1.00</b>	0.03	0.01	0.01	0.03	0.00	0.03	0.02	0.12
P1	0.00	0.09	0.00	0.00	<b>0.28</b>	0.02	0.01	0.05	0.02	0.10	0.03	0.15
P2	0.00	0.14	0.06	0.00	0.09	<b>0.10</b>	0.02	0.02	0.00	0.02	0.02	0.06
P3	0.00	0.16	0.36	0.01	0.25	0.08	<b>0.43</b>	0.36	0.48	0.27	0.27	0.09
P4	0.00	0.38	0.02	0.00	0.05	0.00	0.01	<b>0.14</b>	0.01	0.27	0.00	0.07
T1(n)	0.00	0.05	0.00	0.00	0.01	0.00	0.10	0.02	<b>0.08</b>	0.16	0.23	0.05
T2(n)	0.00	0.03	0.00	0.00	0.06	0.09	0.01	0.01	0.03	<b>0.09</b>	0.05	0.08
T3(n)	0.00	0.07	0.03	0.00	0.16	0.00	0.05	0.08	0.36	0.01	<b>0.10</b>	0.28
T4(n)	0.00	0.03	0.01	0.00	0.01	0.00	0.00	0.02	0.00	0.00	0.18	<b>0.06</b>

Table 19. CWD Classification Results with MLPNN (  $SNR = 10\text{ dB}$  ).

TEST SNR	COSTAS	FRANK	FSK/PSK	FMCW	P1	P2	P3	P4	T1(n)	T2(n)	T3(n)	T4(n)
COSTAS	<b>1.00</b>	0.00	0.00	0.00	0.00	0.00	0.00	0.00	0.00	0.00	0.00	0.00
FRANK	0.00	<b>1.00</b>	0.00	0.00	0.00	0.00	0.00	0.00	0.00	0.00	0.00	0.00
FSK/PSK	0.00	0.00	<b>1.00</b>	0.00	0.00	0.00	0.00	0.00	0.00	0.00	0.00	0.00
FMCW	0.00	0.00	0.00	<b>1.00</b>	0.00	0.00	0.00	0.00	0.00	0.00	0.00	0.00
P1	0.00	0.00	0.00	0.00	<b>0.99</b>	0.00	0.00	0.00	0.00	0.00	0.00	0.00
P2	0.00	0.00	0.00	0.00	0.00	<b>1.00</b>	0.00	0.00	0.00	0.00	0.00	0.00
P3	0.00	0.00	0.00	0.00	0.00	0.00	<b>1.00</b>	0.00	0.00	0.00	0.00	0.00
P4	0.00	0.00	0.00	0.00	0.01	0.00	0.00	<b>1.00</b>	0.00	0.00	0.00	0.00
T1(n)	0.00	0.00	0.00	0.00	0.00	0.00	0.00	0.00	<b>1.00</b>	0.00	0.00	0.00
T2(n)	0.00	0.00	0.00	0.00	0.00	0.00	0.00	0.00	0.00	<b>1.00</b>	0.00	0.00
T3(n)	0.00	0.00	0.00	0.00	0.00	0.00	0.00	0.00	0.00	0.00	<b>1.00</b>	0.00
T4(n)	0.00	0.00	0.00	0.00	0.00	0.00	0.00	0.00	0.00	0.00	0.00	<b>1.00</b>
TEST MODULATION	COSTAS	FRANK	FSK/PSK	FMCW	P1	P2	P3	P4	T1(n)	T2(n)	T3(n)	T4(n)
COSTAS	<b>1.00</b>	0.01	0.01	0.00	0.01	0.00	0.00	0.00	0.00	0.00	0.01	0.00
FRANK	0.00	<b>0.13</b>	0.03	0.04	0.37	0.28	0.51	0.35	0.00	0.00	0.13	0.00
FSK/PSK	0.00	0.01	<b>0.95</b>	0.01	0.00	0.04	0.01	0.01	0.00	0.00	0.01	0.00
FMCW	0.00	0.01	0.00	<b>0.90</b>	0.01	0.00	0.01	0.01	0.01	0.00	0.00	0.00
P1	0.00	0.03	0.00	0.00	<b>0.07</b>	0.03	0.00	0.01	0.00	0.00	0.01	0.05
P2	0.00	0.02	0.00	0.01	0.09	<b>0.52</b>	0.05	0.04	0.00	0.00	0.03	0.01
P3	0.00	0.30	0.01	0.01	0.03	0.03	<b>0.04</b>	0.03	0.02	0.00	0.10	0.01
P4	0.00	0.01	0.00	0.00	0.25	0.02	0.02	<b>0.36</b>	0.00	0.00	0.00	0.01
T1(n)	0.00	0.24	0.00	0.01	0.06	0.00	0.17	0.08	<b>0.62</b>	0.00	0.08	0.02
T2(n)	0.00	0.03	0.00	0.00	0.01	0.06	0.01	0.01	0.14	<b>0.67</b>	0.01	0.01
T3(n)	0.00	0.13	0.00	0.03	0.09	0.03	0.15	0.10	0.08	0.01	<b>0.05</b>	0.24
T4(n)	0.00	0.08	0.02	0.00	0.02	0.02	0.01	0.01	0.13	0.32	0.58	<b>0.65</b>

Table 20. CWD Classification Results with MLPNN (  $SNR = 6\text{ dB}$  ).

TEST SNR	COSTAS	FRANK	FSK/PSK	FMCW	P1	P2	P3	P4	T1(n)	T2(n)	T3(n)	T4(n)
COSTAS	<b>1.00</b>	0.00	0.01	0.00	0.00	0.00	0.00	0.00	0.00	0.00	0.00	0.00
FRANK	0.00	<b>1.00</b>	0.00	0.00	0.00	0.00	0.00	0.00	0.00	0.00	0.00	0.00
FSK/PSK	0.00	0.00	<b>0.99</b>	0.00	0.00	0.00	0.00	0.00	0.00	0.00	0.00	0.00
FMCW	0.00	0.00	0.00	<b>1.00</b>	0.00	0.00	0.00	0.00	0.00	0.00	0.00	0.00
P1	0.00	0.00	0.00	0.00	<b>0.92</b>	0.00	0.00	0.01	0.00	0.00	0.00	0.00
P2	0.00	0.00	0.00	0.00	0.00	<b>1.00</b>	0.00	0.00	0.00	0.00	0.00	0.00
P3	0.00	0.00	0.00	0.00	0.00	0.00	<b>0.87</b>	0.08	0.00	0.00	0.00	0.00
P4	0.00	0.00	0.00	0.00	0.07	0.00	0.12	<b>0.90</b>	0.00	0.00	0.00	0.00
T1(n)	0.00	0.00	0.00	0.00	0.00	0.00	0.00	0.00	<b>1.00</b>	0.00	0.00	0.00
T2(n)	0.00	0.00	0.00	0.00	0.00	0.00	0.00	0.00	0.00	<b>1.00</b>	0.00	0.00
T3(n)	0.00	0.00	0.00	0.00	0.00	0.00	0.00	0.00	0.00	0.00	<b>0.89</b>	0.00
T4(n)	0.00	0.00	0.00	0.00	0.01	0.00	0.00	0.00	0.00	0.00	0.11	<b>1.00</b>
TEST MODULATION	COSTAS	FRANK	FSK/PSK	FMCW	P1	P2	P3	P4	T1(n)	T2(n)	T3(n)	T4(n)
COSTAS	<b>1.00</b>	0.01	0.02	0.01	0.02	0.01	0.02	0.01	0.00	0.00	0.02	0.00
FRANK	0.00	<b>0.07</b>	0.05	0.03	0.36	0.24	0.34	0.35	0.00	0.01	0.09	0.00
FSK/PSK	0.00	0.01	<b>0.90</b>	0.01	0.00	0.08	0.00	0.00	0.00	0.00	0.01	0.00
FMCW	0.00	0.00	0.00	<b>0.84</b>	0.01	0.02	0.02	0.01	0.00	0.00	0.00	0.00
P1	0.00	0.03	0.01	0.00	<b>0.02</b>	0.06	0.01	0.02	0.00	0.00	0.02	0.02
P2	0.00	0.02	0.01	0.02	0.13	<b>0.54</b>	0.10	0.06	0.00	0.00	0.05	0.00
P3	0.00	0.31	0.00	0.04	0.02	0.01	<b>0.09</b>	0.02	0.03	0.00	0.14	0.00
P4	0.00	0.00	0.00	0.00	0.28	0.00	0.05	<b>0.35</b>	0.00	0.00	0.00	0.01
T1(n)	0.00	0.24	0.01	0.00	0.08	0.00	0.27	0.09	<b>0.64</b>	0.00	0.09	0.01
T2(n)	0.00	0.04	0.00	0.01	0.01	0.05	0.02	0.00	0.01	<b>0.68</b>	0.02	0.00
T3(n)	0.00	0.20	0.01	0.06	0.06	0.00	0.07	0.07	0.00	0.11	<b>0.03</b>	0.63
T4(n)	0.00	0.06	0.01	0.00	0.02	0.01	0.02	0.01	0.32	0.19	0.53	<b>0.32</b>



Table 21. CWD Classification Results with MLPNN (  $SNR = 3\text{ dB}$  ).

TEST SNR	COSTAS	FRANK	FSK/PSK	FMCW	P1	P2	P3	P4	T1(n)	T2(n)	T3(n)	T4(n)
COSTAS	<b>0.91</b>	0.00	0.00	0.00	0.01	0.00	0.00	0.00	0.00	0.00	0.00	0.00
FRANK	0.00	<b>1.00</b>	0.00	0.00	0.00	0.00	0.01	0.00	0.00	0.00	0.00	0.00
FSK/PSK	0.02	0.00	<b>1.00</b>	0.00	0.00	0.00	0.00	0.00	0.00	0.00	0.00	0.00
FMCW	0.00	0.00	0.00	<b>1.00</b>	0.00	0.00	0.00	0.00	0.00	0.00	0.00	0.00
P1	0.05	0.00	0.00	0.00	<b>0.72</b>	0.00	0.00	0.17	0.00	0.00	0.00	0.00
P2	0.00	0.00	0.00	0.00	0.00	<b>1.00</b>	0.00	0.00	0.00	0.00	0.00	0.00
P3	0.01	0.00	0.00	0.00	0.00	0.00	<b>0.89</b>	0.08	0.00	0.00	0.00	0.00
P4	0.00	0.00	0.00	0.00	0.27	0.00	0.00	<b>0.74</b>	0.00	0.00	0.00	0.00
T1(n)	0.00	0.00	0.00	0.00	0.00	0.00	0.00	0.00	<b>1.00</b>	0.00	0.00	0.00
T2(n)	0.00	0.00	0.00	0.00	0.00	0.00	0.00	0.00	0.00	<b>1.00</b>	0.00	0.00
T3(n)	0.00	0.00	0.00	0.00	0.00	0.00	0.09	0.00	0.00	0.00	<b>0.83</b>	0.00
T4(n)	0.02	0.00	0.00	0.00	0.00	0.00	0.00	0.00	0.00	0.00	0.17	<b>1.00</b>
TEST MODULATION	COSTAS	FRANK	FSK/PSK	FMCW	P1	P2	P3	P4	T1(n)	T2(n)	T3(n)	T4(n)
COSTAS	<b>1.00</b>	0.01	0.03	0.01	0.01	0.00	0.00	0.01	0.00	0.00	0.04	0.00
FRANK	0.00	<b>0.20</b>	0.12	0.07	0.34	0.25	0.50	0.38	0.00	0.01	0.12	0.00
FSK/PSK	0.00	0.01	<b>0.85</b>	0.02	0.00	0.05	0.01	0.01	0.00	0.00	0.04	0.00
FMCW	0.00	0.01	0.00	<b>0.86</b>	0.02	0.02	0.01	0.01	0.00	0.00	0.00	0.00
P1	0.00	0.03	0.00	0.00	<b>0.08</b>	0.03	0.00	0.03	0.00	0.00	0.01	0.00
P2	0.00	0.00	0.00	0.01	0.11	<b>0.55</b>	0.06	0.06	0.00	0.00	0.06	0.00
P3	0.00	0.38	0.01	0.00	0.06	0.02	<b>0.06</b>	0.03	0.03	0.00	0.21	0.00
P4	0.00	0.00	0.00	0.01	0.23	0.01	0.05	<b>0.31</b>	0.00	0.00	0.00	0.01
T1(n)	0.00	0.14	0.00	0.00	0.07	0.00	0.19	0.05	<b>0.67</b>	0.00	0.09	0.00
T2(n)	0.00	0.01	0.00	0.00	0.01	0.06	0.01	0.02	0.08	<b>0.67</b>	0.00	0.00
T3(n)	0.00	0.15	0.01	0.04	0.04	0.02	0.09	0.10	0.10	0.16	<b>0.04</b>	0.38
T4(n)	0.00	0.06	0.00	0.00	0.03	0.01	0.01	0.00	0.12	0.16	0.38	<b>0.60</b>

Table 22. CWD Classification Results with MLPNN (  $SNR = 0\text{ dB}$  ).

TEST SNR	COSTAS	FRANK	FSK/PSK	FMCW	P1	P2	P3	P4	T1(n)	T2(n)	T3(n)	T4(n)
COSTAS	<b>0.96</b>	0.00	0.00	0.00	0.00	0.00	0.00	0.00	0.00	0.00	0.00	0.00
FRANK	0.01	<b>0.96</b>	0.03	0.00	0.01	0.13	0.22	0.00	0.00	0.00	0.00	0.00
FSK/PSK	0.02	0.00	<b>0.97</b>	0.00	0.00	0.01	0.00	0.00	0.00	0.00	0.00	0.00
FMCW	0.00	0.00	0.00	<b>1.00</b>	0.00	0.00	0.01	0.00	0.00	0.00	0.00	0.00
P1	0.01	0.00	0.00	0.00	<b>0.94</b>	0.00	0.02	0.22	0.00	0.00	0.00	0.00
P2	0.01	0.00	0.00	0.00	0.00	<b>0.71</b>	0.00	0.00	0.00	0.00	0.00	0.00
P3	0.00	0.00	0.00	0.00	0.02	0.01	<b>0.51</b>	0.02	0.01	0.00	0.00	0.00
P4	0.00	0.02	0.00	0.00	0.03	0.00	0.12	<b>0.74</b>	0.00	0.00	0.02	0.00
T1(n)	0.00	0.00	0.01	0.00	0.00	0.11	0.01	0.00	<b>0.98</b>	0.00	0.00	0.00
T2(n)	0.00	0.00	0.00	0.00	0.00	0.02	0.01	0.00	0.01	<b>0.99</b>	0.00	0.00
T3(n)	0.00	0.01	0.00	0.00	0.00	0.02	0.10	0.00	0.00	0.00	<b>0.65</b>	0.01
T4(n)	0.01	0.00	0.00	0.00	0.00	0.00	0.00	0.02	0.00	0.00	0.31	<b>0.98</b>
TEST MODULATION	COSTAS	FRANK	FSK/PSK	FMCW	P1	P2	P3	P4	T1(n)	T2(n)	T3(n)	T4(n)
COSTAS	<b>1.00</b>	0.01	0.01	0.01	0.03	0.00	0.03	0.01	0.00	0.00	0.02	0.00
FRANK	0.00	<b>0.19</b>	0.04	0.10	0.21	0.32	0.43	0.35	0.00	0.00	0.15	0.00
FSK/PSK	0.00	0.00	<b>0.93</b>	0.01	0.01	0.05	0.01	0.00	0.00	0.00	0.01	0.00
FMCW	0.00	0.01	0.00	<b>0.73</b>	0.01	0.01	0.01	0.02	0.00	0.00	0.00	0.01
P1	0.00	0.04	0.01	0.00	<b>0.03</b>	0.01	0.00	0.01	0.00	0.00	0.02	0.03
P2	0.00	0.00	0.00	0.00	0.11	<b>0.50</b>	0.07	0.02	0.00	0.00	0.02	0.01
P3	0.00	0.26	0.01	0.02	0.06	0.01	<b>0.03</b>	0.01	0.09	0.00	0.07	0.02
P4	0.00	0.02	0.00	0.04	0.33	0.02	0.07	<b>0.41</b>	0.01	0.00	0.01	0.02
T1(n)	0.00	0.15	0.00	0.01	0.06	0.00	0.25	0.05	<b>0.59</b>	0.01	0.07	0.01
T2(n)	0.00	0.01	0.00	0.00	0.01	0.08	0.03	0.02	0.01	<b>0.66</b>	0.02	0.01
T3(n)	0.00	0.26	0.00	0.09	0.05	0.01	0.05	0.07	0.00	0.05	<b>0.04</b>	0.45
T4(n)	0.00	0.04	0.02	0.01	0.07	0.01	0.02	0.01	0.29	0.28	0.59	<b>0.43</b>

Table 23. CWD Classification Results with MLPNN (  $SNR = -3dB$  ).

TEST SNR	COSTAS	FRANK	FSK/PSK	FMCW	P1	P2	P3	P4	T1(n)	T2(n)	T3(n)	T4(n)
COSTAS	<b>0.83</b>	0.00	0.09	0.00	0.01	0.00	0.00	0.00	0.00	0.00	0.00	0.00
FRANK	0.04	<b>0.54</b>	0.46	0.01	0.03	0.01	0.02	0.04	0.01	0.02	0.00	0.01
FSK/PSK	0.04	0.00	<b>0.19</b>	0.00	0.00	0.00	0.00	0.00	0.00	0.00	0.00	0.01
FMCW	0.00	0.00	0.00	<b>0.98</b>	0.00	0.00	0.00	0.00	0.00	0.00	0.00	0.00
P1	0.05	0.05	0.02	0.00	<b>0.23</b>	0.00	0.04	0.24	0.00	0.00	0.00	0.01
P2	0.00	0.00	0.03	0.00	0.01	<b>0.81</b>	0.00	0.01	0.01	0.01	0.01	0.00
P3	0.03	0.27	0.01	0.01	0.15	0.02	<b>0.75</b>	0.09	0.00	0.02	0.04	0.01
P4	0.00	0.04	0.00	0.01	0.52	0.10	0.10	<b>0.57</b>	0.00	0.00	0.00	0.16
T1(n)	0.01	0.07	0.01	0.01	0.02	0.04	0.01	0.00	<b>0.97</b>	0.01	0.01	0.00
T2(n)	0.00	0.01	0.00	0.00	0.02	0.01	0.01	0.00	0.01	<b>0.95</b>	0.02	0.02
T3(n)	0.00	0.01	0.14	0.00	0.01	0.02	0.03	0.03	0.00	0.00	<b>0.88</b>	0.01
T4(n)	0.01	0.01	0.08	0.00	0.01	0.01	0.04	0.01	0.00	0.00	0.05	<b>0.77</b>
TEST MODULATION	COSTAS	FRANK	FSK/PSK	FMCW	P1	P2	P3	P4	T1(n)	T2(n)	T3(n)	T4(n)
COSTAS	<b>1.00</b>	0.01	0.01	0.01	0.02	0.01	0.01	0.02	0.00	0.00	0.01	0.00
FRANK	0.00	<b>0.19</b>	0.13	0.11	0.36	0.32	0.47	0.28	0.01	0.01	0.09	0.00
FSK/PSK	0.00	0.02	<b>0.45</b>	0.00	0.00	0.02	0.04	0.01	0.00	0.00	0.01	0.00
FMCW	0.00	0.00	0.00	<b>0.81</b>	0.01	0.03	0.01	0.01	0.00	0.00	0.02	0.00
P1	0.00	0.00	0.00	0.00	<b>0.05</b>	0.04	0.00	0.15	0.00	0.01	0.02	0.01
P2	0.00	0.01	0.03	0.00	0.09	<b>0.47</b>	0.05	0.09	0.00	0.01	0.07	0.00
P3	0.00	0.20	0.02	0.01	0.08	0.04	<b>0.02</b>	0.03	0.07	0.01	0.12	0.07
P4	0.00	0.00	0.02	0.02	0.22	0.02	0.10	<b>0.20</b>	0.09	0.10	0.03	0.05
T1(n)	0.00	0.21	0.03	0.02	0.11	0.00	0.22	0.10	<b>0.61</b>	0.05	0.32	0.04
T2(n)	0.00	0.04	0.00	0.01	0.00	0.06	0.00	0.01	0.05	<b>0.62</b>	0.04	0.08
T3(n)	0.00	0.20	0.01	0.02	0.05	0.01	0.06	0.05	0.14	0.12	<b>0.21</b>	0.31
T4(n)	0.00	0.11	0.33	0.01	0.01	0.01	0.01	0.05	0.03	0.07	0.05	<b>0.45</b>

Table 24. CWD Classification Results with MLPNN (  $SNR = -6dB$  ).

TEST SNR	COSTAS	FRANK	FSK/PSK	FMCW	P1	P2	P3	P4	T1(n)	T2(n)	T3(n)	T4(n)
COSTAS	<b>0.72</b>	0.03	0.07	0.00	0.01	0.00	0.01	0.00	0.02	0.01	0.01	0.06
FRANK	0.06	<b>0.58</b>	0.35	0.00	0.07	0.08	0.05	0.11	0.06	0.03	0.02	0.10
FSK/PSK	0.00	0.01	<b>0.04</b>	0.00	0.01	0.01	0.00	0.00	0.00	0.00	0.00	0.00
FMCW	0.00	0.02	0.02	<b>0.93</b>	0.00	0.01	0.01	0.01	0.01	0.02	0.02	0.02
P1	0.02	0.05	0.00	0.00	<b>0.15</b>	0.00	0.03	0.12	0.00	0.00	0.00	0.09
P2	0.02	0.02	0.16	0.01	0.00	<b>0.65</b>	0.03	0.01	0.05	0.00	0.01	0.05
P3	0.12	0.09	0.08	0.00	0.04	0.04	<b>0.48</b>	0.16	0.02	0.19	0.23	0.15
P4	0.00	0.11	0.03	0.05	0.62	0.05	0.12	<b>0.56</b>	0.05	0.03	0.27	0.04
T1(n)	0.03	0.05	0.06	0.01	0.02	0.09	0.04	0.01	<b>0.62</b>	0.03	0.03	0.03
T2(n)	0.01	0.02	0.00	0.00	0.02	0.05	0.03	0.00	0.03	<b>0.63</b>	0.03	0.01
T3(n)	0.01	0.01	0.13	0.00	0.04	0.02	0.20	0.00	0.13	0.01	<b>0.23</b>	0.12
T4(n)	0.03	0.02	0.08	0.01	0.02	0.01	0.00	0.03	0.01	0.03	0.15	<b>0.34</b>
TEST MODULATION	COSTAS	FRANK	FSK/PSK	FMCW	P1	P2	P3	P4	T1(n)	T2(n)	T3(n)	T4(n)
COSTAS	<b>1.00</b>	0.04	0.00	0.03	0.01	0.00	0.02	0.02	0.00	0.01	0.02	0.01
FRANK	0.00	<b>0.20</b>	0.44	0.12	0.32	0.39	0.24	0.11	0.01	0.11	0.11	0.02
FSK/PSK	0.00	0.04	<b>0.05</b>	0.00	0.00	0.03	0.01	0.00	0.00	0.01	0.02	0.00
FMCW	0.00	0.04	0.01	<b>0.60</b>	0.04	0.02	0.01	0.06	0.01	0.01	0.02	0.03
P1	0.00	0.05	0.00	0.02	<b>0.00</b>	0.02	0.00	0.03	0.00	0.00	0.00	0.00
P2	0.00	0.03	0.16	0.02	0.09	<b>0.34</b>	0.08	0.04	0.01	0.01	0.02	0.02
P3	0.00	0.16	0.04	0.04	0.05	0.10	<b>0.09</b>	0.36	0.34	0.36	0.26	0.06
P4	0.00	0.32	0.06	0.08	0.26	0.05	0.10	<b>0.12</b>	0.05	0.32	0.25	0.24
T1(n)	0.00	0.01	0.12	0.06	0.07	0.01	0.29	0.14	<b>0.40</b>	0.09	0.07	0.07
T2(n)	0.00	0.06	0.00	0.02	0.01	0.04	0.02	0.02	0.12	<b>0.07</b>	0.07	0.11
T3(n)	0.00	0.01	0.10	0.03	0.05	0.00	0.13	0.06	0.06	0.01	<b>0.03</b>	0.22
T4(n)	0.00	0.04	0.04	0.01	0.09	0.02	0.02	0.00	0.00	0.01	0.12	<b>0.22</b>

Table 25. QMFB Classification Results with MLPNN (  $SNR = 10\text{ dB}$  ).

TEST SNR	COSTAS	FRANK	FSK/PSK	FMCW	P1	P2	P3	P4	T1(n)	T2(n)	T3(n)	T4(n)
COSTAS	<b>1.00</b>	0.00	0.00	0.00	0.00	0.00	0.00	0.00	0.00	0.00	0.00	0.00
FRANK	0.00	<b>1.00</b>	0.00	0.00	0.00	0.00	0.00	0.00	0.00	0.00	0.00	0.00
FSK/PSK	0.00	0.00	<b>1.00</b>	0.00	0.00	0.00	0.00	0.00	0.00	0.00	0.00	0.00
FMCW	0.00	0.00	0.00	<b>1.00</b>	0.00	0.00	0.00	0.00	0.00	0.00	0.00	0.00
P1	0.00	0.00	0.00	0.00	<b>1.00</b>	0.00	0.00	0.00	0.00	0.00	0.00	0.00
P2	0.00	0.00	0.00	0.00	0.00	<b>1.00</b>	0.00	0.00	0.00	0.00	0.00	0.00
P3	0.00	0.00	0.00	0.00	0.00	0.00	<b>1.00</b>	0.00	0.00	0.00	0.00	0.00
P4	0.00	0.00	0.00	0.00	0.00	0.00	0.00	<b>1.00</b>	0.00	0.00	0.00	0.00
T1(n)	0.00	0.00	0.00	0.00	0.00	0.00	0.00	0.00	<b>1.00</b>	0.00	0.00	0.00
T2(n)	0.00	0.00	0.00	0.00	0.00	0.00	0.00	0.00	0.00	<b>1.00</b>	0.00	0.00
T3(n)	0.00	0.00	0.00	0.00	0.00	0.00	0.00	0.00	0.00	0.00	<b>1.00</b>	0.00
T4(n)	0.00	0.00	0.00	0.00	0.00	0.00	0.00	0.00	0.00	0.00	0.00	<b>1.00</b>
TEST MODULATION	COSTAS	FRANK	FSK/PSK	FMCW	P1	P2	P3	P4	T1(n)	T2(n)	T3(n)	T4(n)
COSTAS	<b>1.00</b>	0.00	0.01	0.00	0.02	0.00	0.00	0.02	0.00	0.00	0.00	0.00
FRANK	0.00	<b>0.34</b>	0.14	0.01	0.07	0.14	0.47	0.04	0.00	0.00	0.00	0.00
FSK/PSK	0.00	0.01	<b>0.05</b>	0.00	0.00	0.00	0.00	0.00	0.00	0.00	0.01	0.00
FMCW	0.00	0.04	0.02	<b>0.00</b>	0.01	0.02	0.05	0.01	0.00	0.00	0.00	0.00
P1	0.00	0.00	0.15	0.05	<b>0.26</b>	0.35	0.00	0.37	0.00	0.00	0.00	0.33
P2	0.00	0.00	0.10	0.00	0.01	<b>0.00</b>	0.00	0.01	0.00	0.00	0.00	0.00
P3	0.00	0.30	0.01	0.00	0.00	0.12	<b>0.20</b>	0.00	0.00	0.03	0.00	0.00
P4	0.00	0.14	0.04	0.39	0.33	0.02	0.00	<b>0.33</b>	0.00	0.00	0.24	0.13
T1(n)	0.00	0.14	0.28	0.00	0.25	0.01	0.00	0.12	<b>0.33</b>	0.00	0.01	0.00
T2(n)	0.00	0.02	0.11	0.00	0.01	0.01	0.00	0.00	0.19	<b>0.96</b>	0.07	0.00
T3(n)	0.00	0.02	0.00	0.57	0.02	0.34	0.00	0.01	0.31	0.00	<b>0.67</b>	0.53
T4(n)	0.00	0.00	0.10	0.00	0.02	0.01	0.28	0.08	0.17	0.01	0.00	<b>0.00</b>

Table 26. QMFB Classification Results with MLPNN (  $SNR = 6\text{ dB}$  ).

TEST SNR	COSTAS	FRANK	FSK/PSK	FMCW	P1	P2	P3	P4	T1(n)	T2(n)	T3(n)	T4(n)
COSTAS	<b>0.34</b>	0.00	0.01	0.00	0.00	0.00	0.00	0.00	0.00	0.00	0.00	0.00
FRANK	0.01	<b>0.93</b>	0.00	0.00	0.00	0.00	0.07	0.00	0.00	0.00	0.00	0.00
FSK/PSK	0.00	0.00	<b>0.52</b>	0.00	0.00	0.00	0.00	0.00	0.00	0.00	0.00	0.00
FMCW	0.00	0.00	0.00	<b>1.00</b>	0.00	0.00	0.00	0.00	0.00	0.00	0.00	0.00
P1	0.05	0.00	0.22	0.00	<b>0.80</b>	0.00	0.00	0.43	0.00	0.00	0.00	0.00
P2	0.00	0.00	0.03	0.00	0.00	<b>1.00</b>	0.00	0.00	0.00	0.00	0.00	0.00
P3	0.00	0.07	0.00	0.00	0.00	0.00	<b>0.93</b>	0.00	0.00	0.01	0.00	0.00
P4	0.00	0.00	0.00	0.00	0.20	0.00	0.00	<b>0.57</b>	0.00	0.00	0.00	0.00
T1(n)	0.00	0.00	0.00	0.00	0.00	0.00	0.00	0.00	<b>1.00</b>	0.00	0.00	0.00
T2(n)	0.01	0.00	0.00	0.00	0.00	0.00	0.00	0.00	0.00	<b>0.93</b>	0.00	0.00
T3(n)	0.09	0.00	0.00	0.00	0.00	0.00	0.00	0.00	0.00	0.00	<b>0.80</b>	0.00
T4(n)	0.51	0.00	0.24	0.00	0.00	0.00	0.00	0.00	0.00	0.05	0.20	<b>1.00</b>
TEST MODULATION	COSTAS	FRANK	FSK/PSK	FMCW	P1	P2	P3	P4	T1(n)	T2(n)	T3(n)	T4(n)
COSTAS	<b>1.00</b>	0.00	0.00	0.00	0.02	0.00	0.00	0.00	0.00	0.00	0.00	0.00
FRANK	0.00	<b>0.33</b>	0.10	0.01	0.07	0.10	0.07	0.07	0.00	0.01	0.00	0.00
FSK/PSK	0.00	0.00	<b>0.00</b>	0.00	0.01	0.00	0.00	0.01	0.00	0.00	0.00	0.00
FMCW	0.00	0.04	0.09	<b>0.00</b>	0.01	0.02	0.05	0.01	0.00	0.00	0.00	0.00
P1	0.00	0.01	0.26	0.02	<b>0.25</b>	0.37	0.00	0.32	0.00	0.00	0.00	0.33
P2	0.00	0.01	0.26	0.00	0.04	<b>0.02</b>	0.00	0.01	0.00	0.00	0.00	0.00
P3	0.00	0.29	0.04	0.00	0.00	0.11	<b>0.42</b>	0.00	0.00	0.07	0.00	0.00
P4	0.00	0.02	0.00	0.28	0.33	0.02	0.00	<b>0.33</b>	0.00	0.00	0.24	0.00
T1(n)	0.00	0.24	0.01	0.01	0.10	0.00	0.00	0.18	<b>0.33</b>	0.00	0.01	0.00
T2(n)	0.00	0.00	0.00	0.00	0.00	0.00	0.00	0.01	0.03	<b>0.92</b>	0.08	0.00
T3(n)	0.00	0.01	0.00	0.69	0.12	0.35	0.00	0.02	0.12	0.00	<b>0.66</b>	0.67
T4(n)	0.00	0.03	0.26	0.00	0.05	0.03	0.46	0.05	0.51	0.01	0.00	<b>0.00</b>

Table 27. QMFB Classification Results with MLPNN (  $SNR = 3\text{ dB}$  ).

TEST SNR	COSTAS	FRANK	FSK/PSK	FMCW	P1	P2	P3	P4	T1(n)	T2(n)	T3(n)	T4(n)
COSTAS	<b>0.85</b>	0.00	0.01	0.00	0.00	0.00	0.00	0.00	0.00	0.00	0.00	0.00
FRANK	0.00	<b>1.00</b>	0.00	0.00	0.00	0.00	0.00	0.00	0.00	0.00	0.00	0.00
FSK/PSK	0.00	0.00	<b>0.45</b>	0.00	0.00	0.00	0.00	0.00	0.00	0.00	0.00	0.00
FMCW	0.00	0.00	0.00	<b>1.00</b>	0.00	0.16	0.00	0.00	0.00	0.00	0.00	0.00
P1	0.02	0.00	0.19	0.00	<b>1.00</b>	0.00	0.00	0.51	0.00	0.00	0.00	0.00
P2	0.00	0.00	0.16	0.00	0.00	<b>0.83</b>	0.00	0.00	0.00	0.00	0.00	0.00
P3	0.00	0.00	0.04	0.00	0.00	0.01	<b>1.00</b>	0.00	0.00	0.00	0.00	0.00
P4	0.00	0.00	0.00	0.00	0.00	0.00	0.00	<b>0.49</b>	0.00	0.00	0.00	0.00
T1(n)	0.00	0.00	0.01	0.00	0.00	0.00	0.00	0.00	<b>1.00</b>	0.00	0.00	0.00
T2(n)	0.00	0.00	0.00	0.00	0.00	0.00	0.00	0.00	0.00	<b>1.00</b>	0.00	0.00
T3(n)	0.00	0.00	0.03	0.00	0.00	0.00	0.00	0.00	0.00	0.00	<b>0.80</b>	0.00
T4(n)	0.14	0.00	0.14	0.00	0.00	0.00	0.00	0.00	0.00	0.00	0.20	<b>1.00</b>
TEST MODULATION	COSTAS	FRANK	FSK/PSK	FMCW	P1	P2	P3	P4	T1(n)	T2(n)	T3(n)	T4(n)
COSTAS	<b>1.00</b>	0.00	0.00	0.00	0.01	0.00	0.01	0.01	0.00	0.00	0.00	0.00
FRANK	0.00	<b>0.34</b>	0.05	0.00	0.06	0.04	0.54	0.05	0.00	0.00	0.00	0.00
FSK/PSK	0.00	0.02	<b>0.00</b>	0.00	0.00	0.00	0.01	0.02	0.00	0.00	0.00	0.00
FMCW	0.00	0.01	0.02	<b>0.00</b>	0.00	0.04	0.03	0.01	0.00	0.00	0.00	0.00
P1	0.00	0.32	0.27	0.21	<b>0.44</b>	0.47	0.01	0.31	0.00	0.00	0.02	0.33
P2	0.00	0.00	0.08	0.00	0.00	<b>0.00</b>	0.00	0.00	0.00	0.00	0.00	0.00
P3	0.00	0.29	0.05	0.00	0.00	0.15	<b>0.10</b>	0.00	0.00	0.09	0.05	0.00
P4	0.00	0.00	0.00	0.28	0.33	0.01	0.00	<b>0.33</b>	0.00	0.00	0.22	0.08
T1(n)	0.00	0.00	0.00	0.01	0.05	0.00	0.00	0.13	<b>0.33</b>	0.00	0.25	0.00
T2(n)	0.00	0.01	0.00	0.00	0.00	0.00	0.01	0.00	0.09	<b>0.68</b>	0.00	0.00
T3(n)	0.00	0.00	0.00	0.52	0.01	0.32	0.00	0.00	0.12	0.00	<b>0.46</b>	0.59
T4(n)	0.00	0.00	0.53	0.00	0.10	0.00	0.29	0.14	0.45	0.23	0.00	<b>0.00</b>

Table 28. QMFB Classification Results with MLPNN (  $SNR = 0\text{ dB}$  ).

TEST SNR	COSTAS	FRANK	FSK/PSK	FMCW	P1	P2	P3	P4	T1(n)	T2(n)	T3(n)	T4(n)
COSTAS	<b>0.55</b>	0.00	0.02	0.00	0.00	0.00	0.00	0.00	0.01	0.00	0.00	0.00
FRANK	0.00	<b>0.86</b>	0.00	0.00	0.00	0.00	0.16	0.00	0.00	0.00	0.02	0.00
FSK/PSK	0.00	0.00	<b>0.11</b>	0.00	0.00	0.00	0.00	0.00	0.00	0.00	0.00	0.00
FMCW	0.00	0.00	0.00	<b>1.00</b>	0.00	0.00	0.00	0.00	0.00	0.00	0.00	0.00
P1	0.09	0.06	0.33	0.00	<b>0.84</b>	0.19	0.01	0.87	0.08	0.00	0.00	0.01
P2	0.00	0.01	0.04	0.00	0.00	<b>0.76</b>	0.00	0.00	0.01	0.00	0.00	0.00
P3	0.01	0.00	0.02	0.00	0.00	0.00	<b>0.82</b>	0.01	0.00	0.01	0.06	0.00
P4	0.00	0.00	0.00	0.00	0.09	0.00	0.00	<b>0.02</b>	0.00	0.00	0.00	0.00
T1(n)	0.00	0.00	0.00	0.00	0.00	0.00	0.00	0.00	<b>0.79</b>	0.00	0.00	0.00
T2(n)	0.00	0.00	0.00	0.00	0.00	0.00	0.00	0.00	0.00	<b>0.83</b>	0.00	0.00
T3(n)	0.00	0.07	0.00	0.00	0.03	0.00	0.00	0.00	0.03	0.00	<b>0.52</b>	0.20
T4(n)	0.36	0.00	0.50	0.00	0.04	0.05	0.01	0.10	0.07	0.16	0.40	<b>0.79</b>
TEST MODULATION	COSTAS	FRANK	FSK/PSK	FMCW	P1	P2	P3	P4	T1(n)	T2(n)	T3(n)	T4(n)
COSTAS	<b>1.00</b>	0.00	0.00	0.00	0.03	0.00	0.01	0.00	0.00	0.00	0.00	0.00
FRANK	0.00	<b>0.33</b>	0.01	0.00	0.18	0.09	0.11	0.01	0.00	0.00	0.00	0.00
FSK/PSK	0.00	0.01	<b>0.00</b>	0.00	0.02	0.01	0.00	0.01	0.00	0.00	0.00	0.00
FMCW	0.00	0.00	0.00	<b>0.00</b>	0.02	0.03	0.02	0.00	0.00	0.00	0.00	0.00
P1	0.00	0.02	0.79	0.90	<b>0.11</b>	0.41	0.01	0.37	0.00	0.00	0.00	0.29
P2	0.00	0.01	0.03	0.00	0.02	<b>0.00</b>	0.02	0.00	0.00	0.00	0.00	0.00
P3	0.00	0.29	0.00	0.00	0.00	0.13	<b>0.36</b>	0.04	0.00	0.00	0.08	0.00
P4	0.00	0.01	0.00	0.00	0.33	0.01	0.00	<b>0.29</b>	0.00	0.00	0.36	0.05
T1(n)	0.00	0.30	0.00	0.00	0.19	0.01	0.00	0.23	<b>0.33</b>	0.00	0.00	0.00
T2(n)	0.00	0.00	0.00	0.00	0.01	0.00	0.02	0.00	0.06	<b>0.66</b>	0.06	0.00
T3(n)	0.00	0.00	0.00	0.10	0.08	0.33	0.00	0.00	0.25	0.11	<b>0.16</b>	0.65
T4(n)	0.00	0.03	0.18	0.01	0.02	0.01	0.45	0.04	0.36	0.22	0.33	<b>0.00</b>

Table 29. QMFB Classification Results with MLPNN (  $SNR = -3dB$  ).

TEST SNR	COSTAS	FRANK	FSK/PSK	FMCW	P1	P2	P3	P4	T1(n)	T2(n)	T3(n)	T4(n)
COSTAS	<b>0.03</b>	0.00	0.01	0.00	0.00	0.00	0.00	0.00	0.00	0.00	0.00	0.00
FRANK	0.00	<b>0.78</b>	0.05	0.00	0.00	0.15	0.10	0.00	0.00	0.03	0.11	0.00
FSK/PSK	0.00	0.00	<b>0.01</b>	0.00	0.01	0.00	0.00	0.00	0.00	0.00	0.01	0.00
FMCW	0.00	0.03	0.01	<b>1.00</b>	0.01	0.02	0.00	0.00	0.00	0.00	0.01	0.00
P1	0.37	0.10	0.83	0.00	<b>0.63</b>	0.01	0.01	0.78	0.01	0.03	0.02	0.00
P2	0.01	0.01	0.00	0.00	0.01	<b>0.59</b>	0.00	0.01	0.01	0.00	0.01	0.12
P3	0.02	0.02	0.02	0.00	0.01	0.22	<b>0.69</b>	0.01	0.11	0.05	0.06	0.06
P4	0.00	0.00	0.00	0.00	0.33	0.01	0.00	<b>0.15</b>	0.05	0.00	0.11	0.00
T1(n)	0.00	0.00	0.00	0.00	0.00	0.00	0.00	0.00	<b>0.63</b>	0.00	0.00	0.00
T2(n)	0.00	0.00	0.00	0.00	0.00	0.00	0.00	0.00	0.01	<b>0.63</b>	0.02	0.00
T3(n)	0.02	0.02	0.00	0.00	0.00	0.00	0.00	0.00	0.01	0.00	<b>0.25</b>	0.11
T4(n)	0.58	0.04	0.10	0.00	0.00	0.01	0.19	0.06	0.18	0.26	0.41	<b>0.70</b>
TEST MODULATION	COSTAS	FRANK	FSK/PSK	FMCW	P1	P2	P3	P4	T1(n)	T2(n)	T3(n)	T4(n)
COSTAS	<b>1.00</b>	0.00	0.01	0.03	0.02	0.01	0.01	0.00	0.00	0.01	0.00	0.00
FRANK	0.00	<b>0.33</b>	0.01	0.03	0.13	0.01	0.17	0.02	0.00	0.00	0.00	0.08
FSK/PSK	0.00	0.01	<b>0.00</b>	0.01	0.03	0.01	0.00	0.00	0.00	0.00	0.00	0.00
FMCW	0.00	0.00	0.01	<b>0.01</b>	0.01	0.18	0.01	0.00	0.00	0.00	0.00	0.04
P1	0.00	0.35	0.65	0.41	<b>0.26</b>	0.47	0.02	0.46	0.01	0.00	0.15	0.28
P2	0.00	0.00	0.00	0.00	0.01	<b>0.02</b>	0.00	0.00	0.00	0.02	0.00	0.00
P3	0.00	0.11	0.17	0.00	0.01	0.20	<b>0.19</b>	0.00	0.01	0.00	0.07	0.06
P4	0.00	0.00	0.00	0.13	0.23	0.00	0.00	<b>0.33</b>	0.00	0.00	0.15	0.00
T1(n)	0.00	0.00	0.00	0.01	0.15	0.00	0.00	0.02	<b>0.34</b>	0.08	0.01	0.00
T2(n)	0.00	0.00	0.00	0.00	0.01	0.00	0.00	0.00	0.03	<b>0.55</b>	0.12	0.00
T3(n)	0.00	0.00	0.04	0.23	0.06	0.10	0.00	0.01	0.41	0.26	<b>0.21</b>	0.52
T4(n)	0.00	0.18	0.13	0.18	0.08	0.03	0.59	0.16	0.21	0.07	0.28	<b>0.02</b>

Table 30. QMFB Classification Results with MLPNN (  $SNR = -6dB$  ).

TEST SNR	COSTAS	FRANK	FSK/PSK	FMCW	P1	P2	P3	P4	T1(n)	T2(n)	T3(n)	T4(n)
COSTAS	<b>0.00</b>	0.00	0.00	0.00	0.01	0.00	0.00	0.00	0.05	0.00	0.00	0.00
FRANK	0.00	<b>0.71</b>	0.00	0.00	0.00	0.00	0.03	0.00	0.03	0.19	0.17	0.03
FSK/PSK	0.00	0.00	<b>0.00</b>	0.00	0.00	0.00	0.00	0.00	0.00	0.00	0.00	0.00
FMCW	0.03	0.00	0.01	<b>0.94</b>	0.04	0.03	0.00	0.00	0.04	0.00	0.00	0.00
P1	0.33	0.11	0.50	0.00	<b>0.88</b>	0.09	0.10	0.66	0.16	0.01	0.11	0.33
P2	0.00	0.00	0.02	0.00	0.00	<b>0.56</b>	0.00	0.01	0.00	0.00	0.00	0.00
P3	0.00	0.00	0.41	0.06	0.01	0.07	<b>0.75</b>	0.04	0.05	0.00	0.26	0.01
P4	0.00	0.00	0.00	0.00	0.01	0.01	0.00	<b>0.28</b>	0.00	0.00	0.00	0.00
T1(n)	0.00	0.00	0.00	0.00	0.00	0.00	0.00	0.00	<b>0.35</b>	0.20	0.00	0.00
T2(n)	0.00	0.00	0.00	0.00	0.00	0.00	0.00	0.00	0.00	<b>0.20</b>	0.00	0.00
T3(n)	0.00	0.00	0.00	0.00	0.00	0.00	0.00	0.00	0.03	0.00	<b>0.17</b>	0.00
T4(n)	0.65	0.18	0.07	0.00	0.04	0.24	0.12	0.01	0.29	0.40	0.29	<b>0.63</b>
TEST MODULATION	COSTAS	FRANK	FSK/PSK	FMCW	P1	P2	P3	P4	T1(n)	T2(n)	T3(n)	T4(n)
COSTAS	<b>1.00</b>	0.00	0.00	0.01	0.01	0.00	0.01	0.00	0.00	0.00	0.00	0.00
FRANK	0.00	<b>0.16</b>	0.00	0.02	0.01	0.25	0.12	0.00	0.05	0.11	0.33	0.40
FSK/PSK	0.00	0.09	<b>0.00</b>	0.01	0.00	0.00	0.00	0.00	0.00	0.13	0.00	0.00
FMCW	0.00	0.00	0.00	<b>0.00</b>	0.00	0.08	0.04	0.01	0.00	0.01	0.00	0.01
P1	0.00	0.28	0.27	0.41	<b>0.31</b>	0.48	0.10	0.58	0.06	0.11	0.33	0.46
P2	0.00	0.06	0.02	0.00	0.04	<b>0.00</b>	0.00	0.00	0.00	0.00	0.00	0.01
P3	0.00	0.12	0.09	0.00	0.15	0.12	<b>0.08</b>	0.02	0.00	0.21	0.00	0.03
P4	0.00	0.01	0.00	0.00	0.01	0.00	0.00	<b>0.00</b>	0.00	0.00	0.00	0.00
T1(n)	0.00	0.01	0.00	0.14	0.00	0.00	0.00	0.02	<b>0.32</b>	0.12	0.00	0.00
T2(n)	0.00	0.08	0.00	0.00	0.00	0.00	0.00	0.00	0.31	<b>0.00</b>	0.00	0.00
T3(n)	0.00	0.01	0.00	0.43	0.01	0.01	0.00	0.00	0.07	0.01	<b>0.00</b>	0.00
T4(n)	0.00	0.18	0.62	0.00	0.47	0.07	0.64	0.38	0.19	0.30	0.33	<b>0.09</b>

## B. RBFNN CLASSIFICATION CONFUSION MATRICES

Table 31. PWVD Classification Results with RBFNN (  $SNR = 10\text{dB}$  ).

TEST SNR	COSTAS	FRANK	FSK/PSK	FMCW	P1	P2	P3	P4	T1(n)	T2(n)	T3(n)	T4(n)
COSTAS	<b>1.00</b>	0.00	0.00	0.00	0.00	0.00	0.00	0.00	0.00	0.00	0.00	0.00
FRANK	0.00	<b>1.00</b>	0.00	0.00	0.00	0.00	0.00	0.00	0.00	0.00	0.00	0.00
FSK/PSK	0.00	0.00	<b>1.00</b>	0.00	0.00	0.00	0.00	0.00	0.00	0.00	0.00	0.00
FMCW	0.00	0.00	0.00	<b>1.00</b>	0.00	0.00	0.00	0.00	0.00	0.00	0.00	0.00
P1	0.00	0.00	0.00	0.00	<b>1.00</b>	0.00	0.00	0.00	0.00	0.00	0.00	0.00
P2	0.00	0.00	0.00	0.00	0.00	<b>1.00</b>	0.00	0.00	0.00	0.00	0.00	0.00
P3	0.00	0.00	0.00	0.00	0.00	0.00	<b>1.00</b>	0.00	0.00	0.00	0.00	0.00
P4	0.00	0.00	0.00	0.00	0.00	0.00	0.00	<b>1.00</b>	0.00	0.00	0.00	0.00
T1(n)	0.00	0.00	0.00	0.00	0.00	0.00	0.00	0.00	<b>1.00</b>	0.00	0.00	0.00
T2(n)	0.00	0.00	0.00	0.00	0.00	0.00	0.00	0.00	0.00	<b>1.00</b>	0.00	0.00
T3(n)	0.00	0.00	0.00	0.00	0.00	0.00	0.00	0.00	0.00	0.00	<b>1.00</b>	0.00
T4(n)	0.00	0.00	0.00	0.00	0.00	0.00	0.00	0.00	0.00	0.00	0.00	<b>1.00</b>
TEST MODULATION	COSTAS	FRANK	FSK/PSK	FMCW	P1	P2	P3	P4	T1(n)	T2(n)	T3(n)	T4(n)
COSTAS	<b>1.00</b>	0.00	0.00	0.00	0.00	0.00	0.00	0.00	0.00	0.00	0.00	0.00
FRANK	0.00	<b>0.67</b>	0.00	0.00	0.33	0.00	0.33	0.33	0.00	0.00	0.00	0.00
FSK/PSK	0.00	0.00	<b>1.00</b>	0.00	0.00	0.00	0.00	0.00	0.00	0.00	0.00	0.00
FMCW	0.00	0.00	0.00	<b>1.00</b>	0.00	0.00	0.00	0.00	0.00	0.00	0.00	0.00
P1	0.00	0.00	0.00	0.00	<b>0.00</b>	0.00	0.00	0.00	0.00	0.00	0.00	0.00
P2	0.00	0.00	0.00	0.00	0.00	<b>1.00</b>	0.00	0.00	0.00	0.00	0.00	0.00
P3	0.00	0.00	0.00	0.00	0.33	0.00	<b>0.67</b>	0.33	0.33	0.00	0.00	0.00
P4	0.00	0.00	0.00	0.00	0.33	0.00	0.00	<b>0.33</b>	0.00	0.00	0.00	0.00
T1(n)	0.00	0.00	0.00	0.00	0.00	0.00	0.00	0.00	<b>0.33</b>	0.00	0.00	0.00
T2(n)	0.00	0.00	0.00	0.00	0.00	0.00	0.00	0.00	0.00	<b>0.67</b>	0.00	0.00
T3(n)	0.00	0.33	0.00	0.00	0.00	0.00	0.00	0.00	0.33	0.00	<b>0.33</b>	0.00
T4(n)	0.00	0.00	0.00	0.00	0.00	0.00	0.00	0.00	0.00	0.33	0.67	<b>1.00</b>

Table 32. PWVD Classification Results with RBFNN (  $SNR = 6\text{dB}$  ).

TEST SNR	COSTAS	FRANK	FSK/PSK	FMCW	P1	P2	P3	P4	T1(n)	T2(n)	T3(n)	T4(n)
COSTAS	<b>0.50</b>	0.00	0.00	0.00	0.00	0.00	0.00	0.00	0.00	0.00	0.00	0.00
FRANK	0.00	<b>1.00</b>	0.00	0.00	0.00	0.00	0.00	0.00	0.00	0.00	0.00	0.00
FSK/PSK	0.00	0.00	<b>1.00</b>	0.00	0.00	0.00	0.00	0.00	0.00	0.00	0.00	0.00
FMCW	0.00	0.00	0.00	<b>1.00</b>	0.00	0.00	0.00	0.00	0.00	0.00	0.00	0.00
P1	0.00	0.00	0.00	0.00	<b>0.60</b>	0.00	0.00	0.40	0.00	0.00	0.00	0.20
P2	0.00	0.00	0.00	0.00	0.00	<b>1.00</b>	0.00	0.00	0.00	0.00	0.00	0.00
P3	0.00	0.00	0.00	0.00	0.00	0.00	<b>1.00</b>	0.00	0.00	0.00	0.00	0.00
P4	0.50	0.00	0.00	0.00	0.40	0.00	0.00	<b>0.40</b>	0.00	0.00	0.00	0.00
T1(n)	0.00	0.00	0.00	0.00	0.00	0.00	0.00	0.00	<b>1.00</b>	0.00	0.00	0.00
T2(n)	0.00	0.00	0.00	0.00	0.00	0.00	0.00	0.00	0.00	<b>1.00</b>	0.00	0.00
T3(n)	0.00	0.00	0.00	0.00	0.00	0.00	0.00	0.00	0.00	0.00	<b>1.00</b>	0.00
T4(n)	0.00	0.00	0.00	0.00	0.00	0.00	0.00	0.20	0.00	0.00	0.00	<b>0.80</b>
TEST MODULATION	COSTAS	FRANK	FSK/PSK	FMCW	P1	P2	P3	P4	T1(n)	T2(n)	T3(n)	T4(n)
COSTAS	<b>1.00</b>	0.00	0.00	0.00	0.00	0.00	0.00	0.00	0.00	0.00	0.00	0.00
FRANK	0.00	<b>0.33</b>	0.00	0.00	0.00	0.00	0.33	0.33	0.00	0.00	0.00	0.00
FSK/PSK	0.00	0.00	<b>0.50</b>	0.00	0.00	0.00	0.00	0.00	0.00	0.00	0.00	0.00
FMCW	0.00	0.00	0.00	<b>1.00</b>	0.00	0.00	0.00	0.00	0.00	0.00	0.00	0.00
P1	0.00	0.00	0.00	0.00	<b>0.33</b>	0.00	0.00	0.00	0.00	0.00	0.00	0.00
P2	0.00	0.00	0.00	0.00	0.00	<b>1.00</b>	0.00	0.00	0.00	0.00	0.00	0.00
P3	0.00	0.00	0.00	0.00	0.33	0.00	<b>0.67</b>	0.33	0.33	0.00	0.00	0.00
P4	0.00	0.00	0.00	0.00	0.00	0.00	0.00	<b>0.33</b>	0.00	0.00	0.00	0.00
T1(n)	0.00	0.33	0.00	0.00	0.00	0.00	0.00	0.00	<b>0.33</b>	0.00	0.00	0.00
T2(n)	0.00	0.00	0.00	0.00	0.00	0.00	0.00	0.00	0.00	<b>0.67</b>	0.00	0.00
T3(n)	0.00	0.33	0.00	0.00	0.33	0.00	0.00	0.00	0.00	0.00	<b>0.33</b>	0.00
T4(n)	0.00	0.00	0.50	0.00	0.00	0.00	0.00	0.00	0.33	0.33	0.67	<b>1.00</b>

Table 33. PWVD Classification Results with RBFNN (  $SNR = 3\text{ dB}$  ).

TEST SNR	COSTAS	FRANK	FSK/PSK	FMCW	P1	P2	P3	P4	T1(n)	T2(n)	T3(n)	T4(n)
COSTAS	<b>1.00</b>	0.00	0.00	0.00	0.00	0.25	0.00	0.00	0.00	0.00	0.00	0.00
FRANK	0.00	<b>1.00</b>	0.00	0.00	0.00	0.00	0.00	0.00	0.00	0.00	0.00	0.00
FSK/PSK	0.00	0.00	<b>0.50</b>	0.00	0.00	0.00	0.20	0.00	0.00	0.00	0.00	0.00
FMCW	0.00	0.00	0.00	<b>1.00</b>	0.00	0.00	0.00	0.00	0.00	0.00	0.00	0.00
P1	0.00	0.00	0.00	0.00	<b>0.60</b>	0.00	0.00	0.00	0.00	0.00	0.00	0.20
P2	0.00	0.00	0.00	0.00	0.00	<b>0.75</b>	0.00	0.00	0.00	0.00	0.00	0.00
P3	0.00	0.00	0.50	0.00	0.00	0.00	<b>0.80</b>	0.00	0.00	0.00	0.00	0.00
P4	0.00	0.00	0.00	0.00	0.40	0.00	0.00	<b>1.00</b>	0.00	0.00	0.00	0.00
T1(n)	0.00	0.00	0.00	0.00	0.00	0.00	0.00	0.00	<b>1.00</b>	0.00	0.00	0.00
T2(n)	0.00	0.00	0.00	0.00	0.00	0.00	0.00	0.00	0.00	<b>1.00</b>	0.00	0.00
T3(n)	0.00	0.00	0.00	0.00	0.00	0.00	0.00	0.00	0.00	0.00	<b>1.00</b>	0.00
T4(n)	0.00	0.00	0.00	0.00	0.00	0.00	0.00	0.00	0.00	0.00	0.00	<b>0.80</b>
TEST MODULATION	COSTAS	FRANK	FSK/PSK	FMCW	P1	P2	P3	P4	T1(n)	T2(n)	T3(n)	T4(n)
COSTAS	<b>1.00</b>	0.00	0.00	0.00	0.00	0.00	0.00	0.00	0.00	0.00	0.00	0.00
FRANK	0.00	<b>0.33</b>	0.00	0.00	0.33	0.00	0.33	0.33	0.00	0.00	0.33	0.00
FSK/PSK	0.00	0.00	<b>0.50</b>	0.00	0.00	0.00	0.00	0.00	0.00	0.00	0.00	0.00
FMCW	0.00	0.00	0.00	<b>1.00</b>	0.00	0.00	0.00	0.00	0.00	0.00	0.00	0.00
P1	0.00	0.00	0.00	0.00	<b>0.33</b>	0.00	0.00	0.00	0.00	0.00	0.00	0.00
P2	0.00	0.00	0.00	0.00	0.00	<b>1.00</b>	0.00	0.00	0.00	0.00	0.00	0.00
P3	0.00	0.00	0.00	0.00	0.33	0.00	<b>0.67</b>	0.33	0.00	0.00	0.00	0.00
P4	0.00	0.00	0.00	0.00	0.00	0.00	0.00	<b>0.33</b>	0.00	0.00	0.00	0.00
T1(n)	0.00	0.00	0.00	0.00	0.00	0.00	0.00	0.00	<b>0.67</b>	0.00	0.00	0.00
T2(n)	0.00	0.00	0.00	0.00	0.00	0.00	0.00	0.00	0.00	<b>0.67</b>	0.00	0.00
T3(n)	0.00	0.00	0.00	0.00	0.00	0.00	0.00	0.00	0.33	0.00	<b>0.00</b>	0.00
T4(n)	0.00	0.67	0.50	0.00	0.00	0.00	0.00	0.00	0.00	0.33	0.67	<b>1.00</b>

Table 34. PWVD Classification Results with RBFNN (  $SNR = 0\text{ dB}$  ).

TEST SNR	COSTAS	FRANK	FSK/PSK	FMCW	P1	P2	P3	P4	T1(n)	T2(n)	T3(n)	T4(n)
COSTAS	<b>1.00</b>	0.00	0.50	0.00	0.00	0.25	0.00	0.00	0.00	0.00	0.00	0.00
FRANK	0.00	<b>0.80</b>	0.00	0.00	0.00	0.00	0.00	0.00	0.00	0.00	0.00	0.00
FSK/PSK	0.00	0.20	<b>0.50</b>	0.00	0.00	0.00	0.00	0.00	0.00	0.00	0.00	0.00
FMCW	0.00	0.00	0.00	<b>1.00</b>	0.00	0.00	0.00	0.00	0.00	0.00	0.00	0.00
P1	0.00	0.00	0.00	0.00	<b>0.40</b>	0.00	0.00	0.00	0.00	0.00	0.00	0.00
P2	0.00	0.00	0.00	0.00	0.00	<b>0.75</b>	0.00	0.00	0.00	0.00	0.00	0.00
P3	0.00	0.00	0.00	0.00	0.00	0.00	<b>1.00</b>	0.00	0.00	0.00	0.00	0.00
P4	0.00	0.00	0.00	0.00	0.40	0.00	0.00	<b>0.80</b>	0.00	0.00	0.00	0.00
T1(n)	0.00	0.00	0.00	0.00	0.00	0.00	0.00	0.00	<b>1.00</b>	0.00	0.00	0.00
T2(n)	0.00	0.00	0.00	0.00	0.00	0.00	0.00	0.00	0.00	<b>1.00</b>	0.00	0.00
T3(n)	0.00	0.00	0.00	0.00	0.00	0.00	0.00	0.00	0.00	0.00	<b>0.80</b>	0.00
T4(n)	0.00	0.00	0.00	0.00	0.20	0.00	0.00	0.20	0.00	0.00	0.20	<b>1.00</b>
TEST MODULATION	COSTAS	FRANK	FSK/PSK	FMCW	P1	P2	P3	P4	T1(n)	T2(n)	T3(n)	T4(n)
COSTAS	<b>1.00</b>	0.00	0.00	0.00	0.00	0.00	0.00	0.00	0.00	0.00	0.00	0.00
FRANK	0.00	<b>0.33</b>	0.00	0.00	0.00	0.50	0.00	0.00	0.00	0.00	0.00	0.00
FSK/PSK	0.00	0.00	<b>0.50</b>	0.00	0.00	0.00	0.00	0.00	0.00	0.00	0.00	0.00
FMCW	0.00	0.00	0.00	<b>1.00</b>	0.00	0.00	0.00	0.00	0.00	0.00	0.00	0.00
P1	0.00	0.00	0.00	0.00	<b>0.00</b>	0.00	0.00	0.00	0.00	0.00	0.00	0.00
P2	0.00	0.00	0.00	0.00	0.00	<b>0.50</b>	0.00	0.00	0.00	0.00	0.00	0.00
P3	0.00	0.00	0.00	0.00	0.67	0.00	<b>0.67</b>	0.33	0.00	0.00	0.00	0.00
P4	0.00	0.00	0.00	0.00	0.00	0.00	0.00	<b>0.33</b>	0.00	0.00	0.00	0.00
T1(n)	0.00	0.00	0.00	0.00	0.00	0.00	0.00	0.00	<b>0.67</b>	0.00	0.00	0.00
T2(n)	0.00	0.00	0.00	0.00	0.00	0.00	0.00	0.00	0.00	<b>0.67</b>	0.00	0.00
T3(n)	0.00	0.33	0.00	0.00	0.33	0.00	0.33	0.33	0.00	0.00	<b>0.33</b>	0.00
T4(n)	0.00	0.33	0.50	0.00	0.00	0.00	0.00	0.00	0.33	0.33	0.67	<b>1.00</b>

Table 35. PWVD Classification Results with RBFNN (  $SNR = -3\text{dB}$  ).

TEST SNR	COSTAS	FRANK	FSK/PSK	FMCW	P1	P2	P3	P4	T1(n)	T2(n)	T3(n)	T4(n)
COSTAS	<b>1.00</b>	0.00	0.00	0.00	0.00	0.00	0.00	0.00	0.00	0.00	0.00	0.00
FRANK	0.00	<b>1.00</b>	0.00	0.00	0.00	0.00	0.00	0.20	0.00	0.00	0.00	0.00
FSK/PSK	0.00	0.00	<b>0.00</b>	0.00	0.00	0.25	0.00	0.00	0.00	0.00	0.00	0.00
FMCW	0.00	0.00	0.00	<b>1.00</b>	0.00	0.00	0.00	0.00	0.00	0.00	0.00	0.00
P1	0.00	0.00	0.00	0.00	<b>0.60</b>	0.00	0.00	0.00	0.00	0.00	0.00	0.20
P2	0.00	0.00	0.00	0.00	0.00	<b>0.50</b>	0.00	0.00	0.00	0.00	0.00	0.00
P3	0.00	0.00	0.50	0.00	0.00	0.00	<b>0.80</b>	0.00	0.00	0.00	0.20	0.00
P4	0.00	0.00	0.00	0.00	0.20	0.00	0.00	<b>0.60</b>	0.00	0.00	0.00	0.00
T1(n)	0.00	0.00	0.00	0.00	0.00	0.00	0.00	0.00	<b>0.60</b>	0.00	0.00	0.00
T2(n)	0.00	0.00	0.00	0.00	0.00	0.00	0.00	0.00	0.00	<b>1.00</b>	0.00	0.00
T3(n)	0.00	0.00	0.00	0.00	0.00	0.00	0.00	0.00	0.40	0.00	<b>0.60</b>	0.00
T4(n)	0.00	0.00	0.50	0.00	0.20	0.25	0.20	0.20	0.00	0.00	0.20	<b>0.80</b>
TEST MODULATION	COSTAS	FRANK	FSK/PSK	FMCW	P1	P2	P3	P4	T1(n)	T2(n)	T3(n)	T4(n)
COSTAS	<b>1.00</b>	0.33	0.00	0.00	0.00	0.00	0.00	0.00	0.00	0.00	0.00	0.00
FRANK	0.00	<b>0.33</b>	0.00	0.00	0.33	0.00	0.67	0.00	0.00	0.00	0.00	0.00
FSK/PSK	0.00	0.00	<b>0.00</b>	0.00	0.00	0.00	0.00	0.00	0.00	0.00	0.00	0.00
FMCW	0.00	0.00	0.00	<b>1.00</b>	0.00	0.00	0.00	0.00	0.00	0.00	0.00	0.00
P1	0.00	0.00	0.00	0.00	<b>0.00</b>	0.00	0.00	0.00	0.00	0.00	0.00	0.00
P2	0.00	0.00	0.00	0.00	0.00	<b>0.50</b>	0.00	0.00	0.00	0.00	0.00	0.00
P3	0.00	0.00	1.00	0.00	0.33	0.50	<b>0.00</b>	0.00	0.00	0.00	0.33	0.00
P4	0.00	0.00	0.00	0.00	0.33	0.00	0.00	<b>0.33</b>	0.00	0.00	0.00	0.00
T1(n)	0.00	0.00	0.00	0.00	0.00	0.00	0.00	0.33	<b>0.67</b>	0.00	0.00	0.00
T2(n)	0.00	0.00	0.00	0.00	0.00	0.00	0.00	0.00	0.00	<b>0.67</b>	0.00	0.00
T3(n)	0.00	0.33	0.00	0.00	0.00	0.00	0.00	0.33	0.33	0.00	<b>0.00</b>	0.33
T4(n)	0.00	0.00	0.00	0.00	0.00	0.00	0.33	0.00	0.00	0.33	0.67	<b>0.67</b>

Table 36. PWVD Classification Results with RBFNN (  $SNR = -6\text{dB}$  ).

TEST SNR	COSTAS	FRANK	FSK/PSK	FMCW	P1	P2	P3	P4	T1(n)	T2(n)	T3(n)	T4(n)
COSTAS	<b>1.00</b>	0.00	0.00	0.00	0.00	0.00	0.00	0.00	0.00	0.20	0.00	0.00
FRANK	0.00	<b>0.00</b>	0.00	0.00	0.00	0.00	0.20	0.00	0.00	0.00	0.00	0.00
FSK/PSK	0.00	0.00	<b>0.00</b>	0.00	0.00	0.00	0.00	0.00	0.00	0.00	0.00	0.00
FMCW	0.00	0.00	0.00	<b>1.00</b>	0.00	0.00	0.00	0.00	0.00	0.00	0.00	0.00
P1	0.00	0.40	0.00	0.00	<b>0.80</b>	0.00	0.00	0.40	0.00	0.00	0.20	0.00
P2	0.00	0.00	0.00	0.00	0.00	<b>0.25</b>	0.00	0.00	0.00	0.00	0.00	0.00
P3	0.00	0.60	0.50	0.00	0.00	0.50	<b>0.40</b>	0.00	0.40	0.40	0.00	0.00
P4	0.00	0.00	0.50	0.00	0.20	0.00	0.20	<b>0.60</b>	0.00	0.00	0.00	0.20
T1(n)	0.00	0.00	0.00	0.00	0.00	0.00	0.00	0.00	<b>0.60</b>	0.00	0.00	0.00
T2(n)	0.00	0.00	0.00	0.00	0.00	0.00	0.20	0.00	0.00	<b>0.40</b>	0.00	0.00
T3(n)	0.00	0.00	0.00	0.00	0.00	0.00	0.00	0.00	0.00	0.00	<b>0.60</b>	0.20
T4(n)	0.00	0.00	0.00	0.00	0.00	0.25	0.00	0.00	0.00	0.00	0.20	<b>0.60</b>
TEST MODULATION	COSTAS	FRANK	FSK/PSK	FMCW	P1	P2	P3	P4	T1(n)	T2(n)	T3(n)	T4(n)
COSTAS	<b>1.00</b>	0.00	0.00	0.00	0.33	0.00	0.00	0.00	0.00	0.00	0.00	0.00
FRANK	0.00	<b>0.00</b>	0.00	0.00	0.00	0.00	0.33	0.33	0.00	0.00	0.00	0.00
FSK/PSK	0.00	0.00	<b>0.00</b>	0.00	0.00	0.00	0.00	0.00	0.00	0.00	0.00	0.00
FMCW	0.00	0.00	0.00	<b>1.00</b>	0.00	0.00	0.00	0.00	0.00	0.00	0.00	0.00
P1	0.00	0.00	0.00	0.00	<b>0.33</b>	0.00	0.00	0.00	0.00	0.00	0.00	0.00
P2	0.00	0.00	0.00	0.00	0.00	<b>0.00</b>	0.00	0.00	0.00	0.00	0.00	0.00
P3	0.00	0.33	1.00	0.00	0.00	1.00	<b>0.33</b>	0.33	0.00	0.33	0.00	0.00
P4	0.00	0.33	0.00	0.00	0.00	0.00	0.00	<b>0.00</b>	0.00	0.00	0.00	0.00
T1(n)	0.00	0.00	0.00	0.00	0.33	0.00	0.00	0.33	<b>0.67</b>	0.33	0.00	0.00
T2(n)	0.00	0.00	0.00	0.00	0.00	0.00	0.00	0.00	0.00	<b>0.00</b>	0.00	0.00
T3(n)	0.00	0.33	0.00	0.00	0.00	0.00	0.33	0.00	0.33	0.00	<b>0.67</b>	0.00
T4(n)	0.00	0.00	0.00	0.00	0.00	0.00	0.00	0.00	0.00	0.33	0.33	<b>1.00</b>



Table 37. CWD Classification Results with RBFNN (  $SNR = 10\text{dB}$  ).

TEST SNR	COSTAS	FRANK	FSK/PSK	FMCW	P1	P2	P3	P4	T1(n)	T2(n)	T3(n)	T4(n)
COSTAS	<b>1.00</b>	0.00	0.00	0.00	0.00	0.00	0.00	0.00	0.00	0.00	0.00	0.00
FRANK	0.00	<b>1.00</b>	0.00	0.00	0.00	0.00	0.00	0.00	0.00	0.00	0.00	0.00
FSK/PSK	0.00	0.00	<b>1.00</b>	0.00	0.00	0.00	0.00	0.00	0.00	0.00	0.00	0.00
FMCW	0.00	0.00	0.00	<b>1.00</b>	0.00	0.00	0.00	0.00	0.00	0.00	0.00	0.00
P1	0.00	0.00	0.00	0.00	<b>1.00</b>	0.00	0.00	0.00	0.00	0.00	0.00	0.00
P2	0.00	0.00	0.00	0.00	0.00	<b>1.00</b>	0.00	0.00	0.00	0.00	0.00	0.00
P3	0.00	0.00	0.00	0.00	0.00	0.00	<b>1.00</b>	0.00	0.00	0.00	0.00	0.00
P4	0.00	0.00	0.00	0.00	0.00	0.00	0.00	<b>1.00</b>	0.00	0.00	0.00	0.00
T1(n)	0.00	0.00	0.00	0.00	0.00	0.00	0.00	0.00	<b>1.00</b>	0.00	0.00	0.00
T2(n)	0.00	0.00	0.00	0.00	0.00	0.00	0.00	0.00	0.00	<b>1.00</b>	0.00	0.00
T3(n)	0.00	0.00	0.00	0.00	0.00	0.00	0.00	0.00	0.00	0.00	<b>1.00</b>	0.00
T4(n)	0.00	0.00	0.00	0.00	0.00	0.00	0.00	0.00	0.00	0.00	0.00	<b>1.00</b>
TEST MODULATION	COSTAS	FRANK	FSK/PSK	FMCW	P1	P2	P3	P4	T1(n)	T2(n)	T3(n)	T4(n)
COSTAS	<b>1.00</b>	0.00	0.00	0.00	0.00	0.00	0.00	0.00	0.00	0.00	0.00	0.00
FRANK	0.00	<b>0.00</b>	0.00	0.00	0.33	0.00	0.33	0.33	0.00	0.00	0.33	0.00
FSK/PSK	0.00	0.00	<b>1.00</b>	0.00	0.00	0.00	0.00	0.00	0.00	0.00	0.00	0.00
FMCW	0.00	0.00	0.00	<b>1.00</b>	0.00	0.00	0.00	0.00	0.00	0.00	0.00	0.00
P1	0.00	0.00	0.00	0.00	<b>0.00</b>	0.00	0.00	0.00	0.00	0.00	0.00	0.00
P2	0.00	0.00	0.00	0.00	0.33	<b>1.00</b>	0.33	0.00	0.00	0.00	0.00	0.00
P3	0.00	0.00	0.00	0.00	0.00	0.00	<b>0.00</b>	0.00	0.33	0.00	0.00	0.00
P4	0.00	0.00	0.00	0.00	0.00	0.00	0.00	<b>0.33</b>	0.00	0.33	0.00	0.00
T1(n)	0.00	0.00	0.00	0.00	0.00	0.00	0.00	0.00	<b>0.33</b>	0.00	0.00	0.00
T2(n)	0.00	0.00	0.00	0.00	0.00	0.00	0.00	0.00	0.00	<b>0.67</b>	0.00	0.00
T3(n)	0.00	0.67	0.00	0.00	0.33	0.00	0.33	0.33	0.00	0.00	<b>0.33</b>	0.33
T4(n)	0.00	0.33	0.00	0.00	0.00	0.00	0.00	0.00	0.33	0.00	0.33	<b>0.67</b>

Table 38. CWD Classification Results with RBFNN (  $SNR = 6\text{dB}$  ).

TEST SNR	COSTAS	FRANK	FSK/PSK	FMCW	P1	P2	P3	P4	T1(n)	T2(n)	T3(n)	T4(n)
COSTAS	<b>1.00</b>	0.33	0.00	0.00	0.00	0.00	0.00	0.00	0.00	0.00	0.00	0.00
FRANK	0.00	<b>0.80</b>	0.00	0.00	0.00	0.00	0.00	0.00	0.20	0.00	0.00	0.00
FSK/PSK	0.00	0.00	<b>0.50</b>	0.00	0.00	0.00	0.00	0.00	0.00	0.00	0.00	0.00
FMCW	0.00	0.00	0.00	<b>1.00</b>	0.00	0.00	0.00	0.00	0.00	0.00	0.00	0.00
P1	0.00	0.00	0.00	0.00	<b>0.60</b>	0.00	0.00	0.00	0.00	0.00	0.00	0.00
P2	0.00	0.00	0.00	0.00	0.00	<b>1.00</b>	0.00	0.00	0.00	0.00	0.00	0.00
P3	0.00	0.00	0.00	0.00	0.00	0.00	<b>0.80</b>	0.00	0.00	0.00	0.00	0.00
P4	0.00	0.00	0.00	0.00	0.40	0.00	0.00	<b>0.80</b>	0.00	0.00	0.00	0.20
T1(n)	0.00	0.00	0.00	0.00	0.00	0.00	0.20	0.00	<b>0.80</b>	0.00	0.00	0.00
T2(n)	0.00	0.00	0.00	0.00	0.00	0.00	0.00	0.00	0.00	<b>1.00</b>	0.00	0.00
T3(n)	0.00	0.20	0.50	0.00	0.00	0.00	0.00	0.00	0.00	0.00	<b>0.80</b>	0.00
T4(n)	0.00	0.00	0.00	0.00	0.00	0.00	0.00	0.20	0.00	0.00	0.20	<b>0.80</b>
TEST MODULATION	COSTAS	FRANK	FSK/PSK	FMCW	P1	P2	P3	P4	T1(n)	T2(n)	T3(n)	T4(n)
COSTAS	<b>1.00</b>	0.33	0.00	0.00	0.00	0.00	0.00	0.00	0.00	0.00	0.00	0.00
FRANK	0.00	<b>0.00</b>	0.00	0.00	0.00	0.00	0.67	0.33	0.00	0.00	0.00	0.00
FSK/PSK	0.00	0.00	<b>0.50</b>	0.00	0.00	0.00	0.00	0.00	0.00	0.00	0.00	0.00
FMCW	0.00	0.00	0.00	<b>1.00</b>	0.00	0.00	0.00	0.00	0.00	0.00	0.00	0.00
P1	0.00	0.00	0.00	0.00	<b>0.00</b>	0.00	0.00	0.00	0.00	0.00	0.00	0.00
P2	0.00	0.00	0.00	0.00	0.33	<b>1.00</b>	0.33	0.00	0.00	0.00	0.00	0.00
P3	0.00	0.00	0.00	0.00	0.00	0.00	<b>0.00</b>	0.00	0.33	0.00	0.00	0.00
P4	0.00	0.00	0.00	0.00	0.00	0.00	0.00	<b>0.33</b>	0.00	0.00	0.00	0.00
T1(n)	0.00	0.00	0.00	0.00	0.00	0.00	0.00	0.00	<b>0.33</b>	0.00	0.00	0.00
T2(n)	0.00	0.00	0.00	0.00	0.33	0.00	0.00	0.00	0.00	<b>0.67</b>	0.00	0.00
T3(n)	0.00	0.33	0.00	0.00	0.33	0.00	0.00	0.33	0.00	0.33	<b>0.33</b>	0.67
T4(n)	0.00	0.33	0.50	0.00	0.00	0.00	0.00	0.00	0.33	0.00	0.67	<b>0.33</b>

Table 39. CWD Classification Results with RBFNN (  $SNR = 3\text{dB}$  ).

TEST SNR	COSTAS	FRANK	FSK/PSK	FMCW	P1	P2	P3	P4	T1(n)	T2(n)	T3(n)	T4(n)
COSTAS	<b>0.50</b>	0.00	0.00	0.00	0.00	0.00	0.00	0.00	0.00	0.00	0.00	0.00
FRANK	0.00	<b>1.00</b>	0.00	0.00	0.00	0.00	0.00	0.00	0.20	0.00	0.00	0.00
FSK/PSK	0.00	0.00	<b>0.50</b>	0.00	0.00	0.00	0.00	0.00	0.00	0.00	0.00	0.00
FMCW	0.00	0.00	0.00	<b>1.00</b>	0.00	0.00	0.00	0.00	0.00	0.00	0.00	0.00
P1	0.50	0.00	0.00	0.00	<b>0.60</b>	0.00	0.00	0.00	0.00	0.00	0.00	0.00
P2	0.00	0.00	0.00	0.00	0.00	<b>1.00</b>	0.00	0.00	0.00	0.00	0.00	0.00
P3	0.00	0.00	0.00	0.00	0.20	0.00	<b>0.60</b>	0.00	0.00	0.00	0.00	0.00
P4	0.00	0.00	0.00	0.00	0.20	0.00	0.00	<b>1.00</b>	0.00	0.00	0.00	0.20
T1(n)	0.00	0.00	0.00	0.00	0.00	0.00	0.20	0.00	<b>0.80</b>	0.00	0.00	0.00
T2(n)	0.00	0.00	0.00	0.00	0.00	0.00	0.00	0.00	0.00	<b>1.00</b>	0.00	0.00
T3(n)	0.00	0.00	0.50	0.00	0.00	0.00	0.00	0.00	0.00	0.00	<b>0.80</b>	0.20
T4(n)	0.00	0.00	0.00	0.00	0.00	0.00	0.20	0.00	0.00	0.00	0.20	<b>0.60</b>
TEST MODULATION	COSTAS	FRANK	FSK/PSK	FMCW	P1	P2	P3	P4	T1(n)	T2(n)	T3(n)	T4(n)
COSTAS	<b>1.00</b>	0.33	0.00	0.00	0.00	0.00	0.00	0.00	0.00	0.00	0.00	0.00
FRANK	0.00	<b>0.00</b>	0.00	0.00	0.33	0.00	0.67	0.33	0.00	0.33	0.33	0.00
FSK/PSK	0.00	0.00	<b>0.00</b>	0.00	0.00	0.00	0.00	0.00	0.00	0.00	0.00	0.00
FMCW	0.00	0.00	0.00	<b>1.00</b>	0.00	0.00	0.00	0.00	0.00	0.00	0.00	0.00
P1	0.00	0.00	0.00	0.00	<b>0.00</b>	0.00	0.00	0.00	0.00	0.00	0.00	0.00
P2	0.00	0.00	0.00	0.00	0.33	<b>1.00</b>	0.33	0.00	0.00	0.00	0.00	0.00
P3	0.00	0.00	0.00	0.00	0.00	0.00	<b>0.00</b>	0.00	0.33	0.00	0.00	0.00
P4	0.00	0.00	0.00	0.00	0.00	0.00	0.00	<b>0.33</b>	0.00	0.00	0.00	0.00
T1(n)	0.00	0.00	0.00	0.00	0.00	0.00	0.00	0.00	<b>0.33</b>	0.00	0.00	0.00
T2(n)	0.00	0.00	0.00	0.00	0.00	0.00	0.00	0.00	0.00	<b>0.33</b>	0.00	0.00
T3(n)	0.00	0.33	0.00	0.00	0.33	0.00	0.00	0.33	0.00	0.33	<b>0.00</b>	1.00
T4(n)	0.00	0.33	1.00	0.00	0.00	0.00	0.00	0.00	0.33	0.00	0.67	<b>0.00</b>

Table 40. CWD Classification Results with RBFNN (  $SNR = 0\text{dB}$  ).

TEST SNR	COSTAS	FRANK	FSK/PSK	FMCW	P1	P2	P3	P4	T1(n)	T2(n)	T3(n)	T4(n)
COSTAS	<b>1.00</b>	0.00	0.00	0.00	0.00	0.25	0.00	0.00	0.00	0.00	0.00	0.00
FRANK	0.00	<b>0.80</b>	0.00	0.00	0.00	0.00	0.00	0.00	0.00	0.00	0.00	0.00
FSK/PSK	0.00	0.00	<b>0.50</b>	0.00	0.00	0.00	0.00	0.00	0.00	0.00	0.00	0.00
FMCW	0.00	0.00	0.00	<b>1.00</b>	0.00	0.00	0.00	0.00	0.00	0.00	0.00	0.00
P1	0.00	0.00	0.00	0.00	<b>0.40</b>	0.00	0.00	0.00	0.00	0.20	0.00	0.00
P2	0.00	0.00	0.00	0.00	0.00	<b>0.75</b>	0.00	0.00	0.00	0.00	0.00	0.00
P3	0.00	0.00	0.00	0.00	0.00	0.00	<b>0.80</b>	0.00	0.20	0.00	0.00	0.00
P4	0.00	0.20	0.00	0.00	0.40	0.00	0.00	<b>0.60</b>	0.00	0.00	0.00	0.00
T1(n)	0.00	0.00	0.00	0.00	0.00	0.00	0.20	0.00	<b>0.80</b>	0.00	0.00	0.00
T2(n)	0.00	0.00	0.00	0.00	0.00	0.00	0.00	0.00	0.00	<b>0.80</b>	0.00	0.00
T3(n)	0.00	0.00	0.50	0.00	0.00	0.00	0.00	0.00	0.00	0.00	<b>0.60</b>	0.20
T4(n)	0.00	0.00	0.00	0.00	0.20	0.00	0.00	0.40	0.00	0.00	0.40	<b>0.80</b>
TEST MODULATION	COSTAS	FRANK	FSK/PSK	FMCW	P1	P2	P3	P4	T1(n)	T2(n)	T3(n)	T4(n)
COSTAS	<b>1.00</b>	0.00	0.00	0.00	0.00	0.00	0.00	0.00	0.00	0.00	0.00	0.00
FRANK	0.00	<b>0.33</b>	0.00	0.00	0.00	0.00	0.67	0.33	0.00	0.00	0.00	0.00
FSK/PSK	0.00	0.00	<b>1.00</b>	0.00	0.00	0.00	0.00	0.00	0.00	0.00	0.00	0.00
FMCW	0.00	0.00	0.00	<b>1.00</b>	0.00	0.00	0.00	0.00	0.00	0.00	0.00	0.00
P1	0.00	0.00	0.00	0.00	<b>0.00</b>	0.00	0.00	0.00	0.00	0.00	0.00	0.00
P2	0.00	0.00	0.00	0.00	0.00	<b>1.00</b>	0.33	0.00	0.00	0.00	0.00	0.00
P3	0.00	0.00	0.00	0.00	0.00	0.00	<b>0.00</b>	0.00	0.33	0.00	0.00	0.00
P4	0.00	0.00	0.00	0.00	0.33	0.00	0.00	<b>0.33</b>	0.00	0.00	0.00	0.00
T1(n)	0.00	0.00	0.00	0.00	0.00	0.00	0.00	0.00	<b>0.33</b>	0.00	0.00	0.00
T2(n)	0.00	0.00	0.00	0.00	0.00	0.00	0.00	0.00	0.00	<b>0.33</b>	0.00	0.00
T3(n)	0.00	0.33	0.00	0.00	0.33	0.00	0.00	0.33	0.00	0.00	<b>0.00</b>	1.00
T4(n)	0.00	0.33	0.00	0.00	0.33	0.00	0.00	0.00	0.33	0.67	1.00	<b>0.00</b>

Table 41. CWD Classification Results with RBFNN (  $SNR = -3\text{dB}$  ).

TEST SNR	COSTAS	FRANK	FSK/PSK	FMCW	P1	P2	P3	P4	T1(n)	T2(n)	T3(n)	T4(n)
COSTAS	<b>1.00</b>	0.00	0.00	0.00	0.00	0.25	0.00	0.00	0.00	0.00	0.00	0.00
FRANK	0.00	<b>0.80</b>	0.00	0.00	0.00	0.00	0.20	0.00	0.00	0.00	0.00	0.00
FSK/PSK	0.00	0.00	<b>0.50</b>	0.00	0.00	0.00	0.00	0.00	0.00	0.00	0.00	0.00
FMCW	0.00	0.00	0.00	<b>1.00</b>	0.00	0.00	0.00	0.00	0.00	0.00	0.00	0.00
P1	0.00	0.00	0.00	0.00	<b>0.60</b>	0.00	0.00	0.00	0.00	0.20	0.00	0.20
P2	0.00	0.00	0.50	0.00	0.00	<b>0.75</b>	0.00	0.00	0.40	0.00	0.00	0.00
P3	0.00	0.00	0.00	0.00	0.00	0.00	<b>0.80</b>	0.00	0.00	0.00	0.20	0.00
P4	0.00	0.00	0.00	0.00	0.00	0.00	0.00	<b>0.80</b>	0.00	0.20	0.00	0.20
T1(n)	0.00	0.20	0.00	0.00	0.00	0.00	0.00	0.00	<b>0.40</b>	0.00	0.00	0.00
T2(n)	0.00	0.00	0.00	0.00	0.00	0.00	0.00	0.00	0.00	<b>0.60</b>	0.00	0.00
T3(n)	0.00	0.00	0.00	0.00	0.00	0.00	0.00	0.00	0.00	0.00	<b>0.20</b>	0.20
T4(n)	0.00	0.00	0.00	0.00	0.40	0.00	0.00	0.20	0.20	0.00	0.60	<b>0.40</b>
TEST MODULATION	COSTAS	FRANK	FSK/PSK	FMCW	P1	P2	P3	P4	T1(n)	T2(n)	T3(n)	T4(n)
COSTAS	<b>1.00</b>	0.00	0.50	0.00	0.00	0.00	0.00	0.00	0.00	0.00	0.00	0.00
FRANK	0.00	<b>0.33</b>	0.00	0.00	0.33	0.00	1.00	0.00	0.00	0.00	0.00	0.00
FSK/PSK	0.00	0.00	<b>0.00</b>	0.00	0.00	0.00	0.00	0.00	0.00	0.00	0.00	0.00
FMCW	0.00	0.00	0.00	<b>0.50</b>	0.00	0.00	0.00	0.00	0.00	0.00	0.00	0.00
P1	0.00	0.00	0.00	0.00	<b>0.00</b>	0.00	0.00	0.00	0.00	0.00	0.00	0.00
P2	0.00	0.00	0.00	0.00	0.33	<b>0.50</b>	0.00	0.00	0.00	0.00	0.00	0.00
P3	0.00	0.00	0.00	0.00	0.00	0.00	<b>0.00</b>	0.33	0.00	0.33	0.00	0.00
P4	0.00	0.00	0.00	0.00	0.00	0.50	0.00	<b>0.33</b>	0.00	0.00	0.00	0.00
T1(n)	0.00	0.00	0.00	0.00	0.00	0.00	0.00	0.00	<b>0.33</b>	0.00	0.00	0.00
T2(n)	0.00	0.00	0.00	0.00	0.00	0.00	0.00	0.00	0.00	<b>0.33</b>	0.00	0.00
T3(n)	0.00	0.33	0.00	0.00	0.33	0.00	0.00	0.00	0.00	0.33	<b>0.33</b>	0.33
T4(n)	0.00	0.33	0.50	0.50	0.00	0.00	0.00	0.33	0.67	0.00	0.67	<b>0.67</b>

Table 42. CWD Classification Results with RBFNN (  $SNR = -6\text{dB}$  ).

TEST SNR	COSTAS	FRANK	FSK/PSK	FMCW	P1	P2	P3	P4	T1(n)	T2(n)	T3(n)	T4(n)
COSTAS	<b>1.00</b>	0.00	0.00	0.00	0.00	0.25	0.00	0.00	0.00	0.20	0.00	0.00
FRANK	0.00	<b>0.40</b>	0.50	0.00	0.00	0.00	0.20	0.00	0.00	0.20	0.00	0.00
FSK/PSK	0.00	0.00	<b>0.00</b>	0.50	0.00	0.00	0.00	0.00	0.00	0.00	0.00	0.00
FMCW	0.00	0.00	0.00	<b>0.50</b>	0.00	0.00	0.00	0.00	0.00	0.00	0.00	0.00
P1	0.00	0.20	0.00	0.00	<b>0.60</b>	0.00	0.00	0.20	0.00	0.00	0.00	0.00
P2	0.00	0.20	0.50	0.00	0.00	<b>0.75</b>	0.00	0.00	0.40	0.00	0.20	0.00
P3	0.00	0.00	0.00	0.00	0.00	0.00	<b>0.20</b>	0.00	0.00	0.00	0.00	0.00
P4	0.00	0.20	0.00	0.00	0.20	0.00	0.20	<b>0.60</b>	0.00	0.20	0.40	0.20
T1(n)	0.00	0.00	0.00	0.00	0.00	0.00	0.00	0.00	<b>0.40</b>	0.00	0.00	0.00
T2(n)	0.00	0.00	0.00	0.00	0.00	0.00	0.20	0.00	0.00	<b>0.20</b>	0.00	0.00
T3(n)	0.00	0.00	0.00	0.00	0.00	0.00	0.20	0.00	0.00	0.00	<b>0.40</b>	0.00
T4(n)	0.00	0.00	0.00	0.00	0.20	0.00	0.00	0.20	0.00	0.20	0.00	<b>0.80</b>
TEST MODULATION	COSTAS	FRANK	FSK/PSK	FMCW	P1	P2	P3	P4	T1(n)	T2(n)	T3(n)	T4(n)
COSTAS	<b>1.00</b>	0.00	0.00	0.00	0.00	0.00	0.00	0.00	0.00	0.67	0.00	0.00
FRANK	0.00	<b>0.00</b>	0.00	0.00	0.00	0.00	0.00	0.00	0.00	0.00	0.00	0.00
FSK/PSK	0.00	0.00	<b>0.00</b>	0.00	0.00	0.00	0.00	0.00	0.00	0.00	0.00	0.00
FMCW	0.00	0.00	0.00	<b>0.50</b>	0.00	0.00	0.00	0.00	0.00	0.00	0.00	0.00
P1	0.00	0.00	0.00	0.00	<b>0.00</b>	0.00	0.00	0.33	0.00	0.00	0.00	0.00
P2	0.00	0.33	1.00	0.50	0.33	<b>1.00</b>	0.33	0.00	0.00	0.00	0.00	0.00
P3	0.00	0.00	0.00	0.00	0.00	0.00	<b>0.33</b>	0.00	0.33	0.00	0.00	0.00
P4	0.00	0.33	0.00	0.00	0.00	0.00	0.00	<b>0.33</b>	0.00	0.33	0.33	0.00
T1(n)	0.00	0.00	0.00	0.00	0.00	0.00	0.00	0.00	<b>0.33</b>	0.00	0.00	0.00
T2(n)	0.00	0.33	0.00	0.00	0.00	0.00	0.00	0.00	0.33	<b>0.00</b>	0.00	0.00
T3(n)	0.00	0.00	0.00	0.00	0.33	0.00	0.00	0.00	0.00	0.00	<b>0.00</b>	0.33
T4(n)	0.00	0.00	0.00	0.00	0.33	0.00	0.33	0.33	0.00	0.00	0.67	<b>0.67</b>

Table 43. QMFB Classification Results with RBFNN (  $SNR = 10\text{ dB}$  ).

TEST SNR	COSTAS	FRANK	FSK/PSK	FMCW	P1	P2	P3	P4	T1(n)	T2(n)	T3(n)	T4(n)
COSTAS	<b>1.00</b>	0.00	0.00	0.00	0.00	0.00	0.00	0.00	0.00	0.00	0.00	0.00
FRANK	0.00	<b>1.00</b>	0.00	0.00	0.00	0.00	0.00	0.00	0.00	0.00	0.00	0.00
FSK/PSK	0.00	0.00	<b>1.00</b>	0.00	0.00	0.00	0.00	0.00	0.00	0.00	0.00	0.00
FMCW	0.00	0.00	0.00	<b>1.00</b>	0.00	0.00	0.00	0.00	0.00	0.00	0.00	0.00
P1	0.00	0.00	0.00	0.00	<b>1.00</b>	0.00	0.00	0.00	0.00	0.00	0.00	0.00
P2	0.00	0.00	0.00	0.00	0.00	<b>1.00</b>	0.00	0.00	0.00	0.00	0.00	0.00
P3	0.00	0.00	0.00	0.00	0.00	0.00	<b>1.00</b>	0.00	0.00	0.00	0.00	0.00
P4	0.00	0.00	0.00	0.00	0.00	0.00	0.00	<b>1.00</b>	0.00	0.00	0.00	0.00
T1(n)	0.00	0.00	0.00	0.00	0.00	0.00	0.00	0.00	<b>1.00</b>	0.00	0.00	0.00
T2(n)	0.00	0.00	0.00	0.00	0.00	0.00	0.00	0.00	0.00	<b>1.00</b>	0.00	0.00
T3(n)	0.00	0.00	0.00	0.00	0.00	0.00	0.00	0.00	0.00	0.00	<b>1.00</b>	0.00
T4(n)	0.00	0.00	0.00	0.00	0.00	0.00	0.00	0.00	0.00	0.00	0.00	<b>1.00</b>
TEST MODULATION	COSTAS	FRANK	FSK/PSK	FMCW	P1	P2	P3	P4	T1(n)	T2(n)	T3(n)	T4(n)
COSTAS	<b>1.00</b>	0.00	0.00	0.00	0.00	0.00	0.00	0.00	0.00	0.00	0.00	0.00
FRANK	0.00	<b>0.33</b>	0.00	0.00	0.00	0.00	0.33	0.00	0.00	0.00	0.00	0.00
FSK/PSK	0.00	0.00	<b>0.00</b>	0.00	0.00	0.00	0.00	0.00	0.00	0.00	0.00	0.00
FMCW	0.00	0.00	0.00	<b>0.00</b>	0.00	0.00	0.00	0.00	0.00	0.00	0.00	0.00
P1	0.00	0.33	1.00	1.00	<b>0.67</b>	0.50	0.33	0.67	0.33	0.00	0.67	0.33
P2	0.00	0.00	0.00	0.00	0.00	<b>0.50</b>	0.00	0.00	0.00	0.00	0.00	0.00
P3	0.00	0.00	0.00	0.00	0.00	0.00	<b>0.33</b>	0.00	0.00	0.00	0.00	0.00
P4	0.00	0.33	0.00	0.00	0.33	0.00	0.00	<b>0.33</b>	0.00	0.00	0.00	0.00
T1(n)	0.00	0.00	0.00	0.00	0.00	0.00	0.00	0.00	<b>0.33</b>	0.00	0.00	0.00
T2(n)	0.00	0.00	0.00	0.00	0.00	0.00	0.00	0.00	0.00	<b>0.67</b>	0.00	0.00
T3(n)	0.00	0.00	0.00	0.00	0.00	0.00	0.00	0.00	0.00	0.00	<b>0.33</b>	0.67
T4(n)	0.00	0.00	0.00	0.00	0.00	0.00	0.00	0.00	0.33	0.33	0.00	<b>0.00</b>

Table 44. QMFB Classification Results with RBFNN (  $SNR = 6\text{ dB}$  ).

TEST SNR	COSTAS	FRANK	FSK/PSK	FMCW	P1	P2	P3	P4	T1(n)	T2(n)	T3(n)	T4(n)
COSTAS	<b>0.50</b>	0.00	0.00	0.00	0.00	0.00	0.00	0.00	0.00	0.00	0.00	0.00
FRANK	0.00	<b>1.00</b>	0.00	0.00	0.00	0.00	0.00	0.00	0.00	0.00	0.00	0.00
FSK/PSK	0.00	0.00	<b>1.00</b>	0.00	0.00	0.00	0.00	0.00	0.00	0.00	0.00	0.00
FMCW	0.00	0.00	0.00	<b>1.00</b>	0.00	0.00	0.00	0.00	0.00	0.00	0.00	0.00
P1	0.50	0.00	0.00	0.00	<b>0.80</b>	0.00	0.00	0.60	0.00	0.20	0.00	0.00
P2	0.00	0.00	0.00	0.00	0.00	<b>1.00</b>	0.00	0.00	0.00	0.00	0.00	0.00
P3	0.00	0.00	0.00	0.00	0.00	0.00	<b>1.00</b>	0.00	0.00	0.00	0.00	0.00
P4	0.00	0.00	0.00	0.00	0.20	0.00	0.00	<b>0.40</b>	0.00	0.00	0.00	0.00
T1(n)	0.00	0.00	0.00	0.00	0.00	0.00	0.00	0.00	<b>1.00</b>	0.00	0.00	0.00
T2(n)	0.00	0.00	0.00	0.00	0.00	0.00	0.00	0.00	0.00	<b>0.80</b>	0.00	0.00
T3(n)	0.00	0.00	0.00	0.00	0.00	0.00	0.00	0.00	0.00	0.00	<b>1.00</b>	0.00
T4(n)	0.00	0.00	0.00	0.00	0.00	0.00	0.00	0.00	0.00	0.00	0.00	<b>1.00</b>
TEST MODULATION	COSTAS	FRANK	FSK/PSK	FMCW	P1	P2	P3	P4	T1(n)	T2(n)	T3(n)	T4(n)
COSTAS	<b>1.00</b>	0.00	0.00	0.00	0.00	0.00	0.00	0.00	0.00	0.00	0.00	0.00
FRANK	0.00	<b>0.33</b>	0.00	0.00	0.00	0.00	0.33	0.00	0.00	0.00	0.00	0.00
FSK/PSK	0.00	0.00	<b>0.00</b>	0.00	0.00	0.00	0.00	0.00	0.00	0.00	0.00	0.00
FMCW	0.00	0.00	0.00	<b>0.00</b>	0.00	0.00	0.00	0.00	0.00	0.00	0.00	0.00
P1	0.00	0.33	1.00	1.00	<b>0.67</b>	0.50	0.33	0.33	0.33	0.00	0.33	0.33
P2	0.00	0.00	0.00	0.00	0.00	<b>0.50</b>	0.00	0.00	0.00	0.00	0.00	0.00
P3	0.00	0.33	0.00	0.00	0.00	0.00	<b>0.33</b>	0.00	0.00	0.00	0.00	0.00
P4	0.00	0.00	0.00	0.00	0.33	0.00	0.00	<b>0.33</b>	0.00	0.00	0.00	0.00
T1(n)	0.00	0.00	0.00	0.00	0.00	0.00	0.00	0.33	<b>0.33</b>	0.00	0.00	0.00
T2(n)	0.00	0.00	0.00	0.00	0.00	0.00	0.00	0.00	0.00	<b>0.67</b>	0.00	0.00
T3(n)	0.00	0.00	0.00	0.00	0.00	0.00	0.00	0.00	0.00	0.00	<b>0.33</b>	0.67
T4(n)	0.00	0.00	0.00	0.00	0.00	0.00	0.00	0.00	0.33	0.33	0.33	<b>0.00</b>

Table 45. QMFB Classification Results with RBFNN (  $SNR = 3\text{ dB}$  ).

TEST SNR	COSTAS	FRANK	FSK/PSK	FMCW	P1	P2	P3	P4	T1(n)	T2(n)	T3(n)	T4(n)
COSTAS	<b>1.00</b>	0.00	0.00	0.00	0.00	0.00	0.00	0.00	0.00	0.00	0.00	0.00
FRANK	0.00	<b>0.80</b>	0.00	0.00	0.00	0.00	0.00	0.00	0.00	0.00	0.00	0.00
FSK/PSK	0.00	0.00	<b>0.50</b>	0.00	0.00	0.00	0.00	0.00	0.00	0.00	0.00	0.00
FMCW	0.00	0.00	0.00	<b>0.50</b>	0.00	0.00	0.00	0.00	0.00	0.00	0.00	0.00
P1	0.00	0.20	0.50	0.50	<b>1.00</b>	0.00	0.00	0.40	0.00	0.00	0.00	0.20
P2	0.00	0.00	0.00	0.00	0.00	<b>1.00</b>	0.00	0.00	0.00	0.00	0.00	0.00
P3	0.00	0.00	0.00	0.00	0.00	0.00	<b>1.00</b>	0.00	0.00	0.00	0.00	0.00
P4	0.00	0.00	0.00	0.00	0.00	0.00	0.00	<b>0.60</b>	0.00	0.00	0.00	0.00
T1(n)	0.00	0.00	0.00	0.00	0.00	0.00	0.00	0.00	<b>1.00</b>	0.00	0.00	0.00
T2(n)	0.00	0.00	0.00	0.00	0.00	0.00	0.00	0.00	0.00	<b>1.00</b>	0.00	0.00
T3(n)	0.00	0.00	0.00	0.00	0.00	0.00	0.00	0.00	0.00	0.00	<b>1.00</b>	0.00
T4(n)	0.00	0.00	0.00	0.00	0.00	0.00	0.00	0.00	0.00	0.00	0.00	<b>0.80</b>
TEST MODULATION	COSTAS	FRANK	FSK/PSK	FMCW	P1	P2	P3	P4	T1(n)	T2(n)	T3(n)	T4(n)
COSTAS	<b>1.00</b>	0.00	0.00	0.00	0.00	0.00	0.00	0.00	0.00	0.00	0.00	0.00
FRANK	0.00	<b>0.00</b>	0.00	0.00	0.00	0.00	0.33	0.00	0.00	0.00	0.00	0.00
FSK/PSK	0.00	0.00	<b>0.00</b>	0.00	0.00	0.00	0.00	0.00	0.00	0.00	0.00	0.00
FMCW	0.00	0.00	0.00	<b>0.00</b>	0.00	0.00	0.00	0.33	0.00	0.00	0.00	0.00
P1	0.00	0.67	1.00	1.00	<b>0.67</b>	0.50	0.33	0.67	0.33	0.33	0.67	0.33
P2	0.00	0.00	0.00	0.00	0.00	<b>0.50</b>	0.00	0.00	0.00	0.00	0.00	0.00
P3	0.00	0.33	0.00	0.00	0.33	0.00	<b>0.33</b>	0.00	0.00	0.00	0.00	0.00
P4	0.00	0.00	0.00	0.00	0.00	0.00	0.00	<b>0.00</b>	0.00	0.00	0.00	0.00
T1(n)	0.00	0.00	0.00	0.00	0.00	0.00	0.00	0.00	<b>0.33</b>	0.00	0.00	0.00
T2(n)	0.00	0.00	0.00	0.00	0.00	0.00	0.00	0.00	0.00	<b>0.67</b>	0.00	0.00
T3(n)	0.00	0.00	0.00	0.00	0.00	0.00	0.00	0.00	0.00	0.00	<b>0.33</b>	0.67
T4(n)	0.00	0.00	0.00	0.00	0.00	0.00	0.00	0.00	0.33	0.00	0.00	<b>0.00</b>

Table 46. QMFB Classification Results with RBFNN (  $SNR = 0\text{ dB}$  ).

TEST SNR	COSTAS	FRANK	FSK/PSK	FMCW	P1	P2	P3	P4	T1(n)	T2(n)	T3(n)	T4(n)
COSTAS	<b>0.50</b>	0.00	0.00	0.00	0.00	0.00	0.00	0.00	0.00	0.00	0.00	0.00
FRANK	0.00	<b>0.80</b>	0.00	0.00	0.00	0.00	0.00	0.00	0.00	0.00	0.00	0.00
FSK/PSK	0.00	0.00	<b>0.00</b>	0.00	0.00	0.00	0.00	0.00	0.00	0.00	0.00	0.00
FMCW	0.00	0.00	0.00	<b>1.00</b>	0.00	0.00	0.00	0.00	0.00	0.00	0.00	0.00
P1	0.50	0.20	1.00	0.00	<b>1.00</b>	0.50	0.20	1.00	0.40	0.40	0.00	0.20
P2	0.00	0.00	0.00	0.00	0.00	<b>0.50</b>	0.00	0.00	0.00	0.00	0.00	0.00
P3	0.00	0.00	0.00	0.00	0.00	0.00	<b>0.80</b>	0.00	0.00	0.00	0.00	0.00
P4	0.00	0.00	0.00	0.00	0.00	0.00	0.00	<b>0.00</b>	0.00	0.00	0.00	0.00
T1(n)	0.00	0.00	0.00	0.00	0.00	0.00	0.00	0.00	<b>0.60</b>	0.20	0.00	0.00
T2(n)	0.00	0.00	0.00	0.00	0.00	0.00	0.00	0.00	0.00	<b>0.40</b>	0.00	0.00
T3(n)	0.00	0.00	0.00	0.00	0.00	0.00	0.00	0.00	0.00	0.00	<b>0.80</b>	0.00
T4(n)	0.00	0.00	0.00	0.00	0.00	0.00	0.00	0.00	0.00	0.00	0.20	<b>0.80</b>
TEST MODULATION	COSTAS	FRANK	FSK/PSK	FMCW	P1	P2	P3	P4	T1(n)	T2(n)	T3(n)	T4(n)
COSTAS	<b>1.00</b>	0.00	0.00	0.00	0.00	0.00	0.00	0.00	0.00	0.00	0.00	0.00
FRANK	0.00	<b>0.00</b>	0.00	0.00	0.00	0.00	0.00	0.00	0.00	0.00	0.00	0.00
FSK/PSK	0.00	0.00	<b>0.00</b>	0.00	0.00	0.00	0.00	0.00	0.00	0.00	0.00	0.00
FMCW	0.00	0.00	0.00	<b>0.00</b>	0.00	0.00	0.00	0.00	0.00	0.00	0.00	0.00
P1	0.00	0.67	1.00	1.00	<b>0.67</b>	1.00	0.67	0.67	0.33	0.00	0.67	0.67
P2	0.00	0.00	0.00	0.00	0.00	<b>0.00</b>	0.00	0.00	0.00	0.00	0.00	0.00
P3	0.00	0.33	0.00	0.00	0.33	0.00	<b>0.33</b>	0.00	0.00	0.00	0.00	0.00
P4	0.00	0.00	0.00	0.00	0.00	0.00	0.00	<b>0.33</b>	0.00	0.00	0.00	0.00
T1(n)	0.00	0.00	0.00	0.00	0.00	0.00	0.00	0.00	<b>0.33</b>	0.00	0.00	0.00
T2(n)	0.00	0.00	0.00	0.00	0.00	0.00	0.00	0.00	0.00	<b>0.67</b>	0.00	0.00
T3(n)	0.00	0.00	0.00	0.00	0.00	0.00	0.00	0.00	0.00	0.33	<b>0.33</b>	0.33
T4(n)	0.00	0.00	0.00	0.00	0.00	0.00	0.00	0.00	0.33	0.00	0.00	<b>0.00</b>

Table 47. QMFB Classification Results with RBFNN (  $SNR = -3\text{dB}$  ).

TEST SNR	COSTAS	FRANK	FSK/PSK	FMCW	P1	P2	P3	P4	T1(n)	T2(n)	T3(n)	T4(n)
COSTAS	<b>0.00</b>	0.00	0.00	0.00	0.00	0.00	0.00	0.00	0.00	0.00	0.00	0.00
FRANK	0.00	<b>0.40</b>	0.00	0.00	0.00	0.00	0.00	0.00	0.00	0.00	0.00	0.00
FSK/PSK	0.00	0.00	<b>0.00</b>	0.00	0.00	0.00	0.00	0.00	0.00	0.00	0.00	0.00
FMCW	0.00	0.00	0.00	<b>0.50</b>	0.00	0.00	0.00	0.00	0.00	0.00	0.00	0.00
P1	1.00	0.40	1.00	0.50	<b>1.00</b>	0.25	0.20	1.00	0.40	0.60	0.40	0.80
P2	0.00	0.00	0.00	0.00	0.00	<b>0.75</b>	0.00	0.00	0.00	0.00	0.00	0.00
P3	0.00	0.20	0.00	0.00	0.00	0.00	<b>0.80</b>	0.00	0.00	0.00	0.00	0.00
P4	0.00	0.00	0.00	0.00	0.00	0.00	0.00	<b>0.00</b>	0.00	0.00	0.00	0.00
T1(n)	0.00	0.00	0.00	0.00	0.00	0.00	0.00	0.00	<b>0.60</b>	0.00	0.00	0.00
T2(n)	0.00	0.00	0.00	0.00	0.00	0.00	0.00	0.00	0.00	<b>0.40</b>	0.00	0.00
T3(n)	0.00	0.00	0.00	0.00	0.00	0.00	0.00	0.00	0.00	0.00	<b>0.40</b>	0.00
T4(n)	0.00	0.00	0.00	0.00	0.00	0.00	0.00	0.00	0.00	0.00	0.20	<b>0.20</b>
TEST MODULATION	COSTAS	FRANK	FSK/PSK	FMCW	P1	P2	P3	P4	T1(n)	T2(n)	T3(n)	T4(n)
COSTAS	<b>1.00</b>	0.00	0.00	0.00	0.00	0.00	0.00	0.00	0.00	0.00	0.00	0.00
FRANK	0.00	<b>0.00</b>	0.00	0.00	0.00	0.00	0.00	0.00	0.00	0.00	0.00	0.00
FSK/PSK	0.00	0.00	<b>0.00</b>	0.00	0.00	0.00	0.00	0.00	0.00	0.00	0.00	0.00
FMCW	0.00	0.00	0.00	<b>0.00</b>	0.33	0.00	0.00	0.00	0.00	0.00	0.00	0.00
P1	0.00	0.67	1.00	1.00	<b>0.67</b>	1.00	0.67	1.00	0.67	0.67	0.33	0.33
P2	0.00	0.00	0.00	0.00	0.00	<b>0.00</b>	0.00	0.00	0.00	0.00	0.00	0.00
P3	0.00	0.33	0.00	0.00	0.00	0.00	<b>0.33</b>	0.00	0.00	0.00	0.00	0.00
P4	0.00	0.00	0.00	0.00	0.00	0.00	0.00	<b>0.00</b>	0.00	0.00	0.00	0.00
T1(n)	0.00	0.00	0.00	0.00	0.00	0.00	0.00	0.00	<b>0.33</b>	0.00	0.00	0.00
T2(n)	0.00	0.00	0.00	0.00	0.00	0.00	0.00	0.00	0.00	<b>0.33</b>	0.33	0.00
T3(n)	0.00	0.00	0.00	0.00	0.00	0.00	0.00	0.00	0.00	0.00	<b>0.00</b>	0.67
T4(n)	0.00	0.00	0.00	0.00	0.00	0.00	0.00	0.00	0.00	0.00	0.33	<b>0.00</b>

Table 48. QMFB Classification Results with RBFNN (  $SNR = -6\text{dB}$  ).

TEST SNR	COSTAS	FRANK	FSK/PSK	FMCW	P1	P2	P3	P4	T1(n)	T2(n)	T3(n)	T4(n)
COSTAS	<b>0.00</b>	0.00	0.00	0.00	0.00	0.00	0.00	0.00	0.00	0.00	0.00	0.00
FRANK	0.00	<b>0.20</b>	0.00	0.00	0.00	0.00	0.00	0.00	0.00	0.00	0.00	0.00
FSK/PSK	0.00	0.00	<b>0.00</b>	0.00	0.00	0.00	0.00	0.00	0.00	0.00	0.00	0.00
FMCW	0.00	0.00	0.00	<b>1.00</b>	0.00	0.00	0.00	0.00	0.00	0.00	0.00	0.00
P1	1.00	0.80	1.00	0.00	<b>1.00</b>	1.00	1.00	0.80	1.00	0.60	1.00	1.00
P2	0.00	0.00	0.00	0.00	0.00	<b>0.00</b>	0.00	0.00	0.00	0.00	0.00	0.00
P3	0.00	0.00	0.00	0.00	0.00	0.00	<b>0.00</b>	0.00	0.00	0.00	0.00	0.00
P4	0.00	0.00	0.00	0.00	0.00	0.00	0.00	<b>0.00</b>	0.00	0.00	0.00	0.00
T1(n)	0.00	0.00	0.00	0.00	0.00	0.00	0.00	0.00	<b>0.00</b>	0.00	0.00	0.00
T2(n)	0.00	0.00	0.00	0.00	0.00	0.00	0.00	0.00	0.00	<b>0.20</b>	0.00	0.00
T3(n)	0.00	0.00	0.00	0.00	0.00	0.00	0.00	0.20	0.00	0.00	<b>0.00</b>	0.00
T4(n)	0.00	0.00	0.00	0.00	0.00	0.00	0.00	0.00	0.00	0.20	0.00	<b>0.00</b>
TEST MODULATION	COSTAS	FRANK	FSK/PSK	FMCW	P1	P2	P3	P4	T1(n)	T2(n)	T3(n)	T4(n)
COSTAS	<b>1.00</b>	0.00	0.00	0.00	0.00	0.00	0.00	0.00	0.00	0.00	0.00	0.00
FRANK	0.00	<b>0.00</b>	0.00	0.00	0.00	0.00	0.00	0.00	0.00	0.00	0.00	0.00
FSK/PSK	0.00	0.00	<b>0.00</b>	0.00	0.00	0.00	0.00	0.00	0.00	0.00	0.00	0.00
FMCW	0.00	0.00	0.00	<b>0.00</b>	0.00	0.00	0.00	0.00	0.00	0.00	0.00	0.00
P1	0.00	0.67	1.00	1.00	<b>1.00</b>	0.50	1.00	0.67	0.67	1.00	1.00	0.67
P2	0.00	0.00	0.00	0.00	0.00	<b>0.00</b>	0.00	0.00	0.00	0.00	0.00	0.00
P3	0.00	0.00	0.00	0.00	0.00	0.00	<b>0.00</b>	0.33	0.00	0.00	0.00	0.33
P4	0.00	0.00	0.00	0.00	0.00	0.00	0.00	<b>0.00</b>	0.00	0.00	0.00	0.00
T1(n)	0.00	0.00	0.00	0.00	0.00	0.00	0.00	0.00	<b>0.00</b>	0.00	0.00	0.00
T2(n)	0.00	0.00	0.00	0.00	0.00	0.00	0.00	0.00	0.33	<b>0.00</b>	0.00	0.00
T3(n)	0.00	0.00	0.00	0.00	0.00	0.50	0.00	0.00	0.00	0.00	<b>0.00</b>	0.00
T4(n)	0.00	0.33	0.00	0.00	0.00	0.00	0.00	0.00	0.00	0.00	0.00	<b>0.00</b>

### C. PNN CLASSIFICATION CONFUSION MATRICES

Table 49. PWVD Classification Results with PNN (  $SNR = 10\text{dB}$  ).

TEST SNR	COSTAS	FRANK	FSK/PSK	FMCW	P1	P2	P3	P4	T1(n)	T2(n)	T3(n)	T4(n)
COSTAS	<b>1.00</b>	0.00	0.00	0.00	0.00	0.00	0.00	0.00	0.00	0.00	0.00	0.00
FRANK	0.00	<b>1.00</b>	0.00	0.00	0.00	0.00	0.00	0.00	0.00	0.00	0.00	0.00
FSK/PSK	0.00	0.00	<b>1.00</b>	0.00	0.00	0.00	0.00	0.00	0.00	0.00	0.00	0.00
FMCW	0.00	0.00	0.00	<b>1.00</b>	0.00	0.00	0.00	0.00	0.00	0.00	0.00	0.00
P1	0.00	0.00	0.00	0.00	<b>1.00</b>	0.00	0.00	0.00	0.00	0.00	0.00	0.00
P2	0.00	0.00	0.00	0.00	0.00	<b>1.00</b>	0.00	0.00	0.00	0.00	0.00	0.00
P3	0.00	0.00	0.00	0.00	0.00	0.00	<b>1.00</b>	0.00	0.00	0.00	0.00	0.00
P4	0.00	0.00	0.00	0.00	0.00	0.00	0.00	<b>1.00</b>	0.00	0.00	0.00	0.00
T1(n)	0.00	0.00	0.00	0.00	0.00	0.00	0.00	0.00	<b>1.00</b>	0.00	0.00	0.00
T2(n)	0.00	0.00	0.00	0.00	0.00	0.00	0.00	0.00	0.00	<b>1.00</b>	0.00	0.00
T3(n)	0.00	0.00	0.00	0.00	0.00	0.00	0.00	0.00	0.00	0.00	<b>1.00</b>	0.00
T4(n)	0.00	0.00	0.00	0.00	0.00	0.00	0.00	0.00	0.00	0.00	0.00	<b>1.00</b>
TEST MODULATION	COSTAS	FRANK	FSK/PSK	FMCW	P1	P2	P3	P4	T1(n)	T2(n)	T3(n)	T4(n)
COSTAS	<b>1.00</b>	0.00	0.00	0.00	0.00	0.00	0.00	0.00	0.00	0.00	0.00	0.00
FRANK	0.00	<b>0.33</b>	0.00	0.00	0.33	0.00	0.67	0.33	0.00	0.00	0.00	0.00
FSK/PSK	0.00	0.00	<b>1.00</b>	0.00	0.00	0.00	0.00	0.00	0.00	0.00	0.33	0.00
FMCW	0.00	0.00	0.00	<b>1.00</b>	0.00	0.00	0.00	0.00	0.00	0.00	0.00	0.00
P1	0.00	0.00	0.00	0.00	<b>0.33</b>	0.00	0.00	0.00	0.00	0.00	0.00	0.00
P2	0.00	0.00	0.00	0.00	0.00	<b>1.00</b>	0.00	0.00	0.00	0.00	0.00	0.00
P3	0.00	0.00	0.00	0.00	0.33	0.00	<b>0.33</b>	0.33	0.33	0.00	0.00	0.00
P4	0.00	0.00	0.00	0.00	0.00	0.00	0.00	<b>0.33</b>	0.00	0.00	0.00	0.00
T1(n)	0.00	0.33	0.00	0.00	0.00	0.00	0.00	0.00	<b>0.33</b>	0.00	0.00	0.00
T2(n)	0.00	0.00	0.00	0.00	0.00	0.00	0.00	0.00	0.00	<b>0.67</b>	0.00	0.00
T3(n)	0.00	0.33	0.00	0.00	0.00	0.00	0.00	0.00	0.00	0.33	<b>0.67</b>	0.00
T4(n)	0.00	0.00	0.00	0.00	0.00	0.00	0.00	0.00	0.33	0.00	0.00	<b>1.00</b>

Table 50. PWVD Classification Results with PNN (  $SNR = 6\text{dB}$  ).

TEST SNR	COSTAS	FRANK	FSK/PSK	FMCW	P1	P2	P3	P4	T1(n)	T2(n)	T3(n)	T4(n)
COSTAS	<b>0.50</b>	0.00	0.00	0.00	0.00	0.00	0.00	0.00	0.00	0.00	0.00	0.00
FRANK	0.00	<b>1.00</b>	0.00	0.00	0.00	0.00	0.00	0.00	0.00	0.00	0.00	0.00
FSK/PSK	0.00	0.00	<b>1.00</b>	0.00	0.00	0.00	0.00	0.00	0.00	0.00	0.00	0.00
FMCW	0.00	0.00	0.00	<b>1.00</b>	0.00	0.00	0.00	0.00	0.00	0.00	0.00	0.00
P1	0.50	0.00	0.00	0.00	<b>0.60</b>	0.00	0.00	0.40	0.00	0.00	0.00	0.00
P2	0.00	0.00	0.00	0.00	0.00	<b>1.00</b>	0.00	0.00	0.00	0.00	0.00	0.00
P3	0.00	0.00	0.00	0.00	0.00	0.00	<b>1.00</b>	0.00	0.00	0.00	0.00	0.00
P4	0.00	0.00	0.00	0.00	0.40	0.00	0.00	<b>0.60</b>	0.00	0.00	0.00	0.00
T1(n)	0.00	0.00	0.00	0.00	0.00	0.00	0.00	0.00	<b>1.00</b>	0.00	0.00	0.00
T2(n)	0.00	0.00	0.00	0.00	0.00	0.00	0.00	0.00	0.00	<b>1.00</b>	0.00	0.00
T3(n)	0.00	0.00	0.00	0.00	0.00	0.00	0.00	0.00	0.00	0.00	<b>1.00</b>	0.00
T4(n)	0.00	0.00	0.00	0.00	0.00	0.00	0.00	0.00	0.00	0.00	0.00	<b>1.00</b>
TEST MODULATION	COSTAS	FRANK	FSK/PSK	FMCW	P1	P2	P3	P4	T1(n)	T2(n)	T3(n)	T4(n)
COSTAS	<b>1.00</b>	0.00	0.00	0.00	0.00	0.00	0.00	0.00	0.00	0.00	0.00	0.00
FRANK	0.00	<b>0.33</b>	0.00	0.00	0.00	0.00	0.33	0.33	0.00	0.00	0.00	0.00
FSK/PSK	0.00	0.00	<b>1.00</b>	0.00	0.00	0.00	0.00	0.00	0.00	0.00	0.33	0.00
FMCW	0.00	0.00	0.00	<b>1.00</b>	0.00	0.00	0.00	0.00	0.00	0.00	0.00	0.00
P1	0.00	0.00	0.00	0.00	<b>0.33</b>	0.00	0.00	0.00	0.00	0.00	0.00	0.00
P2	0.00	0.00	0.00	0.00	0.00	<b>1.00</b>	0.00	0.00	0.00	0.00	0.00	0.00
P3	0.00	0.00	0.00	0.00	0.33	0.00	<b>0.67</b>	0.33	0.33	0.00	0.00	0.00
P4	0.00	0.00	0.00	0.00	0.00	0.00	0.00	<b>0.33</b>	0.00	0.00	0.00	0.00
T1(n)	0.00	0.00	0.00	0.00	0.00	0.00	0.00	0.00	<b>0.33</b>	0.00	0.00	0.00
T2(n)	0.00	0.00	0.00	0.00	0.33	0.00	0.00	0.00	0.00	<b>0.67</b>	0.00	0.00
T3(n)	0.00	0.67	0.00	0.00	0.00	0.00	0.00	0.00	0.00	0.00	<b>0.33</b>	0.67
T4(n)	0.00	0.00	0.00	0.00	0.00	0.00	0.00	0.00	0.33	0.33	0.33	<b>0.33</b>

Table 51. PWVD Classification Results with PNN (  $SNR = 3\text{dB}$  ).

TEST SNR	COSTAS	FRANK	FSK/PSK	FMCW	P1	P2	P3	P4	T1(n)	T2(n)	T3(n)	T4(n)
COSTAS	<b>1.00</b>	0.00	0.00	0.00	0.00	0.00	0.00	0.00	0.00	0.00	0.00	0.00
FRANK	0.00	<b>1.00</b>	0.00	0.00	0.00	0.00	0.00	0.00	0.00	0.00	0.00	0.00
FSK/PSK	0.00	0.00	<b>1.00</b>	0.00	0.00	0.25	0.00	0.00	0.00	0.00	0.00	0.00
FMCW	0.00	0.00	0.00	<b>1.00</b>	0.00	0.00	0.00	0.00	0.00	0.00	0.00	0.00
P1	0.00	0.00	0.00	0.00	<b>0.80</b>	0.00	0.00	0.00	0.00	0.00	0.00	0.00
P2	0.00	0.00	0.00	0.00	0.00	<b>0.50</b>	0.00	0.00	0.00	0.00	0.00	0.00
P3	0.00	0.00	0.00	0.00	0.00	0.00	<b>1.00</b>	0.00	0.00	0.00	0.00	0.00
P4	0.00	0.00	0.00	0.00	0.20	0.00	0.00	<b>1.00</b>	0.00	0.00	0.00	0.20
T1(n)	0.00	0.00	0.00	0.00	0.00	0.00	0.00	0.00	<b>1.00</b>	0.00	0.00	0.00
T2(n)	0.00	0.00	0.00	0.00	0.00	0.00	0.00	0.00	0.00	<b>1.00</b>	0.00	0.00
T3(n)	0.00	0.00	0.00	0.00	0.00	0.25	0.00	0.00	0.00	0.00	<b>1.00</b>	0.00
T4(n)	0.00	0.00	0.00	0.00	0.00	0.00	0.00	0.00	0.00	0.00	0.00	<b>0.80</b>
TEST MODULATION	COSTAS	FRANK	FSK/PSK	FMCW	P1	P2	P3	P4	T1(n)	T2(n)	T3(n)	T4(n)
COSTAS	<b>1.00</b>	0.00	0.00	0.00	0.00	0.00	0.00	0.00	0.00	0.00	0.33	0.00
FRANK	0.00	<b>0.33</b>	0.00	0.00	0.33	0.00	0.33	0.33	0.00	0.00	0.00	0.00
FSK/PSK	0.00	0.00	<b>1.00</b>	0.00	0.00	0.00	0.00	0.00	0.00	0.00	0.33	0.00
FMCW	0.00	0.00	0.00	<b>1.00</b>	0.00	0.00	0.00	0.00	0.00	0.00	0.00	0.00
P1	0.00	0.00	0.00	0.00	<b>0.33</b>	0.00	0.00	0.00	0.00	0.00	0.00	0.00
P2	0.00	0.00	0.00	0.00	0.00	<b>1.00</b>	0.00	0.00	0.00	0.00	0.00	0.00
P3	0.00	0.00	0.00	0.00	0.33	0.00	<b>0.67</b>	0.33	0.33	0.00	0.00	0.00
P4	0.00	0.00	0.00	0.00	0.00	0.00	0.00	<b>0.33</b>	0.00	0.00	0.00	0.00
T1(n)	0.00	0.33	0.00	0.00	0.00	0.00	0.00	0.00	<b>0.33</b>	0.00	0.00	0.00
T2(n)	0.00	0.00	0.00	0.00	0.00	0.00	0.00	0.00	0.00	<b>0.67</b>	0.00	0.00
T3(n)	0.00	0.33	0.00	0.00	0.00	0.00	0.00	0.00	0.00	0.00	<b>0.00</b>	0.33
T4(n)	0.00	0.00	0.00	0.00	0.00	0.00	0.00	0.00	0.33	0.33	0.33	<b>0.67</b>

Table 52. PWVD Classification Results with PNN (  $SNR = 0\text{dB}$  ).

TEST SNR	COSTAS	FRANK	FSK/PSK	FMCW	P1	P2	P3	P4	T1(n)	T2(n)	T3(n)	T4(n)
COSTAS	<b>0.50</b>	0.00	0.00	0.00	0.00	0.00	0.00	0.00	0.00	0.00	0.00	0.00
FRANK	0.00	<b>1.00</b>	0.00	0.00	0.00	0.00	0.00	0.00	0.00	0.00	0.00	0.00
FSK/PSK	0.00	0.00	<b>1.00</b>	0.00	0.00	0.25	0.00	0.00	0.00	0.00	0.00	0.00
FMCW	0.00	0.00	0.00	<b>1.00</b>	0.00	0.00	0.00	0.00	0.00	0.00	0.00	0.00
P1	0.50	0.00	0.00	0.00	<b>0.80</b>	0.00	0.00	0.20	0.00	0.00	0.00	0.00
P2	0.00	0.00	0.00	0.00	0.00	<b>0.50</b>	0.00	0.00	0.00	0.00	0.00	0.00
P3	0.00	0.00	0.00	0.00	0.00	0.00	<b>1.00</b>	0.00	0.00	0.00	0.00	0.00
P4	0.00	0.00	0.00	0.00	0.20	0.00	0.00	<b>0.60</b>	0.00	0.00	0.00	0.00
T1(n)	0.00	0.00	0.00	0.00	0.00	0.00	0.00	0.00	<b>1.00</b>	0.00	0.00	0.00
T2(n)	0.00	0.00	0.00	0.00	0.00	0.00	0.00	0.00	0.00	<b>1.00</b>	0.00	0.00
T3(n)	0.00	0.00	0.00	0.00	0.00	0.25	0.00	0.00	0.00	0.00	<b>0.60</b>	0.00
T4(n)	0.00	0.00	0.00	0.00	0.00	0.00	0.00	0.20	0.00	0.00	0.40	<b>1.00</b>
TEST MODULATION	COSTAS	FRANK	FSK/PSK	FMCW	P1	P2	P3	P4	T1(n)	T2(n)	T3(n)	T4(n)
COSTAS	<b>1.00</b>	0.00	0.00	0.00	0.00	0.00	0.00	0.00	0.00	0.00	0.00	0.00
FRANK	0.00	<b>0.33</b>	0.00	0.00	0.00	0.00	0.33	0.33	0.00	0.00	0.00	0.00
FSK/PSK	0.00	0.00	<b>1.00</b>	0.00	0.00	0.00	0.00	0.00	0.00	0.00	0.00	0.00
FMCW	0.00	0.00	0.00	<b>1.00</b>	0.00	0.00	0.00	0.00	0.00	0.00	0.00	0.00
P1	0.00	0.00	0.00	0.00	<b>0.33</b>	0.00	0.00	0.00	0.00	0.00	0.00	0.00
P2	0.00	0.00	0.00	0.00	0.00	<b>1.00</b>	0.00	0.00	0.00	0.00	0.00	0.00
P3	0.00	0.00	0.00	0.00	0.33	0.00	<b>0.67</b>	0.33	0.00	0.00	0.00	0.00
P4	0.00	0.00	0.00	0.00	0.00	0.00	0.00	<b>0.33</b>	0.00	0.00	0.00	0.00
T1(n)	0.00	0.33	0.00	0.00	0.00	0.00	0.00	0.00	<b>0.67</b>	0.00	0.00	0.00
T2(n)	0.00	0.00	0.00	0.00	0.00	0.00	0.00	0.00	0.00	<b>0.67</b>	0.33	0.00
T3(n)	0.00	0.33	0.00	0.00	0.33	0.00	0.00	0.00	0.00	0.00	<b>0.67</b>	0.00
T4(n)	0.00	0.00	0.00	0.00	0.00	0.00	0.00	0.00	0.33	0.33	0.00	<b>1.00</b>



Table 53. PWVD Classification Results with PNN (  $SNR = -3\text{dB}$  ).

TEST SNR	COSTAS	FRANK	FSK/PSK	FMCW	P1	P2	P3	P4	T1(n)	T2(n)	T3(n)	T4(n)
COSTAS	<b>0.00</b>	0.20	0.00	0.00	0.00	0.25	0.00	0.00	0.00	0.00	0.00	0.00
FRANK	0.00	<b>0.80</b>	0.00	0.00	0.00	0.00	0.00	0.00	0.00	0.00	0.00	0.00
FSK/PSK	0.00	0.00	<b>1.00</b>	0.00	0.00	0.00	0.20	0.00	0.00	0.00	0.00	0.00
FMCW	0.00	0.00	0.00	<b>1.00</b>	0.00	0.00	0.00	0.00	0.00	0.00	0.00	0.00
P1	0.50	0.00	0.00	0.00	<b>0.60</b>	0.00	0.00	0.00	0.00	0.00	0.00	0.20
P2	0.00	0.00	0.00	0.00	0.00	<b>0.75</b>	0.00	0.00	0.20	0.00	0.00	0.00
P3	0.00	0.00	0.00	0.00	0.00	0.00	<b>0.80</b>	0.00	0.00	0.00	0.25	0.00
P4	0.00	0.00	0.00	0.00	0.20	0.00	0.00	<b>0.80</b>	0.00	0.00	0.00	0.00
T1(n)	0.00	0.00	0.00	0.00	0.00	0.00	0.00	0.00	<b>0.40</b>	0.00	0.00	0.00
T2(n)	0.00	0.00	0.00	0.00	0.00	0.00	0.00	0.00	0.00	<b>1.00</b>	0.00	0.00
T3(n)	0.00	0.00	0.00	0.00	0.20	0.00	0.00	0.00	0.20	0.00	<b>0.50</b>	0.00
T4(n)	0.50	0.00	0.00	0.00	0.00	0.00	0.00	0.20	0.20	0.00	0.25	<b>0.80</b>
TEST MODULATION	COSTAS	FRANK	FSK/PSK	FMCW	P1	P2	P3	P4	T1(n)	T2(n)	T3(n)	T4(n)
COSTAS	<b>1.00</b>	0.00	0.00	0.00	0.00	0.00	0.00	0.00	0.00	0.00	0.00	0.00
FRANK	0.00	<b>0.33</b>	0.00	0.00	0.33	0.00	0.67	0.00	0.00	0.00	0.00	0.00
FSK/PSK	0.00	0.00	<b>1.00</b>	0.00	0.00	0.00	0.00	0.00	0.00	0.00	0.00	0.00
FMCW	0.00	0.00	0.00	<b>1.00</b>	0.00	0.00	0.00	0.00	0.00	0.00	0.00	0.00
P1	0.00	0.00	0.00	0.00	<b>0.33</b>	0.00	0.00	0.00	0.00	0.00	0.00	0.00
P2	0.00	0.00	0.00	0.00	0.00	<b>1.00</b>	0.00	0.00	0.00	0.00	0.00	0.00
P3	0.00	0.33	0.00	0.00	0.33	0.00	<b>0.00</b>	0.33	0.33	0.00	0.00	0.00
P4	0.00	0.00	0.00	0.00	0.00	0.00	0.00	<b>0.33</b>	0.00	0.00	0.00	0.00
T1(n)	0.00	0.00	0.00	0.00	0.00	0.00	0.33	0.00	<b>0.33</b>	0.00	0.33	0.00
T2(n)	0.00	0.00	0.00	0.00	0.00	0.00	0.00	0.33	0.00	<b>0.67</b>	0.00	0.00
T3(n)	0.00	0.33	0.00	0.00	0.00	0.00	0.00	0.33	0.33	0.33	<b>0.00</b>	0.33
T4(n)	0.00	0.00	0.00	0.00	0.00	0.00	0.00	0.00	0.00	0.00	0.67	<b>0.67</b>

Table 54. PWVD Classification Results with PNN (  $SNR = -6\text{dB}$  ).

TEST SNR	COSTAS	FRANK	FSK/PSK	FMCW	P1	P2	P3	P4	T1(n)	T2(n)	T3(n)	T4(n)
COSTAS	<b>0.50</b>	0.00	0.00	0.00	0.00	0.25	0.20	0.00	0.00	0.00	0.00	0.00
FRANK	0.00	<b>0.80</b>	0.00	0.00	0.00	0.00	0.00	0.00	0.00	0.00	0.00	0.00
FSK/PSK	0.00	0.00	<b>1.00</b>	0.00	0.00	0.25	0.00	0.00	0.00	0.00	0.00	0.20
FMCW	0.00	0.00	0.00	<b>1.00</b>	0.00	0.00	0.00	0.00	0.00	0.00	0.00	0.00
P1	0.00	0.00	0.00	0.00	<b>0.80</b>	0.00	0.00	0.20	0.00	0.00	0.00	0.20
P2	0.00	0.00	0.00	0.00	0.00	<b>0.25</b>	0.00	0.00	0.00	0.00	0.20	0.00
P3	0.00	0.20	0.00	0.00	0.00	0.00	<b>0.40</b>	0.00	0.00	0.20	0.20	0.00
P4	0.00	0.00	0.00	0.00	0.20	0.00	0.00	<b>0.80</b>	0.00	0.00	0.20	0.00
T1(n)	0.00	0.00	0.00	0.00	0.00	0.00	0.20	0.00	<b>0.60</b>	0.20	0.00	0.00
T2(n)	0.00	0.00	0.00	0.00	0.00	0.00	0.00	0.00	0.00	<b>0.40</b>	0.00	0.00
T3(n)	0.00	0.00	0.00	0.00	0.00	0.25	0.20	0.00	0.40	0.00	<b>0.20</b>	0.20
T4(n)	0.50	0.00	0.00	0.00	0.00	0.00	0.00	0.00	0.00	0.20	0.20	<b>0.40</b>
TEST MODULATION	COSTAS	FRANK	FSK/PSK	FMCW	P1	P2	P3	P4	T1(n)	T2(n)	T3(n)	T4(n)
COSTAS	<b>1.00</b>	0.00	0.00	0.00	0.00	0.00	0.00	0.33	0.00	0.00	0.00	0.00
FRANK	0.00	<b>0.33</b>	0.00	0.00	0.00	0.00	0.67	0.33	0.00	0.00	0.00	0.00
FSK/PSK	0.00	0.00	<b>1.00</b>	0.00	0.00	0.00	0.00	0.00	0.00	0.00	0.00	0.00
FMCW	0.00	0.00	0.00	<b>1.00</b>	0.00	0.00	0.00	0.00	0.00	0.00	0.33	0.00
P1	0.00	0.00	0.00	0.00	<b>0.33</b>	0.00	0.00	0.00	0.00	0.00	0.00	0.00
P2	0.00	0.00	0.00	0.00	0.00	<b>1.00</b>	0.00	0.00	0.00	0.00	0.00	0.00
P3	0.00	0.67	0.00	0.00	0.33	0.00	<b>0.33</b>	0.00	1.00	0.00	0.00	0.00
P4	0.00	0.00	0.00	0.00	0.00	0.00	0.00	<b>0.33</b>	0.00	0.00	0.00	0.33
T1(n)	0.00	0.00	0.00	0.00	0.00	0.00	0.00	0.00	<b>0.00</b>	0.00	0.00	0.00
T2(n)	0.00	0.00	0.00	0.00	0.00	0.00	0.00	0.00	0.00	<b>0.67</b>	0.00	0.00
T3(n)	0.00	0.00	0.00	0.00	0.33	0.00	0.00	0.00	0.00	0.00	<b>0.33</b>	0.00
T4(n)	0.00	0.00	0.00	0.00	0.00	0.00	0.00	0.00	0.00	0.33	0.33	<b>0.67</b>

Table 55. CWD Classification Results with PNN (  $SNR = 10\text{dB}$  ).

TEST SNR	COSTAS	FRANK	FSK/PSK	FMCW	P1	P2	P3	P4	T1(n)	T2(n)	T3(n)	T4(n)
COSTAS	<b>1.00</b>	0.00	0.00	0.00	0.00	0.00	0.00	0.00	0.00	0.00	0.00	0.00
FRANK	0.00	<b>1.00</b>	0.00	0.00	0.00	0.00	0.00	0.00	0.00	0.00	0.00	0.00
FSK/PSK	0.00	0.00	<b>1.00</b>	0.00	0.00	0.00	0.00	0.00	0.00	0.00	0.00	0.00
FMCW	0.00	0.00	0.00	<b>1.00</b>	0.00	0.00	0.00	0.00	0.00	0.00	0.00	0.00
P1	0.00	0.00	0.00	0.00	<b>1.00</b>	0.00	0.00	0.00	0.00	0.00	0.00	0.00
P2	0.00	0.00	0.00	0.00	0.00	<b>1.00</b>	0.00	0.00	0.00	0.00	0.00	0.00
P3	0.00	0.00	0.00	0.00	0.00	0.00	<b>1.00</b>	0.00	0.00	0.00	0.00	0.00
P4	0.00	0.00	0.00	0.00	0.00	0.00	0.00	<b>1.00</b>	0.00	0.00	0.00	0.00
T1(n)	0.00	0.00	0.00	0.00	0.00	0.00	0.00	0.00	<b>1.00</b>	0.00	0.00	0.00
T2(n)	0.00	0.00	0.00	0.00	0.00	0.00	0.00	0.00	0.00	<b>1.00</b>	0.00	0.00
T3(n)	0.00	0.00	0.00	0.00	0.00	0.00	0.00	0.00	0.00	0.00	<b>1.00</b>	0.00
T4(n)	0.00	0.00	0.00	0.00	0.00	0.00	0.00	0.00	0.00	0.00	0.00	<b>1.00</b>
TEST MODULATION	COSTAS	FRANK	FSK/PSK	FMCW	P1	P2	P3	P4	T1(n)	T2(n)	T3(n)	T4(n)
COSTAS	<b>1.00</b>	0.00	0.00	0.00	0.00	0.00	0.00	0.00	0.00	0.00	0.00	0.00
FRANK	0.00	<b>0.33</b>	0.00	0.00	0.33	0.00	1.00	0.33	0.00	0.33	0.00	0.00
FSK/PSK	0.00	0.00	<b>1.00</b>	0.00	0.00	0.00	0.00	0.00	0.00	0.00	0.00	0.00
FMCW	0.00	0.00	0.00	<b>1.00</b>	0.00	0.00	0.00	0.00	0.00	0.00	0.00	0.00
P1	0.00	0.00	0.00	0.00	<b>0.33</b>	0.00	0.00	0.00	0.00	0.00	0.00	0.00
P2	0.00	0.00	0.00	0.00	0.00	<b>1.00</b>	0.00	0.00	0.00	0.00	0.00	0.00
P3	0.00	0.00	0.00	0.00	0.00	0.00	<b>0.00</b>	0.00	0.00	0.00	0.00	0.00
P4	0.00	0.00	0.00	0.00	0.33	0.00	0.00	<b>0.67</b>	0.00	0.33	0.00	0.33
T1(n)	0.00	0.33	0.00	0.00	0.00	0.00	0.00	0.00	<b>0.67</b>	0.00	0.00	0.00
T2(n)	0.00	0.00	0.00	0.00	0.00	0.00	0.00	0.00	0.00	<b>0.33</b>	0.00	0.00
T3(n)	0.00	0.33	0.00	0.00	0.00	0.00	0.00	0.00	0.00	0.00	<b>0.67</b>	0.00
T4(n)	0.00	0.00	0.00	0.00	0.00	0.00	0.00	0.00	0.33	0.00	0.33	<b>0.67</b>

Table 56. CWD Classification Results with PNN (  $SNR = 6\text{dB}$  ).

TEST SNR	COSTAS	FRANK	FSK/PSK	FMCW	P1	P2	P3	P4	T1(n)	T2(n)	T3(n)	T4(n)
COSTAS	<b>0.50</b>	0.00	0.00	0.00	0.00	0.00	0.00	0.00	0.00	0.00	0.00	0.00
FRANK	0.00	<b>1.00</b>	0.00	0.00	0.00	0.00	0.00	0.00	0.00	0.00	0.00	0.00
FSK/PSK	0.00	0.00	<b>1.00</b>	0.00	0.00	0.00	0.00	0.00	0.00	0.00	0.00	0.00
FMCW	0.00	0.00	0.00	<b>1.00</b>	0.00	0.00	0.00	0.00	0.00	0.00	0.00	0.00
P1	0.00	0.00	0.00	0.00	<b>0.60</b>	0.00	0.00	0.00	0.00	0.00	0.00	0.00
P2	0.00	0.00	0.00	0.00	0.00	<b>0.75</b>	0.00	0.00	0.00	0.00	0.00	0.00
P3	0.00	0.00	0.00	0.00	0.00	0.00	<b>0.80</b>	0.00	0.00	0.20	0.00	0.00
P4	0.00	0.00	0.00	0.00	0.40	0.00	0.00	<b>1.00</b>	0.00	0.00	0.00	0.00
T1(n)	0.00	0.00	0.00	0.00	0.00	0.25	0.20	0.00	<b>1.00</b>	0.00	0.00	0.00
T2(n)	0.00	0.00	0.00	0.00	0.00	0.00	0.00	0.00	0.00	<b>0.80</b>	0.00	0.00
T3(n)	0.50	0.00	0.00	0.00	0.00	0.00	0.00	0.00	0.00	0.00	<b>0.60</b>	0.00
T4(n)	0.00	0.00	0.00	0.00	0.00	0.00	0.00	0.00	0.00	0.00	0.40	<b>1.00</b>
TEST MODULATION	COSTAS	FRANK	FSK/PSK	FMCW	P1	P2	P3	P4	T1(n)	T2(n)	T3(n)	T4(n)
COSTAS	<b>1.00</b>	0.00	0.00	0.00	0.00	0.00	0.00	0.00	0.00	0.00	0.00	0.00
FRANK	0.00	<b>0.00</b>	0.00	0.00	0.33	0.00	1.00	0.33	0.00	0.00	0.00	0.00
FSK/PSK	0.00	0.00	<b>1.00</b>	0.00	0.00	0.00	0.00	0.00	0.00	0.00	0.00	0.00
FMCW	0.00	0.00	0.00	<b>1.00</b>	0.00	0.00	0.00	0.00	0.00	0.00	0.00	0.00
P1	0.00	0.00	0.00	0.00	<b>0.00</b>	0.00	0.00	0.33	0.00	0.00	0.00	0.00
P2	0.00	0.00	0.00	0.00	0.00	<b>1.00</b>	0.00	0.00	0.00	0.00	0.00	0.00
P3	0.00	0.00	0.00	0.00	0.00	0.00	<b>0.00</b>	0.00	0.00	0.33	0.33	0.00
P4	0.00	0.00	0.00	0.00	0.33	0.00	0.00	<b>0.33</b>	0.00	0.33	0.00	0.33
T1(n)	0.00	0.33	0.00	0.00	0.33	0.00	0.00	0.00	<b>0.67</b>	0.00	0.00	0.00
T2(n)	0.00	0.00	0.00	0.00	0.00	0.00	0.00	0.00	0.00	<b>0.33</b>	0.00	0.00
T3(n)	0.00	0.67	0.00	0.00	0.00	0.00	0.00	0.00	0.00	0.00	<b>0.33</b>	0.00
T4(n)	0.00	0.00	0.00	0.00	0.00	0.00	0.00	0.00	0.33	0.00	0.33	<b>0.67</b>

Table 57. CWD Classification Results with PNN (  $SNR = 3\text{ dB}$  ).

TEST SNR	COSTAS	FRANK	FSK/PSK	FMCW	P1	P2	P3	P4	T1(n)	T2(n)	T3(n)	T4(n)
COSTAS	<b>0.50</b>	0.00	0.00	0.00	0.00	0.00	0.00	0.00	0.00	0.00	0.00	0.00
FRANK	0.00	<b>0.80</b>	0.00	0.00	0.00	0.00	0.00	0.00	0.00	0.00	0.00	0.00
FSK/PSK	0.50	0.00	<b>1.00</b>	0.00	0.00	0.25	0.00	0.00	0.00	0.00	0.00	0.00
FMCW	0.00	0.00	0.00	<b>1.00</b>	0.00	0.00	0.00	0.00	0.00	0.00	0.00	0.00
P1	0.00	0.00	0.00	0.00	<b>0.60</b>	0.00	0.20	0.00	0.00	0.00	0.00	0.00
P2	0.00	0.00	0.00	0.00	0.00	<b>0.75</b>	0.00	0.00	0.00	0.00	0.00	0.00
P3	0.00	0.20	0.00	0.00	0.00	0.00	<b>0.80</b>	0.00	0.00	0.00	0.00	0.00
P4	0.00	0.00	0.00	0.00	0.40	0.00	0.00	<b>1.00</b>	0.00	0.00	0.00	0.00
T1(n)	0.00	0.00	0.00	0.00	0.00	0.00	0.00	0.00	<b>1.00</b>	0.00	0.00	0.00
T2(n)	0.00	0.00	0.00	0.00	0.00	0.00	0.00	0.00	0.00	<b>1.00</b>	0.00	0.00
T3(n)	0.00	0.00	0.00	0.00	0.00	0.00	0.00	0.00	0.00	0.00	<b>0.60</b>	0.00
T4(n)	0.00	0.00	0.00	0.00	0.00	0.00	0.00	0.00	0.00	0.00	0.40	<b>1.00</b>
TEST MODULATION	COSTAS	FRANK	FSK/PSK	FMCW	P1	P2	P3	P4	T1(n)	T2(n)	T3(n)	T4(n)
COSTAS	<b>1.00</b>	0.00	0.00	0.00	0.00	0.00	0.00	0.00	0.00	0.00	0.00	0.00
FRANK	0.00	<b>0.00</b>	0.00	0.00	0.33	0.00	0.67	0.33	0.00	0.33	0.00	0.00
FSK/PSK	0.00	0.00	<b>0.50</b>	0.00	0.00	0.00	0.00	0.00	0.00	0.00	0.00	0.00
FMCW	0.00	0.00	0.00	<b>1.00</b>	0.00	0.00	0.00	0.00	0.00	0.00	0.00	0.00
P1	0.00	0.00	0.00	0.00	<b>0.00</b>	0.00	0.00	0.00	0.00	0.00	0.00	0.00
P2	0.00	0.00	0.50	0.00	0.00	<b>1.00</b>	0.00	0.00	0.00	0.00	0.00	0.00
P3	0.00	0.00	0.00	0.00	0.00	0.00	<b>0.00</b>	0.33	0.00	0.00	0.00	0.00
P4	0.00	0.33	0.00	0.00	0.67	0.00	0.00	<b>0.33</b>	0.00	0.00	0.00	0.33
T1(n)	0.00	0.00	0.00	0.00	0.00	0.00	0.33	0.00	<b>0.67</b>	0.00	0.00	0.00
T2(n)	0.00	0.00	0.00	0.00	0.00	0.00	0.00	0.00	0.00	<b>0.33</b>	0.00	0.00
T3(n)	0.00	0.67	0.00	0.00	0.00	0.00	0.00	0.00	0.00	0.00	<b>0.67</b>	0.00
T4(n)	0.00	0.00	0.00	0.00	0.00	0.00	0.00	0.00	0.33	0.33	0.33	<b>0.67</b>

Table 58. CWD Classification Results with PNN (  $SNR = 0\text{ dB}$  ).

TEST SNR	COSTAS	FRANK	FSK/PSK	FMCW	P1	P2	P3	P4	T1(n)	T2(n)	T3(n)	T4(n)
COSTAS	<b>0.50</b>	0.00	0.00	0.00	0.00	0.00	0.00	0.00	0.00	0.00	0.00	0.00
FRANK	0.00	<b>1.00</b>	0.00	0.00	0.00	0.00	0.00	0.00	0.00	0.00	0.00	0.00
FSK/PSK	0.50	0.00	<b>1.00</b>	0.00	0.00	0.00	0.00	0.00	0.00	0.00	0.00	0.00
FMCW	0.00	0.00	0.00	<b>1.00</b>	0.00	0.00	0.00	0.00	0.00	0.00	0.00	0.00
P1	0.00	0.00	0.00	0.00	<b>0.60</b>	0.25	0.00	0.00	0.00	0.00	0.00	0.00
P2	0.00	0.00	0.00	0.00	0.00	<b>0.75</b>	0.00	0.00	0.00	0.00	0.00	0.00
P3	0.00	0.00	0.00	0.00	0.00	0.00	<b>1.00</b>	0.00	0.00	0.00	0.00	0.00
P4	0.00	0.00	0.00	0.00	0.40	0.00	0.00	<b>1.00</b>	0.00	0.00	0.00	0.00
T1(n)	0.00	0.00	0.00	0.00	0.00	0.00	0.00	0.00	<b>1.00</b>	0.00	0.00	0.00
T2(n)	0.00	0.00	0.00	0.00	0.00	0.00	0.00	0.00	0.00	<b>1.00</b>	0.00	0.00
T3(n)	0.00	0.00	0.00	0.00	0.00	0.00	0.00	0.00	0.00	0.00	<b>0.60</b>	0.00
T4(n)	0.00	0.00	0.00	0.00	0.00	0.00	0.00	0.00	0.00	0.00	0.40	<b>1.00</b>
TEST MODULATION	COSTAS	FRANK	FSK/PSK	FMCW	P1	P2	P3	P4	T1(n)	T2(n)	T3(n)	T4(n)
COSTAS	<b>1.00</b>	0.00	0.00	0.00	0.00	0.50	0.00	0.00	0.00	0.00	0.00	0.00
FRANK	0.00	<b>0.33</b>	0.00	0.00	0.33	0.00	0.67	0.33	0.00	0.33	0.00	0.00
FSK/PSK	0.00	0.00	<b>1.00</b>	0.00	0.00	0.00	0.00	0.00	0.00	0.00	0.00	0.00
FMCW	0.00	0.00	0.00	<b>1.00</b>	0.00	0.00	0.00	0.00	0.00	0.00	0.00	0.00
P1	0.00	0.00	0.00	0.00	<b>0.33</b>	0.00	0.00	0.00	0.00	0.00	0.00	0.00
P2	0.00	0.00	0.00	0.00	0.00	<b>0.50</b>	0.00	0.00	0.00	0.00	0.00	0.00
P3	0.00	0.33	0.00	0.00	0.00	0.00	<b>0.00</b>	0.00	0.00	0.00	0.00	0.00
P4	0.00	0.00	0.00	0.00	0.00	0.00	0.00	<b>0.33</b>	0.00	0.00	0.33	0.33
T1(n)	0.00	0.00	0.00	0.00	0.33	0.00	0.33	0.00	<b>0.67</b>	0.00	0.00	0.00
T2(n)	0.00	0.00	0.00	0.00	0.00	0.00	0.00	0.00	0.00	<b>0.33</b>	0.00	0.00
T3(n)	0.00	0.33	0.00	0.00	0.00	0.00	0.00	0.33	0.00	0.00	<b>0.00</b>	0.00
T4(n)	0.00	0.00	0.00	0.00	0.00	0.00	0.00	0.00	0.33	0.33	0.67	<b>0.67</b>

Table 59. CWD Classification Results with PNN (  $SNR = -3dB$  ).

TEST SNR	COSTAS	FRANK	FSK/PSK	FMCW	P1	P2	P3	P4	T1(n)	T2(n)	T3(n)	T4(n)
COSTAS	<b>1.00</b>	0.00	0.50	0.00	0.00	0.00	0.00	0.00	0.00	0.00	0.20	0.00
FRANK	0.00	<b>0.80</b>	0.00	0.00	0.20	0.00	0.20	0.00	0.00	0.00	0.20	0.00
FSK/PSK	0.00	0.00	<b>0.50</b>	0.00	0.00	0.00	0.00	0.00	0.00	0.00	0.00	0.00
FMCW	0.00	0.00	0.00	<b>1.00</b>	0.00	0.00	0.00	0.00	0.00	0.00	0.00	0.00
P1	0.00	0.20	0.00	0.00	<b>0.20</b>	0.25	0.00	0.40	0.00	0.00	0.00	0.00
P2	0.00	0.00	0.00	0.00	0.00	<b>0.50</b>	0.00	0.00	0.00	0.00	0.00	0.00
P3	0.00	0.00	0.00	0.00	0.00	0.00	<b>0.40</b>	0.00	0.00	0.20	0.00	0.00
P4	0.00	0.00	0.00	0.00	0.40	0.00	0.20	<b>0.60</b>	0.00	0.00	0.00	0.00
T1(n)	0.00	0.00	0.00	0.00	0.20	0.25	0.00	0.00	<b>0.80</b>	0.00	0.00	0.00
T2(n)	0.00	0.00	0.00	0.00	0.00	0.00	0.00	0.00	0.00	<b>0.80</b>	0.00	0.00
T3(n)	0.00	0.00	0.00	0.00	0.00	0.00	0.20	0.00	0.00	0.00	<b>0.20</b>	0.00
T4(n)	0.00	0.00	0.00	0.00	0.00	0.00	0.00	0.00	0.20	0.00	0.40	<b>1.00</b>
TEST MODULATION	COSTAS	FRANK	FSK/PSK	FMCW	P1	P2	P3	P4	T1(n)	T2(n)	T3(n)	T4(n)
COSTAS	<b>1.00</b>	0.00	0.00	0.00	0.00	0.00	0.00	0.00	0.00	0.00	0.00	0.00
FRANK	0.00	<b>0.00</b>	0.00	0.00	0.33	0.00	0.33	0.00	0.00	0.00	0.00	0.00
FSK/PSK	0.00	0.00	<b>1.00</b>	0.00	0.00	0.00	0.00	0.00	0.00	0.00	0.00	0.00
FMCW	0.00	0.00	0.00	<b>1.00</b>	0.00	0.00	0.00	0.00	0.00	0.00	0.00	0.00
P1	0.00	0.00	0.00	0.00	<b>0.33</b>	0.00	0.00	0.33	0.00	0.00	0.00	0.00
P2	0.00	0.00	0.00	0.00	0.00	<b>0.50</b>	0.00	0.00	0.00	0.00	0.00	0.00
P3	0.00	0.00	0.00	0.00	0.33	0.00	<b>0.00</b>	0.00	0.00	0.00	0.00	0.00
P4	0.00	0.00	0.00	0.00	0.00	0.00	0.33	<b>0.33</b>	0.00	0.00	0.00	0.00
T1(n)	0.00	0.33	0.00	0.00	0.00	0.00	0.00	0.00	<b>1.00</b>	0.00	0.33	0.00
T2(n)	0.00	0.00	0.00	0.00	0.00	0.00	0.00	0.00	0.00	<b>0.67</b>	0.00	0.00
T3(n)	0.00	0.67	0.00	0.00	0.00	0.50	0.33	0.00	0.00	0.00	<b>0.33</b>	0.33
T4(n)	0.00	0.00	0.00	0.00	0.00	0.00	0.00	0.33	0.00	0.33	0.33	<b>0.67</b>

Table 60. CWD Classification Results with PNN (  $SNR = -6dB$  ).

TEST SNR	COSTAS	FRANK	FSK/PSK	FMCW	P1	P2	P3	P4	T1(n)	T2(n)	T3(n)	T4(n)
COSTAS	<b>1.00</b>	0.00	0.00	0.00	0.00	0.00	0.00	0.00	0.20	0.00	0.00	0.00
FRANK	0.00	<b>0.80</b>	0.00	0.00	0.00	0.00	0.00	0.00	0.20	0.20	0.00	0.20
FSK/PSK	0.00	0.00	<b>1.00</b>	0.00	0.00	0.25	0.00	0.00	0.20	0.00	0.00	0.00
FMCW	0.00	0.00	0.00	<b>1.00</b>	0.00	0.00	0.00	0.00	0.00	0.00	0.00	0.00
P1	0.00	0.00	0.00	0.00	<b>0.20</b>	0.00	0.00	0.40	0.00	0.00	0.20	0.20
P2	0.00	0.20	0.00	0.00	0.00	<b>0.00</b>	0.00	0.00	0.00	0.00	0.00	0.00
P3	0.00	0.00	0.00	0.00	0.00	0.00	<b>0.80</b>	0.00	0.00	0.00	0.00	0.00
P4	0.00	0.00	0.00	0.00	0.60	0.00	0.00	<b>0.60</b>	0.00	0.00	0.00	0.20
T1(n)	0.00	0.00	0.00	0.00	0.00	0.50	0.00	0.00	<b>0.40</b>	0.00	0.20	0.00
T2(n)	0.00	0.00	0.00	0.00	0.00	0.00	0.20	0.00	0.00	<b>0.60</b>	0.00	0.00
T3(n)	0.00	0.00	0.00	0.00	0.00	0.25	0.00	0.00	0.00	0.20	<b>0.40</b>	0.00
T4(n)	0.00	0.00	0.00	0.00	0.20	0.00	0.00	0.00	0.00	0.00	0.20	<b>0.40</b>
TEST MODULATION	COSTAS	FRANK	FSK/PSK	FMCW	P1	P2	P3	P4	T1(n)	T2(n)	T3(n)	T4(n)
COSTAS	<b>1.00</b>	0.00	0.00	0.00	0.00	0.00	0.00	0.00	0.00	0.00	0.00	0.00
FRANK	0.00	<b>0.33</b>	0.00	0.00	0.00	0.00	0.00	0.00	0.00	0.00	0.67	0.00
FSK/PSK	0.00	0.00	<b>1.00</b>	0.50	0.00	0.00	0.00	0.00	0.00	0.00	0.00	0.00
FMCW	0.00	0.00	0.00	<b>0.00</b>	0.00	0.00	0.00	0.00	0.00	0.00	0.00	0.00
P1	0.00	0.00	0.00	0.00	<b>0.67</b>	0.00	0.00	0.33	0.00	0.00	0.00	0.00
P2	0.00	0.00	0.00	0.00	0.00	<b>1.00</b>	0.00	0.00	0.00	0.00	0.00	0.00
P3	0.00	0.33	0.00	0.50	0.00	0.00	<b>0.00</b>	0.00	0.33	0.33	0.00	0.00
P4	0.00	0.00	0.00	0.00	0.33	0.00	0.00	<b>0.33</b>	0.00	0.33	0.00	0.33
T1(n)	0.00	0.00	0.00	0.00	0.00	0.00	0.33	0.00	<b>0.67</b>	0.00	0.33	0.00
T2(n)	0.00	0.33	0.00	0.00	0.00	0.00	0.00	0.00	0.00	<b>0.33</b>	0.00	0.00
T3(n)	0.00	0.00	0.00	0.00	0.00	0.00	0.67	0.33	0.00	0.00	<b>0.00</b>	0.33
T4(n)	0.00	0.00	0.00	0.00	0.00	0.00	0.00	0.00	0.00	0.00	0.00	<b>0.33</b>

Table 61. QMFB Classification Results with PNN (  $SNR = 10\text{ dB}$  ).

TEST SNR	COSTAS	FRANK	FSK/PSK	FMCW	P1	P2	P3	P4	T1(n)	T2(n)	T3(n)	T4(n)
COSTAS	<b>1.00</b>	0.00	0.00	0.00	0.00	0.00	0.00	0.00	0.00	0.00	0.00	0.00
FRANK	0.00	<b>1.00</b>	0.00	0.00	0.00	0.00	0.00	0.00	0.00	0.00	0.00	0.00
FSK/PSK	0.00	0.00	<b>1.00</b>	0.00	0.00	0.00	0.00	0.00	0.00	0.00	0.00	0.00
FMCW	0.00	0.00	0.00	<b>1.00</b>	0.00	0.00	0.00	0.00	0.00	0.00	0.00	0.00
P1	0.00	0.00	0.00	0.00	<b>1.00</b>	0.00	0.00	0.00	0.00	0.00	0.00	0.00
P2	0.00	0.00	0.00	0.00	0.00	<b>1.00</b>	0.00	0.00	0.00	0.00	0.00	0.00
P3	0.00	0.00	0.00	0.00	0.00	0.00	<b>1.00</b>	0.00	0.00	0.00	0.00	0.00
P4	0.00	0.00	0.00	0.00	0.00	0.00	0.00	<b>1.00</b>	0.00	0.00	0.00	0.00
T1(n)	0.00	0.00	0.00	0.00	0.00	0.00	0.00	0.00	<b>1.00</b>	0.00	0.00	0.00
T2(n)	0.00	0.00	0.00	0.00	0.00	0.00	0.00	0.00	0.00	<b>1.00</b>	0.00	0.00
T3(n)	0.00	0.00	0.00	0.00	0.00	0.00	0.00	0.00	0.00	0.00	<b>1.00</b>	0.00
T4(n)	0.00	0.00	0.00	0.00	0.00	0.00	0.00	0.00	0.00	0.00	0.00	<b>1.00</b>
TEST MODULATION	COSTAS	FRANK	FSK/PSK	FMCW	P1	P2	P3	P4	T1(n)	T2(n)	T3(n)	T4(n)
COSTAS	<b>1.00</b>	0.00	0.00	0.00	0.00	0.00	0.33	0.00	0.00	0.00	0.00	0.00
FRANK	0.00	<b>0.33</b>	0.00	0.00	0.00	0.00	0.00	0.00	0.00	0.00	0.00	0.00
FSK/PSK	0.00	0.33	<b>0.00</b>	0.00	0.00	0.50	0.00	0.00	0.00	0.00	0.00	0.00
FMCW	0.00	0.00	1.00	<b>0.00</b>	0.00	0.00	0.00	0.00	0.00	0.00	0.00	0.00
P1	0.00	0.00	0.00	1.00	<b>0.67</b>	0.00	0.00	0.33	0.00	0.00	0.00	0.00
P2	0.00	0.00	0.00	0.00	0.00	<b>0.00</b>	0.00	0.00	0.00	0.00	0.00	0.00
P3	0.00	0.00	0.00	0.00	0.00	0.50	<b>0.67</b>	0.00	0.00	0.00	0.00	0.00
P4	0.00	0.33	0.00	0.00	0.00	0.00	0.00	<b>0.33</b>	0.00	0.00	0.33	0.00
T1(n)	0.00	0.00	0.00	0.00	0.33	0.00	0.00	0.33	<b>0.33</b>	0.00	0.00	0.00
T2(n)	0.00	0.00	0.00	0.00	0.00	0.00	0.00	0.00	0.00	<b>1.00</b>	0.00	0.00
T3(n)	0.00	0.00	0.00	0.00	0.00	0.00	0.00	0.00	0.33	0.00	<b>0.67</b>	1.00
T4(n)	0.00	0.00	0.00	0.00	0.00	0.00	0.00	0.00	0.33	0.00	0.00	<b>0.00</b>

Table 62. QMFB Classification Results with PNN (  $SNR = 6\text{ dB}$  ).

TEST SNR	COSTAS	FRANK	FSK/PSK	FMCW	P1	P2	P3	P4	T1(n)	T2(n)	T3(n)	T4(n)
COSTAS	<b>0.50</b>	0.00	0.00	0.00	0.00	0.00	0.00	0.00	0.00	0.00	0.00	0.00
FRANK	0.00	<b>1.00</b>	0.00	0.00	0.00	0.00	0.00	0.00	0.00	0.00	0.00	0.00
FSK/PSK	0.00	0.00	<b>1.00</b>	0.00	0.00	0.00	0.00	0.00	0.00	0.00	0.00	0.00
FMCW	0.00	0.00	0.00	<b>1.00</b>	0.00	0.00	0.00	0.00	0.00	0.00	0.00	0.00
P1	0.00	0.00	0.00	0.00	<b>0.60</b>	0.00	0.00	0.20	0.00	0.00	0.00	0.00
P2	0.00	0.00	0.00	0.00	0.00	<b>1.00</b>	0.00	0.00	0.00	0.00	0.00	0.00
P3	0.00	0.00	0.00	0.00	0.00	0.00	<b>1.00</b>	0.00	0.00	0.00	0.00	0.00
P4	0.00	0.00	0.00	0.00	0.40	0.00	0.00	<b>0.80</b>	0.00	0.00	0.00	0.00
T1(n)	0.00	0.00	0.00	0.00	0.00	0.00	0.00	0.00	<b>1.00</b>	0.00	0.00	0.00
T2(n)	0.00	0.00	0.00	0.00	0.00	0.00	0.00	0.00	0.00	<b>1.00</b>	0.00	0.00
T3(n)	0.50	0.00	0.00	0.00	0.00	0.00	0.00	0.00	0.00	0.00	<b>1.00</b>	0.00
T4(n)	0.00	0.00	0.00	0.00	0.00	0.00	0.00	0.00	0.00	0.00	0.00	<b>1.00</b>
TEST MODULATION	COSTAS	FRANK	FSK/PSK	FMCW	P1	P2	P3	P4	T1(n)	T2(n)	T3(n)	T4(n)
COSTAS	<b>1.00</b>	0.33	0.00	0.00	0.00	0.00	0.33	0.00	0.00	0.00	0.00	0.00
FRANK	0.00	<b>0.33</b>	0.00	0.00	0.00	0.00	0.00	0.00	0.00	0.00	0.00	0.00
FSK/PSK	0.00	0.00	<b>0.00</b>	0.00	0.00	0.50	0.00	0.00	0.00	0.00	0.00	0.00
FMCW	0.00	0.00	1.00	<b>0.00</b>	0.00	0.50	0.33	0.00	0.00	0.00	0.00	0.00
P1	0.00	0.00	0.00	1.00	<b>0.67</b>	0.00	0.00	0.67	0.00	0.00	0.00	0.00
P2	0.00	0.00	0.00	0.00	0.00	<b>0.00</b>	0.00	0.00	0.00	0.00	0.00	0.00
P3	0.00	0.00	0.00	0.00	0.00	0.00	<b>0.33</b>	0.00	0.00	0.00	0.00	0.00
P4	0.00	0.33	0.00	0.00	0.00	0.00	0.00	<b>0.00</b>	0.00	0.00	0.00	0.00
T1(n)	0.00	0.00	0.00	0.00	0.33	0.00	0.00	0.33	<b>0.33</b>	0.00	0.33	0.00
T2(n)	0.00	0.00	0.00	0.00	0.00	0.00	0.00	0.00	0.00	<b>0.67</b>	0.00	0.00
T3(n)	0.00	0.00	0.00	0.00	0.00	0.00	0.00	0.00	0.00	0.33	<b>0.33</b>	1.00
T4(n)	0.00	0.00	0.00	0.00	0.00	0.00	0.00	0.00	0.67	0.00	0.33	<b>0.00</b>

Table 63. QMFB Classification Results with PNN (  $SNR = 3\text{ dB}$  ).

TEST SNR	COSTAS	FRANK	FSK/PSK	FMCW	P1	P2	P3	P4	T1(n)	T2(n)	T3(n)	T4(n)
COSTAS	<b>1.00</b>	0.00	0.00	0.00	0.00	0.25	0.00	0.00	0.00	0.00	0.00	0.00
FRANK	0.00	<b>1.00</b>	0.00	0.00	0.00	0.00	0.00	0.00	0.00	0.00	0.00	0.00
FSK/PSK	0.00	0.00	<b>0.00</b>	0.00	0.00	0.00	0.00	0.00	0.00	0.00	0.00	0.00
FMCW	0.00	0.00	0.50	<b>1.00</b>	0.00	0.00	0.00	0.00	0.00	0.00	0.00	0.00
P1	0.00	0.00	0.00	0.00	<b>0.60</b>	0.00	0.00	0.40	0.00	0.00	0.00	0.00
P2	0.00	0.00	0.00	0.00	0.00	<b>0.75</b>	0.00	0.00	0.00	0.00	0.00	0.00
P3	0.00	0.00	0.00	0.00	0.00	0.00	<b>1.00</b>	0.00	0.00	0.00	0.00	0.00
P4	0.00	0.00	0.00	0.00	0.40	0.00	0.00	<b>0.60</b>	0.00	0.00	0.00	0.00
T1(n)	0.00	0.00	0.00	0.00	0.00	0.00	0.00	0.00	<b>0.80</b>	0.00	0.00	0.00
T2(n)	0.00	0.00	0.00	0.00	0.00	0.00	0.00	0.00	0.00	<b>1.00</b>	0.00	0.00
T3(n)	0.00	0.00	0.50	0.00	0.00	0.00	0.00	0.00	0.20	0.00	<b>0.80</b>	0.00
T4(n)	0.00	0.00	0.00	0.00	0.00	0.00	0.00	0.00	0.00	0.00	0.20	<b>1.00</b>
TEST MODULATION	COSTAS	FRANK	FSK/PSK	FMCW	P1	P2	P3	P4	T1(n)	T2(n)	T3(n)	T4(n)
COSTAS	<b>1.00</b>	0.00	0.00	0.00	0.00	0.00	0.33	0.00	0.00	0.00	0.00	0.00
FRANK	0.00	<b>0.33</b>	0.00	0.00	0.00	0.00	0.00	0.00	0.00	0.00	0.00	0.00
FSK/PSK	0.00	0.33	<b>0.00</b>	0.00	0.00	0.50	0.00	0.00	0.00	0.00	0.33	0.00
FMCW	0.00	0.00	1.00	<b>0.00</b>	0.00	0.50	0.33	0.00	0.00	0.00	0.00	0.00
P1	0.00	0.33	0.00	1.00	<b>0.67</b>	0.00	0.00	0.67	0.00	0.00	0.00	0.00
P2	0.00	0.00	0.00	0.00	0.00	<b>0.00</b>	0.00	0.00	0.00	0.00	0.00	0.00
P3	0.00	0.00	0.00	0.00	0.00	0.00	<b>0.33</b>	0.00	0.00	0.00	0.00	0.00
P4	0.00	0.00	0.00	0.00	0.00	0.00	0.00	<b>0.00</b>	0.00	0.00	0.00	0.00
T1(n)	0.00	0.00	0.00	0.00	0.33	0.00	0.00	0.33	<b>0.33</b>	0.00	0.00	0.00
T2(n)	0.00	0.00	0.00	0.00	0.00	0.00	0.00	0.00	0.00	<b>0.67</b>	0.00	0.00
T3(n)	0.00	0.00	0.00	0.00	0.00	0.00	0.00	0.00	0.00	0.33	<b>0.67</b>	1.00
T4(n)	0.00	0.00	0.00	0.00	0.00	0.00	0.00	0.00	0.67	0.00	0.00	<b>0.00</b>

Table 64. QMFB Classification Results with PNN (  $SNR = 0\text{ dB}$  ).

TEST SNR	COSTAS	FRANK	FSK/PSK	FMCW	P1	P2	P3	P4	T1(n)	T2(n)	T3(n)	T4(n)
COSTAS	<b>1.00</b>	0.00	0.00	0.00	0.00	0.00	0.00	0.00	0.00	0.00	0.00	0.00
FRANK	0.00	<b>1.00</b>	0.00	0.00	0.00	0.00	0.20	0.00	0.00	0.00	0.00	0.00
FSK/PSK	0.00	0.00	<b>0.50</b>	0.00	0.00	0.00	0.00	0.00	0.00	0.00	0.00	0.00
FMCW	0.00	0.00	0.50	<b>1.00</b>	0.00	0.00	0.00	0.00	0.00	0.00	0.00	0.00
P1	0.00	0.00	0.00	0.00	<b>1.00</b>	0.00	0.00	0.60	0.00	0.00	0.00	0.00
P2	0.00	0.00	0.00	0.00	0.00	<b>1.00</b>	0.00	0.00	0.00	0.00	0.00	0.00
P3	0.00	0.00	0.00	0.00	0.00	0.00	<b>0.80</b>	0.00	0.00	0.00	0.20	0.00
P4	0.00	0.00	0.00	0.00	0.00	0.00	0.00	<b>0.20</b>	0.00	0.00	0.00	0.00
T1(n)	0.00	0.00	0.00	0.00	0.00	0.00	0.00	0.00	<b>0.80</b>	0.00	0.00	0.00
T2(n)	0.00	0.00	0.00	0.00	0.00	0.00	0.00	0.00	0.00	<b>1.00</b>	0.00	0.00
T3(n)	0.00	0.00	0.00	0.00	0.00	0.00	0.00	0.00	0.20	0.00	<b>0.40</b>	0.20
T4(n)	0.00	0.00	0.00	0.00	0.00	0.00	0.00	0.20	0.00	0.00	0.40	<b>0.80</b>
TEST MODULATION	COSTAS	FRANK	FSK/PSK	FMCW	P1	P2	P3	P4	T1(n)	T2(n)	T3(n)	T4(n)
COSTAS	<b>1.00</b>	0.33	0.50	0.00	0.33	0.00	0.33	0.00	0.00	0.00	0.00	0.00
FRANK	0.00	<b>0.33</b>	0.00	0.00	0.00	0.00	0.00	0.00	0.00	0.00	0.00	0.00
FSK/PSK	0.00	0.00	<b>0.00</b>	0.00	0.00	0.50	0.00	0.00	0.00	0.00	0.00	0.00
FMCW	0.00	0.00	0.50	<b>0.00</b>	0.00	0.50	0.33	0.00	0.00	0.00	0.00	0.00
P1	0.00	0.33	0.00	0.50	<b>0.33</b>	0.00	0.00	0.33	0.00	0.00	0.00	0.00
P2	0.00	0.00	0.00	0.00	0.00	<b>0.00</b>	0.00	0.00	0.00	0.00	0.00	0.00
P3	0.00	0.00	0.00	0.00	0.00	0.00	<b>0.33</b>	0.00	0.00	0.00	0.33	0.00
P4	0.00	0.00	0.00	0.00	0.00	0.00	0.00	<b>0.00</b>	0.00	0.00	0.00	0.33
T1(n)	0.00	0.00	0.00	0.00	0.33	0.00	0.00	0.33	<b>0.33</b>	0.00	0.00	0.00
T2(n)	0.00	0.00	0.00	0.00	0.00	0.00	0.00	0.00	0.00	<b>0.67</b>	0.00	0.00
T3(n)	0.00	0.00	0.00	0.50	0.00	0.00	0.00	0.33	0.00	0.00	<b>0.67</b>	0.67
T4(n)	0.00	0.00	0.00	0.00	0.00	0.00	0.00	0.00	0.67	0.33	0.00	<b>0.00</b>

Table 65. QMFB Classification Results with PNN (  $SNR = -3dB$  ).

TEST SNR	COSTAS	FRANK	FSK/PSK	FMCW	P1	P2	P3	P4	T1(n)	T2(n)	T3(n)	T4(n)
COSTAS	<b>1.00</b>	0.00	0.00	0.00	0.00	0.00	0.00	0.00	0.00	0.00	0.00	0.00
FRANK	0.00	<b>0.60</b>	0.00	0.00	0.00	0.00	0.00	0.00	0.00	0.00	0.00	0.00
FSK/PSK	0.00	0.00	<b>0.50</b>	0.00	0.00	0.00	0.00	0.00	0.20	0.00	0.00	0.00
FMCW	0.00	0.20	0.50	<b>1.00</b>	0.00	0.00	0.20	0.20	0.00	0.00	0.00	0.20
P1	0.00	0.00	0.00	0.00	<b>0.80</b>	0.00	0.00	0.80	0.00	0.00	0.00	0.00
P2	0.00	0.00	0.00	0.00	0.00	<b>1.00</b>	0.00	0.00	0.00	0.00	0.20	0.00
P3	0.00	0.20	0.00	0.00	0.00	0.00	<b>0.60</b>	0.00	0.00	0.00	0.00	0.00
P4	0.00	0.00	0.00	0.00	0.00	0.00	0.00	<b>0.00</b>	0.00	0.00	0.00	0.00
T1(n)	0.00	0.00	0.00	0.00	0.00	0.00	0.00	0.00	<b>0.60</b>	0.00	0.00	0.00
T2(n)	0.00	0.00	0.00	0.00	0.00	0.00	0.20	0.00	0.00	<b>0.80</b>	0.00	0.00
T3(n)	0.00	0.00	0.00	0.00	0.20	0.00	0.00	0.00	0.20	0.00	<b>0.60</b>	0.00
T4(n)	0.00	0.00	0.00	0.00	0.00	0.00	0.00	0.00	0.00	0.20	0.20	<b>0.80</b>
TEST MODULATION	COSTAS	FRANK	FSK/PSK	FMCW	P1	P2	P3	P4	T1(n)	T2(n)	T3(n)	T4(n)
COSTAS	<b>1.00</b>	0.33	0.50	0.50	0.33	0.00	0.00	0.00	0.00	0.00	0.00	0.00
FRANK	0.00	<b>0.00</b>	0.00	0.00	0.00	0.00	0.00	0.00	0.00	0.00	0.00	0.00
FSK/PSK	0.00	0.00	<b>0.00</b>	0.00	0.33	0.50	0.00	0.00	0.00	0.00	0.00	0.00
FMCW	0.00	0.33	0.50	<b>0.50</b>	0.00	0.50	0.33	0.67	0.00	0.00	0.00	0.00
P1	0.00	0.00	0.00	0.00	<b>0.33</b>	0.00	0.00	0.33	0.00	0.00	0.00	0.00
P2	0.00	0.00	0.00	0.00	0.00	<b>0.00</b>	0.00	0.00	0.00	0.00	0.00	0.00
P3	0.00	0.33	0.00	0.00	0.00	0.00	<b>0.33</b>	0.00	0.00	0.00	0.00	0.33
P4	0.00	0.00	0.00	0.00	0.00	0.00	0.00	<b>0.00</b>	0.00	0.00	0.00	0.00
T1(n)	0.00	0.00	0.00	0.00	0.00	0.00	0.00	0.00	<b>0.33</b>	0.00	0.33	0.00
T2(n)	0.00	0.00	0.00	0.00	0.00	0.00	0.00	0.00	0.00	<b>0.67</b>	0.00	0.00
T3(n)	0.00	0.00	0.00	0.00	0.00	0.00	0.00	0.00	0.33	0.00	<b>0.33</b>	0.67
T4(n)	0.00	0.00	0.00	0.00	0.00	0.00	0.33	0.00	0.33	0.33	0.33	<b>0.00</b>

Table 66. QMFB Classification Results with PNN (  $SNR = -6dB$  ).

TEST SNR	COSTAS	FRANK	FSK/PSK	FMCW	P1	P2	P3	P4	T1(n)	T2(n)	T3(n)	T4(n)
COSTAS	<b>0.00</b>	0.00	0.00	0.00	0.20	0.00	0.00	0.00	0.40	0.40	0.00	0.20
FRANK	0.00	<b>0.40</b>	0.00	0.00	0.00	0.00	0.00	0.00	0.00	0.00	0.00	0.00
FSK/PSK	0.00	0.00	<b>0.00</b>	0.00	0.00	0.25	0.00	0.00	0.00	0.00	0.00	0.00
FMCW	1.00	0.20	0.50	<b>1.00</b>	0.20	0.50	0.00	0.40	0.40	0.00	0.60	0.00
P1	0.00	0.20	0.00	0.00	<b>0.60</b>	0.00	0.00	0.40	0.00	0.00	0.00	0.00
P2	0.00	0.00	0.00	0.00	0.00	<b>0.25</b>	0.00	0.00	0.00	0.00	0.00	0.00
P3	0.00	0.00	0.00	0.00	0.00	0.00	<b>0.60</b>	0.00	0.00	0.00	0.20	0.00
P4	0.00	0.00	0.00	0.00	0.00	0.00	0.00	<b>0.20</b>	0.00	0.00	0.00	0.00
T1(n)	0.00	0.00	0.00	0.00	0.00	0.00	0.00	0.00	<b>0.20</b>	0.00	0.00	0.00
T2(n)	0.00	0.00	0.00	0.00	0.00	0.00	0.00	0.00	0.00	<b>0.40</b>	0.00	0.00
T3(n)	0.00	0.00	0.00	0.00	0.00	0.00	0.00	0.00	0.00	0.00	<b>0.20</b>	0.40
T4(n)	0.00	0.20	0.50	0.00	0.00	0.00	0.40	0.00	0.00	0.20	0.00	<b>0.40</b>
TEST MODULATION	COSTAS	FRANK	FSK/PSK	FMCW	P1	P2	P3	P4	T1(n)	T2(n)	T3(n)	T4(n)
COSTAS	<b>1.00</b>	0.33	0.00	0.00	0.67	0.00	0.33	0.33	0.00	0.00	0.00	0.00
FRANK	0.00	<b>0.00</b>	0.00	0.00	0.00	0.00	0.00	0.00	0.00	0.00	0.33	0.33
FSK/PSK	0.00	0.33	<b>0.00</b>	0.50	0.00	0.50	0.00	0.33	0.00	0.00	0.00	0.00
FMCW	0.00	0.00	1.00	<b>0.00</b>	0.00	0.50	0.67	0.00	0.00	0.33	0.33	0.33
P1	0.00	0.33	0.00	0.00	<b>0.00</b>	0.00	0.00	0.33	0.00	0.00	0.00	0.00
P2	0.00	0.00	0.00	0.00	0.00	<b>0.00</b>	0.00	0.00	0.00	0.00	0.00	0.00
P3	0.00	0.00	0.00	0.00	0.33	0.00	<b>0.00</b>	0.00	0.00	0.00	0.00	0.00
P4	0.00	0.00	0.00	0.00	0.00	0.00	0.00	<b>0.00</b>	0.00	0.00	0.00	0.00
T1(n)	0.00	0.00	0.00	0.50	0.00	0.00	0.00	0.00	<b>0.33</b>	0.00	0.00	0.00
T2(n)	0.00	0.00	0.00	0.00	0.00	0.00	0.00	0.00	0.00	<b>0.00</b>	0.00	0.00
T3(n)	0.00	0.00	0.00	0.00	0.00	0.00	0.00	0.00	0.67	0.33	<b>0.33</b>	0.33
T4(n)	0.00	0.00	0.00	0.00	0.00	0.00	0.00	0.00	0.00	0.33	0.00	<b>0.00</b>

THIS PAGE INTENTIONALLY LEFT BLANK



## APPENDIX C.

### A. PARAMETER EXTRACTION RESULTS FOR POLYPHASE CODED LPI MODULATIONS USING PWVD IMAGES

Table 67. Original Parameters vs. Extracted Parameters (SNR = 6 dB).

6 dB																
Signal Type	Actual Parameters					Extracted Parameters					Error					
	Signal #	Carrier Frequency	Number of Subcodes	Carrier Cycles per Subcode	Code Period	Bandwidth	Carrier Frequency	Number of Subcodes	Carrier Cycles per Subcode	Code Period	Bandwidth	Error fc	Error Nc	Error cpp	Error T	Error B
Frank	1	1495	36	1	0.0241	1495.0000	1517.5700	37.2600	1.0400	0.0257	1449.2100	0.0151	0.0350	0.0400	0.0673	0.0306
	2	1495	25	2	0.0334	747.5000	1470.0000	25.3900	2.0500	0.0354	716.8000	0.0167	0.0156	0.0250	0.0585	0.0411
	3	1495	9	4	0.0241	373.7500	1517.5700	9.0500	4.3100	0.0257	352.0500	0.0151	0.0056	0.0775	0.0673	0.0581
	4	1495	9	5	0.0301	299.0000	1493.3300	9.2700	5.1000	0.0317	292.4400	0.0011	0.0300	0.0200	0.0531	0.0219
	5	2195	25	3	0.0342	731.6667	2216.6600	25.7200	3.6600	0.0425	604.3300	0.0099	0.0288	0.2200	0.2438	0.1740
	6	2195	16	4	0.0292	548.7500	2187.5000	16.4300	4.8400	0.0364	451.1700	0.0034	0.0269	0.2100	0.2484	0.1778
	7	2195	16	5	0.0364	439.0000	2187.5000	15.6000	6.2800	0.0448	347.8100	0.0034	0.0250	0.2560	0.2292	0.2077
	8	2195	16	6	0.0437	365.8333	2187.5000	15.5600	7.5400	0.0537	289.8400	0.0034	0.0275	0.2567	0.2278	0.2077
P1	1	1495	36	1	0.0241	1495.0000	1517.5700	37.2600	1.0400	0.0257	1449.2100	0.0151	0.0350	0.0400	0.0673	0.0306
	2	1495	25	2	0.0334	747.5000	1467.2000	25.3900	2.0400	0.0354	716.8000	0.0186	0.0156	0.0200	0.0585	0.0411
	3	1495	9	4	0.0241	373.7500	1517.5700	9.9800	3.9200	0.0258	386.2300	0.0151	0.1089	0.0200	0.0714	0.0334
	4	1495	9	5	0.0301	299.0000	1493.3300	8.9600	5.3300	0.0320	280.0000	0.0011	0.0044	0.0660	0.0631	0.0635
	5	2195	16	4	0.0292	548.7500	2187.5000	16.6300	4.7300	0.0360	462.1000	0.0034	0.0394	0.1825	0.2347	0.1579
	6	2195	16	5	0.0364	439.0000	2187.5000	15.9400	6.2100	0.0452	352.1800	0.0034	0.0038	0.0240	0.2402	0.1978
	7	2195	16	6	0.0437	365.8333	2187.5000	16.5300	7.1400	0.0540	306.2500	0.0034	0.0331	0.1900	0.2347	0.1629
	8	2195	25	3	0.0342	731.6667	2216.6600	25.5400	3.6800	0.0424	602.0000	0.0099	0.0216	0.2267	0.2409	0.1772
P2	1	1495	36	1	0.0241	1495.0000	1418.4500	33.5000	1.1000	0.0261	1281.7300	0.0512	0.0694	0.1000	0.0839	0.1427
	2	1495	16	2	0.0214	747.5000	1401.3600	14.1700	2.3200	0.0235	601.5600	0.0626	0.1144	0.1600	0.0979	0.1952
	3	1495	16	3	0.0321	498.3333	1414.5800	14.5300	3.4800	0.0358	405.4100	0.0538	0.0919	0.1600	0.1150	0.1865
	4	2195	36	3	0.0492	731.6667	2284.7200	34.5000	4.2000	0.0635	542.8200	0.0409	0.0417	0.4000	0.2906	0.2581
	5	2195	16	4	0.0292	548.7500	2187.5000	14.8600	5.6300	0.0382	388.2800	0.0034	0.0713	0.4075	0.3101	0.2924
	6	2195	16	5	0.0364	439.0000	2240.0000	18.9000	5.7200	0.0482	391.5600	0.0205	0.1813	0.1440	0.3225	0.1081
	1	1495	36	1	0.0241	1495.0000	1438.9600	37.6400	0.9800	0.0258	1456.0500	0.0375	0.0456	0.0200	0.0714	0.0261
	2	1495	25	2	0.0334	747.5000	1386.0000	11.0200	2.9800	0.0237	464.8000	0.0729	0.5592	0.4900	0.2914	0.3782
P3	3	1495	9	4	0.0241	373.7500	1555.1700	6.9000	5.7500	0.0250	270.0100	0.0402	0.2333	0.4375	0.0382	0.2776
	4	1495	9	5	0.0301	299.0000	1524.4400	7.4600	6.4400	0.0315	236.4400	0.0197	0.1711	0.2880	0.0465	0.2092
	5	2195	25	3	0.0342	731.6667	2226.0000	27.3200	3.4500	0.0424	644.0000	0.0141	0.0928	0.1500	0.2409	0.1198
	6	2195	16	4	0.0292	548.7500	2214.8400	16.4300	4.9000	0.0364	451.1700	0.0090	0.0269	0.2250	0.2484	0.1778
	7	2195	16	6	0.0437	365.8333	2205.7200	15.3400	7.6500	0.0532	288.0200	0.0049	0.0413	0.2750	0.2164	0.2127
	8	2195	16	5	0.0364	439.0000	2187.5000	16.2300	6.0200	0.0447	363.1200	0.0034	0.0144	0.0204	0.2265	0.1728
	1	1495	36	1	0.0241	1495.0000	1555.1700	37.2600	1.0700	0.0257	1449.2100	0.0402	0.0350	0.0700	0.0673	0.0306
	2	1495	25	2	0.0334	747.5000	1498.0000	25.3900	2.0800	0.0354	716.8000	0.0020	0.0156	0.0400	0.0585	0.0411
P4	3	1495	9	4	0.0241	373.7500	1476.5600	9.3300	4.1100	0.0260	358.8800	0.0123	0.0367	0.0275	0.0797	0.0398
	4	1495	9	5	0.0301	299.0000	1493.3300	8.9600	5.3300	0.0320	280.0000	0.0011	0.0044	0.0660	0.0631	0.0635
	5	2195	25	3	0.0342	731.6667	2158.3300	25.5400	3.5800	0.0422	602.0000	0.0167	0.0216	0.1933	0.2351	0.1772
	6	2195	16	4	0.0292	548.7500	2214.8400	16.6300	4.7900	0.0360	462.1000	0.0090	0.0394	0.1975	0.2347	0.1579
	7	2195	16	6	0.0437	365.8333	2205.7200	15.5600	7.6100	0.0537	289.8400	0.0049	0.0275	0.2683	0.2278	0.2077
	8	2195	16	5	0.0364	439.0000	2209.3700	16.6400	6.0100	0.0452	367.5000	0.0065	0.0400	0.0200	0.2402	0.1629

Table 68. Original Parameters vs. Extracted Parameters (SNR = 0 dB).

Signal Type	Actual Parameters						Extracted Parameters						Error			
	Signal #	Carrier Frequency	Number of Subcodes	Carrier Cycles per Subcode	Code Period	Bandwidth	Carrier Frequency	Number of Subcodes	Carrier Cycles per Subcode	Code Period	Bandwidth	Error fc	Error Nc	Error cnp	Error T	Error B
Frank	1	1495	36	1	0.0241	1495.0000	1517.5700	37.2600	1.0400	0.0257	1449.2100	0.0151	0.0350	0.0400	0.0673	0.0306
	2	1495	25	2	0.0334	747.5000	1540.0000	25.3900	2.1400	0.0354	716.8000	0.0301	0.0156	0.0700	0.0585	0.0411
	3	1495	9	4	0.0241	373.7500	1517.5700	9.0500	4.3100	0.0257	352.0500	0.0151	0.0056	0.0775	0.0673	0.0581
	4	1495	9	5	0.0301	299.0000	1493.3300	8.7400	5.3900	0.0315	276.8800	0.0011	0.0289	0.0780	0.0465	0.0740
	5	2195	25	3	0.0342	731.6667	2219.0000	25.7200	3.6700	0.0425	604.3300	0.0109	0.0288	0.2233	0.2438	0.1740
	6	2195	16	4	0.0292	548.7500	2184.7600	16.8000	4.7000	0.0361	464.8400	0.0047	0.0500	0.1750	0.2381	0.1529
	7	2195	16	5	0.0364	439.0000	2187.5000	16.2300	6.0200	0.0447	363.1200	0.0034	0.0144	0.2040	0.2265	0.1728
	8	2195	16	6	0.0437	365.8333	2185.6700	16.1200	7.2200	0.0532	302.6000	0.0043	0.0075	0.2033	0.2164	0.1728
P1	1	1495	36	1	0.0241	1495.0000	1750.0000	37.2600	1.2000	0.0257	1449.2100	0.1706	0.0350	0.2000	0.0673	0.0306
	2	1495	25	2	0.0334	747.5000	1456.0000	25.3900	2.0300	0.0354	716.8000	0.0261	0.0156	0.0150	0.0585	0.0411
	3	1495	9	4	0.0241	373.7500	1459.4700	9.6800	3.9100	0.0260	372.5500	0.0238	0.0756	0.0225	0.0797	0.0032
	4	1495	9	5	0.0301	299.0000	1490.2200	9.0900	5.1500	0.0314	289.3300	0.0032	0.0100	0.0300	0.0432	0.0323
	5	2195	16	4	0.0292	548.7500	2187.5000	16.6300	4.7300	0.0360	462.1000	0.0034	0.0394	0.1825	0.2347	0.1579
	6	2195	16	5	0.0364	439.0000	2187.5000	16.2300	6.0200	0.0447	363.1200	0.0034	0.0144	0.2040	0.2265	0.1728
	7	2195	16	6	0.0437	365.8333	2187.5000	16.3500	7.1800	0.0537	304.4200	0.0034	0.0219	0.1967	0.2278	0.1679
	8	2195	25	3	0.0342	731.6667	2158.3300	25.5400	3.5800	0.0424	602.0000	0.0167	0.0216	0.1933	0.2409	0.1772
P2	1	1495	36	1	0.0241	1495.0000	1380.8500	36.2500	0.9900	0.0260	1394.5300	0.0764	0.0069	0.0100	0.0797	0.0672
	2	1495	16	2	0.0214	747.5000	1401.3600	15.6100	2.1000	0.0234	666.5000	0.0626	0.0244	0.0500	0.0932	0.1084
	3	1495	16	3	0.0321	498.3333	1446.6600	14.1200	3.7000	0.0361	390.8300	0.0323	0.1175	0.2333	0.1244	0.2157
	4	2195	36	3	0.0492	731.6667	2333.3300	38.2300	3.8700	0.0634	602.7700	0.0630	0.0619	0.2900	0.2885	0.1762
	5	2195	16	4	0.0292	548.7500	2187.5000	14.8600	5.6300	0.0382	388.2800	0.0034	0.0713	0.4075	0.3101	0.2924
	6	2195	16	5	0.0364	439.0000	2220.3100	15.3000	7.0400	0.0485	315.0000	0.0115	0.0438	0.4080	0.3307	0.2825
	1	1495	36	1	0.0241	1495.0000	1401.3600	37.6400	0.9800	0.0258	1456.0500	0.0626	0.0456	0.0200	0.0714	0.0261
	2	1495	25	2	0.0334	747.5000	1414.0000	23.9000	2.1000	0.0355	672.0000	0.0542	0.0440	0.0500	0.0614	0.1010
P3	3	1495	9	4	0.0241	373.7500	1555.1700	-1479.7200	0.0300	-0.0328	450.35.1500	0.0402	165.4133	0.9925	2.3621	119.4954
	4	1495	9	5	0.0301	299.0000	1508.8800	7.1300	6.7300	0.0318	224.0000	0.0093	0.2078	0.3460	0.0565	0.2508
	5	2195	25	3	0.0342	731.6667	2251.6600	27.3200	3.4900	0.0424	644.0000	0.0258	0.0928	0.1633	0.2409	0.1198
	6	2195	16	4	0.0292	548.7500	2214.8400	15.6700	5.1200	0.0362	432.0300	0.0090	0.0206	0.2800	0.2415	0.2127
	7	2195	16	6	0.0437	365.8333	2178.3800	16.1200	7.1900	0.0532	302.6000	0.0076	0.0075	0.1983	0.2164	0.1728
	8	2195	16	5	0.0364	439.0000	2187.5000	16.2300	6.0200	0.0447	363.1250	0.0034	0.0144	0.2040	0.2265	0.1728
	1	1495	36	1	0.0241	1495.0000	1476.5600	37.2600	1.0100	0.0257	1449.2100	0.0123	0.0350	0.0100	0.0673	0.0306
	2	1495	25	2	0.0334	747.5000	1526.0000	25.3900	2.1200	0.0354	716.8000	0.0207	0.0156	0.0600	0.0585	0.0411
P4	3	1495	9	4	0.0241	373.7500	1497.0700	8.6500	4.4200	0.0255	338.3700	0.0014	0.0389	0.1050	0.0590	0.0947
	4	1495	9	5	0.0301	299.0000	1490.2200	8.9600	5.3200	0.0320	280.0000	0.0032	0.0044	0.0640	0.0631	0.0635
	5	2195	25	3	0.0342	731.6667	2240.4000	25.5400	3.7200	0.0424	602.0000	0.0205	0.0216	0.2400	0.2409	0.1772
	6	2195	16	4	0.0292	548.7500	2173.8200	16.6300	4.7000	0.0360	462.1000	0.0096	0.0394	0.1750	0.2347	0.1579
	7	2195	16	6	0.0437	365.8333	2196.6100	15.5600	7.5700	0.0537	289.8400	0.0007	0.0275	0.2617	0.2278	0.2077
	8	2195	16	5	0.0364	439.0000	2187.5000	15.6000	6.2800	0.0448	347.8100	0.0034	0.0250	0.2560	0.2292	0.2077

Table 69. Original Parameters vs. Extracted Parameters (SNR = -3 dB).

Signal Type	Actual Parameters					Extracted Parameters					Error				
	Signal #	Carrier Frequency	Number of Subcodes	Carrier Cycles per Subcode	Code Period	Bandwidth	Carrier Frequency	Number of Subcodes	Carrier Cycles per Subcode	Code Period	Bandwidth	Error fc	Error Nc	Error cpp	Error T
Frank	1	1495	36	1	0.0241	1495.0000	1520.9900	37.2600	1.0490	0.0257	1449.2100	0.0174	0.0350	0.0490	0.0673
	2	1495	25	2	0.0334	747.5000	1470.0000	25.8000	2.0300	0.0357	722.4000	0.0167	0.0320	0.0150	0.0336
	3	1495	9	4	0.0241	373.7500	1476.5600	8.8600	4.2300	0.0254	348.6300	0.0123	0.0156	0.0575	0.0672
	4	1495	9	5	0.0301	299.0000	1452.8800	5.2400	8.7400	0.0315	276.8800	0.0282	0.4178	0.7480	0.0465
	5	2195	25	3	0.0342	731.6667	2193.3300	25.7200	3.6200	0.0425	604.3300	0.0008	0.0288	0.2067	0.2438
	6	2195	16	4	0.0292	548.7500	2228.5100	16.4300	4.9300	0.0364	451.1700	0.0153	0.0269	0.2325	0.2484
	7	2195	16	5	0.0364	439.0000	2187.5000	15.4000	6.3200	0.0445	345.6200	0.0034	0.0375	0.2640	0.2210
	8	2195	16	6	0.0437	365.8333	2205.7200	16.1200	7.2800	0.0532	302.6000	0.0049	0.0075	0.2133	0.2164
P1	1	1495	36	1	0.0241	1495.0000	1418.4500	37.2600	0.9700	0.0257	1449.2100	0.0512	0.0350	0.0300	0.0673
	2	1495	25	2	0.0334	747.5000	1363.6000	25.3900	1.9000	0.0354	716.8000	0.0879	0.0156	0.0500	0.0585
	3	1495	9	4	0.0241	373.7500	1514.1600	-64.4200	0.1600	-0.0068	9395.9900	0.0128	8.1578	0.9600	1.2824
	4	1495	9	5	0.0301	299.0000	1487.1100	-206.2400	0.0900	-0.0128	16040.8800	0.0053	23.9156	0.9820	1.4252
	5	2195	16	4	0.0292	548.7500	2242.1800	16.8000	4.8200	0.0361	464.8400	0.0215	0.0500	0.2050	0.2381
	6	2195	16	5	0.0364	439.0000	2231.2500	15.9400	6.3300	0.0452	352.1800	0.0165	0.0038	0.2660	0.2402
	7	2195	16	6	0.0437	365.8333	2187.5000	16.5300	7.1400	0.0540	306.2500	0.0034	0.0331	0.1900	0.2347
	8	2195	25	3	0.0342	731.6667	2179.3300	25.7200	3.6000	0.0425	604.3300	0.0071	0.0288	0.2000	0.2438
P2	1	1495	36	1	0.0241	1495.0000	1582.5100	33.5000	1.2300	0.0261	1281.7300	0.0585	0.0694	0.2300	0.0839
	2	1495	16	2	0.0214	747.5000	1490.2300	17.5600	2.0000	0.0235	745.1100	0.0032	0.0975	0.0000	0.0979
	3	1495	16	3	0.0321	498.3333	1446.6600	168.4200	0.1000	0.0120	14035.0000	0.0323	9.5263	0.9667	0.6263
	4	2195	36	3	0.0492	731.6667	2234.4900	34.5000	4.1100	0.0635	542.8200	0.0180	0.0417	0.3700	0.2906
	5	2195	16	4	0.0292	548.7500	2214.8400	14.8600	5.7000	0.0382	388.2800	0.0090	0.0713	0.4250	0.3101
	6	2195	16	5	0.0364	439.0000	2128.4300	11.0100	7.4200	0.0380	286.5600	0.0303	0.3119	0.4840	0.3472
	1	1495	36	1	0.0241	1495.0000	1442.3800	37.2600	0.9900	0.0257	1449.2100	0.0352	0.0350	0.0100	0.0673
	2	1495	25	2	0.0334	747.5000	1439.2000	16.0000	2.5700	0.0285	560.0000	0.0373	0.3600	0.2850	0.1479
P3	3	1495	9	4	0.0241	373.7500	1538.0800	-114.5600	0.1200	-0.0091	12530.2700	0.0288	13.7289	0.9700	1.3779
	4	1495	9	5	0.0301	299.0000	1524.4400	6.9400	6.9000	0.0314	220.8800	0.0197	0.2289	0.3800	0.0432
	5	2195	25	3	0.0342	731.6667	2125.6600	-733.5600	0.0800	-0.0280	26198.6600	0.0316	30.3424	0.9733	1.8195
	6	2195	16	4	0.0292	548.7500	2176.5600	16.4300	4.8200	0.0364	451.1700	0.0084	0.0269	0.2050	0.2484
	7	2195	16	6	0.0437	365.8333	2185.6700	16.1200	7.2200	0.0532	302.6000	0.0043	0.0075	0.2033	0.2164
	8	2195	16	5	0.0364	439.0000	2121.8700	15.6000	6.1000	0.0448	347.8100	0.0333	0.0250	0.2200	0.2077
	1	1495	36	1	0.0241	1495.0000	1360.3500	37.2600	0.9300	0.0257	1449.2100	0.0901	0.0350	0.0700	0.0673
	2	1495	25	2	0.0334	747.5000	1540.0000	25.1900	2.1500	0.0352	714.0000	0.0301	0.0076	0.0750	0.0525
P4	3	1495	9	4	0.0241	373.7500	1517.5700	9.6800	4.0700	0.0260	372.5500	0.0157	0.0756	0.0175	0.0797
	4	1495	9	5	0.0301	299.0000	1505.7700	8.9600	5.3700	0.0320	280.0000	0.0072	0.0044	0.0740	0.0631
	5	2195	25	3	0.0342	731.6667	2228.3300	25.5400	3.7000	0.0424	602.0000	0.0152	0.0216	0.2333	0.2409
	6	2195	16	4	0.0292	548.7500	2121.8700	16.6300	4.5900	0.0360	462.1000	0.0333	0.0394	0.1475	0.2347
	7	2195	16	6	0.0437	365.8333	2205.7200	16.3500	7.2400	0.0537	304.4200	0.0049	0.0219	0.2067	0.2278
	8	2195	16	5	0.0364	439.0000	2165.6200	16.4300	5.9200	0.0450	365.3100	0.0134	0.0269	0.1840	0.2347

Table 70. Original Parameters vs. Extracted Parameters (SNR = -6 dB).

Signal Type	Actual Parameters					Extracted Parameters					Error				
	Signal #	Carrier Frequency	Number of Subcodes	Carrier Cycles per Subcode	Code Period	Bandwidth	Carrier Frequency	Number of Subcodes	Carrier Cycles per Subcode	Code Period	Bandwidth	Error fc	Error Nc	Error cpp	Error B
Frank	1	1495	36	1	0.0241	1495.0000	1425.2900	37.2600	0.9800	0.0257	1449.2100	0.0466	0.0350	0.0200	0.0306
	2	1495	25	2	0.0334	747.5000	1341.2000	25.3900	1.8700	0.0354	716.8000	0.1029	0.0156	0.0650	0.0411
	3	1495	9	4	0.0241	373.7500	3407.7100	-75.6300	0.3300	-0.0074	10182.1200	1.2794	9.4033	0.9175	1.3073
	4	1495	9	5	0.0301	299.0000	1536.8800	8.7400	5.5500	0.0315	276.8800	0.0280	0.0289	0.1100	0.0465
	5	2195	25	3	0.0342	731.6667	2219.0000	-270.4000	0.1300	-0.0170	15906.3300	0.0109	11.8160	0.9567	20.7399
	6	2195	16	4	0.0292	548.7500	2127.3400	-139.6300	0.1700	-0.0112	12373.0400	0.0308	9.7269	0.9575	1.3841
	7	2195	16	5	0.0364	439.0000	2301.2500	16.4300	6.2900	0.0450	365.3100	0.0484	0.0269	0.2580	0.1679
	8	2195	16	6	0.0437	365.8333	2178.3800	15.5600	7.5100	0.0537	289.8400	0.0076	0.0275	0.2517	0.2077
P1	1	1495	36	1	0.0241	1495.0000	1753.4100	37.2600	1.2000	0.0257	1449.2100	0.1728	0.0350	0.2000	0.0306
	2	1495	25	2	0.0334	747.5000	1318.8000	25.3900	1.8300	0.0354	716.8000	0.1179	0.0156	0.0850	0.0411
	3	1495	9	4	0.0241	373.7500	2221.6700	-67.1500	0.2300	-0.0070	9594.2300	0.4861	8.4611	0.9425	1.2907
	4	1495	9	5	0.0301	299.0000	1505.7700	0.0000	0.0000	0.0000	0.0000	0.0072	1.0000	1.0000	1.0000
	5	2195	16	4	0.0292	548.7500	2873.8200	-201.9400	0.1900	-0.0135	14880.4600	0.3093	13.6213	0.9525	1.4630
	6	2195	16	5	0.0364	439.0000	2229.0600	15.6000	6.4000	0.0448	347.8100	0.0155	0.0250	0.2800	0.2077
	7	2195	16	6	0.0437	365.8333	2171.0900	-88.4400	0.2700	-0.0110	8040.8800	0.0109	6.5275	0.9550	20.9796
	8	2195	25	3	0.0342	731.6667	2172.3300	25.5400	3.6000	0.0424	602.0000	0.1013	0.0216	0.2000	0.1772
P2	1	1495	36	1	0.0241	1495.0000	1028.8000	332.3200	0.0400	0.0155	21341.7900	0.3118	8.2311	0.9600	13.2754
	2	1495	16	2	0.0214	747.5000	1360.3500	144.9800	0.0960	0.0102	14095.7000	0.0901	8.0613	0.9520	17.8571
	3	1495	16	3	0.0321	498.3333	1528.3300	268.1800	0.0800	0.0151	17710.0000	0.0223	15.7613	0.9733	34.5385
	4	2195	36	3	0.0492	731.6667	2407.8700	124.7700	0.2600	0.0138	9004.3900	0.0970	2.4658	0.9133	11.3067
	5	2195	16	4	0.0292	548.7500	2187.5000	189.3900	0.1500	0.0131	14410.1500	0.0034	10.8369	0.9625	0.5507
	6	2195	16	5	0.0364	439.0000	2025.6200	355.8900	0.1100	0.0201	17668.4300	0.0772	21.2431	0.9780	39.2470
	1	1495	36	1	0.0241	1495.0000	1630.3700	39.9900	1.0600	0.0260	1538.0800	0.0905	0.1108	0.0600	0.0288
	2	1495	25	2	0.0334	747.5000	1752.8000	-122.1100	0.1400	-0.0104	11709.6000	0.1724	5.8844	0.9300	1.3110
P3	3	1495	9	4	0.0241	373.7500	957.0300	-5440.1400	0.0100	-0.0630	86351.5600	0.3598	605.4600	0.9975	230.0410
	4	1495	9	5	0.0301	299.0000	1487.1100	-224.9700	0.0800	-0.0134	16753.3300	0.0053	25.9967	0.9840	1.4452
	5	2195	25	3	0.0342	731.6667	2125.6600	-293.5900	0.1200	-0.0177	16573.6600	0.0316	12.7436	0.9600	1.5180
	6	2195	16	4	0.0292	548.7500	2258.5900	-45.3100	0.3200	-0.0064	7049.2100	0.0290	3.8319	0.9200	1.2195
	7	2195	16	6	0.0437	365.8333	2178.3800	15.5600	7.5100	0.0537	289.8400	0.0076	0.0275	0.2517	0.2077
	8	2195	16	5	0.0364	439.0000	2154.6800	-906.3200	0.0700	-0.0321	28196.8700	0.0184	57.6450	0.9860	63.2298
	1	1495	36	1	0.0241	1495.0000	1363.7600	37.2600	0.9400	0.0257	1449.2100	0.0878	0.0350	0.0600	0.0306
	2	1495	25	2	0.0334	747.5000	1677.2000	26.0800	2.2600	0.0352	739.2000	0.1219	0.0432	0.1300	0.0525
P4	3	1495	9	4	0.0241	373.7500	0.0000	-114.5600	0.0000	-0.0091	1370.2700	1.0000	13.7289	1.0000	32.5258
	4	1495	9	5	0.0301	299.0000	1524.4400	-770.8500	0.0400	-0.0248	31011.5500	0.0197	86.6500	0.9920	1.8239
	5	2195	25	3	0.0342	731.6667	2146.6600	25.7200	3.5500	0.0425	604.3300	0.0220	0.0288	0.1833	0.2438
	6	2195	16	4	0.0292	548.7500	2187.5000	16.6300	4.7300	0.0360	462.1000	0.0034	0.0394	0.1825	0.2347
	7	2195	16	6	0.0437	365.8333	2214.8400	16.3500	7.2700	0.0537	304.4200	0.0090	0.0219	0.2117	0.2278
	8	2195	16	5	0.0364	439.0000	2231.2500	-812.1900	0.0800	-0.0304	26691.8700	0.0165	51.7619	0.9840	1.8341
															59.8015

## B. PARAMETER EXTRACTION RESULTS FOR POLYPHASE CODED LPI MODULATIONS USING CWD IMAGES

Table 71. Original Parameters vs. Extracted Parameters (SNR = 6 dB).

Signal Type	Actual Parameters					Extracted Parameters					Error				
	Signal #	Carrier Frequency	Number of Subcodes	Carrier Cycles per Subcode	Code Period	Bandwidth	Carrier Frequency	Number of Subcodes	Carrier Cycles per Subcode	Code Period	Bandwidth	Error fc	Error Nc	Error cpp	Error T
Frank	1	1495	36	1	0.0241	1495.0000	1462.8900	31.6100	1.2600	0.0272	1158.6900	0.0215	0.1219	0.2600	0.1296
	2	1495	25	2	0.0334	747.5000	1447.6000	24.8000	2.0800	0.0357	694.4000	0.0317	0.0080	0.0400	0.0674
	3	1495	9	4	0.0241	373.7500	1421.8700	9.8800	3.9200	0.0272	362.3000	0.0489	0.0978	0.0200	0.1296
	4	1495	9	5	0.0301	299.0000	1546.2200	9.7000	5.1200	0.0321	301.7700	0.0343	0.0778	0.0240	0.0664
	5	2195	25	3	0.0342	731.6667	2167.6600	24.8000	3.7400	0.0428	578.6600	0.0125	0.0080	0.2467	0.2526
	6	2195	16	4	0.0292	548.7500	2184.7600	16.5000	4.8400	0.0365	451.1700	0.0047	0.0313	0.2100	0.2518
	7	2195	16	5	0.0364	439.0000	2104.3700	17.1000	5.6200	0.0457	374.0600	0.0413	0.0688	0.1240	0.2539
	8	2195	16	6	0.0437	365.8333	2225.7800	18.3000	6.6700	0.0548	333.5900	0.0140	0.1438	0.1117	0.2530
P1	1	1495	36	1	0.0241	1495.0000	1476.5600	31.9600	1.2600	0.0274	1165.5200	0.0123	0.1122	0.2600	0.1379
	2	1495	25	2	0.0334	747.5000	1618.4000	25.1000	2.3000	0.0357	702.8000	0.0825	0.0040	0.1500	0.0674
	3	1495	9	4	0.0241	373.7500	1483.3900	11.5000	3.6400	0.0282	406.7300	0.0078	0.2778	0.0900	0.1711
	4	1495	9	5	0.0301	299.0000	1462.2200	10.1000	4.6500	0.0321	314.2200	0.0219	0.1222	0.0700	0.0664
	5	2195	16	4	0.0292	548.7500	2296.8700	15.7000	5.3500	0.0365	429.2900	0.0464	0.0188	0.3375	0.2518
	6	2195	16	5	0.0364	439.0000	2194.0600	17.6000	5.6900	0.0457	385.0000	0.0004	0.1000	0.1380	0.2539
	7	2195	16	6	0.0437	365.8333	2220.3100	17.7000	6.8800	0.0548	322.6500	0.0115	0.1063	0.1467	0.2530
	8	2195	25	3	0.0342	731.6667	2137.3300	26.1000	3.5000	0.0428	609.0000	0.0263	0.0440	0.1667	0.2526
P2	1	1495	36	1	0.0241	1495.0000	1479.9800	30.5300	1.3300	0.0275	1107.4200	0.0100	0.1519	0.3300	0.1420
	2	1495	16	2	0.0214	747.5000	1456.0500	13.9200	2.6200	0.0251	553.7100	0.0261	0.1300	0.3100	0.1726
	3	1495	16	3	0.0321	498.3333	1531.2500	15.6000	3.3600	0.0342	455.0000	0.0242	0.0250	0.1200	0.0652
	4	2195	36	3	0.0492	731.6667	2129.1600	32.4000	4.0500	0.0617	525.0000	0.0300	0.1000	0.3500	0.2540
	5	2195	16	4	0.0292	548.7500	2228.5100	14.7600	5.9900	0.0397	371.8700	0.0153	0.0775	0.4975	0.3616
	6	2195	16	5	0.0364	439.0000	2198.4300	16.5000	6.0900	0.0457	360.9300	0.0016	0.0313	0.2180	0.2539
	1	1495	36	1	0.0241	1495.0000	1565.4200	31.9800	1.3300	0.0272	1172.3600	0.0471	0.1117	0.3300	0.1296
	2	1495	25	2	0.0334	747.5000	1495.2000	18.5000	2.8800	0.0357	518.0000	0.0001	0.2600	0.4400	0.0674
P3	3	1495	9	4	0.0241	373.7500	1483.3900	7.9800	5.3500	0.0288	276.8500	0.0078	0.1133	0.3375	0.1960
	4	1495	9	5	0.0301	299.0000	1452.8800	7.6000	6.1400	0.0321	236.4400	0.0282	0.1556	0.2280	0.0664
	5	2195	25	3	0.0342	731.6667	2223.6600	20.3000	4.6900	0.0428	473.6600	0.0131	0.1880	0.5633	0.2526
	6	2195	16	4	0.0292	548.7500	2108.2000	17.0000	4.5300	0.0365	464.8400	0.0395	0.0625	0.1325	0.2518
	7	2195	16	6	0.0437	365.8333	2265.8800	17.1000	7.2600	0.0548	311.7100	0.0323	0.0688	0.2100	0.2530
	8	2195	16	5	0.0364	439.0000	2145.9300	17.6000	5.5700	0.0457	385.0000	0.0224	0.1000	0.1140	0.2539
	1	1495	36	1	0.0241	1495.0000	1397.9400	28.6400	1.3400	0.0275	1039.0600	0.0649	0.2044	0.3400	0.1420
	2	1495	25	2	0.0334	747.5000	1635.2000	25.7000	2.2700	0.0357	719.6000	0.0938	0.0280	0.1350	0.0674
P4	3	1495	9	4	0.0241	373.7500	1462.8900	11.0300	3.7800	0.0285	386.2300	0.0215	0.2256	0.0550	0.1835
	4	1495	9	5	0.0301	299.0000	1459.1100	10.6000	4.4200	0.0321	329.7700	0.0240	0.1778	0.1160	0.0664
	5	2195	25	3	0.0342	731.6667	2123.3300	25.0000	3.6400	0.0428	583.3300	0.0327	0.0000	0.2133	0.2526
	6	2195	16	4	0.0292	548.7500	2132.8100	15.7400	4.5000	0.0332	473.0400	0.0283	0.0163	0.1250	0.1387
	7	2195	16	6	0.0437	365.8333	2132.8100	18.1000	6.4600	0.0548	329.9400	0.0283	0.1313	0.0767	0.2530
	8	2195	16	5	0.0364	439.0000	2196.2500	17.1000	5.8700	0.0457	374.0600	0.0006	0.0688	0.1740	0.2539

Table 72. Original Parameters vs. Extracted Parameters (SNR = 0 dB).

0 dB																
Signal Type	Signal #	Actual Parameters				Extracted Parameters				Error						
		Carrier Frequency	Number of Subcodes	Carrier Cycles per Subcode	Code Period	Bandwidth	Carrier Frequency	Number of Subcodes	Carrier Cycles per Subcode	Code Period	Bandwidth	Error fc	Error Nc	Error opp	Error T	Error B
Frank	1	1495	36	1	0.0241	1495.0000	1527.8300	28.2500	1.4700	0.0272	1035.6400	0.0220	0.2153	0.4700	0.1296	0.3073
	2	1495	25	2	0.0334	747.5000	1391.6000	24.0000	2.0700	0.0357	672.0000	0.0692	0.0400	0.0350	0.0674	0.1010
	3	1495	9	4	0.0241	373.7500	1425.2900	10.1600	3.8200	0.0272	372.5500	0.0466	0.1289	0.0450	0.1296	0.0032
	4	1495	9	5	0.0301	299.0000	1415.5500	10.1000	4.5000	0.0321	314.2200	0.0531	0.1222	0.1000	0.0664	0.0509
	5	2195	25	3	0.0342	731.6667	2321.6600	27.7000	3.5900	0.0428	646.3300	0.0577	0.1080	0.1967	0.2526	0.1166
	6	2195	16	4	0.0292	548.7500	2179.2900	16.8000	4.7400	0.0365	459.3700	0.0072	0.0500	0.1850	0.2518	0.1629
	7	2195	16	5	0.0364	439.0000	2187.5000	16.0000	5.6800	0.0415	385.0000	0.0034	0.0000	0.1360	0.1387	0.1230
	8	2195	16	6	0.0437	365.8333	2225.7800	19.7000	6.1900	0.0548	359.1100	0.0140	0.2313	0.0317	0.2530	0.0184
P1	1	1495	36	1	0.0241	1495.0000	2173.8200	38.1400	1.5500	0.0272	1397.9400	0.4541	0.0594	0.5500	0.1296	0.0649
	2	1495	25	2	0.0334	747.5000	1503.6000	25.0000	2.1400	0.0357	700.0000	0.0058	0.0000	0.0700	0.0674	0.0635
	3	1495	9	4	0.0241	373.7500	1613.2800	12.2100	3.6000	0.0272	447.7500	0.0791	0.3567	0.1000	0.1296	0.1980
	4	1495	9	5	0.0301	299.0000	1490.2200	10.4000	4.6000	0.0321	323.5500	0.0032	0.1556	0.0800	0.0664	0.0821
	5	2195	16	4	0.0292	548.7500	2132.8100	19.3000	4.3000	0.0390	494.9200	0.0283	0.2063	0.0750	0.3376	0.0981
	6	2195	16	5	0.0364	439.0000	2242.1800	17.9500	6.0200	0.0482	371.8700	0.0215	0.1219	0.2040	0.3225	0.1529
	7	2195	16	6	0.0437	365.8333	2218.4800	18.3000	6.6500	0.0548	333.5900	0.0107	0.1438	0.1083	0.2530	0.0881
	8	2195	25	3	0.0342	731.6667	2226.0000	26.5000	3.6000	0.0428	618.3300	0.0141	0.0600	0.2000	0.2526	0.1549
P2	1	1495	36	1	0.0241	1495.0000	1397.9400	28.3700	1.3700	0.0278	1018.5500	0.0649	0.2119	0.3700	0.1545	0.3187
	2	1495	16	2	0.0214	747.5000	1606.4400	14.0200	2.7900	0.0244	574.2100	0.0745	0.1238	0.3950	0.1399	0.2318
	3	1495	16	3	0.0321	498.3333	1531.2500	15.5000	3.3800	0.0342	452.0800	0.0242	0.0313	0.1267	0.0652	0.0928
	4	2195	36	3	0.0492	731.6667	2129.1600	36.6800	3.7900	0.0654	560.6400	0.0300	0.0189	0.2633	0.3292	0.2337
	5	2195	16	4	0.0292	548.7500	2214.8400	14.6000	5.9500	0.0392	371.8700	0.0090	0.0875	0.4875	0.3444	0.3223
	6	2195	16	5	0.0364	439.0000	2196.2500	19.3000	5.2000	0.0457	422.1800	0.0006	0.2063	0.0400	0.2539	0.0383
	1	1495	36	1	0.0241	1495.0000	1155.2700	32.1100	0.9900	0.0277	1158.6900	0.2272	0.1081	0.0100	0.1503	0.2250
	2	1495	25	2	0.0334	747.5000	1498.0000	18.9000	2.8300	0.0357	529.2000	0.0020	0.2440	0.4150	0.0674	0.2920
P3	3	1495	9	4	0.0241	373.7500	1473.1400	9.4200	4.4800	0.0287	328.1200	0.0146	0.0467	0.1200	0.1918	0.1221
	4	1495	9	5	0.0301	299.0000	1456.0000	7.5000	6.2400	0.0321	233.3300	0.0261	0.1667	0.2480	0.0664	0.2196
	5	2195	25	3	0.0342	731.6667	2228.3300	24.0000	3.9700	0.0428	560.0000	0.0152	0.0400	0.3233	0.2526	0.2346
	6	2195	16	4	0.0292	548.7500	2108.2000	16.2000	4.7500	0.0365	442.9600	0.0395	0.0125	0.1875	0.2518	0.1928
	7	2195	16	6	0.0437	365.8333	2260.4100	17.6000	7.0400	0.0548	320.8300	0.0298	0.1000	0.1733	0.2530	0.1230
	8	2195	16	5	0.0364	439.0000	2174.3700	19.6200	5.4900	0.0495	395.9300	0.0094	0.2263	0.0980	0.3582	0.0981
	1	1495	36	1	0.0241	1495.0000	1883.3000	40.9700	1.7000	0.0370	1107.4200	0.2597	0.1381	0.7000	0.5365	0.2593
	2	1495	25	2	0.0334	747.5000	1517.6000	25.6600	2.2300	0.0377	680.4000	0.0014	0.0264	0.1150	0.1272	0.0898
P4	3	1495	9	4	0.0241	373.7500	1497.0700	10.2800	4.0500	0.0278	369.1400	0.0014	0.1422	0.0125	0.1545	0.0123
	4	1495	9	5	0.0301	299.0000	1459.1100	11.2000	4.1800	0.0321	348.4400	0.0240	0.2444	0.1640	0.0664	0.1654
	5	2195	25	3	0.0342	731.6667	2088.3300	25.4000	3.5200	0.0428	592.6600	0.0486	0.0160	0.1733	0.2526	0.1900
	6	2195	16	4	0.0292	548.7500	2310.5400	15.7000	5.3800	0.0365	429.2900	0.0526	0.0188	0.3450	0.2518	0.2177
	7	2195	16	6	0.0437	365.8333	2138.2800	18.1000	6.4800	0.0548	329.9400	0.0258	0.1313	0.0800	0.2530	0.0981
	8	2195	16	5	0.0364	439.0000	2183.1200	19.9000	5.4500	0.0497	400.3100	0.0054	0.2438	0.0900	0.3636	0.0881

Table 73. Original Parameters vs. Extracted Parameters (SNR = -3 dB).

-3 dB																
Signal Type	Signal #	Actual Parameters				Extracted Parameters				Error						
		Carrier Frequency	Number of Subcodes	Carrier Cycles per Subcode	Code Period	Bandwidth	Carrier Frequency	Number of Subcodes	Carrier Cycles per Subcode	Code Period	Bandwidth	Error fc	Error Nc	Error cpp	Error T	Error B
Frank	1	1495	36	1	0.0241	1495.0000	1746.5800	30.3600	1.7900	0.0312	970.7000	0.1683	0.1567	0.7900	0.2957	0.3507
	2	1495	25	2	0.0334	747.5000	1486.8000	32.1000	1.8000	0.0390	823.2000	0.0055	0.2840	0.1000	0.1661	0.1013
	3	1495	9	4	0.0241	373.7500	1493.6500	9.4700	4.4500	0.0282	334.9600	0.0009	0.0556	0.1125	0.1711	0.1038
	4	1495	9	5	0.0301	299.0000	1540.0000	8.6800	4.7500	0.0268	323.5500	0.0301	0.0352	0.0500	0.1096	0.0821
	5	2195	25	3	0.0342	731.6667	2132.6600	16.4100	3.9900	0.0307	534.3300	0.0284	0.3436	0.3300	0.1015	0.2697
	6	2195	16	4	0.0292	548.7500	2220.3100	17.9000	4.5300	0.0365	489.4500	0.0115	0.1188	0.1325	0.2518	0.1081
	7	2195	16	5	0.0364	439.0000	2253.1200	14.9400	5.2500	0.0348	428.7500	0.0265	0.0663	0.0500	0.0452	0.0233
	8	2195	16	6	0.0437	365.8333	2174.7300	16.1200	6.6600	0.0494	326.3000	0.0092	0.0075	0.1100	0.1295	0.1081
P1	1	1495	36	1	0.0241	1495.0000	1401.3600	46.8900	1.2900	0.0432	1083.4900	0.0626	0.3025	0.2900	0.7940	0.2753
	2	1495	25	2	0.0334	747.5000	1400.0000	22.6400	1.9600	0.0317	714.0000	0.0635	0.0944	0.0200	0.0522	0.0448
	3	1495	9	4	0.0241	373.7500	1486.8100	11.6800	3.5000	0.0275	423.8200	0.0055	0.2978	0.1250	0.1420	0.1340
	4	1495	9	5	0.0301	299.0000	1521.3300	11.9500	4.3200	0.0340	351.5500	0.0176	0.3278	0.1360	0.1296	0.1758
	5	2195	16	4	0.0292	548.7500	2028.9000	27.0200	4.5800	0.0610	442.9600	0.0757	0.6888	0.1450	1.0921	0.1928
	6	2195	16	5	0.0364	439.0000	2218.1200	20.3000	4.9900	0.0457	444.0600	0.0105	0.2688	0.0020	0.2539	0.0115
	7	2195	16	6	0.0437	365.8333	2231.2500	20.2000	6.0500	0.0548	368.2200	0.0165	0.2625	0.0083	0.2530	0.0065
	8	2195	25	3	0.0342	731.6667	1992.6600	43.5000	3.2700	0.0714	609.0000	0.0922	0.7400	0.0900	1.0896	0.1677
P2	1	1495	36	1	0.0241	1495.0000	1415.0300	23.4100	1.7100	0.0284	823.7300	0.0535	0.3497	0.7100	0.1794	0.4490
	2	1495	16	2	0.0214	747.5000	1551.7500	14.1800	2.7100	0.0248	570.8000	0.0380	0.1138	0.3550	0.1586	0.2364
	3	1495	16	3	0.0321	498.3333	1548.7500	16.1000	3.2900	0.0342	469.5800	0.0360	0.0063	0.0967	0.0652	0.0577
	4	2195	36	3	0.0492	731.6667	2121.0600	30.9000	4.2300	0.0617	500.6900	0.0337	0.1417	0.4100	0.2540	0.3157
	5	2195	16	4	0.0292	548.7500	2305.0700	14.2000	5.9300	0.0365	388.2800	0.0501	0.1125	0.4825	0.2518	0.2924
	6	2195	16	5	0.0364	439.0000	2198.4300	15.9000	6.3200	0.0457	347.8100	0.0016	0.0062	0.2640	0.2539	0.2077
	1	1495	36	1	0.0241	1495.0000	1746.5800	49.6800	1.2800	0.0364	1363.7600	0.1683	0.3800	0.2800	0.5116	0.0878
	2	1495	25	2	0.0334	747.5000	1621.2000	13.2400	3.1200	0.0255	518.0000	0.0844	0.4704	0.5600	0.2376	0.3070
P3	3	1495	9	4	0.0241	373.7500	1469.7200	8.9500	4.4700	0.0272	328.1200	0.0169	0.0056	0.1175	0.1296	0.1221
	4	1495	9	5	0.0301	299.0000	1468.4400	8.4500	6.0500	0.0348	242.6600	0.0178	0.0611	0.2100	0.1561	0.1884
	5	2195	25	3	0.0342	731.6667	2198.0000	25.1400	3.9000	0.0447	562.3300	0.0014	0.0056	0.3000	0.3082	0.2314
	6	2195	16	4	0.0292	548.7500	2124.6000	26.0200	4.9800	0.0610	426.5600	0.0321	0.6263	0.2450	1.0921	0.2227
	7	2195	16	6	0.0437	365.8333	2200.2600	20.2800	6.5200	0.0601	337.2300	0.0024	0.2675	0.0867	0.3742	0.0782
	8	2195	16	5	0.0364	439.0000	2170.0000	18.8000	5.2700	0.0457	411.2500	0.0114	0.1750	0.0540	0.2539	0.0632
	1	1495	36	1	0.0241	1495.0000	1934.5700	34.4600	1.5600	0.0278	1237.3000	0.2940	0.0428	0.5600	0.1545	0.1724
	2	1495	25	2	0.0334	747.5000	1489.6000	29.4800	1.9700	0.0391	753.2000	0.0036	0.1792	0.0150	0.1691	0.0076
P4	3	1495	9	4	0.0241	373.7500	1309.0800	15.5700	2.8500	0.0340	458.0070	0.1244	0.7300	0.2875	0.4119	0.2254
	4	1495	9	5	0.0301	299.0000	1480.8800	12.1100	4.1300	0.0338	357.7700	0.0094	0.3456	0.1740	0.1229	0.1966
	5	2195	25	3	0.0342	731.6667	2228.3300	25.5800	3.1100	0.0357	716.3300	0.0152	0.0232	0.0367	0.0448	0.0210
	6	2195	16	4	0.0292	548.7500	2214.8400	18.0200	4.7900	0.0390	462.1000	0.0090	0.1263	0.1975	0.3376	0.1579
	7	2195	16	6	0.0437	365.8333	2218.4800	16.9000	7.2000	0.0548	308.0700	0.0107	0.0562	0.2000	0.2530	0.1579
	8	2195	16	5	0.0364	439.0000	2187.5000	17.4000	5.7400	0.0457	380.6200	0.0034	0.0875	0.1480	0.2539	0.1330

Table 74. Original Parameters vs. Extracted Parameters (SNR = -6 dB).

- 6dB																
Signal Type	Signal #	Actual Parameters				Extracted Parameters				Error						
		Carrier Frequency	Number of Subcodes	Carrier Cycles per Subcode	Code Period	Bandwidth	Carrier Frequency	Number of Subcodes	Carrier Cycles per Subcode	Code Period	Bandwidth	Error fc	Error Nc	Error cpp	Error T	Error B
Frank	1	1495	36	1	0.0241	1495.0000	1397.9400	24.8400	1.2700	0.0227	1093.7500	0.0649	0.3100	0.2700	0.0573	0.2684
	2	1495	25	2	0.0334	747.5000	1274.0000	36.5900	1.7700	0.0508	719.6000	0.1478	0.4636	0.1150	0.5189	0.0373
	3	1495	9	4	0.0241	373.7500	1750.0000	20.1200	3.9300	0.0452	444.3300	0.1706	1.2356	0.0175	0.8771	0.1888
	4	1495	9	5	0.0301	299.0000	1443.5500	9.8500	3.9300	0.0268	367.1100	0.0344	0.0944	0.2140	0.1096	0.2278
	5	2195	25	3	0.0342	731.6667	2242.3300	29.6200	4.0500	0.0535	553.0000	0.0216	0.1848	0.3500	0.5658	0.2442
	6	2195	16	4	0.0292	548.7500	2105.4600	21.4200	3.7100	0.0378	566.0100	0.0408	0.3388	0.0725	0.2964	0.0315
	7	2195	16	5	0.0364	439.0000	2209.3700	18.0000	5.8300	0.0475	378.4300	0.0065	0.1250	0.1660	0.3033	0.1380
	8	2195	16	6	0.0437	365.8333	2211.1900	21.8200	6.0600	0.0598	364.5800	0.0074	0.3638	0.0100	0.3673	0.0034
P1	1	1495	36	1	0.0241	1495.0000	1708.9800	38.6600	1.5700	0.0355	1086.9100	0.1431	0.0739	0.5700	0.4742	0.2730
	2	1495	25	2	0.0334	747.5000	1402.8000	27.6600	1.8800	0.0371	744.8000	0.0617	0.1064	0.0600	0.1093	0.0036
	3	1495	9	4	0.0241	373.7500	1456.0500	7.1800	3.9000	0.0192	372.5500	0.0261	0.2022	0.0250	0.2027	0.0032
	4	1495	9	5	0.0301	299.0000	1568.0000	7.9400	4.5400	0.0230	345.3300	0.0488	0.1178	0.0920	0.2359	0.1549
	5	2195	16	4	0.0292	548.7500	2203.9000	16.1600	5.3300	0.0391	412.8900	0.0041	0.0100	0.3325	0.3410	0.2476
	6	2195	16	5	0.0364	439.0000	2128.4300	22.5000	4.3200	0.0457	492.1800	0.0303	0.4063	0.1360	0.2539	0.1211
	7	2195	16	6	0.0437	365.8333	2145.5700	19.0000	6.1900	0.0548	346.3500	0.0225	0.1875	0.0317	0.2530	0.0533
	8	2195	25	3	0.0342	731.6667	2366.0000	23.2400	3.4000	0.0334	695.3300	0.0779	0.0704	0.1333	0.0225	0.0497
P2	1	1495	36	1	0.0241	1495.0000	1869.6200	23.3100	1.7700	0.0221	1052.7300	0.2506	0.3525	0.7700	0.0822	0.2958
	2	1495	16	2	0.0214	747.5000	998.0400	23.8500	1.4800	0.0354	673.3300	0.3324	0.4906	0.2600	0.6538	0.0992
	3	1495	16	3	0.0321	498.3333	1717.9100	15.1600	3.2300	0.0285	550.8300	0.1491	0.0525	0.0767	0.1123	0.0652
	4	2195	36	3	0.0492	731.6667	2262.0300	64.6500	3.4300	0.0982	667.8700	0.0305	0.7958	0.1433	0.9958	0.0872
	5	2195	16	4	0.0292	548.7500	2102.7300	14.1300	5.6500	0.0380	371.8700	0.0420	0.1169	0.4125	0.3033	0.3223
	6	2195	16	5	0.0364	439.0000	2235.6000	23.6200	5.4000	0.0571	413.4300	0.0185	0.4763	0.0800	0.5667	0.0582
	1	1495	36	1	0.0241	1495.0000	1647.4609	41.1900	1.2100	0.0302	1360.3500	0.1020	0.1442	0.2100	0.2541	0.0901
	2	1495	25	2	0.0334	747.5000	1503.6000	23.4300	1.9200	0.0300	781.2000	0.0058	0.0628	0.0400	0.1030	0.0451
P3	3	1495	9	4	0.0241	373.7500	1503.9000	8.7700	3.8900	0.0227	386.2300	0.0060	0.0256	0.0275	0.0573	0.0334
	4	1495	9	5	0.0301	299.0000	1446.6600	10.2700	5.6700	0.0402	255.1100	0.0323	0.1411	0.1340	0.3355	0.1468
	5	2195	25	3	0.0342	731.6667	2230.6600	23.1200	5.1600	0.0535	431.6600	0.0162	0.0752	0.7200	0.5658	0.4100
	6	2195	16	4	0.0292	548.7500	2206.6400	22.9000	3.5200	0.0365	626.1700	0.0053	0.4313	0.1200	0.2518	0.1411
	7	2195	16	6	0.0437	365.8333	2174.7300	23.4800	7.2700	0.0785	298.9500	0.0092	0.4675	0.2117	0.7949	0.1828
	8	2195	16	5	0.0364	439.0000	2303.4300	14.6800	5.9800	0.0381	385.0000	0.0494	0.0825	0.1960	0.0454	0.1230
	1	1495	36	1	0.0241	1495.0000	1281.7300	79.6100	0.8900	0.0558	1425.2900	0.1427	1.2114	0.1100	1.3173	0.0466
	2	1495	25	2	0.0334	747.5000	1458.8000	20.7400	2.0500	0.0292	708.4000	0.0242	0.1704	0.0250	0.1269	0.0523
P4	3	1495	9	4	0.0241	373.7500	1613.2800	13.9400	3.9300	0.0340	410.1500	0.0791	0.5489	0.0175	0.4119	0.0974
	4	1495	9	5	0.0301	299.0000	1431.1100	16.7900	3.9300	0.0461	364.0000	0.0427	0.8656	0.2140	0.5315	0.2174
	5	2195	25	3	0.0342	731.6667	2163.0000	19.7000	4.0300	0.0367	536.6600	0.0146	0.2120	0.3433	0.0741	0.2665
	6	2195	16	4	0.0292	548.7500	2214.8400	14.5800	3.9700	0.0261	557.8100	0.0090	0.0888	0.0075	0.1049	0.0165
	7	2195	16	6	0.0437	365.8333	2275.0000	19.7700	6.6300	0.0577	342.7000	0.0364	0.2356	0.1050	0.3193	0.0632
	8	2195	16	5	0.0364	439.0000	2082.5000	29.8000	5.2300	0.0748	398.1200	0.0513	0.8625	0.0460	1.0523	0.0931



## C. COMPARATIVE PARAMETER EXTRACTION RESULTS

### 1. Results for P1 Code

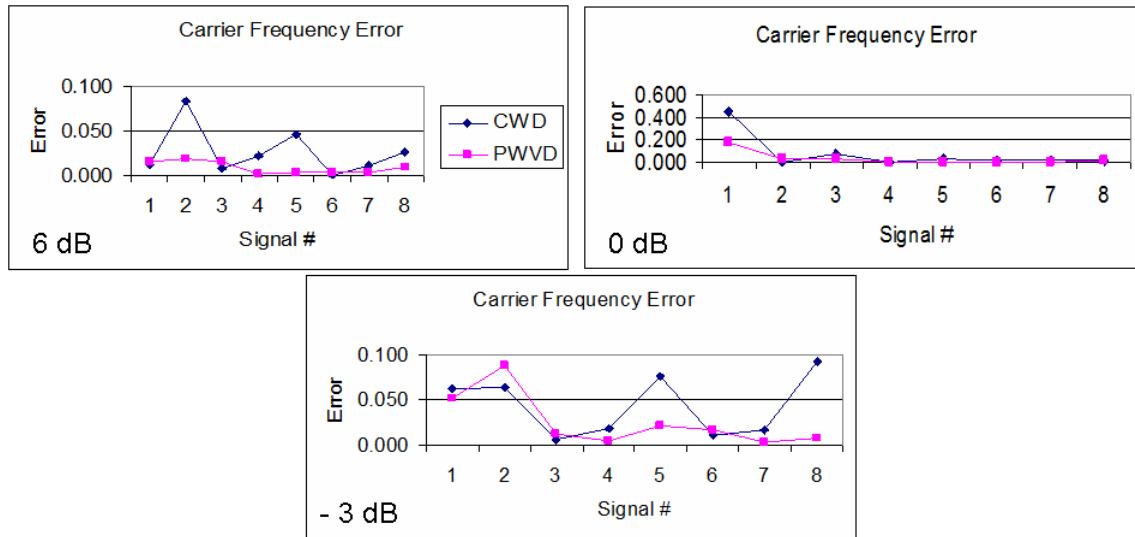


Figure 92. Carrier Frequency Error for P1 Code.

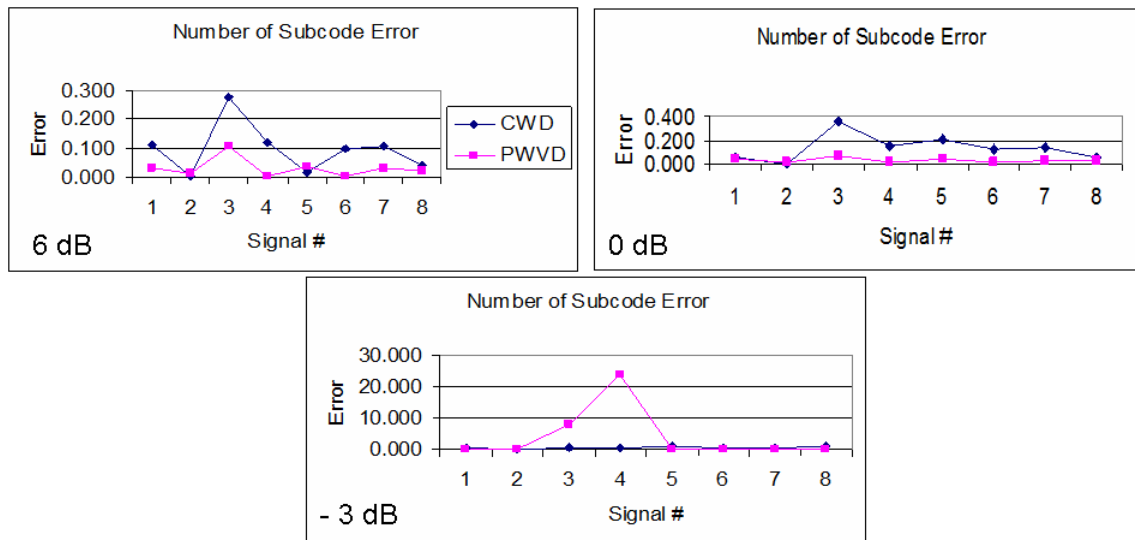


Figure 93. Number of Subcode Error for P1 Code.

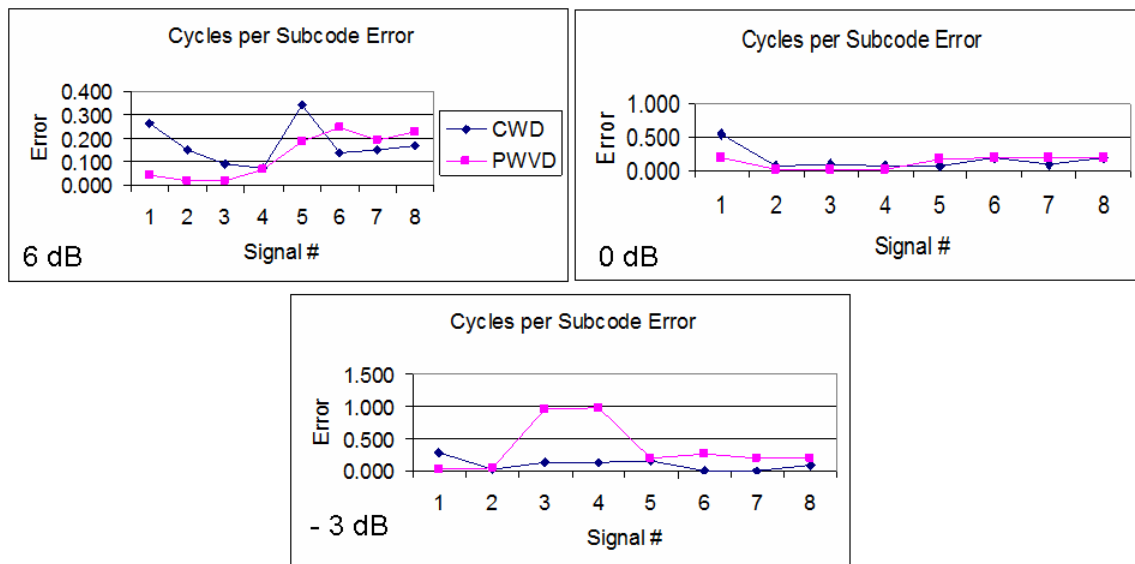


Figure 94. Cycles per Subcode Error for P1 Code.

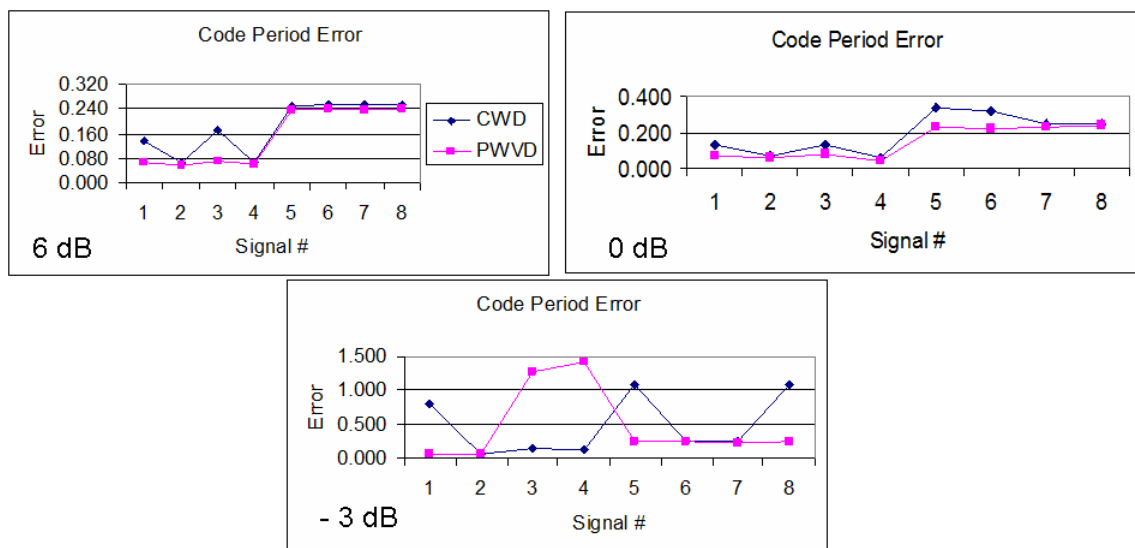


Figure 95. Code Period Error for P1 Code.

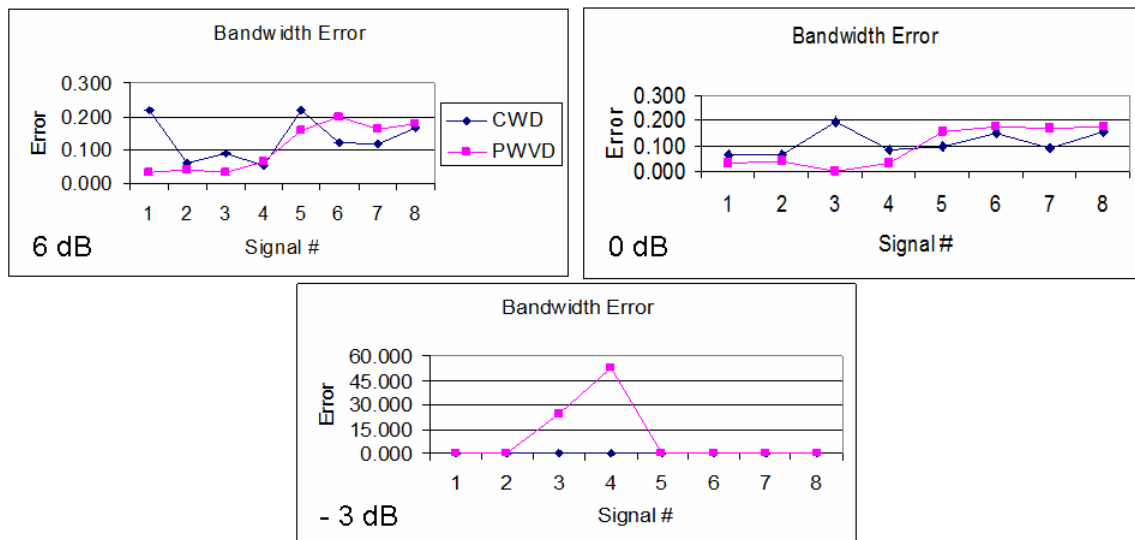


Figure 96. Bandwidth Error for P1 Code

## 2. Results for P2 Code

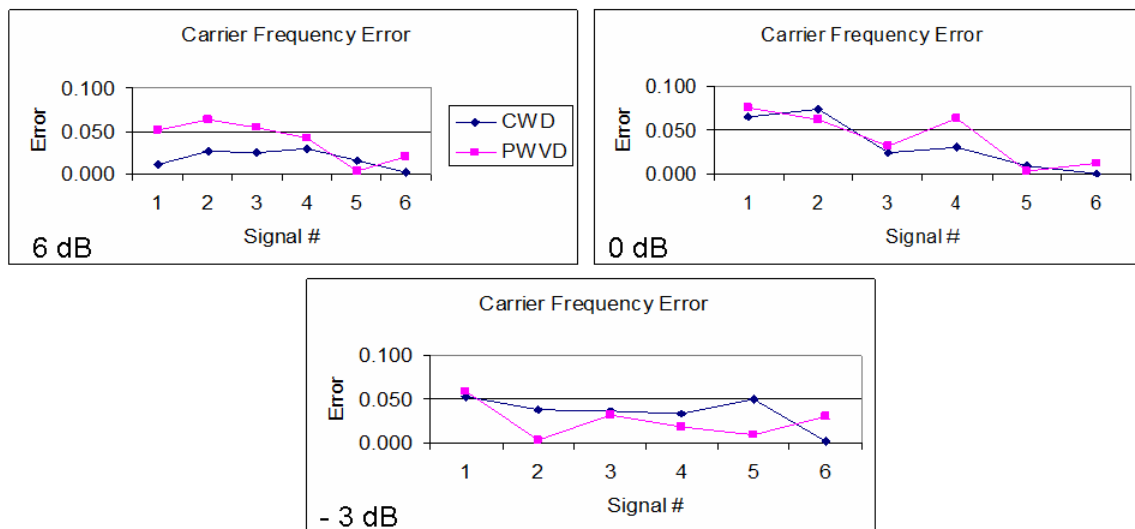


Figure 97. Carrier Frequency Error for P2 Code.

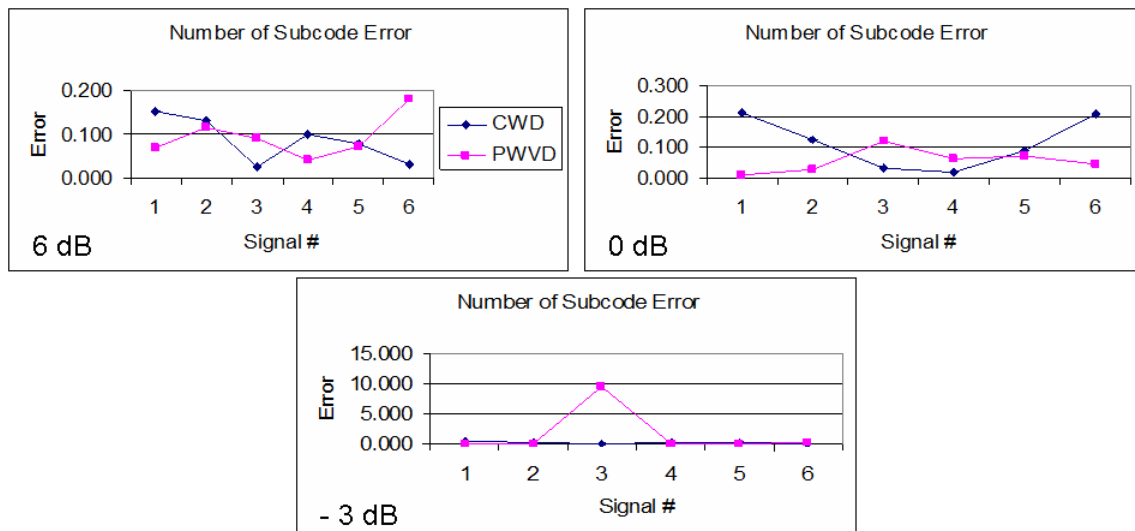


Figure 98. Number of Subcode Error for P2 Code.

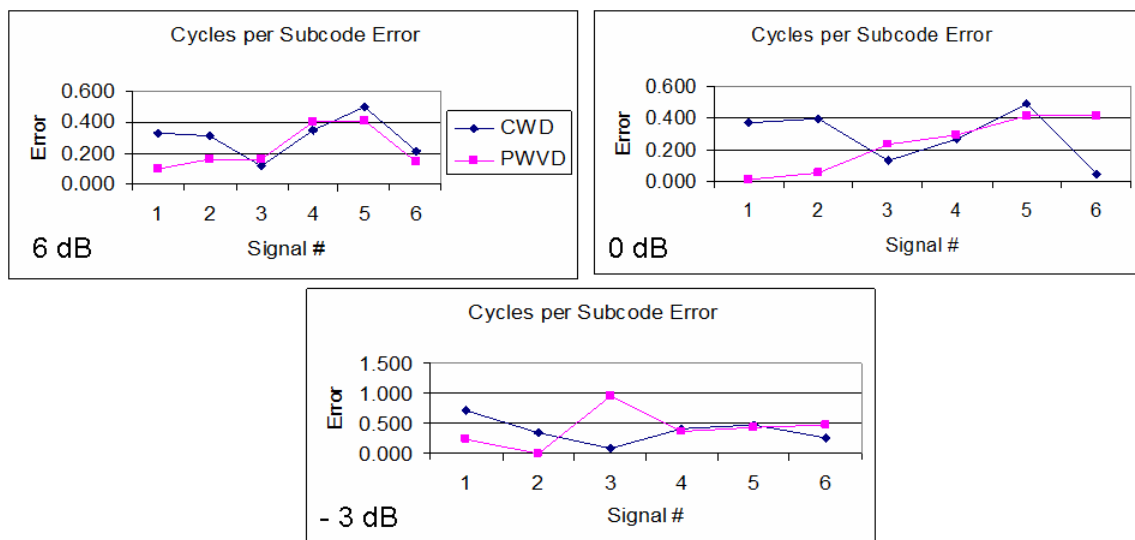


Figure 99. Cycles per Subcode Error for P2 Code.

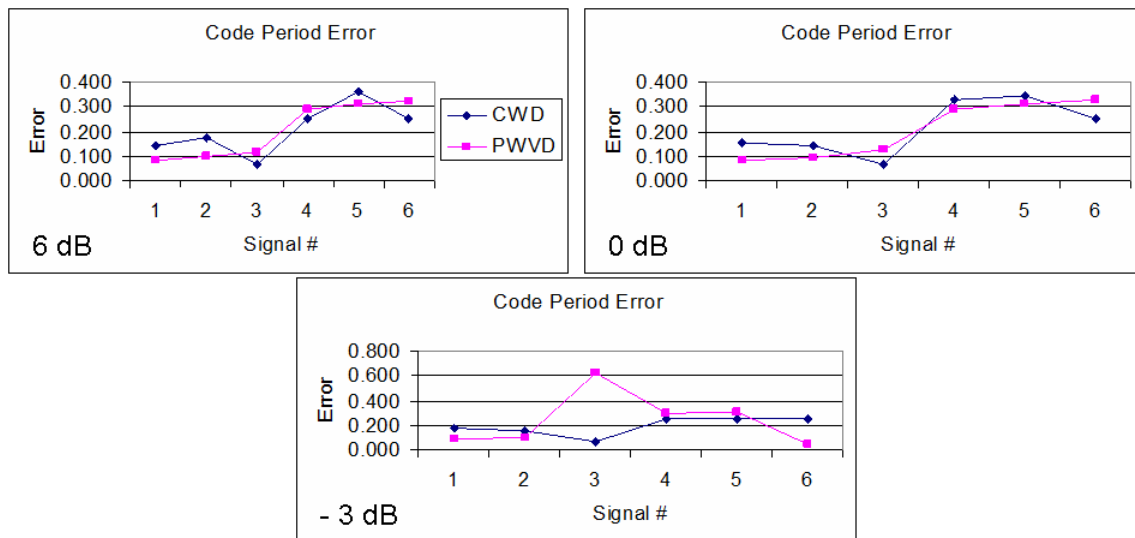


Figure 100. Code Period Error for P2 Code.

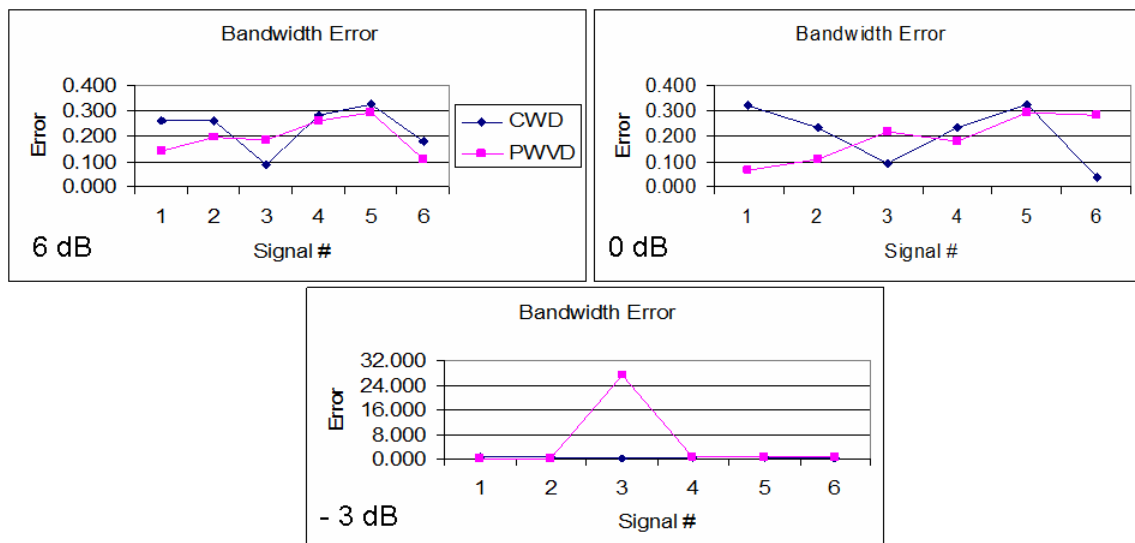


Figure 101. Bandwidth Error for P2 Code.

### 3. Results for P3 Code

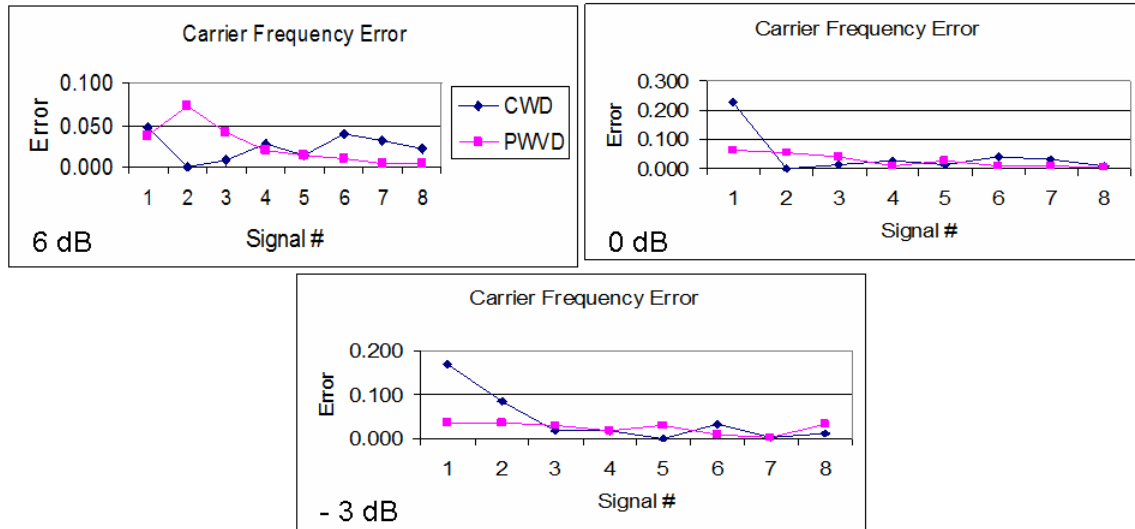


Figure 102. Carrier Frequency Error for P3 Code.

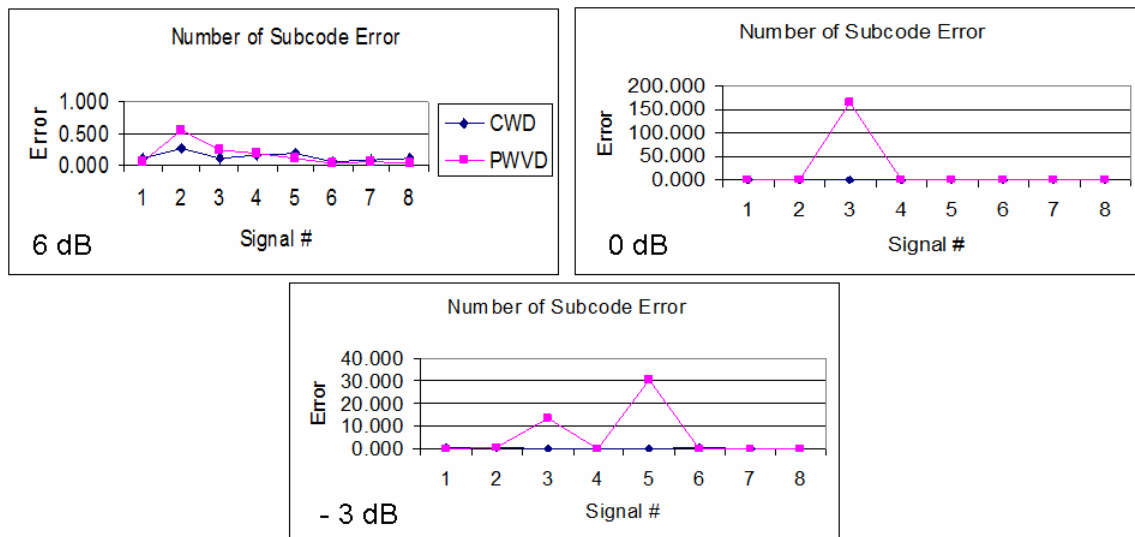


Figure 103. Number of Subcode Error for P3 Code.

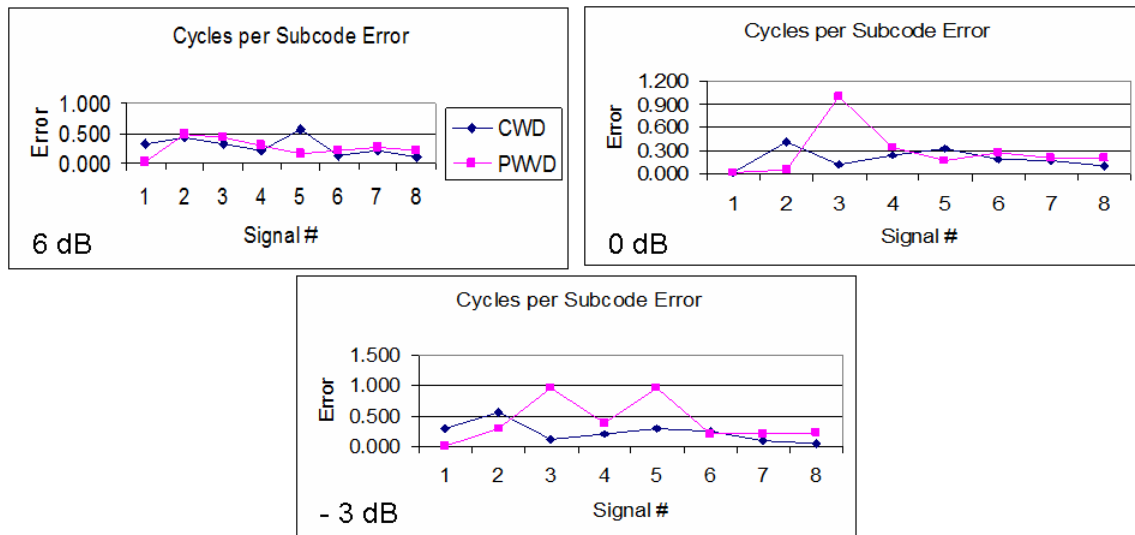


Figure 104. Cycles per Subcode Error for P3 Code.

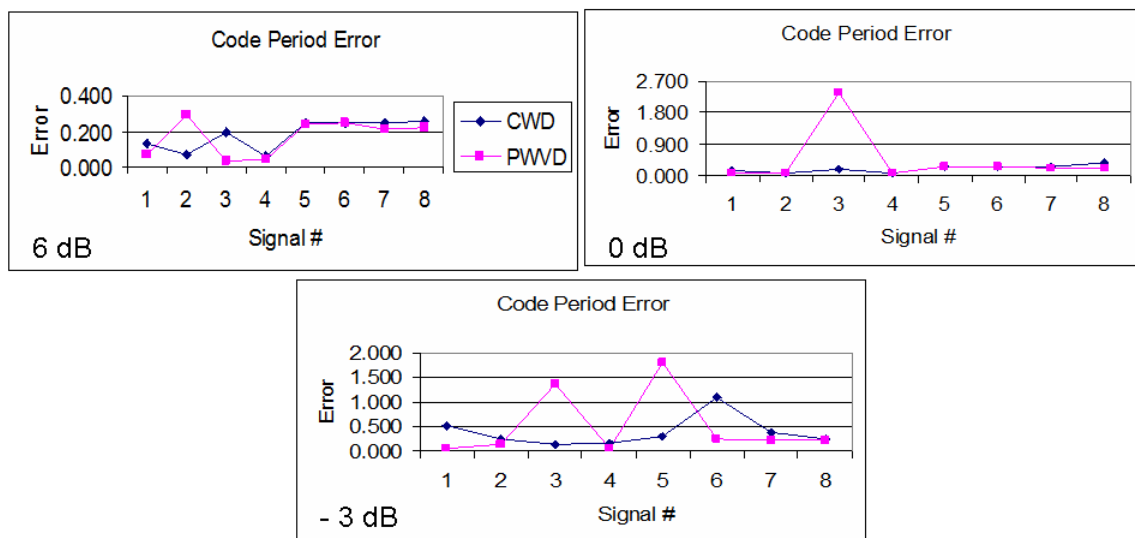


Figure 105. Code Period Error for P3 Signal.

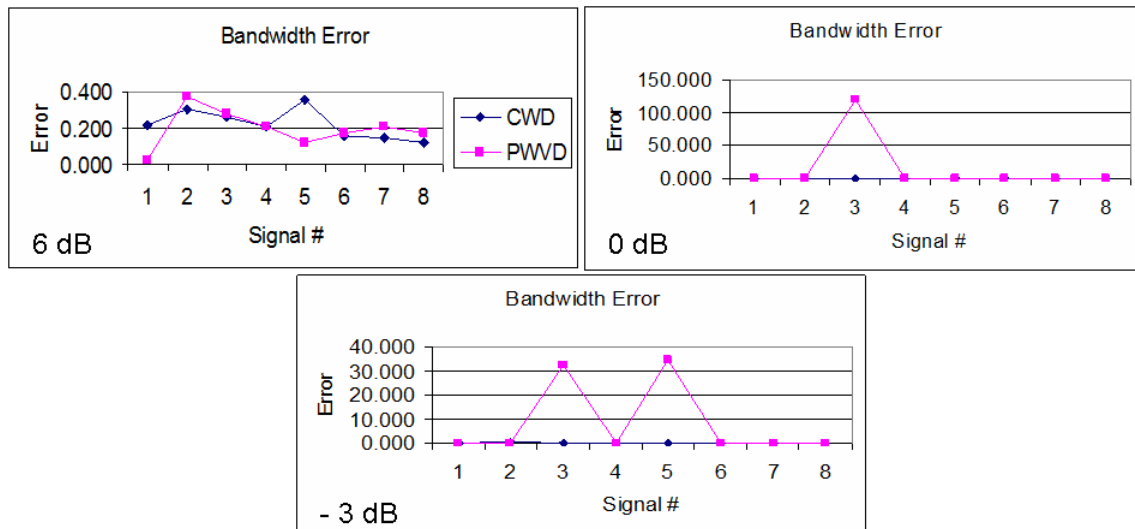


Figure 106. Bandwidth Error for P3 Code.

#### 4. Results for P4 Code

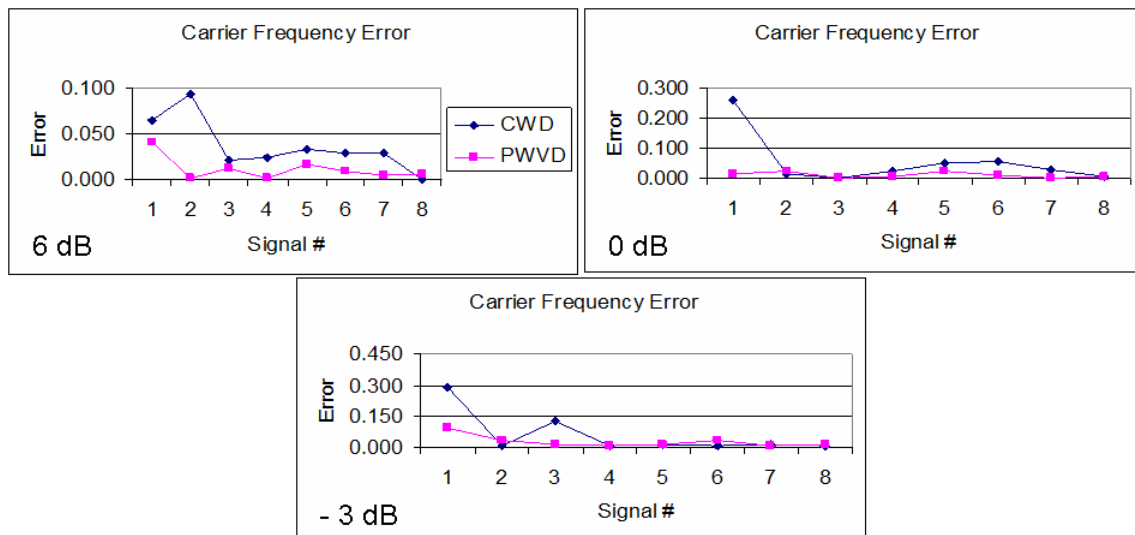


Figure 107. Carrier Frequency Error for P4 Code.



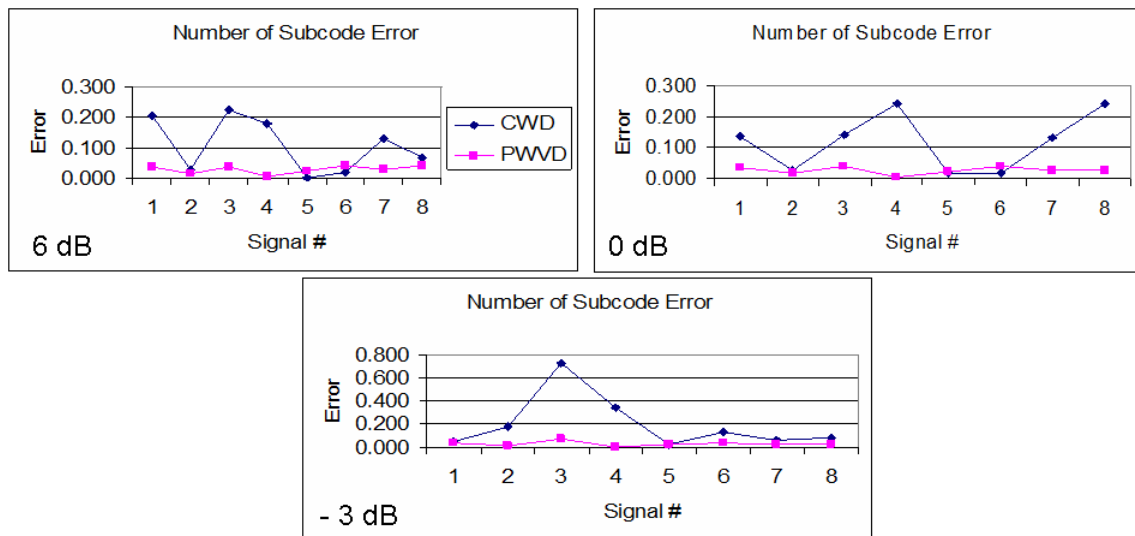


Figure 108. Number of Subcode Error for P4 Code.

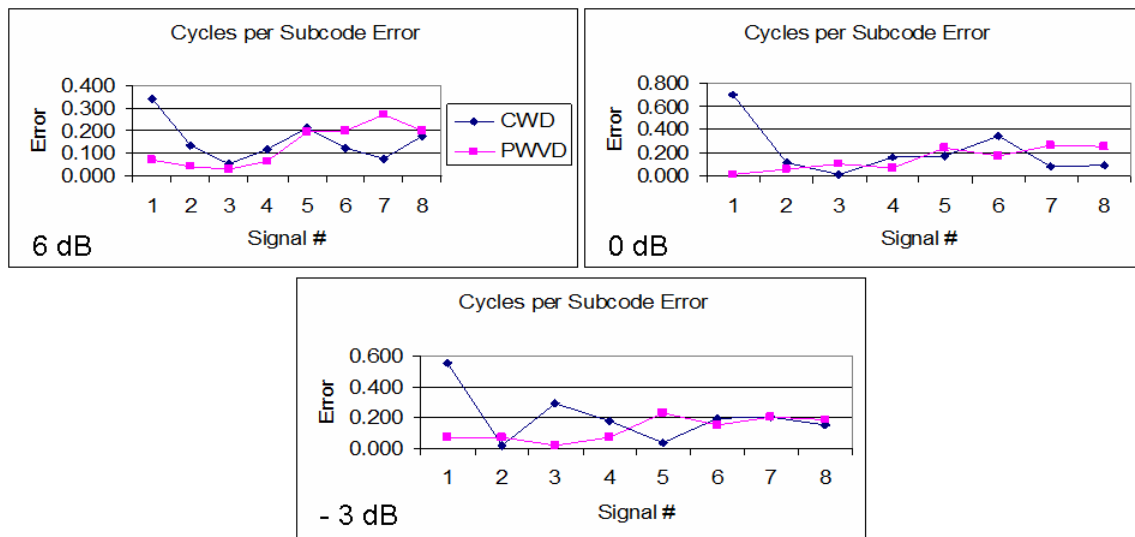


Figure 109. Cycles per Subcode Error for P4 Code.

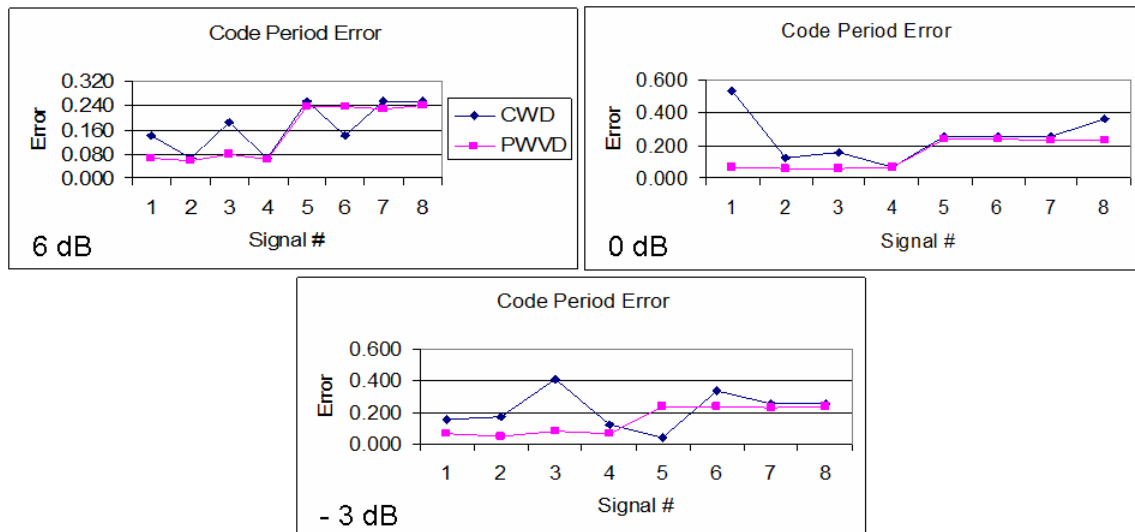


Figure 110. Code Period Error for P4 Code.

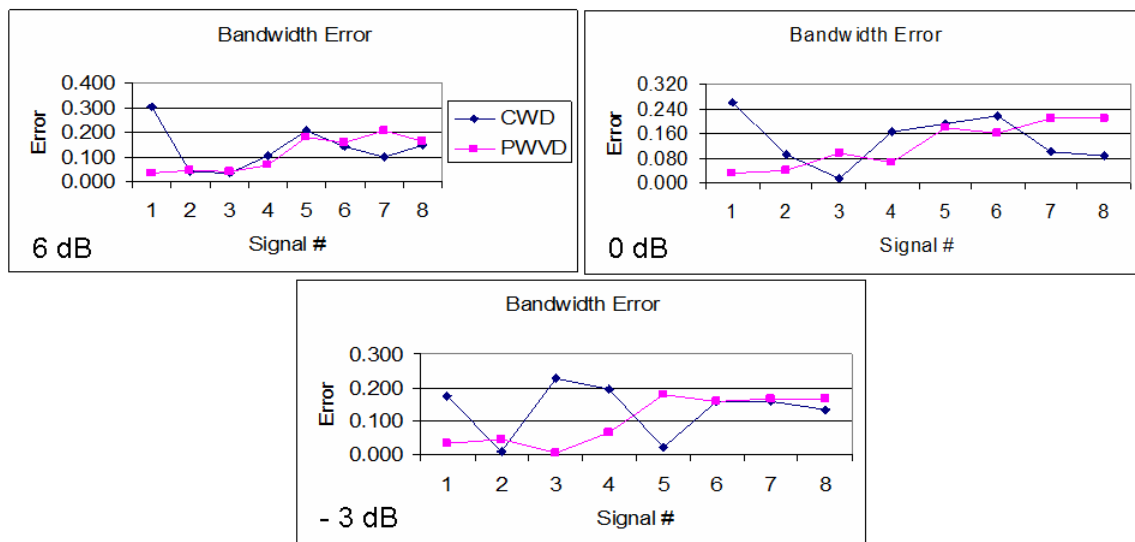


Figure 111. Bandwidth Error for P4 Code.

## LIST OF REFERENCES

- [1] R. G. Wiley, *ELINT: The Interception and Analysis of Radar Signals*, Artech House, 2006.
- [2] P. E. Pace, *Detecting and Classifying Low Probability of Intercept Radar*, Norwood, MA: Artech House, 2004.
- [3] A. Denk, "Detecting and Jamming Low Probability of Intercept (LPI) Radars," Master's Thesis, Naval Postgraduate School, Monterey, CA, 2006.
- [4] D. L. Adamy, *EW102 A Second Course in Electronic Warfare*, Horizon House Publications, Inc., 2004.
- [5] G. Schrick and R. G. Wiley, "Interception of LPI radar signals," *Record of the IEEE International Radar Conference*, Arlington, VA, pp. 108-111, 7-10 May 1990.
- [6] D. D. Vaccaro, *Electronic Warfare Receiving Systems*, Norwood, MA: Artech House, 1993.
- [7] C. Breakenridge, "Nonstationary signal classification using time-frequency optimization," *Proceedings of the 2003 10th IEEE International Conference*, 14-17 December 2003, Vol. 1, pp. 132-135, July 2003.
- [8] G. Roberts, A. M. Zoubir, and B. Boashash, "Time-frequency classification using a multiple hypothesis test: an application to the classification of humpback whale signals," *IEEE International Conference on Acoustics, Speech, and Signal Processing*, Vol. 1, pp. 563-566, 1997.
- [9] C. Breakenridge, and M. Mesbah, "Minimum classification error using time-frequency analysis," *Proceedings of the 3rd IEEE International Symposium*, pp. 717-720, 14-17 December 2003.
- [10] T. Wang, J. Deng, and B. He, "Classification of motor imagery EEG patterns and their topographic representation," *Proceedings of the 26<sup>th</sup> Annual International Conference of the IEEE EMBS*, pp. 4359-4362, 1-5 September 2004.
- [11] N. Gache, P. Chevret, and V. Zimpfer, "Target classification near complex interfaces using time-frequency filters," *Proceedings of the 1998 IEEE International Conference*, Vol. 4, pp. 2433-2436, 12-15 May 1998.
- [12] K.-T. Kim, I.-S. Choi, and H.-T. Kim, "Efficient radar target classification using adaptive joint time-frequency processing," *IEEE Trans. On Antennas and Propagation*, Vol. 48, No. 12, pp. 1789-1801, December 2000.

- [13] M. V. Chilukuri, P. K. Dash, and K. P. Basu, "Time-frequency based pattern recognition technique for detection and classification of power quality disturbances," *2004 IEEE Region 10 Conference*, Vol. 3, pp. 260-263, 21-24 November 2004.
- [14] B. W. Gillespie, and L. E. Atlas, "Optimizing time-frequency kernels for classification," *IEEE Trans. On Signal Processing*, Vol. 49, No. 3, pp. 485-496, March 2001.
- [15] L. Atlas, L. Owsley, J. McLaughlin, and G. Bernard, "Automatic feature-finding for time-frequency distributions," *Proceedings of the IEEE-SP International Symposium*, pp. 333-336, 18-21 June 1996.
- [16] E. Azzouz, and A. K. Nandi, *Automatic Modulation Recognition of Communication Signals*, Kluwer Academic Publishers, 1996.
- [17] C. Louis, and P. Sehier, "Automatic modulation recognition with a hierarchical neural network," *Record of the IEEE Military Communications Conference, MILCOM '94*, Vol. 3, pp. 713-717, October 1994.
- [18] Y-C. Lin, and C-C. J. Kuo, "Modulation classification using wavelet transform," *Proc. SPIE* Vol. 2303, pp. 260-271, *Wavelet Applications in Signal and Image Processing II*, Andrew F. Laine, Michael A. Unser; Eds., October 1994.
- [19] E. E. Azzouz, and A. K. Nandi, "Automatic identification of digital modulation types," *Signal Processing*, Vol. 47, No. 1, pp. 55-69, 1995.
- [20] J. Reichert, "Automatic classification of communication signals using higher order statistics," *Proceedings of the 1992 IEEE International Conference on Acoustics, Speech and Signal Processing*, Vol. 5, pp. 221-224, 23-26 March 1992.
- [21] C. Schreyogg, K. Kittel, U. Kressel, and J. Reichert, "Robust classification of modulation types using spectral features applied to HMM," *Proceedings of MILCOM*, Vol. 3, pp. 1377-1381, 2-5 November 1997.
- [22] A. K. Nandi, and E. E. Azzouz, "Algorithms for automatic modulation recognition of communication signals," *IEEE Transactions on Communications*, Vol. 46, No. 4, pp. 431-436, April 1998.
- [23] H. Ketterer, F. Jondral, and A. H. Costa, "Classification of modulation modes using time-frequency methods," *Proceedings of the 1999 IEEE International Conference on Acoustics, Speech, and Signal Processing*, 1999. Vol. 5, pp. 2471-2474, 15-19 March 1999.

- [24] M. L. D. Wong, and A. K. Nandi, "Automatic digital modulation recognition using artificial neural network and genetic algorithm," *Signal Processing*, Vol. 84, No. 2, pp. 351-365, February 2004.
- [25] A. K. Mishra and B. Mulgrew, "Radar signal classification using PCA-based features," *Proceedings of the 2006 IEEE International Conference on Acoustics, Speech, and Signal Processing*, Vol. 3, pp. 1104-1107, 14-19 May 2006.
- [26] W. Soares-Filho, J. M. de Seixas and L. P. Caloba, "Principal component analysis for classifying passive sonar signals," *The 2001 IEEE International Symposium on Circuits and Systems*, Vol. 3, pp. 592-595, 6-9 May 2001.
- [27] T. O. Gulum, P. E. Pace, "Time-Frequency Feature Extraction for Classification of LPI Radar Modulations using Principal Components Analysis," *2008 IEEE International Conference on Acoustics, Speech and Signal Processing* (in review).
- [28] T. O. Gulum, P. E. Pace, "Autonomous Parameter Extraction Algorithms for LPI Radar Polyphase Modulations," *2008 IEEE International Conference on Acoustics, Speech and Signal Processing* (in review).
- [29] E. R. Zilberman, "Autonomous Time-Frequency Cropping and Feature Extraction Algorithms for Classification of LPI Radar Modulations," Master's Thesis, Naval Postgraduate School, Monterey, CA, 2006.
- [30] S. O. Piper, "Receiver frequency resolution for range resolution in homodyne FMCW radar," *Proceedings National Telesystems Conference, Commercial Applications and Dual-Use Technology*, pp. 169-173, 1993.
- [31] S. O. Piper, "Homodyne FMCW radar range resolution effects with sinusoidal nonlinearities in the frequency sweep," *Record of the IEEE International Radar Conference*, pp. 563-567, 1995.
- [32] W. D. Wirth, "Polyphase coded CW radar," *Proc. of the IEEE Fourth International Symposium on Spread Spectrum Techniques and Applications*, Mainz, Germany, Vol. 1, pp. 186-190, 22-25 September 1996.
- [33] R. L. Frank, "Polyphase codes with good nonperiodic correlation properties," *IEEE Transactions on Information Theory*, Vol. 9, No. 1, pp. 43-45, 1963.
- [34] B. L. Lewis, F. F. Kretschmer and W. W. Shelton, *Aspects of Radar Signal Processing*, Artech House Inc., Norwood, MA, 1986.
- [35] J. E. Fielding, "Polytime coding as a means of pulse compression," *IEEE Trans. on Aerospace and Electronic Systems*, Vol. 35, No. 2, pp. 716-721, April 1999.
- [36] S. Qian, *Introduction to Time-Frequency and Wavelet Transforms*, Upper Saddle River, NJ: Prentice Hall, 2002.

- [37] F. Auger, P. Flandrin, P. Goncalves, O. Lemoine, *Time Frequency Toolbox*, CNRS, France, 1996.
- [38] L. Cohen, "Time-frequency distributions-A review," *Proceedings of the IEEE*, Vol. 77, No. 7, pp. 941-981, July 1989.
- [39] T. Farrell, and G. Prescott, "A nine-tile algorithm for LPI signal detection using QMF filter bank trees," *Proceedings of the IEEE Conference on Military Communications MILCOM '96*, Vol. 3, pp. 974-978, 1996.
- [40] P. Jarpa, "Quantifying the Differences in Low Probability of Intercept Radar Waveforms Using Quadrature Mirror Filtering," Master's Thesis, Naval Postgraduate School, Monterey, California, 2002.
- [41] Rafael C. Gonzales, Richard E. Woods and Steven L. Eddins, *Digital Image Processing Using Matlab*, Upper Saddle River, NJ, Prentice Hall, 2004.
- [42] J. S. Lim, *Two-Dimensional Signal and Image Processing*, Englewood Cliffs, NJ: Prentice Hall, 1990.
- [43] A. V. Oppenheim, A. S. Willsky, S. H. Nawab, *Signals and Systems*, Upper Saddle River, NJ: Prentice Hall, 1997.
- [44] M. P. Fargues, "Investigation of Feature dimension Reduction Schemes for Classification Applications," Naval Postgraduate School, Monterey, CA, NPS-EC-01-005, June 2001.
- [45] C. K. Lee, "infrared Face Recognition," Master's Thesis, Naval Postgraduate School, Monterey, California, 2004.
- [46] C.W. Therrien, *Discrete Random Signals and Statistical Signal Processing*, Prentice Hall, Englewood Cliffs, New Jersey, 1991.
- [47] S. Haykin, *Neural Networks-A Comprehensive Foundation*, Second Ed., Upper Saddle River, New Jersey: Prentice Hall, 1999.
- [48] G. Bulbulla, "Recognition of In-Ear Microphone Speech Data Using Multi-Layer Neural networks," Master's Thesis, Naval Postgraduate School, Monterey, California, 2006.
- [49] S. Theodoridis, K. Koutroumbas, *Pattern Recognition*, Third Ed., San Diego, CA: Academic Press, 2006.
- [50] H. B. Demuth, and M. H. Beale, *Neural Network Toolbox User's Guide*, Version 4, Natick, MA: The MathWorks, Inc., 2005.

- [51] C. Christodoulou, M. Georgiopoulos, *Applications of Neural Networks in Electromagnetics*, Norwood, MA: Artech House, 2001.
- [52] H. Husain, M. Khalid, R. Yusof, "Nonlinear Function Approximation using Radial Basis Function Neural Networks," *Student Conference on Research and Development*, pp. 326-329, July 2002.
- [53] H. Deshuang, M. Songde, "A New Radial Basis Probabilistic Neural Network Model," *IEEE 3rd International Conference on Signal Processing*, Vol. 2, pp. 1449-1452, October 1996.
- [54] L. Rutkowski, "Adaptive Probabilistic Neural Networks for Pattern Classification in Time-Varying Environment," *IEEE Transactions on Neural Networks*, Vol. 15, No. 4, pp. 811-827, July 2004.
- [55] M. R. Hejazi, G. Shevlyakov, Y-S Ho, "Modified Discrete Radon Transforms and Their Application to Rotation-Invariant Image Analysis," *IEEE 8th Workshop on Multimedia Signal Processing*, pp. 429-434, October 2006.
- [56] *Image Processing Toolbox 5 User's Guide*, Natick, MA: The MathWorks, Inc., 2007.

THIS PAGE INTENTIONALLY LEFT BLANK



## INITIAL DISTRIBUTION LIST

1. Defense Technical Information Center  
Ft. Belvoir, Virginia
2. Dudley Knox Library  
Naval Postgraduate School  
Monterey, California
3. Chairman  
Department of Information Sciences  
Naval Postgraduate School  
Monterey, California
4. Chairman  
Department of Electrical and Computer Engineering  
Naval Postgraduate School  
Monterey, California
5. Professor Phillip E. Pace  
Department of Electrical and Computer Engineering  
Naval Postgraduate School  
Monterey, California
6. Professor Roberto Cristi  
Department of Electrical and Computer Engineering  
Naval Postgraduate School  
Monterey, California
7. Dr. Peter Craig  
Office of Naval Research, Code 312  
Arlington, Virginia
8. LTJG Taylan O. Gulum  
Turkish Navy  
Ankara, Turkey